EXPLORING POLYPHOSPHATE BIOLOGY REGULATION IN *SACCHAROMYCES CEREVISIAE*

By: Liam McCarthy

A thesis submitted to the
University of Ottawa, Faculty of Medicine
In partial fulfilment of requirements for the
Doctorate in Philosophy Degree in Cellular and Molecular Medicine

Department of Cellular and Molecular Medicine
Faculty of Medicine
University of Ottawa

© Liam McCarthy, Ottawa, Canada, 2025

AUTHORIZATIONS

Manuscripts used as chapters in thesis:

Manuscript #1 – Chapter 2

McCarthy, L.*, Bentley-DeSousa*, A., Denoncourt, A., Tseng, Y. C., Gabriel, M., & Downey, M. (2020). Proteins required for vacuolar function are targets of lysine polyphosphorylation in yeast. *FEBS Letters*, 594(1), 21–30. https://doi.org/10.1002/1873-3468.13588
*Co-first authors

License Number: 6013820171050
License date: Apr 21, 2025
Licensed Content Publisher: John Wiley & Sons
Licensed Content Publication: FEBS Letters

Manuscript #2 – Chapter 3

McCarthy, L., Abramchuk, I., Wafy, G., Denoncourt, A., Lavallée-Adam, M., & Downey, M. (2022). Ddp1 cooperates with Ppx1 to counter a stress response initiated by nonvacuolar polyphosphate. *mBio*, 13(4), e0039022. https://doi.org/10.1128/mbio.00390-22

© 2022 McCarthy et al. This is an open-access article distributed under the terms of the Creative Commons Attribution 4.0 International (CC BY) license.

Manuscript #3 (In preparation) – Chapter 4

McCarthy, L., Ononye, O., & Downey, M. (In preparation). Exploring the structure and function of the Ddp1 polyphosphatase phosphohydrolase in yeast.

Manuscripts not used as chapters in thesis:

Manuscript #4
Note: Parts of this review have been used in the introduction (Chapter 1) and the discussion (Chapter 5). See *statement of rights and permissions* section of these chapters for specific details.

McCarthy, L., & Downey, M. (2023). The emerging landscape of eukaryotic polyphosphatases. *FEBS Letters*, 597(11), 1447–1461. https://doi.org/10.1002/1873-3468.14584

License Number: 6013820606011
License date: Apr 21, 2025
Licensed Content Publisher: John Wiley & Sons
Licensed Content Publication: FEBS Letters

Manuscript #5
Note: Parts of this review have been used in the introduction (Chapter 1) and the discussion (Chapter 5). See *statement of rights and permissions* section of these chapters for specific details.

McCarthy, L.*, Baijal, K.*, Downey, M. (2025) A framework for understanding and investigating polyphosphate-protein interactions. *Biochem Soc Trans*, 21:BST20240678.
https://doi.org/10.1042/BST20240678
*Co-first authors

© 2025 McCarthy et al. This is an open access article published by Portland Press Limited on behalf of the Biochemical Society and distributed under the Creative Commons Attribution 4.0 International (CC BY) license.

Manuscript #6 – Not included in thesis

Bondy-Chorney, E., Abramchuk, I., Nasser, R., Holinier, C., Denoncourt, A., Baijal, K., **McCarthy, L.**, Khacho, M., Lavallée-Adam, M., & Downey, M. (2020). A broad response to intracellular long-chain polyphosphate in human cells. *Cell Reports*, 33(4), 108318. https://doi.org/10.1016/j.celrep.2020.108318

Manuscript #7 – Not included in thesis

Milhaven M., Hastings E., Brister D., Cevallos L., Chilukuri S., Diyya A., Garg A., Hernandez R., Kelly D., Lazo K., Le J., Maag G., Marfatia P.D., Mehta R., Nejad A., Porche J., Queiroz A., Sackett D., Santos Molina P., Slade T., So M., Thakur K., Urquidez Negrete A., Wackett S., Weiss S., **McCarthy L.**, Wheaton K., Rudner AD.., McCutcheon J.P., Pfeifer S.P. (2021). Complete genome sequence of microbacterium bacteriophage Erla. Microbiology resource announcements, 10(3), e01354-20. https://doi.org/10.1128/MRA.01354-20

ABSTRACT

Polyphosphate (polyP) is a polymer of inorganic phosphate residues that can range from three residues to thousands in length. These polymers are conserved across most organisms where they participate in a multitude of cellular functions. In yeast, polyP is synthesized and stored within the vacuole where it is involved in phosphate, ion, and pH homeostasis. Despite growing interest in polyP's role in a variety of diseases there are still many questions relating to its fundamental biology that remain unanswered.

We first set out to expand the scope of polyP-binding proteins in yeast. We performed an expanded screen of 200 yeast proteins that were not screened in our groups previous screen for polyP-binding proteins published in 2018. We identify 8 new polyP-binding proteins that interact genetically and physically with previous targets involved in ribosome biogenesis. These include two proteins involved in vacuolar function – the Prb1 protease and the Apl5 subunit of the AP-3 complex. The ability of polyP to bind to these proteins suggests a model for feedback regulation of polyP synthesis in the vacuole.

In many cell types, polyphosphate is concentrated in subcellular compartments or organelles. In budding yeast, polyP synthesis by the membrane-bound vacuolar transporter chaperone (VTC) complex is coupled to its translocation into the lumen of the vacuole, a lysosome-like organelle, where it is stored at high concentrations. In contrast, the ectopic expression of the bacterial polyphosphate kinase (PPK) results in the toxic accumulation of polyP outside the vacuole. We used label-free mass spectrometry to investigate the mechanisms underlying this toxicity. We find that PPK expression results in the activation of a stress response mediated in part by the Hog1 and Yak1 kinases and the Msn2/Msn4 transcription factors as well as changes in protein kinase A (PKA) activity. This response is countered by the combined action of the Ddp1

and Ppx1 polyphosphatases that function together to counter polyP accumulation and downstream toxicity.

Finally, we performed a protein mutagenesis screen to explore the structure and function of the Ddp1 endopolyphosphatase. We used our ectopic PPK expression system (described above) to compare the ability of Ddp1 mutants and wild-type Ddp1 to rescue the PPK-induced toxicity. Our screen confirms many phosphate recognition residues important for Ddp1's polyphosphatase activity *in vivo*. We also developed a plasmid shuffle system in a pyrophosphatase mutant strain that presumably accumulates toxic levels of 1,5-bisdiphosphoinositol tetrakisphosphate (1,5-IP8) to expand our Ddp1 mutagenesis screen and study the regulation of its pyrophosphatase activity *in vivo*. Moreover, DIPP1, the mammalian homologue of Ddp1, can complement the loss of the yeast protein, highlighting that this system could be used to perform mutagenesis screens on other pyrophosphatases in the future.

Together this work expands on potential functions of polyP in yeast and provides insight into the importance of polyP compartmentalization in eukaryotes. Moreover, it provides insight into the multiple functions of Ddp1 and how they might be regulated *in vivo*.

TABLE OF CONTENTS

List of tables by chapter **X**

List of figures by chapter **XI**

List of abbreviations **XIII**

Acknowledgements **XVI**

Chapter 1 – Introduction **1**
Statement of rights and permissions 1

1.1. Renewed interest in an old molecule 2
1.2. PolyP synthesis and localization 3
1.2.1. Bacteria 3
1.2.2. Yeast 3
1.2.3. Mammalian cells 6
1.3. Enzymes involved in polyP degradation 6
1.3.1. Polyphosphatases in bacteria 7
1.3.2. Polyphosphatases in yeast 7
1.3.2.1. Vacuolar polyphosphatases 7
1.3.2.1.1. Ppn1 9
1.3.2.1.2. Ppn2 11
1.3.2.1.3. Pho8 12
1.3.2.2. Nonvacuolar polyphosphatases 13
1.3.2.2.1. Ddp1 13
1.3.2.2.2. Ppx1 16
1.3.3. Polyphosphatases in mammalian cells 16
1.3.3.1. DIPP1/NUDT3 17
1.3.3.2. Prune 18
1.3.3.3. Alkaline and acid phosphatases 20
1.4. Functions of polyP 22
1.5. The current landscape of polyP-protein interactions 24
1.6. Revisiting defining characteristics of polyphosphorylation 25
1.7. A unified nomenclature for polyP-protein interactions 29
1.8. Outcomes of polyP-protein interactions 29
1.8.1. Protein chaperone activity 30
1.8.2. Modulation of protein-protein interactions 32
1.8.2.1. Promoting interactions 32
1.8.2.2. Disrupting interactions 33
1.8.3. Modulation of cell signalling 34

1.8.4. Regulation of enzymatic activity 35
1.8.5. Modulation of protein-nucleic acid interactions and protein-lipid interactions 35
1.9. Open questions in the field of polyP biology 36
1.10. Description of rationales and hypotheses 37
1.10.1. Objective 1: An expanded screen for the identification of novel polyP-binding proteins. 37
1.10.1.1. Rationale 37
1.10.1.2. Hypothesis 37
1.10.2. Objective 2: Explore polyP compartmentalization in yeast and identify the molecular mechanisms that make nonvacuolar polyP accumulation toxic 38
1.10.2.1. Rationale 38
1.10.2.2. Hypothesis 38
1.10.3. Objective 3: Explore the structure and function of the Ddp1 polyphosphatase and uncover how it is regulated *in vivo* 39
1.10.3.1 Rationale 39
1.10.3.2 Hypothesis 39
1.11. References 40

Chapter 2 – Manuscript #1 **52**
Title: Proteins required for vacuolar function are targets of lysine polyphosphorylation in yeast.

2.1. Abstract 54
2.2. Introduction 55
2.3. Results and discussion 57
2.4. Methods 67
2.5. Acknowledgements 71
2.6. References 72
2.7. Supplemental figures (S1 Figure –S4 Figure) 76
2.8. Supplemental tables (S1 Table – S3 Table) 81

Chapter 3 – Manuscript #2 **88**
Title: Ddp1 cooperates with Ppx1 to counter a stress response initiated by nonvacuolar polyphosphate.

3.1. Abstract 90
3.2. Importance 91
3.3. Introduction 92
3.4. Results 94
3.4.1. Remodeling of the yeast proteome in response to ectopic PPK expression 94
3.4.2. Vacuolar polyP does not impact the cellular response to PPK expression 96
3.4.3. Expression changes for proteins involved in fundamental metabolism in PPK-expressing cells 98
3.4.4. An Msn2/Msn4-dependent signaling pathway limits viability in PPK-expressing cells 99

3.4.5. Ddp1 cooperates with Ppx1 to degrade nonvacuolar polyP 103
3.5. Discussion 109
3.5.1. Nonvacuolar polyP reprograms the yeast proteome 109
3.5.2. Ddp1 and Ppx1 limit the toxic effects of nonvacuolar polyP 110
3.5.3. PolyP as an activator of stress signaling 112
3.5.4. Endogenous functions of nonvacuolar polyP 112
3.5.5. Regulation of polyP in human cells 113
3.6. Methods 115
3.7. Acknowledgements 126
3.8. References 127
3.9. Supplemental figures (S1 Figure – S5 Figure) 132
3.10. Supplemental tables (S1 Table – S5 Table) 141

Chapter 4 – Manuscript (in preparation) #3 **151**
Title: Exploring the structure and function of the Ddp1 polyphosphate phosphohydrolase in yeast.

4.1. Abstract 153
4.2. Introduction 154
4.3. Results 157
4.3.1. Confirming Ddp1 polyphosphate recognition sites *in vivo* 157
4.3.2. The nose and the intrinsically disordered N-terminus are dispensable for polyphosphatase activity 160
4.3.3. The nose is involved in nucleic acid binding 164
4.3.4. A plasmid shuffle system for studying the structure and function of pyrophosphatases *in vivo* 165
4.4. Discussion 170
4.5. Methods 175
4.6. Acknowledgements 182
4.7. References 183
4.8. Supplemental figures 187
4.9. Supplemental tables 191

Chapter 5 – General discussion **200**

5.1. Role of polyP-protein interactions and vacuolar function 201
5.2. Characteristics of polyP-binding elements 202
5.3. Methodological considerations for studying polyP-binding proteins 203
5.4. Regulation of polyP binding by post-translation modifications (PTMs) 204
5.5. Regulation of polyP binding by polyphosphatases 204
5.6. Importance of polyP compartmentalization 205
5.7. Physiological scenarios of nonvacuolar polyP accumulation 207
5.8. Protein kinase A (PKA) regulation by polyP 208
5.9. Regulation of Ddp1 activity 209

5.10. Could Ddp1 dephosphorylate pyrophosphorylated proteins? 211
5.11. 1,5-IP8 toxicity in yeast 212
5.12. Concluding remarks 213
5.13. References 216

LIST OF TABLES BY CHAPTER

Only the tables included in this thesis are listed here. See list of tables for each chapter for links to all tables included in the published manuscript.

Chapter 1 – Introduction
No tables presented.

Chapter 2 – Manuscript #1
Title: Proteins required for vacuolar function are targets of lysine polyphosphorylation in yeast.

S1 Table PASK containing proteins screened for polyphosphorylation in this study.

S2 Table Yeast strains used in this study.

Chapter 3 – Manuscript #2
Title: Ddp1 cooperates with Ppx1 to counter a stress response initiated by nonvacuolar polyphosphate.

S1 Table Mass spectrometry data.

S2 Table Summary of MS data set confirmations.

S3 Table Yeast strains used in this work.

S4 Table Antibodies used in this work.

S5 Table Plasmids and qPCR primers used in this work.

Chapter 4 – Manuscript #3
Title: Exploring the structure and function of the Ddp1 polyphosphate phosphohydrolase in yeast.

S1 Table Summary of the Ddp1 mutant screen.

S2 Table Strains and plasmids used in this work.

Chapter 5 – Discussion
No tables presented.

LIST OF FIGURES BY CHAPTER

Chapter 1 – Introduction

Figure 1 Schematic representation of a polyP chain.

Figure 2 Schematic representation of polyP synthesis enzymes in bacteria and yeast.

Figure 3 Schematic of eukaryotic polyphosphatases including yeast and mammalian enzymes.

Figure 4 Domain structure of eukaryotic endo- and exopolyphosphatase enzymes.

Figure 5 The many ascribed functions of yeast Ddp1.

Figure 6 NuPAGE gel mobility shift analysis of polyP-binding protein.

Figure 7 PolyP-binding sequence element motifs.

Figure 8 Outcomes of polyP-protein binding.

Chapter 2 – Manuscript #1

Title: Proteins required for vacuolar function are targets of lysine polyphosphorylation in yeast.

Figure 1 Identification of new polyphosphorylated targets in yeast.

Figure 2 Polyphosphorylated targets are connected by genetic and physical interactions.

Figure 3 Analysis of Prb1 polyphosphorylation.

Figure 4 Analysis of Apl5 polyphosphorylation.

S1 Figure Collapse of polyphosphate-induced shifts on SDS-PAGE gels.

S2 Figure Analysis of Prb1 and Apl5 polyphosphorylation.

S3 Figure PASK sequences within the AP3 complex.

S4 Figure Strategy for TAG checking.

Chapter 3 – Manuscript #2

Title: Ddp1 cooperates with Ppx1 to counter a stress response initiated by nonvacuolar polyphosphate.

Figure 1 The proteome of PPK-expressing yeast.

Figure 2 The response to PPK expression is not impacted by the presence of vacuolar polyP.

Figure 3 The Msn2 and Msn4 transcription factors limit viability in PPK-expressing cells.

Figure 4 Yak1 and Hog1 kinases modulate the response to PPK expression.

Figure 5 PolyP accumulation outside the vacuole is countered by Ppx1 and Ddp1.

Figure 6 Working model for the cellular response to nonvacuolar polyP in yeast.
S1 Figure Changes to the *S. cerevisiae* proteome with ectopic PPK expression.
S2 Figure Supplementing media with excess metals does not rescue PPK-induced growth defects.
S3 Figure PolyP quantification, qPCR analysis of Msn2/Msn4 targets, and HA-PPK levels in the *HOG1* and *YAK1* mutants.
S4 Figure HA-PPK regulation in polyphosphatase mutants.
S5 Figure Overexpression of potential mammalian polyphosphatases.

Chapter 4 – Manuscript #3
Title: Exploring the structure and function of the Ddp1 polyphosphate phosphohydrolase in yeast.

Figure 1 Using the PPK system to identify critical Ddp1 polyphosphate binding sites *in vivo*.
Figure 2 The disordered N-terminus and nose of Ddp1 are not required for polyphosphatase activity, but the nose might be involved in RNA binding.
Figure 3 Ddp1's N-terminus is required for pyrophosphatase activity.
S1 Figure Mutation of DIPP1's RHPDR sequence to AHKKR does not significantly improve rescue.
S2 Figure Ddp1 does not interact with itself.
S3 Figure The *ddp1*Δ *siw14*Δ and *siw14*Δ *vip1*Δ *VIP1(H548A)* mutant strains are viable *in S. cerevisiae.*
S4 Figure The first 20 amino acids of Ddp1 are important for its pyrophosphatase activity.

Chapter 5 – Discussion
No tables presented.

LIST OF ABBREVIATIONS

1-IP7	1-diphosphoinositol pentakisphosphate
1,5-IP8	1,5-bisdiphosphoinositol tetrakisphosphate
5-IP7	5-diphosphoinositol pentakisphosphate
ADP	Adenosine diphosphate
ALP	Alkaline phosphatase
ALS	Amyotrophic lateral sclerosis
AP-3	Adaptor protein-3
APS	Ammonium persulfate
ATP	Adenosine triphosphate
BioGRID	Biological General Repository for Interaction Datasets
BME	β-mercaptoethanol
BSA	Bovine serum albumin
cAMP	Cyclic adenosine monophosphate
CHAD	Conserved histidine α-helical domain
Co	Cobalt
DAPI	4',6-diamidino-2-phenylindole
DDA	Data-dependent acquisition
DEX	Dextrose
DMSO	Dimethyl sulfoxide
DNA	Deoxyribonucleic acid
DTT	Dithiothreitol
ER	Endoplasmic reticulum
FDR	False discovery rate
GAL	Galactose
GFP	Green fluorescent protein
GPD	Glyceraldehyde-3-phosphate dehydrogenase
GTP	Guanosine triphosphate
H2O2	Hydrogen peroxide
HA	Hemagglutinin
His	Histidine
HPS	Hermansky-Pudlak Syndrome
IDR	Intrinsically disordered region
IP6	Inositol hexaphosphate
kDa	Kilodalton
LB	Luria broth
LDH	Lactate dehydrogenase
Leu	Leucine
Mg	Magnesium

mM	Millimolar
Mn	Manganese
mRNA	Messenger ribonucleic acid
MS	Mass spectrometry
MVB	Multivesicular body
NLS	Nuclear localization signal
nM	Nanomolar
NMIHBA	Neurodevelopmental disorder with microcephaly, hypotonia, and variable brain anomalies
Nudix	Nucleoside diphosphate linked to a variable moiety X
P130	Polyphosphate with a chain length of 130 phosphate units
P14	Polyphosphate with a chain length of 14 phosphate units
P60	Polyphosphate with a chain length of 60 phosphate units
PAGE	Polyacrylamide gel electrophoresis
PASK	Polyacidic serine and lysine rich
PCR	Polymerase chain reaction
PHO	Phosphate
PKA	Protein kinase A
polyHis	Histidine repeats
polyHis	Lysine repeats
polyP	Polyphosphate
PPBD	Polyphosphate binding domain
PPK	Polyphosphate kinase
PTM	Post-translational modification
PVDF	Polyvinylidene fluoride
RNA	Ribonucleic acid
RT-qPCR	Quantitative reverse transcription polymerase chain reaction
SC	Synthetic complete
SDS	Sodium dodecyl sulfate
SPX	Syg1 Pho81 Xpr1
STRE	Stress response element
TBE	Tris-Borate-EDTA
TBST	Tris-Buffered Saline with Tween 20
TBST	Trichloroacetic acid
TEMED	N,N,N′,N′-Tetramethylethylenediamine
TRAP	Tartrate-resistant acid phosphatase
Ura	Uracil
vec.	Empty vector
VTC	Vacuolar transporter chaperone
VWF	von Willebrand Factor
YEP	Yeast extract peptone

YPD	Yeast extract peptone dextrose
Zn	Zinc

ACKNOWLEDGEMENTS

I'd like to start off by thanking my supervisor Michael Downey for his unwavering support, mentorship, and guidance throughout this journey. I am forever grateful for the role you have played in helping me become the scientist that I am today. Thank you for helping me achieve so many of the goals that I had set out to accomplish.

I'd also like to thank Adam Rudner for his mentorship and guidance. Thank you for introducing me to the fascinating world of phages, I am forever grateful for the opportunities you provided and for allowing me to teach so many students over the years.

To my partner, Dr. Kanchi Baijal (who beat me to the finish line), thank you for your constant support and for always listening to my crazy theories and ideas.

To our dog, Yana, for her unconditional love and companionship.

Finally, I'd like to thank my sister Alaina, my mom Claire, and my dad Brad for their support.

CHAPTER 1 – INTRODUCTION

Statement of rights and permissions

The articles listed below are used under the following licences:

(1) **McCarthy, L.**, & Downey, M. (2023). The emerging landscape of eukaryotic polyphosphatases. *FEBS Letters*, 597(11), 1447–1461. https://doi.org/10.1002/1873-3468.14584

License Number: 6013820606011
License date: Apr 21, 2025
Licensed Content Publisher: John Wiley & Sons
Licensed Content Publication: FEBS Letters

Note: Section 1.3: Enzymes involved in polyP degradation was taken from this review article. Slight modifications were made to section *1.3.2.2.1. Ddp1* based on recently published data that was not available at the time of the original publication. This includes clarification of increased 1-IP7 in *ddp1*Δ mutants, the role of inositol pyrophosphate as a regulator of VTC activity, and Mn^{2+} as a cation for *in vitro* polyphosphatase activity. Additionally, Figures 3 and 4 were reused from this review.

(2) **McCarthy, L.**, Baijal, K., Downey, M. (2025) A framework for understanding and investigating polyphosphate-protein interactions. *Biochem Soc Trans*, 21:BST20240678. https://doi.org/10.1042/BST20240678

© 2025 McCarthy et al. This is an open access article published by Portland Press Limited on behalf of the Biochemical Society and distributed under the Creative Commons Attribution 4.0 International (CC BY) license.

Note: Sections 1.5, 1.6, 1.7, and 1.8 were taken from this review article with no modifications made. Additionally, Figures 7 and 8 were reused from this review.

1.1. Renewed interest in an old molecule

Polyphosphate (polyP) is a polymer of at least three inorganic phosphate residues linked by high energy phosphoanhydride bonds (1) (**Figure 1**). These polymers are conserved across most organisms, except for plants where they have not conclusively been detected (2). Although these chains were first discovered over a century ago, and may have arisen during the prebiotic era (3,4), polyP research has only more recently gained significant interest. This is largely because there is growing evidence that polyP is involved in various physiological disorders (5–8). Despite the recent boom in polyP research there are still many questions relating to its basic biology that remain unanswered. Work in mammalian cells is complicated by a lack of knowledge about the enzymes that produce and degrade polyP (9). Nonetheless, this has not stopped researchers from identifying a multitude of potential functions of polyP in higher eukaryotes. However, the lack of candidate enzymes responsible for polyP synthesis in mammalian cells has made the budding yeast *Saccharomyces cerevisiae* a workhorse in the polyP field (10).

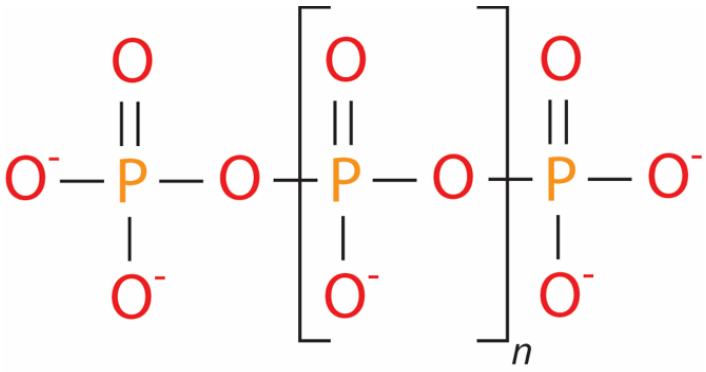


Figure 1. Schematic representation of a polyP chain. PolyP chains are polymers of at least three phosphate residues joined together by high energy phosphoanhydride bonds. These chains range from three to hundreds of phosphate units in length. The negative charge imparted by the oxygen atoms make these chains highly anionic.

1.2. PolyP synthesis and localization

1.2.1. Bacteria

In bacteria, polyP is synthesized by a highly conserved polyphosphate kinase (PPK) that uses ATP to add phosphate residues to growing chains (11–13) (**Figure 2**). PolyP levels are kept low under optimal conditions, such as growth in rich media (14). However, when cells are starved for nutrients, polyP levels rapidly accumulate to help the cells adapt to stress (14). How polyP accumulation is regulated is still unclear, but it may be post-translational. PPK is autophosphorylated before polyP synthesis occurs (12) and its dimerization is also likely critical (15). PolyP synthesis machinery is well conserved across bacteria and most bacteria have a single PPK enzyme. However, some bacteria also have a PPK2 enzyme which primarily degrades polyP to make GTP, but can also synthesize polyP from ATP (16,17). The PPK synthetase from *Escherichia coli* is thought to act as a homodimer or homotetramer and is localized to the inner membrane (15,18). Although bacteria lack membrane bound organelles, the polyP produced by PPK is often localized into granules within the cytosol (19–21). Recent work in *E. coli* has demonstrated that during nitrogen starvation polyP co-localizes with Hfq to form Hfq-PolyP (HP) bodies which segregate specific types of RNAs until nitrogen repletion (22). The formation of polyP granules may serve as a way of regulating polyP localization and function in the absence of membrane-bound organelles.

1.2.2. Yeast

In yeast, polyP synthesis is accomplished via the vacuolar transporter chaperone (VTC) complex which is predominantly localized to the vacuolar membrane (23) (**Figure 2**). The VTC complex is composed of multiple individual subunits: Vtc1, Vtc2 or Vtc3, and Vtc4 (24–26). The complex stoichiometry consists of 3 Vtc1 subunits, 1 Vtc2 or Vtc3 subunit, and 1 Vtc4 subunit (25–27).

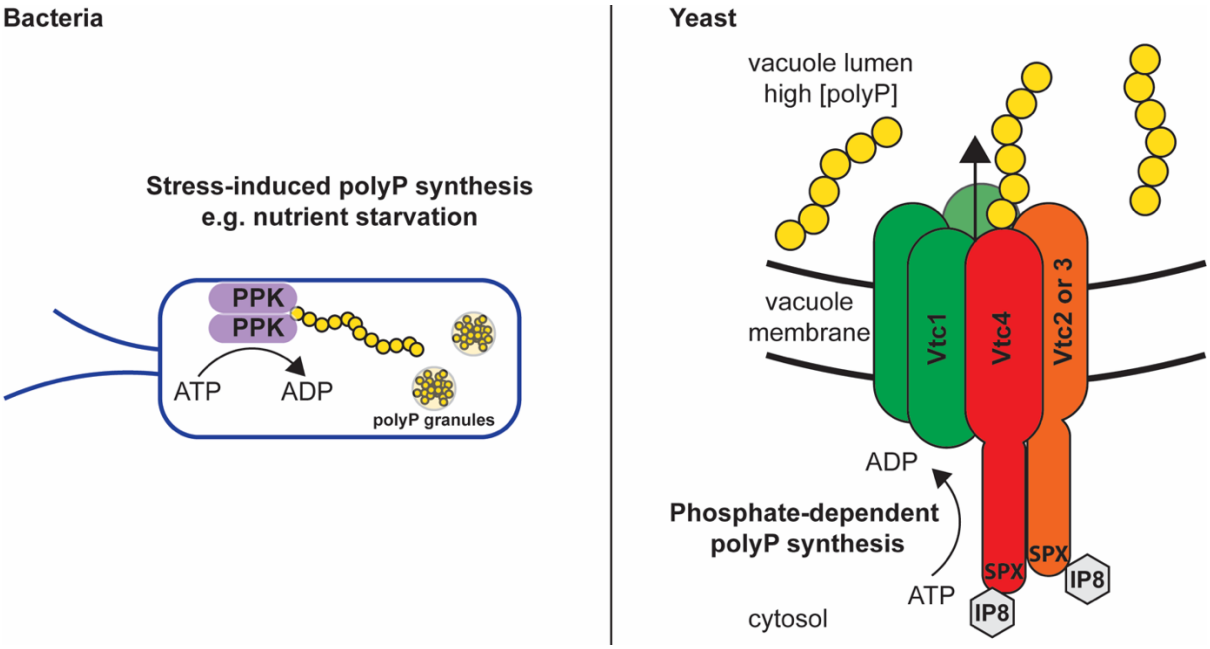


Figure 2. Schematic representation of polyP synthesis enzymes in bacteria and yeast. Bacterial polyP is synthesized by the polyP kinase PPK during stress conditions, such as nutrient starvation. PPK is thought to act as a membrane-bound dimer or homotetramer. PolyP localizes into granules in the cytosol of bacteria. Yeast polyP is synthesized by the membrane-bound VTC complex, which is composed of 3 Vtc1 subunits, 1 Vtc2 or Vtc3 subunit, and 1 Vtc4 subunit. Vtc4 and Vtc2/3 contain SPX domains which can be bound by inositol pyrophosphates, such as IP8, to stimulate polyP synthesis. In yeast, polyP synthesis simultaneously drives the transport of polyP into the vacuole where it is stored in high concentration.

Additionally, Vtc5, which is not required for polyP synthesis, can be recruited to increase the rate of synthesis of the complex (28). Vtc4 is the central catalytic subunit of the complex and uses the γ-phosphate of ATP to grow chains of polyP (23). The VTC complex is regulated by phosphate availability in the cell. Individual subunits of the VTC complex belong to the PHO regulon and their transcription is induced during phosphate starvation (29). Moreover, the catalytic activity of the complex is directly stimulated by inositol pyrophosphates, which are important phosphate signaling molecules that communicate cytosolic inorganic phosphate levels via SPX (Syg1 Pho81 Xpr1) domain binding (25–27,30–32). Recent work demonstrated that inositol pyrophosphate binding to the SPX domains of Vtc2/3 and Vtc4 disrupts SPX-SPX domain interactions between the subunits and activates Vtc4-dependent polyP synthesis (27). During synthesis, the growing polyP chains are simultaneously transported into the vacuolar lumen where they are stored at high concentrations (33). The coupled synthesis and transport of polyP is thought to be important to prevent the toxic effects of polyP accumulation outside of the vacuole (33). Indeed, ectopic expression of *E. coli* PPK, encoding the bacterial polyP synthetase, leads to cytoplasmic polyP accumulation which is toxic suggesting that vacuolar sequestration of polyP is important (33,34). This segregation of polyP stores appears to be conserved across eukaryotes, including trypanosomes and mammals, where it is also often localized within acidocalcisome-like organelles (33,35). Although polyP is compartmentalized within the vacuole it has also been detected in other subcellular compartments in lower concentrations, such as the nucleus (36,37), the cytoplasm (38), and the mitochondria (39,40). Whether these small pools of polyP are synthesized locally or transported from the vacuole is still unclear. Interestingly, VTC subunits localize around the nucleus (believed to be the endoplasmic reticulum) and the cell periphery under phosphate replete conditions (23,41), but whether this population of the VTC complex produces polyP is still unclear.

Nonetheless, understanding why polyP is stored in the vacuole and how it might localize to other compartments under specific conditions remains an important question for future research.

1.2.3. Mammalian cells

Despite the explosion of recent interest in polyP and its links to various physiological disorders in mammalian systems, the enzymes that produce and degrade polyP in higher eukaryotes are not well characterized (9). Efforts to identify proteins with homology to bacterial PPK and yeast VTC proteins have been unsuccessful and have made the identification of a mammalian polyP synthetase difficult (9,42). More recently, the mitochondrial F_OF1-ATP synthase has been shown to synthesize and hydrolyse polyP in assays using isolated mitochondria (43), but it's contribution to polyP levels *in vivo* has not been demonstrated. Because the enzymes responsible for polyP production have not been identified researchers have resorted to manipulating polyP levels via exogenous addition of polyP or via the expression of polyP producing and degrading enzymes from bacteria and yeast. Similarly to yeast, polyP is also compartmentalized into acidocalcisome-like organelles. For example, polyP is stored in the dense granules of platelet cells and is important for activating the blood clotting cascade when needed (44). In astrocytes, polyP is also localized to vesicle-like structures and is released in a calcium-dependent manner to activate nearby neurons (45). Thus, compartmentalization of polyP into specific organelles appears to be a conserved mode of regulation across eukaryotes.

1.3. Enzymes involved in polyP degradation

Enzymes that degrade polyP are termed polyphosphatases. These enzymes can be classified into two groups: endopolyphosphatases which cleave internal phosphoanhydride bonds to generate two

shorter chains, or exopolyphosphatases which cleave terminal bonds to release a single phosphate residue and produce a shorter chain (**Figure 3**). These polyphosphatase enzymes often use specific cations for their enzymatic function and play important roles in regulating polyP levels as well as chain lengths.

1.3.1. Polyphosphatases in bacteria

The only known polyphosphatase enzyme in bacteria is the PPX exopolyphosphatase. The PPX enzyme is conserved across bacteria and functions as a dimer that hydrolyzes polyP chains processively from the terminal phosphate residue (46). Cells lacking PPX have higher levels of polyP during stress conditions compared to wild-type cells (47). The N-terminus contains its catalytic site and shares homology with the acetate and sugar kinase/Hsp70/actin (ASKHA) phosphotransferase superfamily (48). The C-terminus contains the polyP binding domain, which is often used as a probe to detect polyP via microscopy in fixed cells (38). Interestingly, a linker that links the N- and C-terminal regions is important for determining polyphosphatase activity *in vitro* (49). The length of this linker appears to directly correlate with polyphosphatase activity (49). Since bacteria only possess an exopolyphosphatase, the endopolyphosphatase function of polyP degrading enzymes likely arose during evolution in eukaryotes.

1.3.2. Polyphosphatases in yeast

1.3.2.1. Vacuolar polyphosphatases

The enzymes involved in degrading polyP in yeast are better characterized than in higher eukaryotes, making it an ideal model for studying polyP biology. However, there are still many open questions in terms of the *in vivo* roles for polyphosphatases. The genetic tools available for yeast may permit rapid dissection of such functional and regulatory pathways. The majority of polyP synthesized by the VTC complex in yeast is simultaneously transported and stored in the

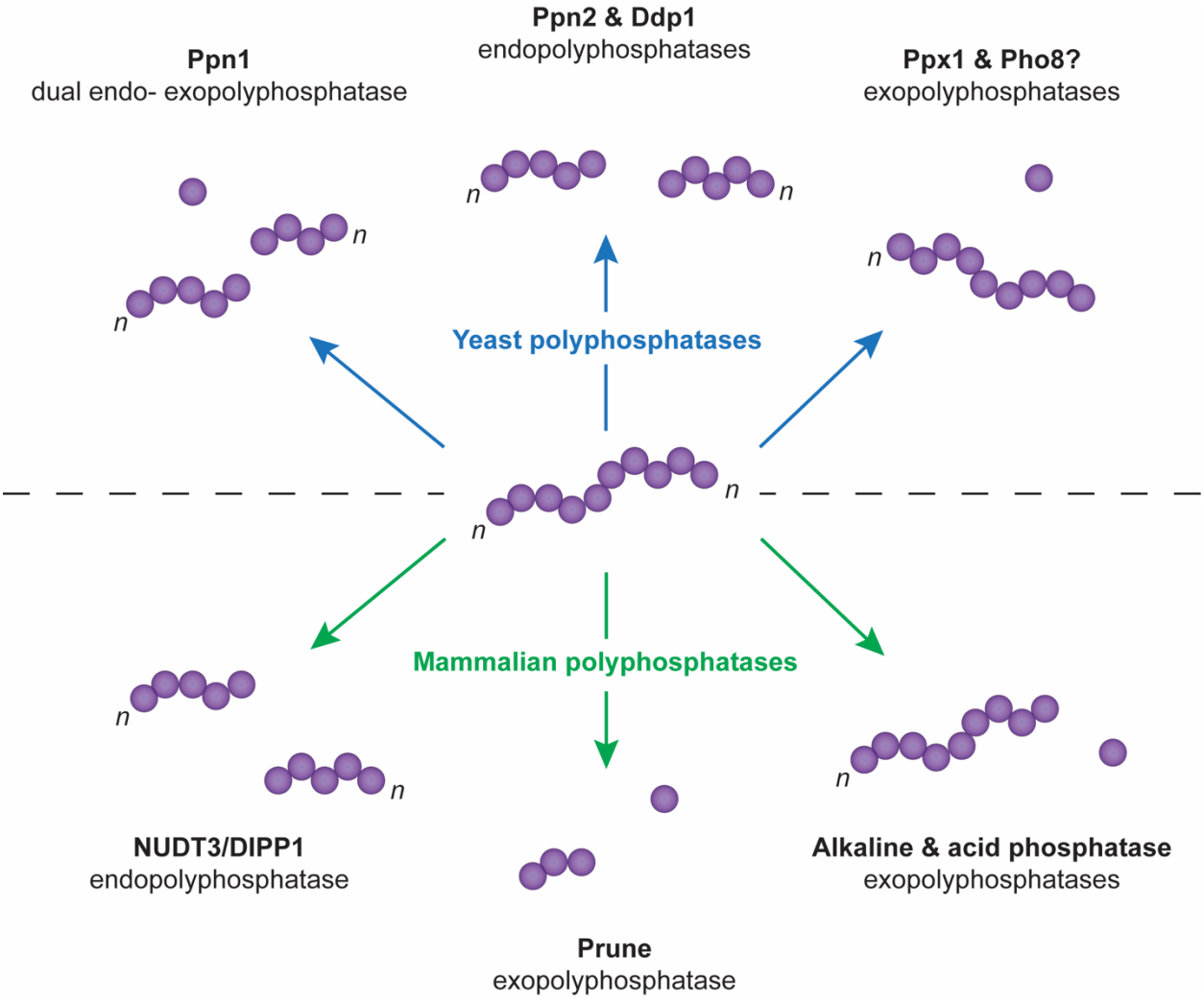


Figure 3. Schematic of eukaryotic polyphosphatases including yeast and mammalian enzymes. Characterized and proposed polyphosphatases are classified as endopolyphosphatases or exopolyphosphatases based on their activity.

vacuole (33). Here reside two polyphosphatases that directly regulate polyP levels and chain length, and a phosphatase that impacts polyP levels via an unknown mechanism.

1.3.2.1.1. Ppn1

The Ppn1 polyphosphatase is thought to act as a homotetramer composed of four 35 kDa subunits (50). Notably, it is a dual-activity polyphosphatase that can cleave internal phosphoanhydride bonds to generate two shorter chains, or cleave terminal bonds to release a single inorganic phosphate (50,51). How this dual endo- and exopolyphosphatase activity is regulated is unclear, but *in vitro* data suggest that Ppn1 catalytic activity might be modulated by specific divalent cations. Although Ppn1 displays endopolyphosphatase activity in the presence of Mn^{2+}, Mg^{2+}, Co^{2+}, or Zn^{2+}, addition of Co^{2+} was shown to specifically promote its exopolyphosphatase activity (52–54). However, it is unclear how these metal cofactors impact the polyphosphatase activity within the vacuole itself, where a multitude of metal ions are stored and likely compete to interact with polyP (55). The *in vitro* activity of Ppn1 has been tested across a wide range of pHs and optimal activity was observed around pH 7.5 (54). However, it maintained some activity at lower pHs overlapping with those suggested for the vacuole, which is mildly acidic under various growth conditions (56).

Notably, Ppn1 is first synthesized as a 78 kDa protein precursor (**Figure 4**) that is trafficked to the vacuole through the multivesicular body (MVB) pathway, a process that is dependent on Rsp5 and Tul1-mediated ubiquitination (57,58). Within the vacuole lumen, the Ppn1 precursor is N- and C-terminally cleaved by vacuolar proteases to generate the mature polypeptide (51). Activation appears to be dependent on glycosylation since the mutation of three asparagine residues predicted to be modification sites abolishes polyphosphatase activity (50), which may represent an important mechanism for regulation. Importantly, expression of only the predicted

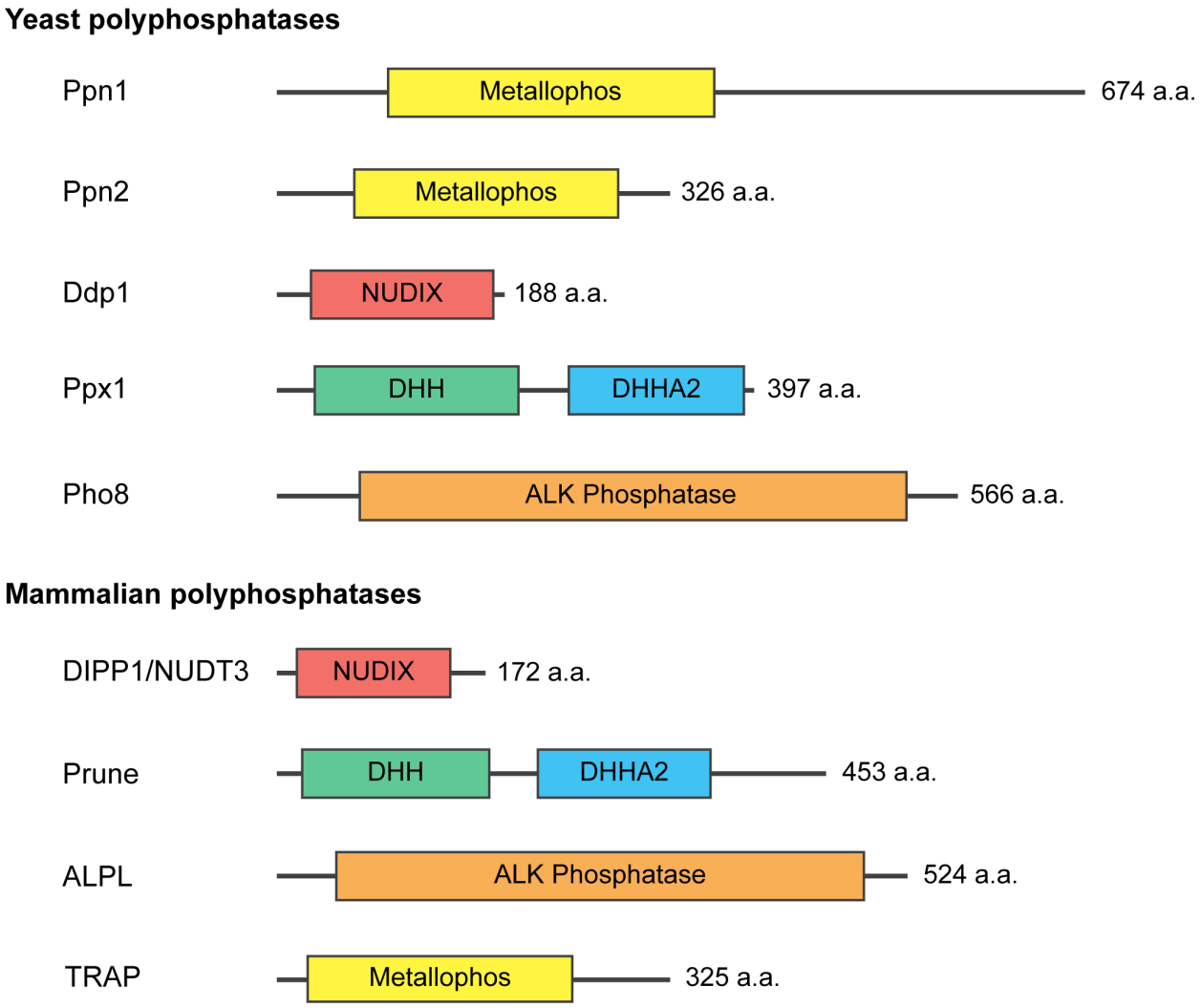


Figure 4. Domain structure of eukaryotic endo- and exopolyphosphatase enzymes. Coordinates based on Pfam (http://pfam-legacy.xfam.org/) (59).

mature form of Ppn1 does not result in an active enzyme (51). This suggests that the actual process of maturation is important for the enzyme's function, perhaps via facilitation of polypeptide folding.

Ppn1 is thought to play a role in phosphate homeostasis by processing long-chain polyP into inorganic phosphate which can then be exported from the vacuole when phosphate levels are low. Its expression is upregulated during low phosphate conditions, and *ppn1*Δ mutants accumulate longer chain polyP and lower levels of orthophosphate (29,60). Additionally, there is evidence to suggest that the role of Ppn1 in regulating chain length is particularly prominent during the stationary phase when nutrients have been expended (50,61). Therefore, it is tempting to speculate that Ppn1 trafficking to the vacuole or its processing by vacuolar proteases may be regulated by changes in nutrient availability.

1.3.2.1.2. Ppn2

The Ppn2 polyphosphatase is also localized to the vacuole where it acts as an endopolyphosphatase that can cleave polyP chains into shorter ones (61). It belongs to the phosphoprotein phosphatase family of metallophosphatases (**Figure 4**), defined by three highly conserved sequence motifs, which contain two catalytic aspartic acid residues (61). Mutating either of these aspartic acids to asparagine was shown to ablate Ppn2 polyphosphatase activity *in vitro* (61). The endopolyphosphatase activity of Ppn2 is Zn^{2+} or Co^{2+}-dependent *in vitro*, but is likely Zn^{2+}-dependent *in vivo* (61). It is unclear if Ppn2 acts a monomer or in a complex, and structural studies are still needed to address this question. Additionally, since its *in vitro* activity has been assayed only at pH 6.8 (61) and 7.2 (53), testing under acidic conditions is warranted. Ppn2 is also thought to be trafficked via the MVB pathway to the vacuole lumen (61), but there is no evidence to suggest that proteolytic processing is necessary for its activity. Cells deleted for *PPN2* accumulate longer

polyP chains during early logarithmic growth, however, this effect is much more drastic in *ppn1*Δ *ppn2*Δ cells at all phases of growth, suggesting Ppn1 and Ppn2 function redundantly (61). How the enzymatic activity of these two vacuolar polyphosphatases is balanced during specific growth periods remains an interesting avenue for future studies.

1.3.2.1.3. Pho8

The Pho8 alkaline phosphatase (ALP) of yeast is homologous to the mammalian ALPs (**Figure 4**). It is synthesized as an inactive precursor that is trafficked to the vacuole through the secretory pathway, where it is activated by Pep4 or Prb1 via a C-terminal cleavage event (62–64). Within the vacuole, the active enzyme can exist as a membrane-bound or a soluble form that also lacks 62 amino acids on the N-terminus (62,64,65). Pho8 is a Zn^{2+} and Mg^{2+}-dependent protein phosphatase that dephosphorylates p-nitrophenyl phosphate and phosphopeptides *in vitro*, suggesting that it dephosphorylates proteins in the vacuole to recycle phosphate (64,66,67). Additionally, it was shown that purified Pho8 has activity towards fructose 2,6-biphosphate, and extracts from *pho8*Δ mutants did not possess fructose-2,6-bisphosphate 6-phosphatase activity (68). It is also involved in nicotinamide adenine dinucleotide metabolism by potentially converting nicotinamide mononucleotide into nicotinamide riboside in the vacuole (69).

More recently, it was shown that *pho8*Δ mutants accumulate higher levels of polyP than wild-type cells, although the chain lengths of extracted polyP were not affected (70). This could suggest that Pho8 does not directly act as a polyphosphatase, but may instead regulate the accumulation of polyP through other pathways. However, direct polyphosphatase activity of Pho8 has not been ruled out and there is evidence to suggest that the ALP isolated from the yeast *Candida utilis* is active in this regard (71). Interestingly, Gerasimaitė et al. showed that Pho8 co-immunoprecipitated with Ppn2 at equal levels, suggesting they might form a complex (61).

However, Ppn2 immunoprecipitated from *pho8*Δ mutants still possessed polyphosphatase activity *in vitro*, indicating that Pho8 is not required for Ppn2 activity (61). Nevertheless, this does not rule out the possibility that Pho8 might regulate Ppn2 activity *in vivo* via other means. An interesting possibility is that Pho8 might act as an exopolyphosphatase and that the Ppn2-Pho8 complex works by processively cleaving long-chains into shorter chains via Ppn2, followed by Pho8-dependent conversion of those short chains into inorganic phosphate.

1.3.2.2. Nonvacuolar polyphosphatases

The prevailing idea that polyP levels are kept high in the vacuole and kept low in other compartments would suggest a tight regulation of polyP levels outside the vacuole. There are two enzymes that are thought to degrade polyP beyond the vacuole: the endopolyphosphatase Ddp1 and the exopolyphosphatase Ppx1, but their functional roles *in vivo* remain unclear.

1.3.2.2.1. Ddp1

The diadenosine and diphosphoinositol polyphosphate phosphohydrolase (Ddp1) appears to be largely localized in the cytoplasm, but is also detected in the nucleus (37,72,73). It is a relatively small 21.5 kDa protein from the Nudix hydrolase family (**Figure 4**) that has been ascribed a number of enzymatic activities (**Figure 5**). First, it is an inositol pyrophosphatase that dephosphorylates 1-IP7 with the greatest affinity, and *ddp1*Δ mutants accumulate high levels of 1-IP7 (30,74–78). However, Ddp1 can also hydrolyse 5-IP7 and 1,5-IP8 with lower affinity *in vitro* (77,79), and *ddp1*Δ mutants have also been shown to accumulate higher levels of 1,5-IP8 (30). Inositol pyrophosphates are high-energy molecules composed of an inositol ring modified by mono- or diphosphates and are involved in eukaryotic cell signalling (80). Interestingly, inositol pyrophosphates have been shown to regulate VTC activity and polyP synthesis by binding to SPX domains (31,32). 5-IP7 was shown to have the greatest stimulatory effect on the VTC complex *in*

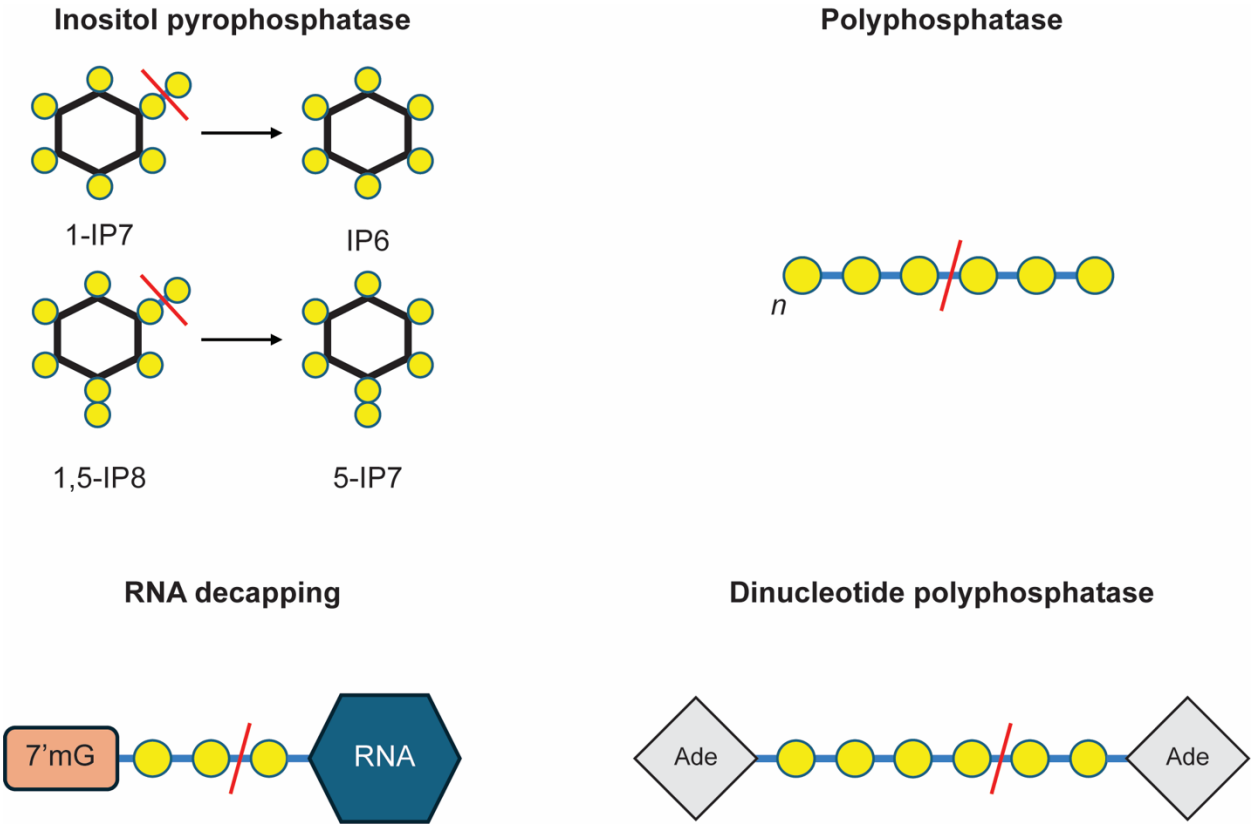


Figure 5: The many ascribed functions of yeast Ddp1. Ddp1 can cleave 1-IP7 into IP6, and 1,5-IP8 into 5-IP7 *in vivo*. As an endopolyphosphatase, Ddp1 can cleave polyP chains internally to generate two shorter chains *in vivo*. Ddp1 has also been shown to cleave the 5'-7-methlyguanosine (7'mG) cap of RNA *in vitro*. Finally, Ddp1 was first characterized as a nucleotide polyphosphatase able to cleave diadenosine hexaphosphate *in vitro*.

vivo, whereas high levels of 1-IP7 did not stimulate VTC-dependent polyP synthesis (32). More recent work has demonstrated that inositol pyrophosphate binding to the Vtc2 and Vtc3 subunits disrupts SPX-SPX interactions with Vtc4 to promote polyP synthesis (27). Here, 1,5-IP8 was shown to have the strongest stimulatory effect on VTC activity, followed by 5-IP7 and IP6 (27). This link between inositol pyrophosphate and polyP metabolism suggests that Ddp1 might indirectly affect polyP levels via its inositol pyrophosphate activity in a manner that is still unclear. Second, Ddp1 might directly impact polyP levels as a polyphosphatase considering it has also been shown to degrade polyP *in vitro* at pH 6.8–8, and deletion of *DDP1* impacts polyP levels in the cell (34,76). Specifically, cells deleted for *DDP1* accumulate 20% less polyP than wild-type cells (76), but overexpression of Ddp1 in cells ectopically expressing *E. coli* PPK reduces PPK-synthesized nonvacuolar polyP to background levels (34). This polyphosphatase activity is largely dependent on Mg^{2+}, Co^{2+}, or Mn^{2+} cofactors *in vitro* (76,81). Notably, Ddp1 has been shown to have a higher affinity for polyP than inositol pyrophosphates (76). Finally, it has been shown to degrade diadenosine polyphosphate (74,82), and can cleave 7-methylguanosine caps from the 5′ end of mRNA *in vitro* (83), although these functions have not been investigated *in vivo*. The latter functions appear dependent on Mn^{2+} *in vitro*, but higher concentrations of Mg^{2+} can promote diadenosine polyphosphate hydrolysis (82,83). Mutation of two glutamic acids within the Nudix box (**Figure 4**) has been shown to abrogate polyphosphatase and decapping activity *in vitro* (76,83). More recently, the molecular structure of Ddp1 bound to pyrophosphates, diadenosine polyphosphates, and polyP has been determined (84). This work revealed the phosphate binding moieties important for substrate binding and reaffirmed Ddp1 preference for polyP (84). Considering its many ascribed functions *in vitro*, it will be important to fully explore the functions

of Ddp1 *in vivo* and to study its regulatory regions to uncover how the cell might coordinate these various activities.

1.3.2.2.2. Ppx1

The Ppx1 exopolyphosphatase is a 40–45 kDa monomeric enzyme that degrades polyP by cleaving terminal phosphoanhydride bonds to remove a single phosphate and thereby generate a shorter chain (85–88). It is the only known yeast polyphosphatase that possesses only exopolyphosphatase activity. Despite its name, it does not share homology with the *E. coli* polyphosphatase PPX (87). Instead, it belongs to the DHH phosphoesterase superfamily (**Figure 4**) and is structurally similar to the family II pyrophosphatases (87,88). However, unlike Ddp1, Ppx1 cannot act on inositol pyrophosphates (76). The catalytic activity of Ppx1 is dependent on Mg^{2+}, Mn^{2+}, or Co^{2+} and is optimal between pH 6.8 and 8.8 *in vitro* (86,88). It is mainly thought to localize to the cytoplasm (72), although it is notable that *ppx1*Δ mutants have decreased exopolyphosphatase activity in mitochondrial fractions, indicating that Ppx1 might localize in part to the mitochondria (89). The functional role of Ppx1 remains unclear and there are no tractable phenotypes described for *ppx1*Δ mutants. The expression of Ppx1 is not affected by levels of phosphate in the cell suggesting that it is not regulated by the PHO regulon (29), while its post-translational regulation has yet to be explored. Furthermore, *ppx1*Δ mutants do not show obvious changes in polyP chain length (76), although this could be because it is not localized to the vacuole lumen where most of the polyP is stored. Despite a lack of clear phenotypes in *ppx1*Δ cells, Ppx1 might be important for regulating the polyphosphorylation of proteins by removing the modification from target lysines. Indeed, this activity has been described *in vitro* for both Ppx1 and Ddp1 (36).

1.3.3. Polyphosphatases in mammalian cells

While mechanisms of polyP synthesis in human cells remain poorly characterized, there has been

some progress in identifying candidate polyphosphatase enzymes. Still, the context under which these enzymes are relevant and how their activities may be regulated *in vivo* is unclear. In this section, we focus on the intracellular DIPP1 and Prune proteins, as well as alkaline and acid phosphatases, which are proposed to degrade extracellular pools of polyP.

1.3.3.1. DIPP1/NUDT3

Work from Lonetti et al. (76) demonstrated that Ddp1 homologs DIPP1 (**Figure 4**), DIPP2 and DIPP3, have endopolyphosphatase activity *in vitro* at pH 8–9. While this activity was first measured at a much lower level than that of Ddp1 (76), subsequent work showed that inclusion of Zn^{2+} or Mn^{2+} as the divalent cation greatly improves DIPP1 ability to cleave polyP chains (90). Moreover, the enzyme is active in reaction conditions spanning physiological pH (90). Using the Xpress-PPBD probe to detect nuclear polyP, Samper-Martín et al. (90) demonstrated a Zn^{2+}-dependent reduction of polyP with DIPP1 overexpression, and a corresponding increase in polyP following its knockdown. Since the available level of Zn^{2+} in the cell is usually quite low (90), one might question when this activity would be relevant. The authors present evidence suggesting that treatment of cells with H_2O_2 causes an increase in available zinc, coincident with a DIPP1-dependent decrease in nuclear polyP (90). Functionally, DIPP1 is required for limiting accumulation of gamma-H2AX foci, a marker of DNA damage, and preservation of viability after H_2O_2 treatment (90). The mechanism by which polyP is acting in this scenario is currently unknown, but this remains an exciting area for future work.

Interestingly, in contrast to yeast Ddp1, ectopic expression of human DIPP1 in yeast failed to decrease polyP levels or rescue toxicity associated with accumulation of nonvacuolar polyP made by the *E. coli* PPK enzyme (34). This remained true even when cells were supplemented with high levels of zinc (34). This could simply reflect a failure of ectopically expressed DIPP1 to

localize to compartments that house PPK-synthesized polyP, or an inability of DIPP1 to target the very long polyP chains that PPK makes. More interesting is the possibility that this seemingly contradictory result reflects the requirement for cofactors unique to mammalian cells, at least for *in vivo* activity.

Finally, DIPP1 also functions in inositol pyrophosphate metabolism (77) and mRNA decapping (91,92). How these various functions might be coordinated is unknown, although it is noteworthy that Zn^{2+} does not stimulate the inositol pyrophosphatase activity of DIPP1, which instead requires Mg^{2+} (90). As DIPP1 localizes to both the nucleus and cytoplasm (90), it is possible that various activities are dictated in part by cation concentrations in these compartments.

1.3.3.2. Prune

The name Prune comes from the protein homology to a *Drosophila* protein of the same name whose mutation results in a loss of red pigmentation in the eyes (93,94). Human Prune is a 453 amino acid protein that is mostly cytoplasmic (95,96), and can be conceptually segmented into two halves. The larger N-terminal region (roughly 370 amino acids) contains two globular domains (97). The C-terminal region contains a segment that is thought be intrinsically disordered, with subsections that have a propensity to form alpha helices, followed by a small compact domain at the very end of the protein (97). The N-terminal region encodes a catalytic domain with homology to Ppx1 (**Figure 4**) (98), originally characterized as having phosphodiesterase activity against cAMP (99). Subsequent work described an exopolyphosphatase activity for Prune at pH 7.2 that is three orders of magnitude greater than its phosphodiesterase activity, calling into question the relevant *in vivo* activity (98). In contrast to Ppx1, Prune prefers very short chains of 3–4 phosphate moieties in length, with limited to no activity against polyP chains of 25 moieties or longer (98,100). Like other exopolyphosphatases, Prune requires metal cofactors, such as Mg^{2+} or Co^{2+}.

In contrast, its activity is inhibited by Zn^{2+} (98).

To our knowledge, there are no studies that link Prune expression to changes in polyP levels *in vivo*. It is unclear if the type of very short chains preferred by Prune (e.g. triphosphates) even exist to any appreciable extent in human cells (101). Of course, it could indeed be the action of Prune which keeps triphosphate levels low. Prune could also work in concert with endopolyphosphatase enzymes to increase the conversion of longer chains to orthophosphate. As a starting point, it would be interesting to test the impact of Prune overexpression or knockdown using the probes employed by Samper-Martín et al. for the study of DIPP1 (90). Notably, like DIPP1, ectopic expression of Prune fails to reduce polyP levels in PPK-expressing yeast cells accumulating long-chain polyP outside of the vacuole (34). However, this may be in part due to the preference of Prune for very short polyP chains (98). As suggested for DIPP1, the contribution of Prune to polyP metabolism *in vivo* may only become apparent under specific conditions or in the presence of cofactors unique to higher eukaryotes.

One reason why interest in Prune remains high is that its elevated expression is a proposed biomarker for the progression of diverse cancers. Here, we point the reader to an excellent review by Bibbo et al. (102). This role is thought to stem from Prune interaction, via its C-terminal region, with a number of proteins such as GSK-3β and an inhibitor of metastasis called Nm23-H1 (97,103,104). In cancer cells, the binding of Prune to GSK-3β inhibits its function and promotes Wnt signalling, in part by promoting GSK-3β sequestration into multivesicular bodies (95). On the other hand, Prune is thought to cooperate with GSK-3β in the regulation of focal adhesions to promote cell migration (103). Prune also inhibits the function of Nm23-H1, and this is associated with increased cell motility in breast cancer cell models (96,99). Importantly, Nm23-H1 acts as an inhibitor of Prune polyphosphatase activity (98), but increases its cAMP phosphodiesterase

activity (99). It is possible that the binding of Prune C-terminal region to different partners functions in part to toggle its various enzymatic activities. In turn, the interactions could be regulated by various signalling cascades responding to internal or external stimuli. To this end, it is noteworthy that the Prune-Nm23-H1 interaction requires phosphorylation of Nm23-H1 by casein kinase II (96). However, there has been no substantial follow-up of the role of Prune's polyphosphatase activity in cancer cell metastasis.

Finally, mutations in Prune are also thought to give rise to neurodevelopmental disorder with microcephaly, hypotonia, and variable brain anomalies (NMIHBA) (100,102,105). Prune mutations contributing to the disease can both increase (105) and decrease (100) polyphosphatase activity, suggesting a complicated relationship between polyP levels and the phenotypes associated with the disease. Whether NMIHBA represents a true 'polyPathy' warrants continued investigation.

From a clinical perspective, the field will benefit from proteomic studies that define the full complement of proteins that interact with Prune in wild-type and disease cells of different origin. The BioGRID (106) database shows Prune interacting physically with 21 distinct proteins. Some of these contain enzymatic activities and could function as modulators of Prune activity *in vivo* via post-translational modifications. Future studies should begin by testing if these interactors are interdependent or mutually exclusive, and whether they impact Prune exopolyphosphatase activity or substrate preference.

1.3.3.3. Alkaline and acid phosphatases

Alkaline phosphatase is a membrane protein found in different cell types throughout the body. It shows robust exopolyphosphatase activity *in vitro*, including in some assays conducted at physiological pH (107–109). It is thought that polyP accumulating on the outside of certain types

of cells, such as osteoblasts, can be processed by ALP to generate free phosphate that drives mineralization. Mechanistically, liberated phosphate may play a direct role in mineralization or serve as an energy source to drive reactions required for the process via ATP (re)generation (110–112). At some cell surfaces, polyP may function to inhibit ALP action against other substrates such as pyrophosphate, which negatively regulates the mineralization process (109,113,114). Thus, the impact of polyP in mineralization appears very context-specific, with length of polyP chains, ion concentrations, and ALP expression levels potentially dictating outcomes (108,109,114–116). Different isoforms of ALP (e.g. placental, tissue-nonspecific (**Figure 4**), and intestinal ALP) seem to have different enzymatic properties and ion dependencies (107–109), which could add complexity to the regulation of polyP hydrolysis across different tissues.

Importantly, ALP action on polyP at the cell surface could have important consequences beyond mineralization. For example, polyP is thought to bind at the cell surface by interacting directly with receptors imbedded in the plasma membrane (e.g. $P2Y_1$) or receptor ligands (e.g. HMGB1, ligand of the RAGE receptor), to impact downstream signalling events in endothelial cells (117,118). These receptors are likely to differ between cell types. For example, the impact of polyP on macrophages is independent of $P2Y_1$ and RAGE (119). Regardless, we theorize that ALP could play a role in degrading polyP bound at cell surfaces to turn off signalling cascades. ALP could also play a role in degrading polyP released by bacterial pathogens during infection (119). Finally, it is likely responsible for the short half-life of polyP in blood (5).

Tartrate-resistant acid phosphatase (TRAP) is a metalloenzyme (**Figure 4**) that carries two iron atoms at its active site (120). It can cleave short polyP chains of 40 moieties in length to release free phosphate, suggestive of exopolyphosphatase activity (121). Long-chain polyP (e.g. P300) can also inhibit phosphatase activity of TRAP towards other substrates, even though it is

not actively degraded. It is theorized that this may be important for regulation of bone resorption by osteoclasts (121). Like ALP, the polyphosphatase activity of TRAP is proposed to occur at the cell surface (121). As such, a caveat of this work is that *in vitro* polyphosphatase assays were carried out at pH 5.5 (121). It is unclear if this enzyme is also active at physiological pH. Alternatively, transient microenvironments at cell surfaces *in vivo* may permit its action outside the pH range normally measured for whole cells and tissues (120). While to our knowledge there are no additional studies regarding its role in polyP turnover, TRAP is certainly worthy of further investigation. Understanding how polyP is targeted outside of the cell will be critical for efforts aimed at delivering polyP for therapeutic purposes.

1.4. Functions of polyP

PolyP has been shown to play a role in various cellular functions in all kingdoms of life. Its function has been well studied in bacteria, which normally have low levels of polyP, but rapidly accumulate polyP in response to various stressors such as salt stress (14), nutrient starvation (14), and oxidative stress (122). During oxidative stress polyP can act as a protein chaperone by binding to partially unfolded proteins to promote their proper refolding and prevent protein aggregation (122). Cells lacking PPK have impaired virulence, biofilm formation, and are more susceptible to antibiotics suggesting that polyP is important for bacterial pathogenesis (123). In fact, bacterial polyP is involved in host-pathogen interactions and can directly interfere with the innate immune response (119). Thus PPK has been suggested as a potential target in the fight against antibiotic resistant bacterial infections (124,125).

In yeast, polyP can exceed 200 mM in terms of free phosphate (60) and is primarily stored within the vacuole where it is involved in phosphate (126,127), pH (128), and ion homeostasis

(129,130). PolyP accumulation in yeast is dependent on phosphate availability and is directly regulated by inositol pyrophosphate (27,32,127). PolyP stores are degraded by polyphosphatases during phosphate limitation and are likely exported as inorganic phosphate by Pho91 to buffer cytosolic phosphate levels (61,131–133). Recent metabolomic work demonstrated that cells lacking polyP show phosphate starvation features even when grown in the presence of phosphate (127). The VTC complex has also been shown to be involved in regulating microautophagy but direct evidence for a role by polyP is unclear (41). Moreover, polyP accumulation in the vacuole is important for driving vacuolar fusion (24,134). However, the potential functions of polyP beyond the vacuole remain unclear. Of note, polyP may be degraded by polyphosphatases in a cell cycle-dependent manner to provide phosphate for dNTP synthesis during DNA replication (135).

In mammalian cells, which have relatively low micromolar concentrations of polyP (136), it has been shown that polyP is stored in platelet dense granules in high concentrations (local millimolar concentrations) and released upon their activation (44). Here, polyP plays a regulatory role in blood clotting by interacting with various clotting factors of the blood coagulation cascade (137). The inability to produce and store polyP in dense granules can lead to bleeding disorders. Patients affected by Hermansky-Pudlak syndrome (HPS) are unable to generate various lysosome-related organelles, including dense granules (138–140). As a result, they are unable to store polyP in their platelets and are affected by bleeding disorders (138,139). Exogenous polyP addition to platelets derived from HPS patients is able to restore blood coagulation (141). PolyP has also been shown to be involved in calcium signaling of neuronal cells. PolyP is released from astrocytes in a calcium-dependent manner and ultimately activates nearby neurons (45). A recent study demonstrated that astrocytes from patients with ALS release excessive amounts of polyP which drives pathogenesis (7). Links between polyP dysregulation and diseases has sparked new interest

in the field of polyP in recent years. However, better characterization of the enzymes that produce and degrade polyP will be critical to study these links and begin to treat polyP driven disorders.

1.5. The current landscape of polyP-protein interactions

PolyP impacts a wide variety of biological processes, from stress resistance in bacteria to blood clotting in mammals (142). How does such a simple molecule impart its diverse functions at a molecular level? We don't expect there to be a single answer to this question. However, there are likely to be common mechanisms at play that can guide our understanding of polyP biology across evolution. One interesting possibility was proposed by Azevedo et al. (36), who in 2015 provided evidence that polyP chains could be covalently linked to lysine residues within two yeast proteins, Nsr1 and Top1, in a non-enzymatic reaction. Mutations that abrogate so called 'polyphosphorylation' also altered protein subcellular localization and resulted in changes to Top1's topoisomerase activity *in vitro* (36). For both proteins, polyphosphorylation occurred in polyacidic serine and lysine rich (abbreviated as PASK) motifs (36).

The idea that polyP can bind to proteins to impact their function is not new. In bacteria, early work by Arthur Kornberg's lab showed that polyP can bind to the Lon protease and stimulate its role in degrading ribosomal proteins during starvation (143). In mammals, polyP impacts blood coagulation by binding to various clotting factors (137). Finally, the conserved histidine α-helical (CHAD) domain, conserved in prokaryotes and eukaryotes, has been characterized as a polyP-binding domain (144).

Yet, the thought that polyP could alternatively function as a new lysine-based post-translational modification (PTM) is particularly interesting, especially in light of the idea that it could directly compete with other modifications that occur on lysines, such as methylation,

acetylation, or ubiquitylation (145). The evidence for covalent attachment of polyP to proteins rested in large part on the intriguing observation that Top1 and Nsr1 isolated from wild-type cells display a dramatic decrease in electrophoretic mobility, relative to proteins isolated from polyP-deficient *vtc4*Δ mutants, when analyzed on Bis-Tris polyacrylamide gels (NuPAGE) (36) (**Figure 6**). The 'polyP shift' persisted when extracts were generated under harsh denaturing conditions (e.g. urea or SDS) (36), usually assumed to disrupt non-covalent interactions.

The following years saw an explosion in the identification of proteins that shifted via NuPAGE analysis in the presence of polyP. Our lab initially published 15 PASK-containing targets, with enrichment of proteins localized to the nucleolus and involved in various aspects of ribosome biogenesis and translation control (146). We also provided the first evidence for polyphosphorylation of human proteins, with the identification of six targets (146). Work with human proteins was extended by Azevedo et al. (147), who used a protein microarray to screen for polyP-binding proteins. They confirmed six targets that fit previously established criteria for polyphosphorylation, namely a polyP-dependent shift on NuPAGE gels (147). In addition, they identified five proteins that did not undergo polyP shifts on NuPAGE gels, but still seemed to interact with polyP as judged by mobility shift on native PAGE or by chromatography, suggesting non-covalent binding (147). The fact that some polyP-binding proteins behave differently on NuPAGE gels is consistent with alternative modes of polyP interaction.

1.6. Revisiting defining characteristics of polyphosphorylation

The collective work between 2015 and 2020 raised the exciting possibility that polyP is a global effector of protein function. Indeed, PASK motifs appear often across eukaryotic species (146).

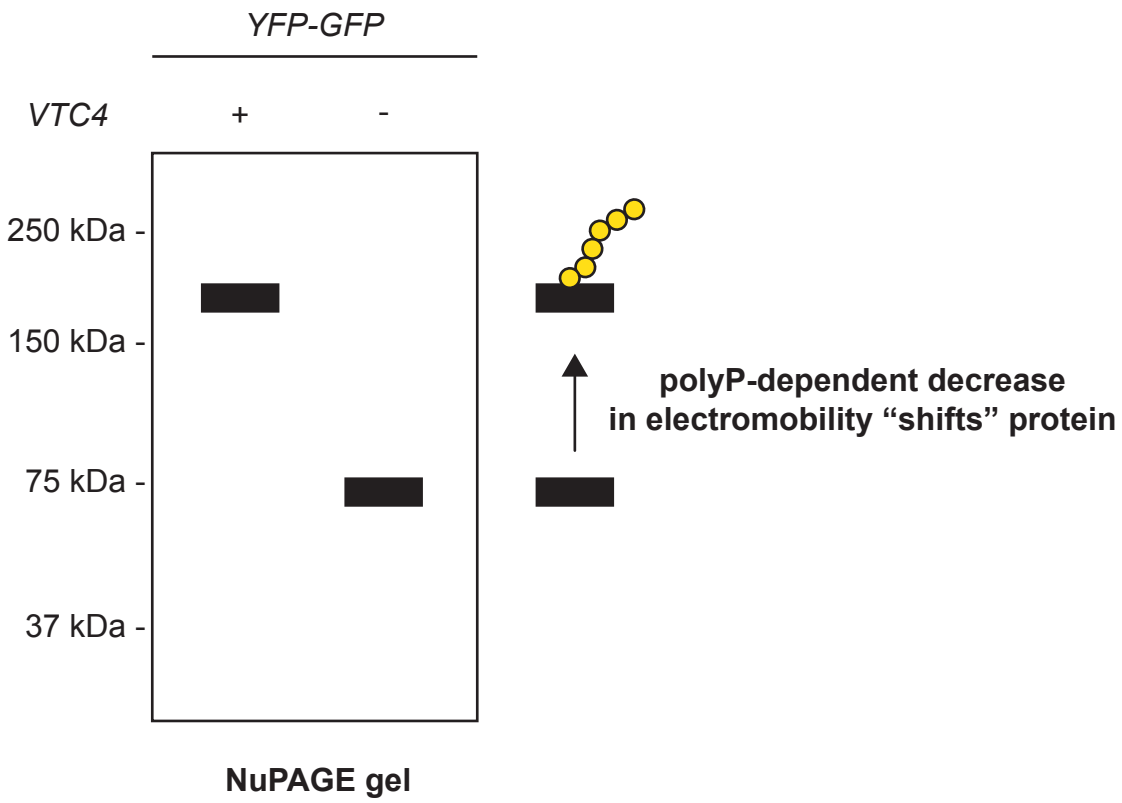


Figure 6. NuPAGE gel mobility shift analysis of polyP-binding protein. Your favourite protein (YFP) can be epitope tagged (e.g. GFP) and screened for polyP binding using a gel shift assay. When polyP-binding proteins are extracted from wild-type cells producing polyP, they run at a higher apparent molecular weight than expected on NuPAGE gels. If the *VTC4* gene is deleted, polyP synthesis is abolished, and the protein runs at its expected molecular weight.

Recent efforts, including contributions from our group, demonstrated that histidine and lysine repeats (polyHis and polyLys) can also interact with polyP molecules (148,149) (**Figure 7**). In contrast with what was originally proposed for lysine polyphosphorylation, the salt and pH sensitivity of polyP interaction with polyHis repeat proteins suggested non-covalent binding — despite the fact that the interaction slowed migration on NuPAGE gels (148). Beyond expanding the scope of proteins that can interact with polyP, the polyHis study called into question the use of NuPAGE gels to discern covalent versus non-covalent interactions, and prompted a re-analysis of the biochemical characteristics of lysine polyphosphorylation. Neville et al. (149) showed that the NuPAGE shift for lysine polyphosphorylation targets was lost when reactions carried out on beads were subsequently washed with high salt or high pH buffers. Importantly, these salt and pH sensitivities were confirmed in separate experiments using size exclusion chromatography (149). Together, these results challenged the assertion that polyphosphorylation is covalent, since we expect covalent modifications to be resistant to these conditions.

We note that the findings of Neville et al. are seemingly at odds with a more recent experiment conducted by Azevedo et al. (150) where protein extracts adjusted to 500 mM salt concentration are permissive for polyP-induced shifts for yeast Nsr1 and human nucleolin proteins, previously described as polyphosphorylated targets. A key difference between these works is that in Neville et al. (149) excess polyP was washed away from the target protein prior to analysis. The ability of targets to shift on NuPAGE gels may depend on the absolute quantity of polyP in the sample. Regardless, we conclude that shifts on NuPAGE (or other types of gels for that matter), while indicative of interaction with polyP, are a poor proxy for distinguishing covalent versus non-covalent interactions.

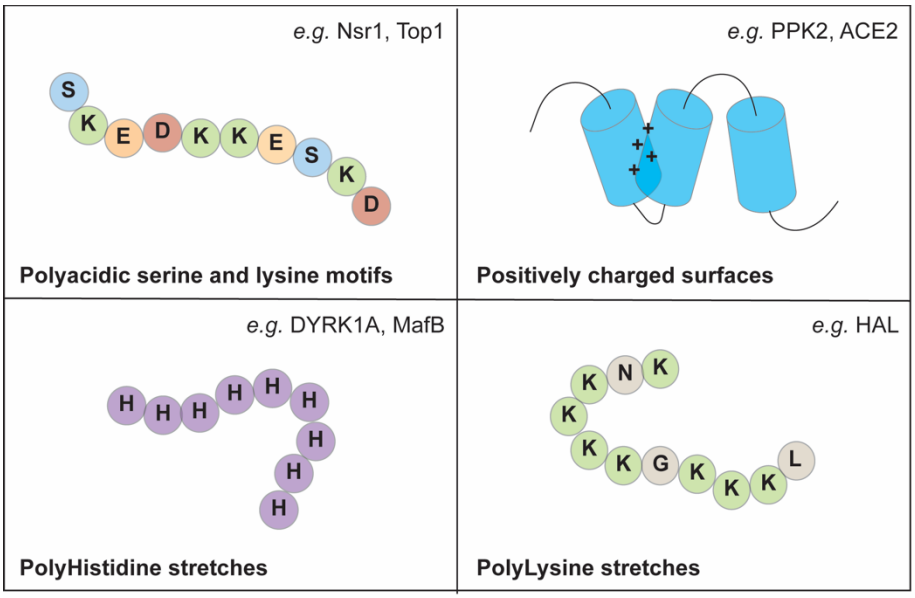


Figure 7. PolyP-binding sequence element motifs. PolyP has been shown to bind proteins containing polyacidic serine and lysine-rich (PASK) motifs, positively charged surfaces, histidine repeats (polyHis), and lysine repeats (polyLys). Examples (e.g.) of proteins with known modes of polyP binding that were discussed in the review are provided.

1.7. A unified nomenclature for polyP-protein interactions

With these new findings, we now consider the evidence for covalent attachment of polyP to proteins to be lacking. Of course, we cannot say for certain that covalent attachment of polyP to lysine or other amino acids never happens. For example, it is possible that polyP interaction with some targets is covalent *in vivo*. While there is currently no evidence to support this idea, models are made to be broken. Despite a reinterpretation of the mode of polyP interaction, the original work from Azevedo et al. (36) remains an outstanding contribution.

At this time, the term polyphosphorylation – with -ylation almost exclusively denoting a PTM – seems somewhat confusing. Other terms for non-covalent polyP interaction with proteins have been suggested. For example, our colleagues have proposed the term 'histidine and lysine polyP modification' (151). However, the introduction of new language seems largely unnecessary when the terms 'polyP binding' and 'polyP-binding proteins' suffice.

1.8. Outcomes of polyP-protein interactions

It appears that polyP-binding proteins are not exactly rare. To date, at least 100 targets have been validated across prokaryotic and eukaryotic species (**See Supplementary Table S1 in published online article**), with additional candidates identified via large scale analyses. PolyP-binding proteins include PASK, polyHis, and polyLys containing proteins, as well as those that interact with polyP via a collection of positive charges concentrated on (or across) a target's surface (**Figure 7**). Below, we highlight key molecular outcomes of polyP-protein interactions and provide examples for each case. For now, we consider these outcomes independent of the proposed mode of binding (i.e. covalent versus varied types of non-covalent interactions), but it is not impossible that distinct interactions could preferentially lead to certain fates. Importantly, outcomes are not

necessarily mutually exclusive, and polyP's impact on a given target could certainly be context specific. A summary is presented in **Figure 8**.

1.8.1. Protein chaperone activity

PolyP performs a chaperone-like role in stabilizing intermediate structures of 'client' proteins including citrate synthase (122), luciferase (122), and lactate dehydrogenase (LDH) (152) when these proteins are partially unfolded. Size exclusion chromatography experiments conducted with LDH suggest that polyP behaves analogous to a protein chaperone, that binds the partially unfolded protein, to promote the formation of intermediate stabilizing structures composed of soluble beta-sheets (152). Additionally, in the case of LDH, intermediate structures formed in the presence of polyP could be refolded by actual protein chaperones upon removal of the thermal stressor that was initially used to unfold it (152,153). How the activities of polyP and protein chaperones are co-ordinated during refolding is deserving of further investigation. This type of protein stabilization may have physiological relevance during conditions of heat or oxidative stress (122,152). As noted previously, the mammalian NUDT3 polyphosphatase is proposed to regulate polyP levels during oxidative stress (90), and we wonder if changes in the folding of nuclear proteins could explain increases in H2AX phosphorylation, a marker of DNA damage, in NUDT3 depleted cells (90). On the other hand, polyP has been shown to bind amyloidogenic proteins that have a propensity to aggregate, oligomerize, and nucleate (154). For these proteins, polyP binding results in a different fate. It accelerates the aggregation and nucleation of these proteins, causing them to form compact, insoluble structures (154). An example is the fibrillation of the *E. coli* CsgA protein (155). Here, polyP plays a role in stabilization of the protein to promote biofilm formation (155). Other proteins that are structurally reorganized by polyP include those involved in the progression of neurodegenerative Alzheimer's and Parkinson's diseases such as $A\beta_{1–40/42}$, Tau, β_2-

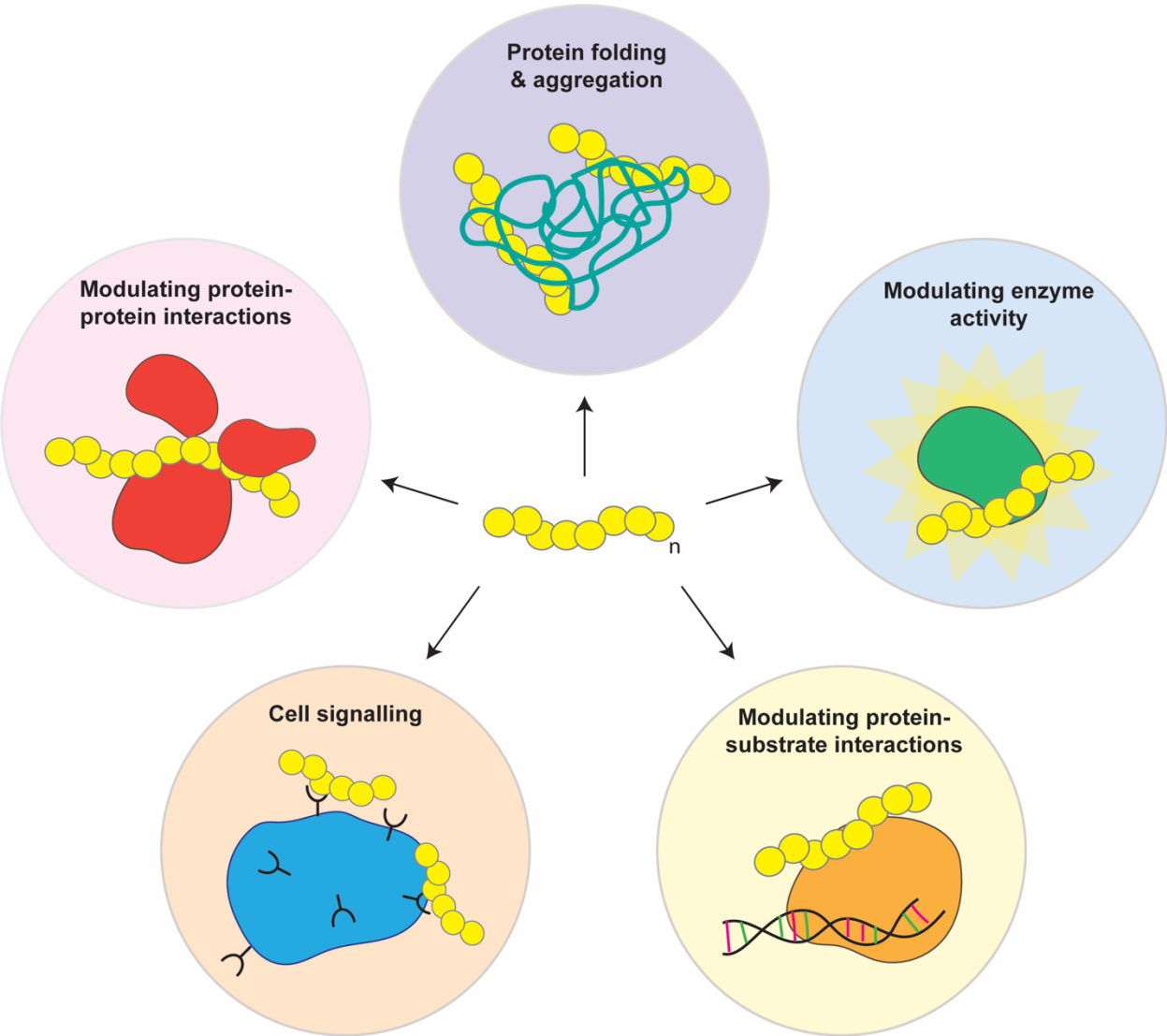


Figure 8. Outcomes of polyP-protein binding. PolyP binding to proteins can disrupt or promote protein-protein interactions or protein-substrate interactions. PolyP binding can also stabilize partially unfolded proteins or play a role in promoting protein aggregation. Additionally, polyP binding events can modulate the enzymatic activity of proteins or contribute to the regulation of signaling pathways within cells. Overall, polyP has wide-reaching roles in the regulation of protein function and activity through direct binding.

microglobulin, and alpha-synuclein proteins (155–157). Interestingly, fibrillation of proteins can happen in the absence of polyP, at a slower rate, presumably resulting in less compact fibrils that are cytotoxic and contribute to faster disease progression (155). Work in neuronal cell lines and *Caenorhabditis elegans* neurodegenerative models suggests that polyP-stabilized alpha-synuclein fibrils are less cytotoxic and more susceptible to proteolytic degradation compared with their unstabilized counterparts (155). Two key residues (K43 and K45) within a lysine-rich region of alpha-synuclein may be critical for polyP binding (157). An open question is whether polyP can stabilize fibrils as they come apart and act as a chaperone to modulate their refolding. Understanding the residues or regions of proteins that interact to promote aggregate formation will help better predict the outcome of polyP binding to partially unfolded proteins and how it could play a role in reversing protein aggregation.

1.8.2. Modulation of protein-protein interactions

Beyond its role in modulating protein folding, polyP can impact target interactions with other proteins.

1.8.2.1. Promoting interactions

One of the earliest descriptions of a polyP-binding protein was made by Kuroda et al. (143), who showed that polyP binding facilitates degradation of target proteins by the Lon protease in *E. coli*. In this scenario, polyP is suggested to bind both Lon and the target, serving as a molecular adaptor. This was first proposed to play a role in the targeting of Lon to ribosomal subunits and nucleoid proteins, during starvation, as part of a broader response that allows cells to adapt to the lack of nutrients (143,158,159). Subsequent work found that this mechanism also contributes to the arrest of DNA replication initiation in *E. coli* by regulating the pool of replication initiator protein, DnaA, when bound to ADP (160). An interesting proposal by Ropelewska et al. (161) is that most

substrates degraded by Lon in a polyP-dependent manner also bind polyP themselves. As another example, two-hybrid assays suggest that polyP binding promotes formation of a heterodimer complex between the *Francisella tularensis* transcription factors MglA and SspA (162). However, it is unclear if disruption of this complex in *ppk-ppx* mutant strains is due to the direct loss of polyP or a downstream effect of the mutations themselves (162).

The effect of polyP may be particularly impactful when it binds to multiple proteins functioning in the same pathway. PolyP's role in the blood coagulation contact pathway is an excellent example. PolyP binds to diverse coagulation factor proteins (FV (163), FXI (164), FXII (165), and thrombin (166)) and plays a role in activating them either directly, or indirectly by accelerating the rate of their interactions. We speculate that polyP may play a similar role in bridging transient interactions in other cases where it interacts with multiple proteins in close proximity. For example, we previously identified many polyP interacting proteins that localize to the nucleolus (146), and theorize that transient interactions mediated by polyP may be important for ribosome biogenesis.

1.8.2.2. Disrupting interactions

In addition to promoting interactions, polyP can also disrupt or prevent interactions between two or more proteins. For example, polyP competes with FVIII to bind von Willebrand Factor (VWF) (167), and instead promotes VWF interaction with glycoprotein Ib (168). This mechanism plays a role in increasing VWF binding to platelets, which is required for platelet activation and aggregation (167,168). PolyP has also been reported to disrupt the interaction between PASK-containing Nsr1 and Top1 *in vitro* (36). Whether polyP impacts interaction of these proteins *in vivo* is not clear, but it is tempting to speculate that this mechanism serves to regulate localization of both proteins to the nucleolus, which is more pronounced in *vtc4*Δ mutant cells that cannot make

polyP (36). Notably, similar polyP-induced changes in localization have been observed for the mammalian kinase DYRK1A (148), which has wide reaching roles in neurogenesis (169), cell proliferation (170,171), and cell homeostasis (172). Specifically, in the presence of excess polyP synthesized by ectopically-expressed bacterial PPK, DYRK1A failed to form nuclear speckles (148). We surmise that this effect and other changes in localization ultimately stem from changes to protein-protein interactions. For example, occlusion of a nuclear localization signal (which often contain lysine residues (173)) by polyP binding could alter a protein's subcellular distribution.

1.8.3. Modulation of cell signaling

Notably, polyP also directly interacts with cell surface receptors to initiate intracellular signaling events. While these receptors are also proteins, this function of polyP is deserving of special attention since the source of polyP is extracellular (e.g. from microorganisms (119), damaged cells (7), or dense granules of platelets (44)). For instance, polyP binding to RAGE and possibly P2Y1 receptors of endothelial cells leads to the activation of pathways like mTORC2 signaling (174) and inflammatory responses involving H4 and HMGB1, which also bind polyP with high affinity (118). Additionally, the predicted binding of polyP to P2Y1 is thought to activate calcium signaling and release of internal polyP stores by astrocytes (45). Intriguingly, released polyP can also act as a neurotransmitter to influence activation of neighboring cells and their uptake of polyP (45). Conversely, polyP can also block receptor binding sites for other ligands. For example, polyP binding to the ACE2 receptor is thought to block the binding of the SARS-CoV-2 Spike protein, thereby preventing viral entry (6,175). In these examples, polyP is proposed to act at the cell surface. However, it is also plausible that polyP may actually enter the cell during receptor internalization (175). For example, via ACE2 internalization, bound polyP could enter the cell and

potentially serve as an intracellular signaling molecule or perform one or more of the functions listed above.

1.8.4. Regulation of enzymatic activity

PolyP binding may also inhibit the enzymatic activity of proteins. For example, *in vitro* assays show that in the presence of polyP, Top1 loses the ability to relax supercoiled DNA (36). Similarly, polyP inhibited the *in vitro* kinase activity of DYRK1A (148). PolyP also inhibits the catalytic activity of HAL, a histidase from *Trypanosoma cruzi* proposed to interact with polyP, via its lysine-rich intrinsically disordered region (176). Of note, it is unclear how the ability of polyP to chelate ions contributes to *in vitro* enzymatic assays and this is deserving of additional consideration in future work. Conversely, polyP could promote enzyme activation. We note that Wang et al. (177) demonstrated that polyP stimulates the kinase activity of mTOR, the master regulator of cellular homeostasis, in a concentration-dependent manner *in vitro*. *In vivo*, ectopic expression of the yeast exopolyphosphatase Ppx1 reduced phosphorylation of mTOR target PHAS-1 and reduced cell viability (177). Given this evidence, it would be important to establish if mTOR regulation occurs via direct binding to polyP.

1.8.5. Modulation of protein-nucleic acid interactions and protein-lipid interactions

PolyP binding can modulate the affinity of targets for other molecules besides proteins. For instance, polyP has been shown to compete with DNA for binding to the mammalian transcription factor MafB, which is unable to bind DNA when polyP-bound (148). However, it is also possible for polyP to alter the RNA or DNA binding specificity of target proteins. This activity of polyP has been shown for the *E. coli* DNA- and RNA-binding protein Hfq (178), and a similar effect is proposed for the sigma factor σ80 of *Heliobacter pylori* (179). Here we speculate that polyP binding stimulates changes in protein conformation or cofactor interactions that alter target binding

specificity. In another example, polyP-stabilized lipopolysaccharide micelles bind to the TLR4 receptor of macrophages more readily than in the absence of polyP (180). However, in this case, it is unclear if polyP directly interacts with TLR4 receptors or if its role is more indirect.

1.9. Open questions in the field of polyphosphate biology

Many questions about fundamental aspects of polyP biology remain unanswered. Without knowing the identity of the enzymes that synthesize and degrade polyP in higher eukaryotes yeast will remain a key model for answering some of these questions. In yeast, it is still unclear how polyphosphatases are regulated inside the vacuole to prevent the continuous degradation of polyP as is it synthesized by the VTC complex. Moreover, the compartmentalization of polyP within the vacuole is like that observed in other eukaryotes where polyP is often localized into acidocalcisome-like organelles. Understanding why polyP is compartmentalized and the consequences of mislocalized polyP could provide insight into potential links between polyP and various physiological disorders. In some cases, lack of polyP may drive physiological disorders, such as Hermansky-Pudlak syndrome, whereas in other cases too much polyP seems to be detrimental, like in the case of ALS patients. Polyphosphatases which are well positioned to regulate polyP levels within cells may be key regulators of various polyP-driven disorders. These enzymes may be able to regulate polyP levels, as well as polyP-protein interactions. Better characterizing these enzymes in mammalian cells will be imperative. However, there is still much to learn about the regulation of polyphosphatases in yeast and these modes of regulation could be conserved in higher eukaryotes. Overall, our work provides novel insights into novel effectors of polyP binding, functions of polyP, and mechanisms by which polyP metabolism is regulated in yeast.

1.10. Description of rationales and hypothesis

In this thesis, I present a manuscript that expands the scope of known polyP-binding proteins in yeast. A second manuscript that examines the importance of polyP compartmentalization in acidocalcisome like-organelles in eukaryotes and identifies pathways dysregulated by nonvacuolar polyP accumulation. Finally, a third manuscript in preparation that examines the structure and function of the Ddp1 polyphophosphatase. Together, these works contribute to the field by establishing new potential functions of polyP and the regulation of polyP metabolism in yeast.

1.10.1. Objective 1: An expanded screen for the identification of novel polyP-binding proteins.

1.10.1.1. Rationale

We and other groups have previously identified numerous polyP-binding proteins in yeast by screening proteins that contain polyacidic serine and lysine rich (PASK) motifs. Following our groups first published screen that examined 90 PASK-containing proteins there remained ~337 proteins that had not yet been screened. We successfully screened ~200 of these remaining proteins for their ability to bind polyP using the NuPAGE analysis.

1.10.1.2. Hypothesis

I hypothesized that other unscreened proteins would also bind polyP and that these proteins might localize to other compartments of the cell. Based on the high concentrations of polyP in the vacuole, I hypothesized that PASK-containing vacuolar proteins would bind polyP and would more likely act as effectors of polyP binding events.

1.10.2. Objective 2: Explore polyP compartmentalization in yeast and identify the molecular mechanisms that make nonvacuolar polyP accumulation toxic.

1.10.2.1. Rationale

Many eukaryotic organisms store polyP within membrane bound acidocalcisome-like organelles and release it when needed. In yeast, forced synthesis of polyP outside the vacuole is toxic to cells highlighting the importance of polyP compartmentalization.

1.10.2.2. Hypothesis

I hypothesized that polyP is compartmentalized to prevent the non-specific interaction of this anionic polymer with proteins and other molecules. This compartmentalization allows for the tight spatiotemporal control of polyP when needed. By using mass spectrometry to identify dysregulated proteins in cells expressing PPK we could begin to identify the molecular mechanisms of its toxicity and identify potential pathways that could be regulated by nonvacuolar polyP under certain physiological conditions.

1.10.3. Objective 3: Explore the structure and function of the Ddp1 polyphosphatase and uncover how it is regulated *in vivo.*

1.10.3.1. Rationale

We identified the Ddp1 endopolyphosphatase as a key regulator of nonvacuolar polyP levels using the PPK expression system. Ddp1 is a Nudix family protein that has been shown to have broad specificity towards a variety of substrates. Despite its many ascribed functions how it regulates these activities within the context of the cell is still unclear.

1.10.3.2. Hypothesis

I hypothesized that Ddp1's catalytic activities are regulated to select between its various substrates *in vivo*. Using our PPK expression system, we could perform a protein mutagenesis screen to identify regions and amino acids that are important for Ddp1's regulation and function.

1.11. References

1. Kornberg A, Rao N, Ault-Riché D. Inorganic polyphosphate: a molecule of many functions. Prog Mol Subcell Biol. 1999;23:1–18.
2. Zhu J, Loubéry S, Broger L, Zhang Y, Lorenzo-Orts L, Utz-Pugin A, et al. A genetically validated approach for detecting inorganic polyphosphates in plants. Plant J [Internet]. 2020;102(3):507–16. Available from: https://onlinelibrary.wiley.com/doi/abs/10.1111/tpj.14642
3. Yamagata Y, Watanabe H, Saitoh M, Namba T. Volcanic production of polyphosphates and its relevance to prebiotic evolution. Nature [Internet]. 1991;352(6335):516–9. Available from: https://doi.org/10.1038/352516a0
4. Kornberg A. Inorganic polyphosphate: toward making a forgotten polymer unforgettable. J Bacteriol. 1995;177(3):491–6.
5. Morrissey JH, Choi SH, Smith SA. Polyphosphate: an ancient molecule that links platelets, coagulation, and inflammation. Blood, J Am Soc Hematol. 2012;119(25):5972–9.
6. Neufurth M, Wang X, Tolba E, Lieberwirth I, Wang S, Schroeder HC, et al. The inorganic polymer, polyphosphate, blocks binding of SARS-CoV-2 spike protein to ACE2 receptor at physiological concentrations. Biochem Pharmacol. 2020;182:114215.
7. Arredondo C, Cefaliello C, Dyrda A, Jury N, Martinez P, Díaz I, et al. Excessive release of inorganic polyphosphate by ALS/FTD astrocytes causes non-cell-autonomous toxicity to motoneurons. Neuron. 2022;110(10):1656-1670.e12.
8. Lempart J, Jakob U. Role of polyphosphate in amyloidogenic processes. Cold Spring Harb Perspect Biol. 2019;11(5):a034041.
9. Desfougères Y, Saiardi A, Azevedo C. Inorganic polyphosphate in mammals: where's Wally? Biochem Soc Trans. 2020;48(1):95–101.
10. Denoncourt A, Downey M. Model systems for studying polyphosphate biology: a focus on microorganisms. Curr Genet. 2021;67(3):331–46.
11. Kornberg SR. Adenosine triphosphate synthesis from polyphosphate by an enzyme from Escherichia coli. BBA - Biochim Biophys Acta. 1957;26(2):294–300.
12. Ahn K, Kornberg A. Polyphosphate kinase from Escherichia coli: Purification and demonstration of a phosphoenzyme intermediate. J Biol Chem [Internet]. 1990;265(20):11734–9. Available from: http://dx.doi.org/10.1016/S0021-9258(19)38459-5
13. Akiyama M, Crooke E, Kornberg A. The polyphosphate kinase gene of Escherichia coli: Isolation and sequence of the ppk gene and membrane location of the protein. J Biol Chem [Internet]. 1992;267(31):22556–61. Available from: http://dx.doi.org/10.1016/S0021-9258(18)41708-5
14. Ault-Riché D, Fraley CD, Tzeng CM, Kornberg A. Novel assay reveals multiple pathways regulating stress-induced accumulations of inorganic polyphosphate in Escherichia coli. J Bacteriol. 1998;180(7):1841–7.
15. Zhu Y, Huang W, Lee SSK, Xu W. Crystal structure of a polyphosphate kinase and its implications for polyphosphate synthesis. EMBO Rep. 2005;6(7):681–7.
16. Ishige K, Zhang H, Kornberg A. Polyphosphate kinase (PPK2), a potent, polyphosphate-driven generator of GTP. Proc Natl Acad Sci U S A. 2002;99(26):16684–8.
17. Zhang H, Ishige K, Kornberg A. A polyphosphate kinase (PPK2) widely conserved in

bacteria. Proc Natl Acad Sci U S A. 2002;99(26):16678–83.
18. Kumble KD, Ahn K, Kornberg A. Phosphohistidyl active sites in polyphosphate kinase of Escherichia coli. Proc Natl Acad Sci U S A. 1996;93(25):14391–5.
19. Ward SK, Heintz JA, Albrecht RM, Talaat AM. Single-cell elemental analysis of bacteria: quantitative analysis of polyphosphates in Mycobacterium tuberculosis. Front Cell Infect Microbiol. 2012;2(May 2012):63.
20. Henry JT, Crosson S. Chromosome replication and segregation govern the biogenesis and inheritance of inorganic polyphosphate granules. Mol Biol Cell. 2013;24(20):3177–86.
21. Racki LR, Tocheva EI, Dieterle MG, Sullivan MC, Jensen GJ, Newman DK. Polyphosphate granule biogenesis is temporally and functionally tied to cell cycle exit during starvation in Pseudomonas aeruginosa. Proc Natl Acad Sci U S A. 2017;114(12):E2440–9.
22. Guan J, Hurto RL, Rai A, Azaldegui CA, Ortiz-Rodríguez LA, Biteen JS, et al. HP-Bodies – Ancestral Condensates that Regulate RNA Turnover and Protein Translation in Bacteria. bioRxiv [Internet]. 2025 Jan 1;2025.02.06.636932. Available from: http://biorxiv.org/content/early/2025/02/06/2025.02.06.636932.abstract
23. Hothorn M, Neumann H, Lenherr ED, Wehner M, Rybin V, Hassa PO, et al. Catalytic core of a membrane-associated eukaryotic polyphosphate polymerase. Science (80-). 2009;324(5926):513–6.
24. Müller O, Bayer MJ, Peters C, Andersen JS, Mann M, Mayer A. The Vtc proteins in vacuole fusion: coupling NSF activity to V_0 *trans*‐complex formation. EMBO J [Internet]. 2002 Feb 1;21(3):259–69. Available from: https://doi.org/10.1093/emboj/21.3.259
25. Guan Z, Chen J, Liu R, Chen Y, Xing Q, Du Z, et al. The cytoplasmic synthesis and coupled membrane translocation of eukaryotic polyphosphate by signal-activated VTC complex. Nat Commun [Internet]. 2023;14(1):718. Available from: https://doi.org/10.1038/s41467-023-36466-4
26. Liu W, Wang J, Comte-Miserez V, Zhang M, Yu X, Chen Q, et al. Cryo-EM structure of the polyphosphate polymerase VTC reveals coupling of polymer synthesis to membrane transit. EMBO J [Internet]. 2023 May 15;42(10):e113320. Available from: https://doi.org/10.15252/embj.2022113320
27. Pipercevic J, Kohl B, Gerasimaite R, Comte-Miserez V, Hostachy S, Müntener T, et al. Inositol pyrophosphates activate the vacuolar transport chaperone complex in yeast by disrupting a homotypic SPX domain interaction. Nat Commun [Internet]. 2023;14(1):2645. Available from: https://doi.org/10.1038/s41467-023-38315-w
28. Desfougères Y, Gerasimaite R, Jessen HJ, Mayer A. Vtc5, a novel subunit of the vacuolar transporter chaperone complex, regulates polyphosphate synthesis and phosphate homeostasis in yeast. J Biol Chem. 2016;291(42):22262–75.
29. Ogawa N, DeRisi J, Brown PO. New components of a system for phosphate accumulation and polyphosphate metabolism in Saccharomyces cerevisiae revealed by genomic expression analysis. Mol Biol Cell. 2000;11(12):4309–21.
30. Chabert V, Kim G-D, Qiu D, Liu G, Michaillat Mayer L, Jamsheer K M, et al. Inositol pyrophosphate dynamics reveals control of the yeast phosphate starvation program through 1,5-IP8 and the SPX domain of Pho81. Gutjahr C, Ron D, editors. Elife [Internet]. 2023;12:RP87956. Available from: https://doi.org/10.7554/eLife.87956
31. Wild R, Gerasimaite R, Jung JY, Truffault V, Pavlovic I, Schmidt A, et al. Control of

eukaryotic phosphate homeostasis by inositol polyphosphate sensor domains. Science (80-). 2016;352(6288):986–90.
32. Gerasimaite R, Pavlovic I, Capolicchio S, Hofer A, Schmidt A, Jessen HJ, et al. Inositol Pyrophosphate Specificity of the SPX-Dependent Polyphosphate Polymerase VTC. ACS Chem Biol. 2017;12(3):648–53.
33. Gerasimaitė R, Sharma S, Desfougères Y, Schmidt A, Mayer A. Coupled synthesis and translocation restrains polyphosphate to acidocalcisome-like vacuoles and prevents its toxicity. J Cell Sci. 2014;127(23):5093–104.
34. McCarthy L, Abramchuk I, Wafy G, Denoncourt A, Lavallée-Adam M, Downey M. Ddp1 Cooperates with Ppx1 to Counter a Stress Response Initiated by Nonvacuolar Polyphosphate. MBio. 2022;13(4).
35. Lander N, Cordeiro C, Huang G, Docampo R. Polyphosphate and acidocalcisomes. Biochem Soc Trans [Internet]. 2016 Feb 9;44(1):1–6. Available from: https://doi.org/10.1042/BST20150193
36. Azevedo C, Livermore T, Saiardi A. Protein polyphosphorylation of lysine residues by inorganic polyphosphate. Mol Cell [Internet]. 2015;58(1):71–82. Available from: http://dx.doi.org/10.1016/j.molcel.2015.02.010
37. Azevedo C, Desfougères Y, Jiramongkol Y, Partington H, Trakansuebkul S, Singh J, et al. Development of a yeast model to study the contribution of vacuolar polyphosphate metabolism to lysine polyphosphorylation. J Biol Chem. 2020;295(6):1439–51.
38. Saito K, Ohtomo R, Kuga-Uetake Y, Aono T, Saito M. Direct labeling of polyphosphate at the ultrastructural level in Saccharomyces cerevisiae by using the affinity of the polyphosphate binding domain of Escherichia coli exopolyphosphatase. Appl Environ Microbiol. 2005;71(10):5692–701.
39. Beauvoit B, Rigoulet M, Guerin B, Canioni P. Polyphosphates as a source of high energy phosphates in yeast mitochondria: A 31P NMR study. FEBS Lett. 1989;252(1–2):17–21.
40. Kulakovskaya T V., Lichko LP, Vagabov VM, Kulaev IS. Inorganic polyphosphates in mitochondria. Biochem. 2010;75(7):825–31.
41. Uttenweiler A, Schwarz H, Neumann H, Mayer A. The vacuolar transporter chaperone (VTC) complex is required for microautophagy. Mol Biol Cell. 2007;18(1):166–75.
42. Brown MRW, Kornberg A. Inorganic polyphosphate in the origin and survival of species. Proc Natl Acad Sci [Internet]. 2004 Nov 16;101(46):16085–7. Available from: https://doi.org/10.1073/pnas.0406909101
43. Baev AY, Angelova PR, Abramov AY. Inorganic polyphosphate is produced and hydrolyzed in F0F1-ATP synthase of mammalian mitochondria. Biochem J. 2020;477(8):1515–24.
44. Ruiz FA, Lea CR, Oldfield E, Docampo R. Human platelet dense granules contain polyphosphate and are similar to acidocalcisomes of bacteria and unicellular eukaryotes. J Biol Chem. 2004;279(43):44250–7.
45. Holmström KM, Marina N, Baev AY, Wood NW, Gourine A V, Abramov AY. Signalling properties of inorganic polyphosphate in the mammalian brain. Nat Commun [Internet]. 2013;4(1):1362. Available from: https://doi.org/10.1038/ncomms2364
46. Akiyama M, Crooke E, Kornberg A. An exopolyphosphatase of Escherichia coli. The enzyme and its ppx gene in a polyphosphate operon. J Biol Chem. 1993;268(1):633–9.
47. Rudat AK, Pokhrel A, Green TJ, Gray MJ. Mutations in Escherichia coli polyphosphate kinase that lead to dramatically increased in vivo polyphosphate levels. J Bacteriol.

2018;200(6):1–20.
48. Alvarado J, Ghosh A, Janovitz T, Jauregui A, Hasson MS, Sanders DA. Origin of Exopolyphosphatase Processivity: Fusion of an ASKHA Phosphotransferase and a Cyclic Nucleotide Phosphodiesterase Homolog. Structure [Internet]. 2006 Aug 1;14(8):1263–72. Available from: https://doi.org/10.1016/j.str.2006.06.009
49. Dai S, Wang B, Ye R, Zhang D, Xie Z, Yu N, et al. Structural Evolution of Bacterial Polyphosphate Degradation Enzyme for Phosphorus Cycling. Adv Sci [Internet]. 2024 Jul 1;11(26):2309602. Available from: https://doi.org/10.1002/advs.202309602
50. Shi X, Kornberg A. Endopolyphosphatase in Saccharomyces cerevisiae undergoes post-translational activations to produce short-chain polyphosphates. FEBS Lett. 2005;579(9):2014–8.
51. Sethuraman A, Rao NN, Kornberg A. The endopolyphosphatase gene: Essential in Saccharomyces cerevisiae. Proc Natl Acad Sci U S A [Internet]. 2001;98(15):8542–7. Available from: http://www.pnas.org/content/98/15/8542.abstract
52. Andreeva N, Trilisenko L, Eldarov M, Kulakovskaya T. Polyphosphatase PPN1 of Saccharomyces cerevisiae: Switching of Exopolyphosphatase and Endopolyphosphatase Activities. PLoS One. 2015;10(3):1–11.
53. Andreeva N, Ledova L, Ryazanova L, Tomashevsky A, Kulakovskaya T, Eldarov M. Ppn2 endopolyphosphatase overexpressed in Saccharomyces cerevisiae: Comparison with Ppn1, Ppx1, and Ddp1 polyphosphatases. Biochimie [Internet]. 2019;163:101–7. Available from: https://doi.org/10.1016/j.biochi.2019.06.001
54. Kumble KD, Kornberg A. Endopolyphosphatases for long chain inorganic polyphosphate in yeast and mammals. J Biol Chem. 1996;271(43):27146–51.
55. Nguyen TQ, Dziuba N, Lindahl PA. Isolated Saccharomyces cerevisiae vacuoles contain low-molecular-mass transition-metal polyphosphate complexes†. Metallomics [Internet]. 2019 Jul 17;11(7):1298–309. Available from: https://doi.org/10.1039/c9mt00104b
56. Li SC, Kane PM. The yeast lysosome-like vacuole: Endpoint and crossroads. Biochim Biophys Acta - Mol Cell Res [Internet]. 2009;1793(4):650–63. Available from: https://www.sciencedirect.com/science/article/pii/S0167488908002814
57. Reggiori F, Pelham HR. Sorting of proteins into multivesicular bodies. EMBO J. 2001;20(18):5176–86.
58. Hettema EH, Valdez-Taubas J, Pelham HRB. Bsd2 binds the ubiquitin ligase Rsp5 and mediates the ubiquitination of transmembrane proteins. EMBO J [Internet]. 2004 Mar 24;23(6):1279–88. Available from: https://doi.org/10.1038/sj.emboj.7600137
59. Mistry J, Chuguransky S, Williams L, Qureshi M, Salazar GA, Sonnhammer ELL, et al. Pfam: The protein families database in 2021. Nucleic Acids Res. 2021;49(D1):D412–9.
60. Auesukaree C, Homma T, Tochio H, Shirakawa M, Kaneko Y, Harashima S. Intracellular Phosphate Serves as a Signal for the Regulation of the PHO Pathway in Saccharomyces cerevisiae. J Biol Chem [Internet]. 2004;279(17):17289–94. Available from: http://dx.doi.org/10.1074/jbc.M312202200
61. Gerasimaitė R, Mayer A. Ppn2, a novel Zn^{2+} -dependent polyphosphatase in the acidocalcisome-like yeast vacuole. J Cell Sci [Internet]. 2017;130(9):1625–36. Available from: http://jcs.biologists.org/lookup/doi/10.1242/jcs.201061
62. Klionsky DJ, Emr SD. Membrane protein sorting: biosynthesis, transport and processing of yeast vacuolar alkaline phosphatase. EMBO J. 1989;8(8):2241–50.
63. Merz AJ, Wickner WT. Resolution of organelle docking and fusion kinetics in a cell-free

assay. Proc Natl Acad Sci. 2004;101(32):11548–53.
64. Qiao W, Ellis C, Steffen J, Wu C, Eide DJ. Zinc status and vacuolar zinc transporters control alkaline phosphatase accumulation and activity in Saccharomyces cerevisiae. Mol Microbiol. 2009;72(2):320–34.
65. Song L. A soluble form of phosphatase in Saccharomyces cerevisiae capable of converting farnesyl diphosphate into E, E-farnesol. Appl Biochem Biotechnol. 2006;128:149–57.
66. Murphy JE, Tibbitts TT, Kantrowitz ER. Mutations at positions 153 and 328 inEscherichia coliAlkaline phosphatase provide insight towards the structure and function of mammalian and yeast alkaline phosphatases. J Mol Biol. 1995;253(4):604–17.
67. Donella-Deana A, Ostojić S, Pinna LA, Barbarić S. Specific dephosphorylation of phosphopeptides by the yeast alkaline phosphatase encoded by PHO8 gene. Biochim Biophys Acta (BBA)-Molecular Cell Res. 1993;1177(2):221–8.
68. Plankert U, Purwin C, Holzer H. Yeast fructose-2, 6-bisphosphate 6-phosphatase is encoded by PHO8, the gene for nonspecific repressible alkaline phosphatase. Eur J Biochem. 1991;196(1):191–6.
69. Lu S-P, Lin S-J. Phosphate-responsive signaling pathway is a novel component of NAD+ metabolism in Saccharomyces cerevisiae. J Biol Chem. 2011;286(16):14271–81.
70. Kizawa K, Aono T, Ohtomo R. PHO8 gene coding alkaline phosphatase of Saccharomyces cerevisiae is involved in polyphosphate metabolism. J Gen Appl Microbiol. 2016;62(6):297–302.
71. Fernandez MP, Gascon S, Schwencke J. Some enzymatic properties of vacuolar alkaline phosphatase from yeast. Curr Microbiol. 1981;6:121–6.
72. Huh, K. W, Falvo, V. J, Gerke, C. L, et al. Global analysis of protein localization in budding yeast. Nature [Internet]. 2003;425(6959):686–91. Available from: http://yeastgfp.ucsf.edu
73. Koh JLY, Chong YT, Friesen H, Moses A, Boone C, Andrews BJ, et al. CYCLoPs: A comprehensive database constructed from automated analysis of protein abundance and subcellular localization patterns in Saccharomyces cerevisiae. G3 Genes, Genomes, Genet. 2015;5(6):1223–32.
74. Safrany ST, Ingram SW, Cartwright JL, Falck JR, McLennan AG, Barnes LD, et al. The diadenosine hexaphosphate hydrolases from Schizosaccharomyces pombe and Saccharomyces cerevisiae are homologues of the human diphosphoinositol polyphosphate. Overlapping substrate specificities in a Mutt-type protein phosphohydrolase. J Biol Chem [Internet]. 1999;274(31):21735–40. Available from: http://dx.doi.org/10.1074/jbc.274.31.21735
75. York SJ, Armbruster BN, Greenwell P, Petes TD, York JD. Inositol diphosphate signaling regulates telomere length. J Biol Chem [Internet]. 2005;280(6):4264–9. Available from: http://dx.doi.org/10.1074/jbc.M412070200
76. Lonetti A, Szijgyarto Z, Bosch D, Loss O, Azevedo C, Saiardi A. Identification of an evolutionarily conserved family of inorganic polyphosphate endopolyphosphatases. J Biol Chem. 2011;286(37):31966–74.
77. Kilari RS, Weaver JD, Shears SB, Safrany ST. Understanding inositol pyrophosphate metabolism and function: Kinetic characterization of the DIPPs. FEBS Lett. 2013;587(21):3464–70.
78. Padmanabhan U, Dollins DE, Fridy PC, York JD, Downes CP. Characterization of a

selective inhibitor of inositol hexakisphosphate kinases. Use in defining biological roles and metabolic relationships of inositol pyrophosphates. J Biol Chem. 2009;284(16):10571–82.
79. Mulugu S, Bai W, Fridy PC, Bastidas RJ, Otto JC, Dollins DE, et al. A Conserved Family of Enzymes That Phosphorylate Inositol Hexakisphosphate. Science (80-). 2008;106(2007):106–9.
80. Shears SB. Inositol pyrophosphates: Why so many phosphates? Adv Biol Regul. 2015;57:203–16.
81. Moser S, Hans G, Saiardi A, Bru S, Taskin AA, Meisinger C, et al. A Screening Approach Unveils an Unknown Mn²⁺-dependent Endopolyphosphatase Activity in Yeast. bioRxiv [Internet]. 2025 Jan 1;2025.01.19.633793. Available from: http://biorxiv.org/content/early/2025/01/19/2025.01.19.633793.abstract
82. Cartwright JL, McLennan AG. The Saccharomyces cerevisiae YOR163w gene encodes a diadenosine 5',5'''- P1,P6-hexaphosphate (Ap6A) hydrolase member of the MutT motif (Nudix hydrolase) family. J Biol Chem [Internet]. 1999;274(13):8604–10. Available from: http://dx.doi.org/10.1074/jbc.274.13.8604
83. Song MG, Bail S, Kiledjian M. Multiple Nudix family proteins possess mRNA decapping activity. Rna. 2013;19(3):390–9.
84. Márquez-Moñino MÁ, Ortega-García R, Shipton ML, Franco-Echevarría E, Riley AM, Sanz-Aparicio J, et al. Multiple substrate recognition by yeast diadenosine and diphosphoinositol polyphosphate phosphohydrolase through phosphate clamping. Sci Adv. 2021;7(17):1–16.
85. Wurst H, Shiba T, Kornberg A. The gene for a major exopolyphosphatase of Saccharomyces cerevisiae. J Bacteriol. 1995;177(4):898–906.
86. Wurst H, Kornberg A. A soluble exopolyphosphatase of Saccharomyces cerevisiae. Purification and characterization. J Biol Chem. 1994;269(15):10996–1001.
87. Ugochukwu E, Lovering AL, Mather OC, Young TW, White SA. The crystal structure of the cytosolic exopolyphosphatase from Saccharomyces cerevisiae reveals the basis for substrate specificity. J Mol Biol. 2007;371(4):1007–21.
88. Tammenkoski M, Moiseev V, Lahti M, Ugochukwu E, Brondijk THC, White SA, et al. Kinetic and mutational analyses of the major cytosolic exopolyphosphatase from Saccharomyces cerevisiae. J Biol Chem. 2007;282(13):9302–11.
89. Lichko LP, Pestov NA, Kulakovskaya T V, Kulaev IS. Effect of PPX1 inactivation on the exopolyphosphatase spectra in cytosol and mitochondria of the yeast Saccharomyces cerevisiae. Biochem. 2003;68:740–6.
90. Samper-Martín B, Sarrias A, Lázaro B, Pérez-Montero M, Rodríguez-Rodríguez R, Ribeiro MPC, et al. Polyphosphate degradation by Nudt3-Zn2+ mediates oxidative stress response. Cell Rep. 2021;37(7).
91. Sahu S, Wang Z, Jiao X, Gu C, Jork N, Wittwer C, et al. InsP7 is a small-molecule regulator of NUDT3-mediated mRNA decapping and processing-body dynamics. Proc Natl Acad Sci U S A. 2020;117(32):19245–53.
92. Grudzien-Nogalska E, Jiao X, Song MG, Hart RP, Kiledjian M. Nudt3 is an mRNA decapping enzyme that modulates cell migration. Rna. 2016;22(5):773–81.
93. Timmons L, Shearn A. Germline transformation using a prune cDNA rescues prune/killer of prune lethality and the prune eye color phenotype in Drosophila. Genetics. 1996;144(4):1589–600.

94. Aravind L, Koonin E V. A novel family of predicted phosphoesterases includes Drosophila prune protein and bacterial RecJ exonuclease. Trends Biochem Sci. 1998;23(1):17–9.
95. Carotenuto M, De Antonellis P, Liguori L, Benvenuto G, Magliulo D, Alonzi A, et al. H-Prune through GSK-3β interaction sustains canonical WNT/β-catenin signaling enhancing cancer progression in NSCLC. Oncotarget. 2014;5(14):5736.
96. Garzia L, D'angelo A, Amoresano A, Knauer SK, Cirulli C, Campanella C, et al. Phosphorylation of nm23-H1 by CKI induces its complex formation with h-prune and promotes cell motility. Oncogene. 2008;27(13):1853–64.
97. Carotenuto M, Pedone E, Diana D, de Antonellis P, Džeroski S, Marino N, et al. Neuroblastoma tumorigenesis is regulated through the Nm23-H1/h-Prune C-terminal interaction. Sci Rep. 2013;3(1):1351.
98. Tammenkoski M, Koivula K, Cusanelli E, Zollo M, Steegborn C, Baykov AA, et al. Human metastasis regulator protein H-prune is a short-chain exopolyphosphatase. Biochemistry. 2008;47(36):9707–13.
99. D'Angelo A, Garzia L, André A, Carotenuto P, Aglio V, Guardiola O, et al. Prune cAMP phosphodiesterase binds nm23-H1 and promotes cancer metastasis. Cancer Cell. 2004;5(2):137–49.
100. Nistala H, Dronzek J, Gonzaga-Jauregui C, Chim SM, Rajamani S, Nuwayhid S, et al. NMIHBA results from hypomorphic PRUNE1 variants that lack short-chain exopolyphosphatase activity. Hum Mol Genet. 2020;29(21):3516–31.
101. Kohn G, Delvaux D, Lakaye B, Servais A-C, Scholer G, Fillet M, et al. High inorganic triphosphatase activities in bacteria and mammalian cells: identification of the enzymes involved. 2012;
102. Bibbò F, Sorice C, Ferrucci V, Zollo M. Functional genomics of PRUNE1 in neurodevelopmental disorders (NDDs) tied to medulloblastoma (MB) and other tumors. Front Oncol. 2021;11:758146.
103. Kobayashi T, Hino S, Oue N, Asahara T, Zollo M, Yasui W, et al. Glycogen synthase kinase 3 and h-prune regulate cell migration by modulating focal adhesions. Mol Cell Biol. 2006;
104. Reymond A, Volorio S, Merla G, Al-Maghtheh M, Zuffardi O, Bulfone A, et al. Evidence for interaction between human PRUNE and nm23-H1 NDPKinase. Oncogene. 1999;18(51):7244–52.
105. Zollo M, Ahmed M, Ferrucci V, Salpietro V, Asadzadeh F, Carotenuto M, et al. PRUNE is crucial for normal brain development and mutated in microcephaly with neurodevelopmental impairment. Brain. 2017;140(4):940–52.
106. Oughtred R, Rust J, Chang C, Breitkreutz B, Stark C, Willems A, et al. The BioGRID database: A comprehensive biomedical resource of curated protein, genetic, and chemical interactions. Protein Sci. 2021;30(1):187–200.
107. Lorenz B, Schröder HC. Mammalian intestinal alkaline phosphatase acts as highly active exopolyphosphatase. Biochim Biophys Acta - Protein Struct Mol Enzymol. 2001;1547(2):254–61.
108. Omelon S, Georgiou J, Henneman ZJ, Wise LM, Sukhu B, Hunt T, et al. Control of vertebrate skeletal mineralization by polyphosphates. PLoS One. 2009;4(5):e5634.
109. Hoac B, Kiffer-Moreira T, Millán JL, McKee MD. Polyphosphates inhibit extracellular matrix mineralization in MC3T3-E1 osteoblast cultures. Bone. 2013;53(2):478–86.

110. Müller WEG, Tolba E, Schröder HC, Wang X. Polyphosphate: a morphogenetically active implant material serving as metabolic fuel for bone regeneration. Macromol Biosci. 2015;15(9):1182–97.
111. Müller WEG, Tolba E, Feng Q, Schröder HC, Markl JS, Kokkinopoulou M, et al. Amorphous Ca2+ polyphosphate nanoparticles regulate the ATP level in bone-like SaOS-2 cells. J Cell Sci. 2015;128(11):2202–7.
112. Müller WEG, Wang S, Neufurth M, Kokkinopoulou M, Feng Q, Schröder HC, et al. Polyphosphate as a donor of high-energy phosphate for the synthesis of ADP and ATP. J Cell Sci. 2017;130(16):2747–56.
113. Addison WN, Azari F, Sørensen ES, Kaartinen MT, McKee MD. Pyrophosphate inhibits mineralization of osteoblast cultures by binding to mineral, up-regulating osteopontin, and inhibiting alkaline phosphatase activity. J Biol Chem. 2007;282(21):15872–83.
114. Millán JL. The role of phosphatases in the initiation of skeletal mineralization. Calcif Tissue Int. 2013;93:299–306.
115. Wang X, Schröder HC, Diehl-Seifert B, Kropf K, Schlossmacher U, Wiens M, et al. Dual effect of inorganic polymeric phosphate/polyphosphate on osteoblasts and osteoclasts in vitro. J Tissue Eng Regen Med. 2013;7(10):767–76.
116. Ariganello MB, Omelon S, Variola F, Wazen RM, Moffatt P, Nanci A. Osteogenic cell cultures cannot utilize exogenous sources of synthetic polyphosphate for mineralization. J Cell Biochem. 2014;115(12):2089–102.
117. Hassanian SM, Ardeshirylajimi A, Dinarvand P, Rezaie AR. Inorganic polyphosphate promotes cyclin D1 synthesis through activation of mTOR/Wnt/β-catenin signaling in endothelial cells. J Thromb Haemost. 2016;14(11):2261–73.
118. Dinarvand P, Hassanian SM, Qureshi SH, Manithody C, Eissenberg JC, Yang L, et al. Polyphosphate amplifies proinflammatory responses of nuclear proteins through interaction with receptor for advanced glycation end products and P2Y1 purinergic receptor. Blood, J Am Soc Hematol. 2014;123(6):935–45.
119. Roewe J, Stavrides G, Strueve M, Sharma A, Marini F, Mann A, et al. Bacterial polyphosphates interfere with the innate host defense to infection. Nat Commun [Internet]. 2020;11(1):1–12. Available from: http://dx.doi.org/10.1038/s41467-020-17639-x
120. Oddie GW, Schenk G, Angel NZ, Walsh N, Guddat LW, De Jersey J, et al. Structure, function, and regulation of tartrate-resistant acid phosphatase. Bone. 2000;27(5):575–84.
121. Harada K, Itoh H, Kawazoe Y, Miyazaki S, Doi K, Kubo T, et al. Polyphosphate-mediated inhibition of tartrate-resistant acid phosphatase and suppression of bone resorption of osteoclasts. PLoS One. 2013;8(11):e78612.
122. Gray MJ, Wholey WY, Wagner NO, Cremers CM, Mueller-Schickert A, Hock NT, et al. Polyphosphate Is a Primordial Chaperone. Mol Cell [Internet]. 2014;53(5):689–99. Available from: http://dx.doi.org/10.1016/j.molcel.2014.01.012
123. Rao NN, Gómez-García MR, Kornberg A. Inorganic Polyphosphate: Essential for Growth and Survival. Annu Rev Biochem [Internet]. 2009;78(1):605–47. Available from: http://www.annualreviews.org/doi/10.1146/annurev.biochem.77.083007.093039
124. Neville N, Roberge N, Ji X, Stephen P, Lu JL, Jia Z. A dual-specificity inhibitor targets polyphosphate kinase 1 and 2 enzymes to attenuate virulence of Pseudomonas aeruginosa. MBio. 2021;12(3):10–1128.
125. Baijal K, Abramchuk I, Herrera CM, Mah T-F, Trent MS, Lavallée-Adam M, et al. Polyphosphate kinase regulates LPS structure and polymyxin resistance during starvation

in E. coli. Plos Biol. 2024;22(3):e3002558.
126. Bostian KA, Lemire JM, Halvorson HO. Physiological control of repressible acid phosphatase gene transcripts in Saccharomyces cerevisiae. Mol Cell Biol. 1983;3(5):839–53.
127. Kim G-D, Qiu D, Jessen HJ, Mayer A. Metabolic consequences of polyphosphate synthesis and imminent phosphate limitation. MBio. 2023;14(3):e00102-23.
128. Eskes E, Deprez MA, Wilms T, Winderickx J. pH homeostasis in yeast; the phosphate perspective. Curr Genet. 2018;64(1):155–61.
129. Dunn T, Gable K, Beeler T. Regulation of cellular Ca2+ by yeast vacuoles. J Biol Chem. 1994;269(10):7273–8.
130. Klompmaker SH, Kohl K, Fasel N, Mayer A. Magnesium uptake by connecting fluid-phase endocytosis to an intracellular inorganic cation filter. Nat Commun. 2017;8(1):1879.
131. Hürlimann HC, Stadler-Waibel M, Werner TP, Freimoser FM. Pho91 is a vacuolar phosphate transporter that regulates phosphate and polyphosphate metabolism in Saccharomyces cerevisiae. Mol Biol Cell. 2007;18(11):4438–45.
132. Austin S, Mayer A. Phosphate Homeostasis − A Vital Metabolic Equilibrium Maintained Through the INPHORS Signaling Pathway. Front Microbiol [Internet]. 2020;Volume 11. Available from: https://www.frontiersin.org/journals/microbiology/articles/10.3389/fmicb.2020.01367
133. Thomas MR, O'Shea EK. An intracellular phosphate buffer filters transient fluctuations in extracellular phosphate levels. Proc Natl Acad Sci. 2005;102(27):9565–70.
134. Desfougères Y, Neumann H, Mayer A. Organelle size control–increasing vacuole content activates SNAREs to augment organelle volume through homotypic fusion. J Cell Sci. 2016;129(14):2817–28.
135. Bru S, Martínez-Laínez JM, Hernández-Ortega S, Quandt E, Torres-Torronteras J, Martí R, et al. Polyphosphate is involved in cell cycle progression and genomic stability in Saccharomyces cerevisiae. Mol Microbiol. 2016;101(3):367–80.
136. Kumble KD, Kornberg A. Inorganic Polyphosphate in Mammalian Cells and Tissues. J Biol Chem [Internet]. 1995 Mar 17;270(11):5818–22. Available from: http://www.jbc.org/content/270/11/5818.abstract
137. Travers RJ, Smith SA, Morrissey JH. Polyphosphate, platelets, and coagulation. Int J Lab Hematol [Internet]. 2015 May 1;37(S1):31–5. Available from: https://doi.org/10.1111/ijlh.12349
138. Huizing M, Boissy RE, Gahl WA. Hermansky–Pudlak syndrome: vesicle formation from yeast to man. Pigment cell Res. 2002;15(6):405–19.
139. Huizing M, Anikster Y, Gahl WA. Hermansky–Pudlak syndrome and related disorders of organelle formation. Traffic. 2000;1(11):823–35.
140. Huizing M, Malicdan MC V, Wang JA, Pri-Chen H, Hess RA, Fischer R, et al. Hermansky–Pudlak syndrome: mutation update. Hum Mutat. 2020;41(3):543–80.
141. Müller F, Mutch NJ, Schenk WA, Smith SA, Esterl L, Spronk HM, et al. Platelet polyphosphates are proinflammatory and procoagulant mediators in vivo. Cell. 2009;139(6):1143–56.
142. Schoeppe R, Waldmann M, Jessen HJ, Renné T. An Update on Polyphosphate In Vivo Activities. Biomolecules 2024, 14, 937. 2024.
143. Kuroda A, Nomura K, Ohtomo R, Kato J, Ikeda T, Takiguchi N, et al. Role of Inorganic

Polyphosphate in Promoting Ribosomal Protein Degradation by the Lon Protease in E. coli. Science (80-) [Internet]. 2001 Jul 27;293(5530):705–8. Available from: https://doi.org/10.1126/science.1061315

144. Lorenzo-Orts L, Hohmann U, Zhu J, Hothorn M. Molecular characterization of CHAD domains as inorganic polyphosphate-binding modules. Life Sci Alliance [Internet]. 2019 Jun 1;2(3):e201900385. Available from: http://www.life-science-alliance.org/content/2/3/e201900385.abstract
145. Azevedo C, Saiardi A. Why always lysine? The ongoing tale of one of the most modified amino acids. Adv Biol Regul [Internet]. 2016;60:144–50. Available from: https://www.sciencedirect.com/science/article/pii/S2212492615300142
146. Bentley-DeSousa A, Holinier C, Moteshareie H, Tseng YC, Kajjo S, Nwosu C, et al. A Screen for Candidate Targets of Lysine Polyphosphorylation Uncovers a Conserved Network Implicated in Ribosome Biogenesis. Cell Rep [Internet]. 2018;22(13):3427–39. Available from: https://doi.org/10.1016/j.celrep.2018.02.104
147. Azevedo C, Singh J, Steck N, Hofer A, Ruiz FA, Singh T, et al. Screening a Protein Array with Synthetic Biotinylated Inorganic Polyphosphate to Define the Human PolyP-ome. ACS Chem Biol. 2018;13(8):1958–63.
148. Neville N, Lehotsky K, Yang Z, Klupt KA, Denoncourt A, Downey M, et al. Modification of histidine repeat proteins by inorganic polyphosphate. Cell Rep [Internet]. 2023 Sep 26;42(9). Available from: https://doi.org/10.1016/j.celrep.2023.113082
149. Neville N, Lehotsky K, Klupt KA, Downey M, Jia Z. Polyphosphate attachment to lysine repeats is a non-covalent protein modification. Mol Cell [Internet]. 2024 May 2;84(9):1802-1810.e4. Available from: https://doi.org/10.1016/j.molcel.2024.03.028
150. Azevedo C, Borghi F, Su XB, Saiardi A. On the covalent nature of lysine polyphosphorylation. Mol Cell [Internet]. 2024 May 2;84(9):1811-1815.e3. Available from: https://doi.org/10.1016/j.molcel.2024.03.029
151. Neville N, Lehotsky K, Jia Z. Back on the chain gang: polyphosphate modification of proteins. Trends Biochem Sci [Internet]. 2024 Sep 1;49(9):757–60. Available from: https://doi.org/10.1016/j.tibs.2024.06.010
152. Yoo NG, Dogra S, Meinen BA, Tse E, Haefliger J, Southworth DR, et al. Polyphosphate stabilizes protein unfolding intermediates as soluble amyloid-like oligomers. J Mol Biol. 2018;430(21):4195–208.
153. Sasahara K, Yamaguchi K, So M, Goto Y. Polyphosphates diminish solubility of a globular protein and thereby promote amyloid aggregation. J Biol Chem. 2019;294(42):15318–29.
154. Guan J, Jaksob U. The protein scaffolding functions of polyphosphate. J Mol Biol. 2024;436(14):168504.
155. Cremers CM, Knoefler D, Gates S, Martin N, Dahl JU, Lempart J, et al. Polyphosphate: A Conserved Modifier of Amyloidogenic Processes. Mol Cell [Internet]. 2016;63(5):768–80. Available from: http://dx.doi.org/10.1016/j.molcel.2016.07.016
156. Wickramasinghe SP, Lempart J, Merens HE, Murphy J, Huettemann P, Jakob U, et al. Polyphosphate initiates tau aggregation through intra-and intermolecular scaffolding. Biophys J. 2019;117(4):717–28.
157. Zhang C, Yamaguchi K, So M, Sasahara K, Ito T, Yamamoto S, et al. Possible mechanisms of polyphosphate-induced amyloid fibril formation of β2-microglobulin. Proc Natl Acad Sci. 2019;116(26):12833–8.

158. Kuroda A. A polyphosphate-lon protease complex in the adaptation of Escherichia coli to amino acid starvation. Biosci Biotechnol Biochem. 2006;70(2):325–31.
159. Nomura K, Kato J, Takiguchi N, Ohtake H, Kuroda A. Inorganic polyphosphate stimulates lon-mediated proteolysis of nucleoid proteins in Escherichia coli. Cell Mol Biol. 2006;52(4):23–9.
160. Gross MH, Konieczny I. Polyphosphate induces the proteolysis of ADP-bound fraction of initiator to inhibit DNA replication initiation upon stress in Escherichia coli. Nucleic Acids Res. 2021;48(10):5457–66.
161. Ropelewska M, Gross MH, Konieczny I. DNA and polyphosphate in directed proteolysis for DNA replication control. Front Microbiol. 2020;11:585717.
162. Wrench AP, Gardner CL, Siegel SD, Pagliai FA, Malekiha M, Gonzalez CF, et al. MglA/SspA complex interactions are modulated by inorganic polyphosphate. PLoS One. 2013;8(10):e76428.
163. Choi SH, Smith SA, Morrissey JH. Polyphosphate accelerates factor V activation by factor XIa. Thromb Haemost. 2015;113(03):599–604.
164. Choi SH, Smith SA, Morrissey JH. Polyphosphate is a cofactor for the activation of factor XI by thrombin. Blood, J Am Soc Hematol. 2011;118(26):6963–70.
165. Malik RA, Zhou J, Fredenburgh JC, Truong TK, Crosby JR, Revenko AS, et al. Polyphosphate-induced thrombosis in mice is factor XII dependent and is attenuated by histidine-rich glycoprotein. Blood Adv. 2021;5(18):3540–51.
166. Mutch NJ, Myles T, Leung LLK, Morrissey JH. Polyphosphate binds with high affinity to exosite II of thrombin. J Thromb Haemost. 2010;8(3):548–55.
167. Montilla M, Atienza-Navarro I, García-Cozar FJ, Castro C, Rodríguez-Martorell FJ, Ruiz FA. Polyphosphate activates von Willebrand factor interaction with glycoprotein Ib in the absence of factor VIII in vitro. Int J Mol Sci. 2022;23(22):14118.
168. Montilla M, Hernandez-Ruiz L, Garcia-Cozar FJ, Alvarez-Laderas I, Rodriguez-Martorell J, Ruiz FA. Polyphosphate binds to human von Willebrand factor in vivo and modulates its interaction with glycoprotein Ib. J Thromb Haemost. 2012;10(11):2315–23.
169. Martinez de Lagran M, Benavides-Piccione R, Ballesteros-Yañez I, Calvo M, Morales M, Fillat C, et al. Dyrk1A influences neuronal morphogenesis through regulation of cytoskeletal dynamics in mammalian cortical neurons. Cereb cortex. 2012;22(12):2867–77.
170. Dirice E, Walpita D, Vetere A, Meier BC, Kahraman S, Hu J, et al. Inhibition of DYRK1A stimulates human β-cell proliferation. Diabetes. 2016;65(6):1660–71.
171. Rammohan M, Harris E, Bhansali RS, Zhao E, Li LS, Crispino JD. The chromosome 21 kinase DYRK1A: emerging roles in cancer biology and potential as a therapeutic target. Oncogene. 2022;41(14):2003–11.
172. Barzowska A, Pucelik B, Pustelny K, Matsuda A, Martyniak A, Stępniewski J, et al. DYRK1A kinase inhibitors promote β-cell survival and insulin homeostasis. Cells. 2021;10(9):2263.
173. Lu J, Wu T, Zhang B, Liu S, Song W, Qiao J, et al. Types of nuclear localization signals and mechanisms of protein import into the nucleus. Cell Commun Signal. 2021;19(1):60.
174. Hassanian SM, Dinarvand P, Smith SA, Rezaie AR. Inorganic polyphosphate elicits pro-inflammatory responses through activation of the mammalian target of rapamycin complexes 1 and 2 in vascular endothelial cells. J Thromb Haemost. 2015;13(5):860–71.
175. Ferrucci V, Kong D-Y, Asadzadeh F, Marrone L, Boccia A, Siciliano R, et al. Long-chain

polyphosphates impair SARS-CoV-2 infection and replication. Sci Signal. 2021;14(690):eabe5040.
176. Mantilla BS, Azevedo C, Denny PW, Saiardi A, Docampo R. The histidine ammonia lyase of Trypanosoma cruzi is involved in acidocalcisome alkalinization and is essential for survival under starvation conditions. MBio. 2021;12(6):e01981-21.
177. Wang L, Fraley CD, Faridi J, Kornberg A, Roth RA. Inorganic polyphosphate stimulates mammalian TOR, a kinase involved in the proliferation of mammary cancer cells. Proc Natl Acad Sci U S A. 2003;100(20):11249–54.
178. Beaufay F, Amemiya HM, Guan J, Basalla J, Meinen BA, Chen Z, et al. Polyphosphate drives bacterial heterochromatin formation. Sci Adv. 2021;7(52).
179. Yang ZX, Zhou YN, Yang Y, Jin DJ. Polyphosphate binds to the principal sigma factor of RNA polymerase during starvation response in Helicobacter pylori. Mol Microbiol. 2010;77(3):618–27.
180. Ito T, Yamamoto S, Yamaguchi K, Sato M, Kaneko Y, Goto S, et al. Inorganic polyphosphate potentiates lipopolysaccharide-induced macrophage inflammatory response. J Biol Chem. 2020;295(12):4014–23.

CHAPTER 2 – MANUSCRIPT #1

Proteins required for vacuolar function are targets of lysine polyphosphorylation in yeast

Publication information:
McCarthy, L., Bentley-DeSousa, A., Denoncourt, A., Tseng, Y. C., Gabriel, M., & Downey, M. (2020). Proteins required for vacuolar function are targets of lysine polyphosphorylation in yeast. *FEBS Letters*, 594(1), 21–30. https://doi.org/10.1002/1873-3468.13588

Authors' contributions:
Conceptualization: L.M., A.B.D., M.D. Methodology: L.M., A.B.D., M.D. Investigation: L.M., A.B.D., A.D., Y.C.T., M.G., M.D. Supervision: M.D. Writing – original draft: L.M., A.B.D., M.D. Writing – review and editing: All authors.

Proteins required for vacuolar function are targets of lysine polyphosphorylation in yeast

Liam McCarthy[1,2#], Amanda Bentley-DeSousa[1,2#], Alix Denoncourt[1,2], Yi-Chieh Tseng[1,2], Matthew Gabriel[1,2], and Michael Downey[1,2*]

1. Department of Cellular and Molecular Medicine, University of Ottawa, Ottawa, Ontario, Canada, K1H 8M5

2. Ottawa Institute of Systems Biology, University of Ottawa, Ottawa, Ontario, Canada, K1H 8M5

Liam McCarthy and Amanda Bentley-DeSousa contributed equally to this work.

* Correspondence: mdowne2@uottawa.ca

2.1. Abstract

Polyphosphates (polyP) are long chains of inorganic phosphates that can be attached to lysine residues of target proteins as a nonenzymatic post-translational modification. This modification, termed polyphosphorylation, may be particularly prevalent in bacterial and fungal species that synthesize large quantities of polyP. In this study, we evaluated the polyphosphorylation status of over 200 candidate targets in Saccharomyces cerevisiae. We report eight new polyphosphorylated proteins that interact genetically and physically with previous targets implicated in ribosome biogenesis. The expanded target network includes vacuolar proteins Prb1 and Apl5, whose modification with polyP suggests a model for feedback regulation of polyP synthesis, while raising questions regarding the location of polyphosphorylation *in vivo*.

2.2. Introduction

Polyphosphate (polyP) is a polymer of inorganic phosphate moieties joined together in linear chains ranging from 3 to 1000 s of residues in length. Evidence suggests that these chains exist in all cells, although their length and concentration vary widely. PolyP is particularly abundant in the budding yeast *Saccharomyces cerevisiae*, comprising upward of 10% of the dry weight of the cell and reaching internal concentrations of over 200 mM in terms of individual phosphate units (1,2). Most of the polyP in yeast is stored in the vacuole following synthesis by the vacuolar membrane-bound VTC complex (3). Overall chain length is controlled by exo- and endopolyphosphatases Ddp1, Ppn1, Ppn2, and Ppx1 (4). In addition to its role in ion homeostasis and phosphate metabolism (5,6), Azevedo *et al*. (7) showed that polyP chains can be noncovalently added to lysine residues as a post-translational modification (PTM). They characterized this modification on proteins Nsr1 and Top1, providing evidence that polyP chains can regulate protein interactions and topoisomerase activity of purified Top1 *in vitro*, as well as the localization of Nsr1 and Top1 *in vivo*. Polyphosphorylation is nonenzymatic and occurs in polyacidic serine and lysine rich (PASK) motifs (7,8). While the sequence requirements for polyP addition are unclear, lysine residues appear to be the modified site (7,9,10). Consistent with this, mutation of lysine residues within predicted PASK motifs to arginine prevents polyphosphorylation of Nsr1, Top1, and Rpa34 (7,9). Polyphosphorylation causes dramatic electrophoretic shifts when protein extracts are run on denaturing Bis-Tris NuPAGE gels, but this same shift does not occur with traditional SDS/PAGE gels (7,9). The underlying reasons for this difference are not completely clear, although it could be related to the use of TEMED in the polymerization of SDS/PAGE gels (9).

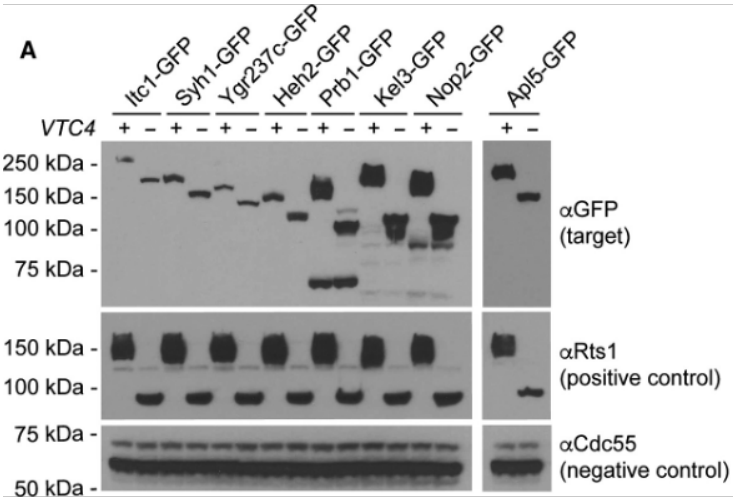
Recently, we reported the identification of an additional 15 polyphosphorylation targets in yeast, including a conserved network implicated in ribosome biogenesis (9). Many of the PASK

motifs in these proteins are contained within intrinsically disordered regions that appear to be under evolutionary selection (11). Based on enrichment in ribosome-related functions, we uncovered a novel function for *VTC4*, encoding the catalytic subunit of the VTC complex (12), in polysome assembly (9). We also demonstrated that six human proteins, including homologs of our novel yeast targets, could be polyphosphorylated following the ectopic expression of *Escherichia coli* PPK, the bacterial polyP polymerase, in HEK293T cells (9). Subsequent studies using protein microarrays identified an additional eight human proteins as targets, in addition to five proteins that appear to bind polyP chains noncovalently (13). Altogether, work from our group and others suggests that lysine polyphosphorylation has the capacity to be a global protein modifier, akin to other lysine-based modifications such as acetylation or ubiquitylation (8,14).

Our previous strategy to identify targets of lysine polyphosphorylation in yeast took advantage of a set of strains wherein each open reading frame is expressed as a fusion with the GFP epitope (15). Candidate fusions from this set were crossed into a wild-type or *vtc4*Δ mutant background prior to analysis by NuPAGE and immunoblotting with an antibody against GFP. In this assay, a *VTC4*-dependent electrophoretic shift signals a candidate polyphosphorylated protein. In our previous work (9), we prioritized 90 targets from 427 proteins containing putative PASK motifs, defined by a sliding window of 20 amino acids with 75% D, E, S, or K amino acids with at least 1 K. This set of 90 proteins was enriched for multiple or long PASK motifs containing many lysine residues. In an attempt to further define the landscape of polyphosphorylation in *S. cerevisiae*, we have now screened the remainder of the candidates present in this GFP collection (See *Methods* section) using a similar strategy.

2.3. Results and discussion

Using our previously defined screening approach, we have now uncovered an additional eight candidate targets. As observed in our previous work, the shifts conferred by polyP (i.e., in the presence of a functional *VTC4* gene) are dramatic and quantitative, with the whole population of target proteins being affected (**Figure 1**). We attribute this 'all or nothing' pattern to the high concentration of polyP in cells and in extracts following cell lysis, which could be quantitatively modifying proteins *in vitro*. *In vivo* polyphosphorylation of any given target may be sub-stoichiometric. As we previously found for other targets (9), polyP-induced shifts collapsed when samples were analyzed *via* SDS/PAGE instead of NuPAGE (**Figure S1**). New polyphosphorylated targets uncovered in our screen include homologs of proteins implicated in human disease (**Figure 1**, see below). Despite the identification of proteins predicted to function in diverse processes, new targets display extensive physical and genetic interactions with previously identified polyphosphorylated proteins (**Figure 2**). Heh2 is an inner nuclear membrane protein involved in ensuring the quality control of nuclear pore complexes (18). Ygr237c and Kel3 are uncharacterized proteins with diverse physical and genetic interactions and putative cytoplasmic localization (19). Itc1 is a member of the Itc1-Isw2 chromatin remodeling complex involved in meiotic gene repression (20). Nop2 is an rRNA methyltransferase required for 27S rRNA processing and 60S ribosome biogenesis (21,22). While largely uncharacterized, Syh1 co-purifies with ribosomes (23), suggesting that it too functions in translation or ribosome assembly. *SYH1* also displays genetic interaction with *EBP2*, encoding a protein involved in 60S biogenesis (24). The identification of Nop2 and Syh1 is consistent with our previous observation that *vtc4*Δ cells show defects in polysome formation and the previous identification of negative genetic interactions between *vtc4*Δ mutants and deletions of genes impacting ribosome biogenesis (*RPP1A*, *MAK11*,



B

Protein	Description or Function	Homolog
Itc1	Chromatin remodeller	N/A
Syh1	Unknown	GIGYF1/2
Ygr237c	Unknown	N/A
Heh2	Inner nuclear membrane	LEMD2/3
Prb1	Vacuolar protease	PCSK9
Kel3	Unknown	KLHDC2
Nop2	rRNA methyltransferase	**NOP2**
Apl5	Cargo transport to vacuole	**AP3δ1**

Figure 1. Identification of new polyphosphorylated targets in yeast. (**A**) NuPAGE analysis of polyphosphorylated proteins. Paired GFP-tagged proteins were extracted from wild-type or *vtc4*Δ mutant cells using TCA lysis prior to NuPAGE analysis, western blotting to PVDF membrane and detection using the indicated antibodies. Rts1 serves as a positive control. Cdc55 serves as a negative control. Images representative of N = 4 or greater for each target. (**B**) Table of new polyphosphorylated targets uncovered in this study. Human homologs were determined using the YeastMINE tool. Bold indicates the presence of a PASK sequence in human homolog (as defined by Bentley-DeSousa *et al.* (9)).

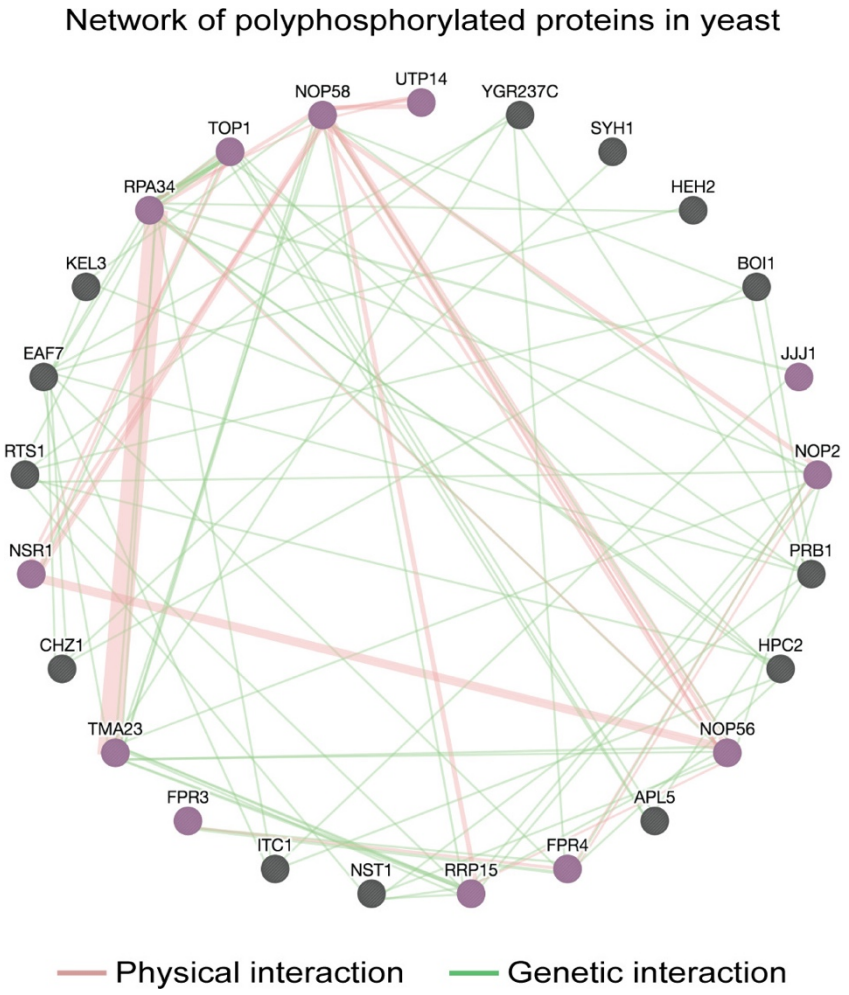


Figure 2. Polyphosphorylated targets are connected by genetic and physical interactions. Genetic and physical associations between new and previously identified targets were computed using the GeneMANIA tool (see *Methods* section). Each node (circle) represents an individual polyphosphorylated protein (n = 22). Physical and genetic interactions are indicated with green and pink lines, respectively. Purple nodes indicate localization to the nucleolus (n = 12; FDR = 1.85 × 10−7).

and *RPC25*) and translation (*ELP3*, *ELP6*, and *MNR1*) (25,26). These data are also consistent with findings in other eukaryotes. In particular, polyP localizes to the nucleolus, the site of ribosome biogenesis, and interacts with nucleolar proteins in trypanosomes (27). Nucleolar polyP is also thought to regulate RNA polymerase I in myeloma cells (28). Our expanded target list also included a number of proteins associated with vacuolar biology. Prb1 encodes the yeast vacuolar proteinase B (29). Apl5 is involved in transporting protein cargo from the ER-Golgi system to the vacuole (30). Since the vast majority of polyP localizes to the vacuole in *S. cerevisiae*, these proteins are ideal candidate effectors of polyP-mediated signaling. Therefore, we carried out further experiments to validate the polyphosphorylation of these new targets and to determine amino acid sequences required for the modification.

We first sought to confirm that the electrophoretic shift detected for Prb1-GFP in the presence of *VTC4* was due to polyP. Since polyphosphorylation occurs nonenzymatically even in harsh conditions (7), we added synthetic polyP of 75 units in length to *vtc4*Δ whole-cell protein extracts generated *via* a trichloroacetic acid (TCA) lysis protocol. PolyP addition caused a concentration-dependent electrophoretic shift (**Figure 3A**). Addition of 5 mM polyP conferred an electrophoretic shift to Prb1-GFP in *vtc4*Δ extracts that was equal to the shift observed in the wild-type control. In contrast, the same concentration of sodium phosphate had no impact on the mobility of Prb1-GFP, confirming that polyP is required for the modification (**Figure 3A**). PolyP-induced shifts also scaled with chain length, with longer chains producing a more dramatic change in electrophoretic mobility (**Figure S2A**).

The Prb1 protease is a heavily processed protein that undergoes a series of glycosylations and programed cleavages to convert the zymogen precursor (pre-pro) form to the fully active enzyme (mPrb1) (31). Processing occurs in step with its transit through the ER-Golgi system to

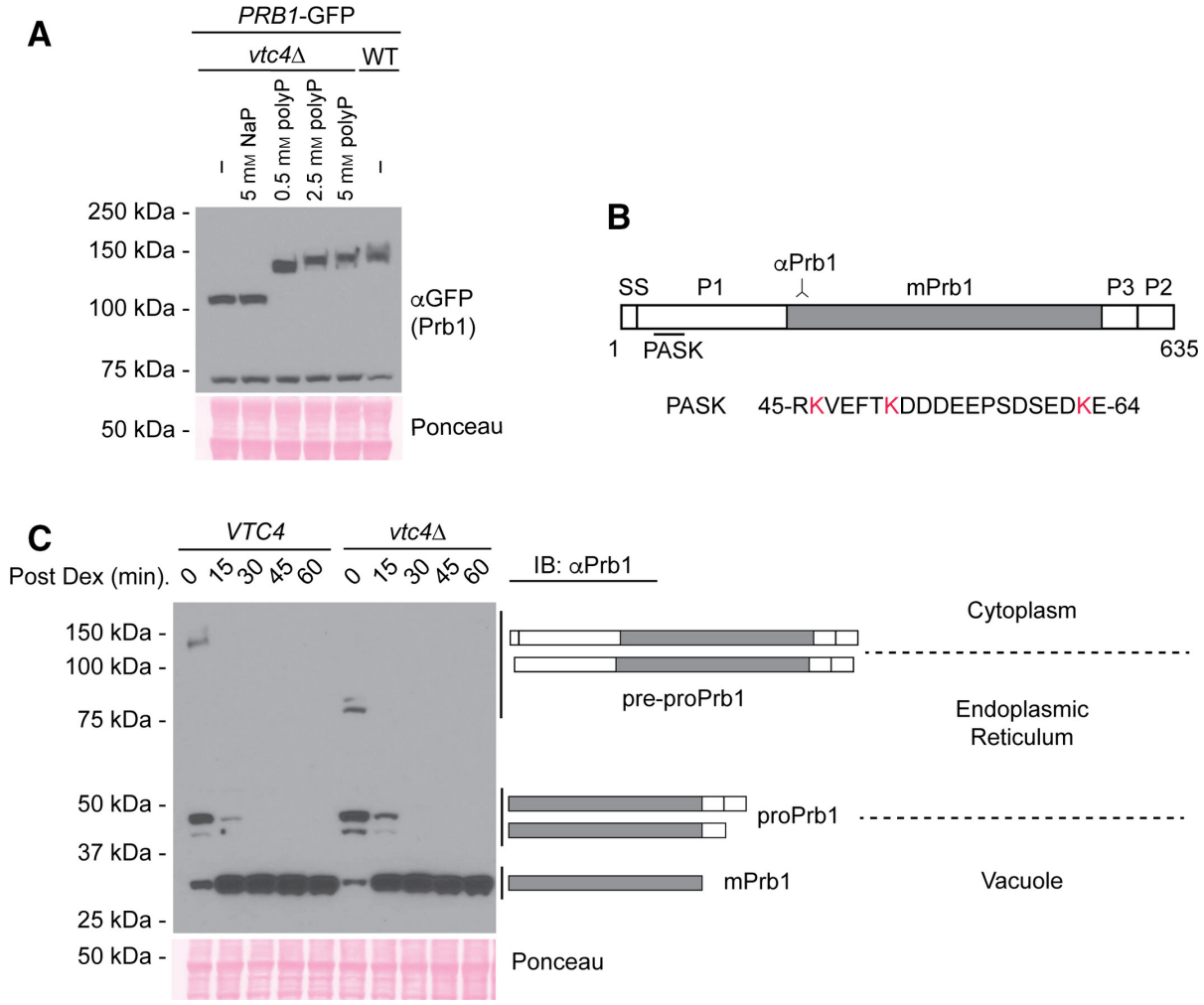


Figure 3. Analysis of Prb1 polyphosphorylation. (**A**) Indicated concentrations of polyP (75 units) or sodium phosphate control were added to *vtc4*Δ mutant cell extracts expressing GFP-tagged Prb1 and polyP-induced shifts were analyzed by western blotting with an antibody against GFP after NuPAGE analysis. The band at the bottom is likely a breakdown product containing GFP. Representative of N = 2. (**B**) Schematic of inactive pre-pro form of Prb1. The region recognized by the antibody is shown. Red lysines indicate candidate sites for polyP attachment. (**C**) Prb1 was expressed under the GAL promoter (see *Methods* section) for 2 h prior to the addition of glucose to stop transcription. Processing and polyphosphorylation of Prb1 at the indicated time points was monitored via NuPAGE analysis. The proposed schematic for Prb1 processing indicated on the right was adapted from that proposed in Mark *et al.* (33). Representative of N = 2.

the vacuole (**Figure 3B** and **Figure 3C**). Since the C-terminal GFP tag of Prb1-GFP is predicted to be removed during its processing, **Figure 1A** and **Figure 3A** only confirmed polyphosphorylation of pre-proPrb1. In order to study polyphosphorylation of Prb1 in the context of its processing from zymogen to active enzyme, we used a previously described galactose overexpression system (32). Induction of *PRB1* transcription with the addition of galactose, followed by addition of glucose to turn off that transcription, allowed for the production of a population of native Prb1 whose processing could be monitored over time. Following analysis by NuPAGE and western blotting, we detected Prb1 with a previously published antibody that recognizes the first 14 amino acids of the fully processed and active (mPrb1) protein (**Figure 3B**) (31). We expect this antibody to detect all forms of Prb1. Only pre-proPrb1, but not any of the processed forms, exhibited an electrophoretic shift in *VTC4* strains relative to *vtc4*Δ mutants (**Figure 3C**). As a control, the previously identified target Rts1 (9) showed polyphosphorylation throughout the time course in *VTC4* cells (**Supplementary Figure 2B**). These data suggest that the P1 segment of Prb1, which is removed in the first self-catalyzed cleavage event within the endoplasmic reticulum (31), is the modified species. Indeed, the predicted PASK motif is located in the P1 fragment, as indicated in **Figure 3B**. Importantly, analysis of these same samples *via* traditional SDS/PAGE, which does not resolve polyP-induced shifts (9), showed identical migration of all species, consistent with the electrophoretic shift being due to polyphosphorylation (**Supplementary Figure 2C**). In this analysis, we also observed slightly delayed processing of Prb1 in *vtc4*Δ mutants, although it is unclear if this is biologically meaningful (**Supplementary Figure 2C**).

Polyphosphorylation of the P1 fragment may be required to ensure early processing steps occur in a manner consistent with the production of an active mPrb1 protein. In this capacity, polyP

may function redundantly or in coordination with other PTMs, including glycosylations. Alternatively, polyP may function in a quality control capacity to regulate the function or degradation of Prb1 that is improperly processed by the ER-Golgi system. A similar role has been suggested for the SCF^{Saf1} ubiquitin ligase, which ubiquitylates Prb1 but does not impact the bulk turnover of the protein population (32,33). The hypothesis that polyP modulates protein stability is consistent with its previously described role as a molecular chaperone in other biological systems (34).

Prb1 is an interesting target in part because it emphasizes the importance of determining where within the cell polyphosphorylation occurs. While most polyP is localized to the yeast vacuole, it has also been detected in other compartments including the mitochondria, cytoplasm, and nucleus (7,35-37). Importantly, the bioavailability of these pools of polyP to act in polyphosphorylation reactions *in vivo* is not clear. To our knowledge, polyP localization to the ER lumen has not been well-documented. But, a fraction of the polyP-synthesizing VTC complex was proposed to reside at the ER membrane (38).

Apl5, the second vacuole-related protein uncovered in our screen, functions as a member of the conserved AP3 complex. AP3 selectively transports protein cargo from the Golgi to lysosome-related organelles such as the yeast vacuole (39,40). As with Prb1-GFP, Apl5-GFP polyphosphorylation was rescued by the addition of increasing concentrations of polyP to *vtc4*Δ extracts, and polyP-induced shifts scaled with chain length (**Figure 4A** and **Supplementary Figure 2D**). Other subunits of AP3 were not polyphosphorylated (**Figure 4B**), suggesting that Apl5 may be a focal point for AP3 regulation by polyP. As predicted, the PASK motif of Apl5 is required for the electrophoretic shift observed in *VTC4* strains (**Figure 4C**). This PASK motif is located in the 'ear domain' of the protein (**Figure 4D**), previously demonstrated to be required for

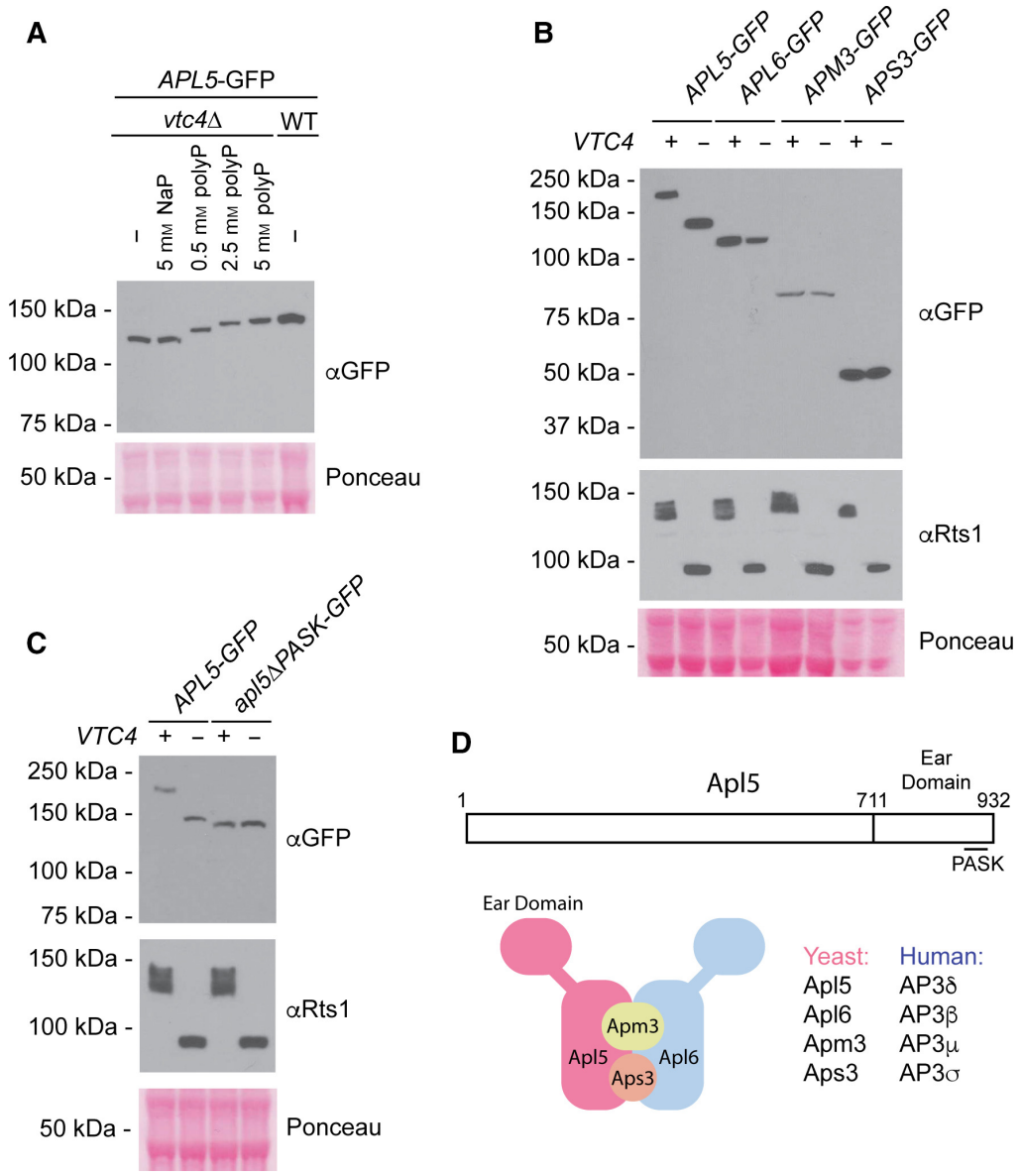


Figure 4. Analysis of Apl5 polyphosphorylation. (**A**) Indicated concentrations of polyP (75 units) or sodium phosphate control were added to vtc4Δ mutant cell extracts expressing GFP-tagged Apl5 and polyP-induced shifts were analyzed by western blotting with an antibody against GFP after NuPAGE analysis. Representative of N = 3. (**B**) The indicated components of the AP3 complex were expressed as GFP fusions in WT and *vtc4*Δ strains and analyzed by western blotting following NuPAGE analysis of protein extracts. Representative of N = 3. (**C**) The PASK motif of Apl5 is required for its polyphosphorylation. Protein extracts from the indicated strains were analyzed as described in B. Representative of N = 3. (**D**) Representation of the conserved Apl5 protein and the AP3 complex. The schematic of the AP3 complex is adapted from that proposed previously (39).

interaction with AP3 regulators such as Vps41 (30,41). This interaction is thought to occur when Vps41 is integrated into the HOPS complex and promotes AP3 docking to the vacuole membrane, which allows proper delivery of vacuolar cargo (30). The other large subunit of the AP3 complex, Apl6, also has a PASK motif (9), although we did not detect reproducible Vtc4-dependent electrophoretic shifts of this protein on NuPAGE gels (**Figure 4B**). Notably, Apl6 only has two lysines in its PASK motif, compared to 13 for Apl5 (**Supplementary Figure 3A**). Since we previously found that electrophoretic shifts due to polyphosphorylation scale in proportion to the number of lysines in the PASK motif (9), it is possible that Apl6 polyphosphorylation is not easily detected *via* this method.

AP3 mutant strains were previously described as having low levels of polyP (42). AP3 could impact polyP synthesis by transporting proteins involved in polyP synthesis or storage to the vacuole (42-44). In the context of this model, polyphosphorylation of AP3 may serve as means of feedback to regulate AP3 function. Importantly, the impact of AP3 on polyP metabolism could be mediated by multiple cargos, as over 200 genes are known to impact polyP synthesis in *S. cerevisiae* (42). In humans, mutations in the AP3β and AP3δ subunits of the AP3 complex, homologs of Apl6 and Apl5, respectively (**Figure 4D**) (39), give rise to Hermansky–Pudlak syndrome (HPS) subtypes 2 and 10 (45-47). HPS is a pleiotropic disease characterized by defects in the transport of proteins to lysosome-related organelles (48-49). Notably, a hallmark of HPS is bleeding diathesis and a failure to accumulate or retain polyP in the dense granules of platelets (48,49). PolyP has a well-characterized role in the blood coagulation cascade and works by stimulating activation of several clotting factors (50). AP3β1, AP3β2, and AP3δ also have PASK motifs as defined by our criteria (**Supplementary Figure 3B**), and Azevedo *et al*. (13) provided evidence that AP3β1 can be polyphosphorylated. Direct regulation

by polyP may be a conserved feature of AP3 biology. As with Prb1, where within the transit pathway to the vacuole AP3 subunits interact with polyP is a critical question that remains to be answered.

Altogether, our work expands the scope of polyphosphorylation in yeast and provides new avenues for exploring the functional consequences of this intriguing PTM. Expanding the catalog of polyphosphorylated proteins in other eukaryotes will be a critical step in understanding the molecular and cellular functions of polyP in these systems.

2.4. Methods

Yeast strains

All strains are in the S288C BY474 background and were generated using standard methods. Strains were analyzed *via* PCR in a manner similar to that described by the yeast deletion consortium (http://www-sequence.stanford.edu/group/yeast_deletion_project/protocols.html) to confirm the presence of the knockout cassette and the absence of the wild-type open reading frame for gene deletions and the correct position of the tag-marker cassette for epitope-tagged strains. This analysis was also done for strains streaked or generated from strains taken from the GFP-tagged set. Here, a common forward primer was used to check the position of GFP-*HIS3MX* cassette with a gene-specific reverse primer outside of the area of homology used for recombination at the 3′ end of the gene (typically 300–500 bp downstream of the stop codon). The common forward primer P1 (also known in our lab as KandCV) has the sequence 5′-TTCGCCTCGACATCATCTGCCC-3′ and primes in the common *TEF* terminator of the 'MX' style cassettes. Thus, this primer is useful in confirming cassette positions associated with other yeast collections including the TAP-tagged and deletion libraries. A sample PCR analysis is shown in **Supplementary Figure 4**. Strain confirmations were always done on colony-purified isolates, whose genotypes are described in **Supplementary Table 1**. For the GAL shut-off experiment used to examine Prb1 processing, wild-type *GALpr-PRB1* and *GALpr-PRB1 vtc4*Δ mutant strains were grown in synthetic complete (SC) media with 2% raffinose overnight. Cells were diluted to OD_{600} = 0.3 in SC media with 2% raffinose and grown until OD_{600} = 0.6. Cultures were then supplemented with 2% galactose for 30 min to induce Prb1 expression. Subsequently, glucose was added to a final concentration of 2% and time points were taken every 15 min. For all other

experiments, cells were grown in YPD media supplemented with 0.005% adenine and tryptophan. All strains were grown at 30 °C.

Screening protocol

Candidate target strains were recovered from the yeast GFP-tagged collection and the *vtc4*Δ and *ppn1*Δ mutations were crossed into the strains as previously described (9). Paired protein extracts were generated and analyzed using NuPAGE analysis following the preparation of protein extracts *via* TCA lysis (see below). Rts1 was used as a control polyphosphorylated protein for each sample analyzed. Candidates were confirmed in a secondary screen before streaking strains for single colonies and confirming the correct position of the GFP tag. As described throughout the results section, select hits were reconfirmed by re-tagging candidates in wild-type and *vtc4*Δ strains and/or with the use of antibodies directed against native targets. A list of screened targets and their predicted PASK motifs is included in **Supplementary Table 1**. We have now analyzed 321 of 427 PASK containing proteins in yeast.

Protein analysis

Protein extraction was done using a TCA lysis method that has been described previously (9). A similar protocol is reiterated here. Briefly, 3–6 OD_{600} equivalents of yeast cells were lysed in 300 µL of 20% TCA with 100 µL of acid-washed glass beads. Supernatant was recovered and beads were washed with 300 µL of 5% TCA and combined with the first supernatant. Samples were centrifuged at 16 000 ***g*** for 4 min at 4 °C. Pellets were resuspended in 100 µL SDS/PAGE sample buffer (0.8 mL 3× SDS/PAGE sample buffer, 100 µL 1.5 M Tris-HCl pH 8.8, 100 µL 1 M DTT). Samples were boiled for 5 min and centrifuged again at 16 000 ***g*** for 4 min. Supernatant was removed for immediate analysis or stored at −80 °C until use. Typically, 10 µL of extract (~ 75 µg) was loaded for each lane, but this varied depending on the expression of the protein

under analysis. We have observed that protein samples tend to lose their polyphosphorylation after multiple freeze thaw cycles. We recommend same-day NuPAGE analysis of extracted proteins.

Western blotting

Buffers used for NuPAGE and SDS/PAGE analysis were described previously (9). SDS/PAGE gels used for this work were 10% final concentration made with 30% acrylamide/bis solution at a ratio of 37.5 : 1 (BioRad 1610158, Hercules, CA, USA). Please note that SDS/PAGE analysis does not resolve polyP-induced shifts. PVDF membrane (Biorad 162-0177) was used for Western blotting of separated protein samples. Primary and secondary antibodies used for immunoblotting, including dilution information for each antibody, are described in **Supplementary Table 2**. Washed blots were exposed to ECL from Millipore (Burlington, MA, USA: Sigma WBKLS0500 or WBLUF0500). Ponceau S stain (Sigma P-3504, St. Louis, MO, USA) was used to verify equal loading across the blots and to monitor the quality of transfer for each blot.

Homologs and Network analysis

Homologs were determined *via* the YeastMINE tool (16). Genetic networks were generated using GeneMANIA (GeneMANIA.org; June 12, 2019) (17). Gene attributes were set to zero, only genetic and physical interactions were computed and shown, all other settings were left as default. FDR displayed was as calculated for nucleolar localization by the GeneMANIA tool.

***In vitro* polyphosphorylation assays**

In vitro polyphosphorylation assays were carried out by mixing the indicated concentrations of polyP with TCA-style protein preps, followed by incubation at room temperature for 20 min before re-boiling of reactions and NuPAGE analysis, as described above. PolyP chains used for this analysis are an average of 75 units in length and were purchased from Kerafast (Medium chain, EUI005, Boston, MA, USA). For supporting *in vitro* analyses, short (14 units), medium (60 units),

and long (130 units) chains were gifted by T. Shiba (Regentiss, Kunitachi City, Japan). Extra-long polyP chains (700 units) were from Kerafast (EUI002).

2.5. Acknowledgements

We thank the members of the Downey lab for critical reading of the manuscript and reviewers for insightful comments. We thank Dr. Elizabeth Jones' lab for the anti-Prb1 antibody and T. Shiba for polyP standards. ABD was supported by an Ontario Graduate Scholarship. This work was funded by a Canadian Institutes of Health Research Project Grant to MD (PJT-148722). We also acknowledge funding from a Rare Disease Foundation Microgrant (grant number 1937).

2.6. References

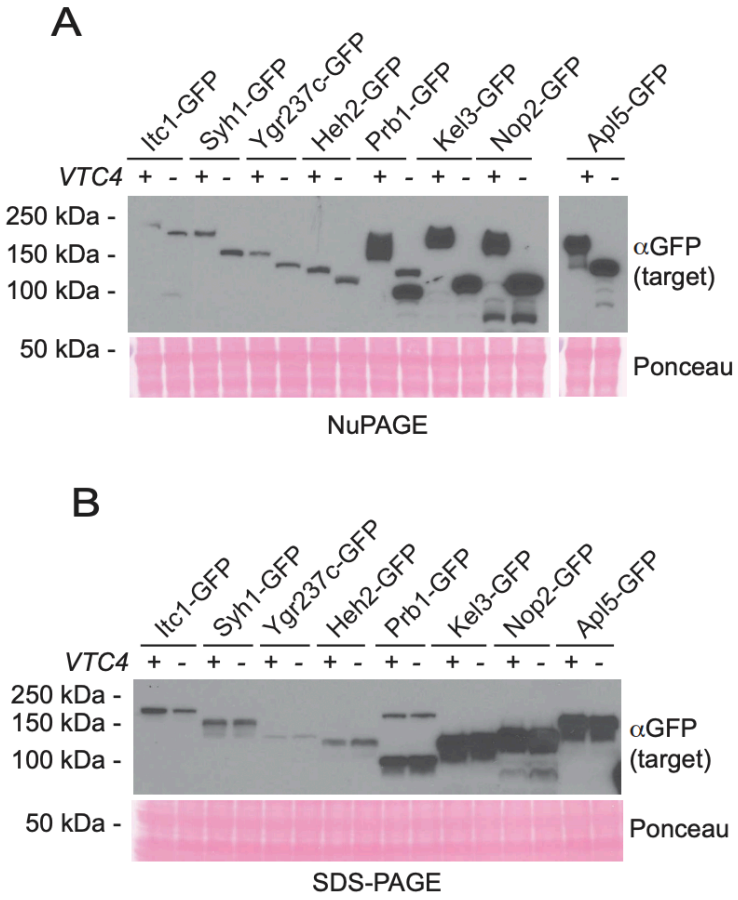
1. Auesukaree C, Homma T, Tochio H, Shirakawa M, Kaneko Y and Harashima S (2004) Intracellular phosphate serves as a signal for the regulation of the PHO pathway in Saccharomyces cerevisiae. J Biol Chem 279, 17289–17294.
2. Kornberg A, Rao NN and Ault-Riche D (1999) Inorganic polyphosphate: a molecule of many functions. Annu Rev Biochem 68, 89–125.
3. Gerasimaite R, Sharma S, Desfougeres Y, Schmidt A and Mayer A (2014) Coupled synthesis and translocation restrains polyphosphate to acidocalcisomelike vacuoles and prevents its toxicity. J Cell Sci 127, 5093–5104.
4. Gerasimaite R and Mayer A (2017) Ppn2, a novel Zn (2+)-dependent polyphosphatase in the acidocalcisomelike yeast vacuole. J Cell Sci 130, 1625–1636.
5. Eskes E, Deprez MA, Wilms T and Winderickx J (2018) pH homeostasis in yeast; the phosphate perspective. Curr Genet 64, 155–161.
6. Rosenfeld L, Reddi AR, Leung E, Aranda K, Jensen LT and Culotta VC (2010) The effect of phosphate accumulation on metal ion homeostasis in Saccharomyces cerevisiae. J Biol Inorg Chem 15, 1051– 1062.
7. Azevedo C, Livermore T and Saiardi A (2015) Protein polyphosphorylation of lysine residues by inorganic polyphosphate. Mol Cell 58, 71–82.
8. Azevedo C and Saiardi A (2016) Why always lysine? The ongoing tale of one of the most modified amino acids. Adv Biol Regul 60, 144–150.
9. Bentley-DeSousa A, Holinier C, Moteshareie H, Tseng YC, Kajjo S, Nwosu C, Amodeo GF, Bondy-Chorney E, Sai Y, Rudner A et al. (2018) A screen for candidate targets of lysine polyphosphorylation uncovers a conserved network implicated in ribosome biogenesis. Cell Rep 22, 3427–3439.
10. Azevedo C and Saiardi A (2016) The new world of inorganic polyphosphates. Biochem Soc Trans 44, 13–17.
11. Zarin T, Strome B, Nguyen Ba AN, Alberti S, FormanKay JD and Moses AM (2019) Proteome-wide signatures of function in highly diverged intrinsically disordered regions. Elife 8, e46883. https://doi.org/10. 7554/eLife.46883
12. Hothorn M, Neumann H, Lenherr ED, Wehner M, Rybin V, Hassa PO, Uttenweiler A, Reinhardt M, Schmidt A, Seiler J et al. (2009) Catalytic core of a membrane-associated eukaryotic polyphosphate polymerase. Science 324, 513–516.
13. Azevedo C, Singh J, Steck N, Hofer A, Ruiz FA, Singh T, Jessen HJ and Saiardi A (2018) Screening a protein array with synthetic biotinylated inorganic polyphosphate to define the human PolyP-ome. ACS Chem Biol 13, 1958–1963.
14. Bentley-DeSousa A and Downey M (2019) From underlying chemistry to therapeutic potential: open questions in the new field of lysine polyphosphorylation. Curr Genet 65, 57–64.
15. Huh WK, Falvo JV, Gerke LC, Carroll AS, Howson RW, Weissman JS and O'Shea EK (2003) Global analysis of protein localization in budding yeast. Nature 425, 686–691.
16. Balakrishnan R, Park J, Karra K, Hitz BC, Binkley G, Hong EL, Sullivan J, Micklem G and Cherry JM (2012) YeastMINE–an integrated data warehouse for Saccharomyces cerevisiae data as a multipurpose toolkit. Database (Oxford) 2012, bar062.

17. Warde-Farley D, Donaldson SL, Comes O, Zuberi K, Badrawi R, Chao P, Franz M, Grouios C, Kazi F, Lopes CT et al. (2010) The GeneMANIA prediction server: biological network integration for gene prioritization and predicting gene function. Nucleic Acids Res 38, W214–W220.
18. Webster BM, Colombi P, Jager J and Lusk CP (2014) Surveillance of nuclear pore complex assembly by ESCRT-III/Vps4. Cell 159, 388–401.
19. Cherry JM, Hong EL, Amundsen C, Balakrishnan R, Binkley G, Chan ET, Christie KR, Costanzo MC, Dwight SS, Engel SR et al. (2012) Saccharomyces genome database: the genomics resource of budding yeast. Nucleic Acids Res 40, D700–D705.
20. Sugiyama M and Nikawa J (2001) The Saccharomyces cerevisiae Isw2p-Itc1p complex represses INO1 expression and maintains cell morphology. J Bacteriol 183, 4985–4993.
21. Hong B, Brockenbrough JS, Wu P and Aris JP (1997) Nop2p is required for pre-rRNA processing and 60S ribosome subunit synthesis in yeast. Mol Cell Biol 17, 378–388.
22. Sharma S, Yang J, Watzinger P, Kotter P and Entian KD (2013) Yeast Nop2 and Rcm1 methylate C2870 and C2278 of the 25S rRNA, respectively. Nucleic Acids Res 41, 9062–9076.
23. Fleischer TC, Weaver CM, McAfee KJ, Jennings JL and Link AJ (2006) Systematic identification and functional screens of uncharacterized proteins associated with eukaryotic ribosomal complexes. Genes Dev 20, 1294–1307.
24. Okano A, Wan K, Kanda K, Yabuki Y, Funato K and Mizuta K (2015) SMY2 and SYH1 suppress defects in ribosome biogenesis caused by ebp2 mutations. Biosci Biotechnol Biochem 79, 1481–1483.
25. Chatr-Aryamontri A, Oughtred R, Boucher L, Rust J, Chang C, Kolas NK, O'Donnell L, Oster S, Theesfeld C, Sellam A et al. (2017) The BioGRID interaction database: 2017 update. Nucleic Acids Res 45, D369–D379.
26. Costanzo M, VanderSluis B, Koch EN, Baryshnikova A, Pons C, Tan G, Wang W, Usaj M, Hanchard J, Lee SD et al. (2016) A global genetic interaction network maps a wiring diagram of cellular function. Science 353, aaf1420.
27. Negreiros RS, Lander N, Huang G, Cordeiro CD, Smith SA, Morrissey JH and Docampo R (2018) Inorganic polyphosphate interacts with nucleolar and glycosomal proteins in trypanosomatids. Mol Microbiol 110, 973–994.
28. Jimenez-Nunez MD, Moreno-Sanchez D, HernandezRuiz L, Benitez-Rondan A, Ramos-Amaya A, Rodriguez-Bayona B, Medina F, Brieva JA and Ruiz FA (2012) Myeloma cells contain high levels of inorganic polyphosphate which is associated with nucleolar transcription. Haematologica 97, 1264–1271.
29. Moehle CM, Aynardi MW, Kolodny MR, Park FJ and Jones EW (1987) Protease B of Saccharomyces cerevisiae: isolation and regulation of the PRB1 structural gene. Genetics 115, 255–263.
30. Angers CG and Merz AJ (2009) HOPS interacts with Apl5 at the vacuole membrane and is required for consumption of AP-3 transport vesicles. Mol Biol Cell 20, 4563–4574.
31. Moehle CM, Dixon CK and Jones EW (1989) Processing pathway for protease B of Saccharomyces cerevisiae. J Cell Biol 108, 309–325.
32. Mark KG, Simonetta M, Maiolica A, Seller CA and Toczyski DP (2014) Ubiquitin ligase trapping identifies an SCF(Saf1) pathway targeting unprocessed vacuolar/ lysosomal proteins. Mol Cell 53, 148–161.

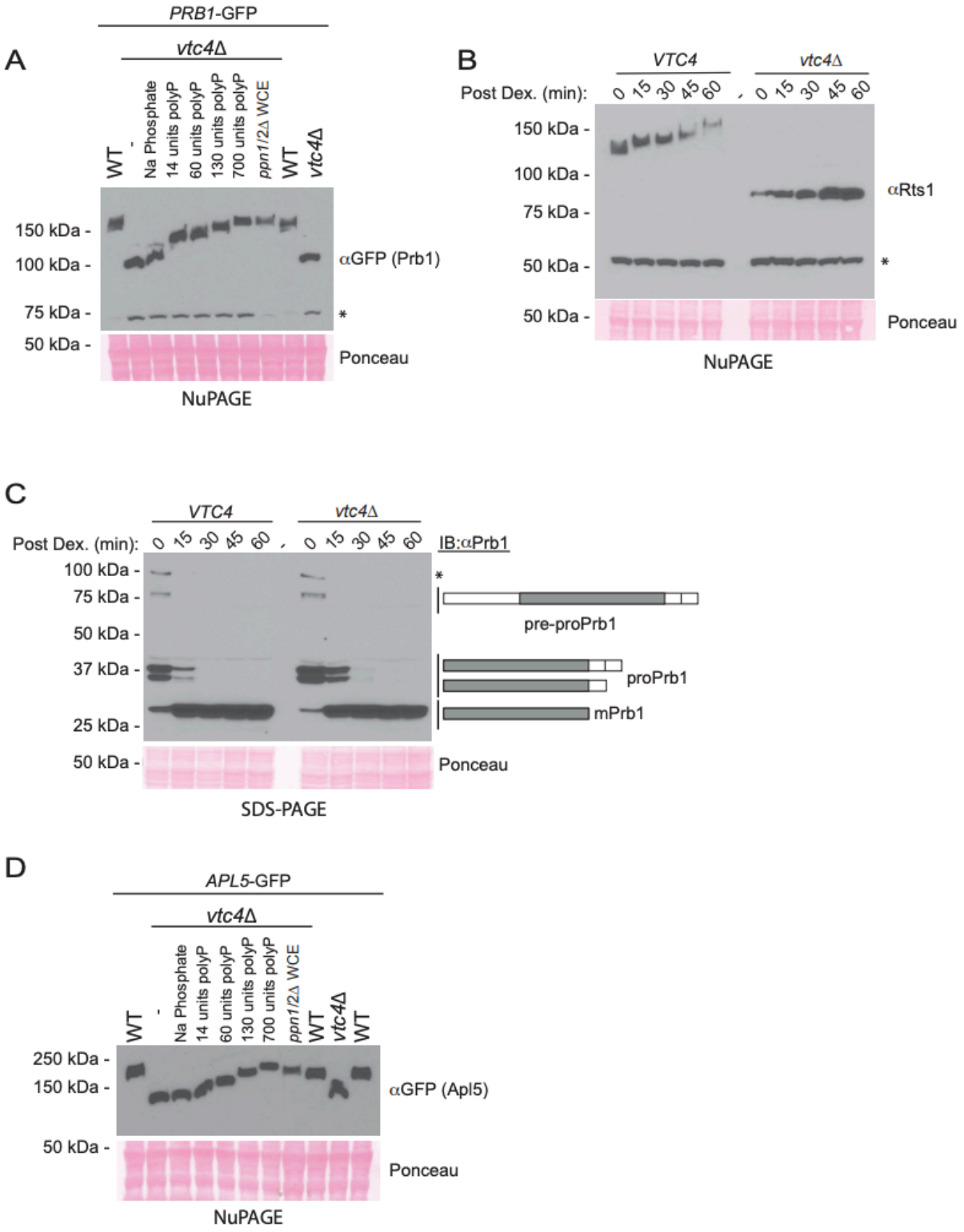
33. Mark KG, Meza-Gutierrez F, Johnson JR, Newton BW, Krogan NJ and Toczyski DP (2015) Prb1 protease activity is required for its recognition by the FBox protein Saf1. Biochemistry 54, 4423–4426.
34. Gray MJ, Wholey WY, Wagner NO, Cremers CM, Mueller-Schickert A, Hock NT, Krieger AG, Smith EM, Bender RA, Bardwell JC et al. (2014) Polyphosphate is a primordial chaperone. Mol Cell 53, 689–699.
35. Breus NA, Ryazanova LP, Dmitriev VV, Kulakovskaya TV and Kulaev IS (2012) Accumulation of phosphate and polyphosphate by Cryptococcus humicola and Saccharomyces cerevisiae in the absence of nitrogen. FEMS Yeast Res 12, 617–624.
36. Saito K, Ohtomo R, Kuga-Uetake Y, Aono T and Saito M (2005) Direct labeling of polyphosphate at the ultrastructural level in Saccharomyces cerevisiae by using the affinity of the polyphosphate binding domain of Escherichia coli exopolyphosphatase. Appl Environ Microbiol 71, 5692–5701.
37. Pestov NA, Kulakovskaya TV and Kulaev IS (2004) Inorganic polyphosphate in mitochondria of Saccharomyces cerevisiae at phosphate limitation and phosphate excess. FEMS Yeast Res 4, 643–648.
38. Gerasimaite R and Mayer A (2016) Enzymes of yeast polyphosphate metabolism: structure, enzymology and biological roles. Biochem Soc Trans 44, 234–239.
39. Cowles CR, Odorizzi G, Payne GS and Emr SD (1997) The AP-3 adaptor complex is essential for cargoselective transport to the yeast vacuole. Cell 91, 109– 118.
40. Odorizzi G, Cowles CR and Emr SD (1998) The AP-3 complex: a coat of many colours. Trends Cell Biol 8, 282–288.
41. Rehling P, Darsow T, Katzmann DJ and Emr SD (1999) Formation of AP-3 transport intermediates requires Vps41 function. Nat Cell Biol 1, 346–353.
42. Freimoser FM, Hurlimann HC, Jakob CA, Werner TP and Amrhein N (2006) Systematic screening of polyphosphate (poly P) levels in yeast mutant cells reveals strong interdependence with primary metabolism. Genome Biol 7, R109.
43. Besteiro S, Tonn D, Tetley L, Coombs GH and Mottram JC (2008) The AP3 adaptor is involved in the transport of membrane proteins to acidocalcisomes of Leishmania. J Cell Sci 121, 561–570.
44. Huang G, Fang J, SantAnna C, Li ZH, Wellems DL, Rohloff P and Docampo R (2011) Adaptor protein-3 (AP-3) complex mediates the biogenesis of acidocalcisomes and is essential for growth and virulence of Trypanosoma brucei. J Biol Chem 286, 36619–36630.
45. Wenham M, Grieve S, Cummins M, Jones ML, Booth S, Kilner R, Ancliff PJ, Griffiths GM and Mumford AD (2010) Two patients with Hermansky Pudlak syndrome type 2 and novel mutations in AP3B1. Haematologica 95, 333–337.
46. Mohammed M, Al-Hashmi N, Al-Rashdi S, Al-Sukaiti N, Al-Adawi K, Al-Riyami M and Al-Maawali A (2018) Biallelic mutations in AP3D1 cause HermanskyPudlak syndrome type 10 associated with immunodeficiency and seizure disorder. Eur J Med Genet.
47. Ammann S, Schulz A, Krageloh-Mann I, Dieckmann NM, Niethammer K, Fuchs S, Eckl KM, Plank R, Werner R, Altmuller J et al. (2016) Mutations in AP3D1 associated with immunodeficiency and seizures define a new type of Hermansky-Pudlak syndrome. Blood 127, 997–1006.
48. Huizing M, Anikster Y and Gahl WA (2000) Hermansky-Pudlak syndrome and related disorders of organelle formation. Traffic 1, 823–835.

49. Huizing M, Boissy RE and Gahl WA (2002) Hermansky-Pudlak syndrome: vesicle formation from yeast to man. Pigment Cell Res 15, 405–419.
50. Travers RJ, Smith SA and Morrissey JH (2015) Polyphosphate, platelets, and coagulation. Int J Lab Hematol 37 (Suppl 1), 31–35.

2.7. Supplemental figures

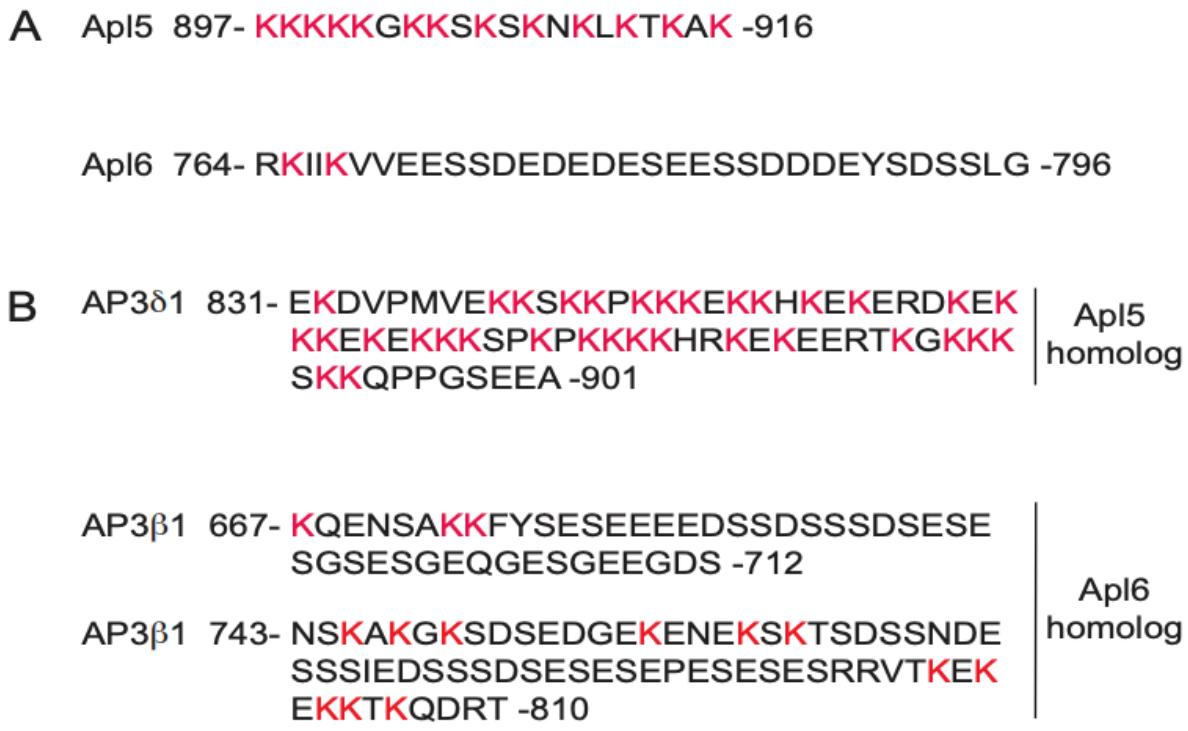


S1 Figure. Collapse of polyphosphate-induced shifts on SDS-PAGE gels. (**A**) analysis of protein samples from the indicated strains by NuPAGE was followed by immunoblotting with anti-GFP antibody. Representative of at least N=4 for each target. (**B**) As in A but with separation on SDS-PAGE gels instead of NuPAGE. Representative of N=2. Relates to Figure 1.

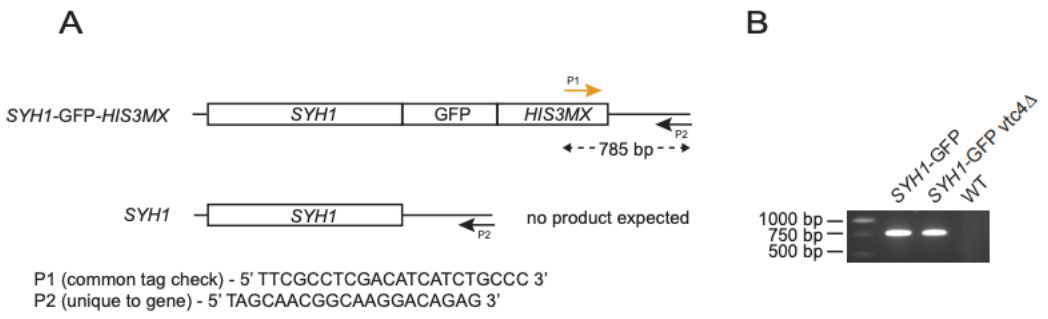


S2 Figure. Analysis of Prb1 and Apl5 polyphosphorylation. (**A**) Chain length dependence of polyP-induced shifts. 10 mM chains of the indicated lengths or extracts from ppn1Δ *ppn2*Δ

deletion mutants were mixed with extracts from *vtc4*Δ cells expressing Prb1-GFP and resolved via NuPAGE. The band marked with an asterisk at the bottom is likely a breakdown product containing GFP. Representative of N=2. (**B**) Polyphosphorylation of Rts1 was monitored during the experiment presented in Figure 3C using an antibody against Rts1. The band marked with an asterisk at the bottom is likely a breakdown product containing GFP. Representative of N=2. (**C**) Processing of pre-pro Prb1 was monitored for the experiment presented in Figure 3C using SDS-PAGE and immunoblotting with an antibody against Prb1. Note: SDS-PAGE does not resolve shifts due to lysine polyphosphorylation. Asterisk may represent a previously uncharacterized form of Prb1. Representative of N=2. (**D**) 10 mM chains of the indicated lengths or extracts from ppn1Δ *ppn2*Δ deletion mutants were mixed with extracts from *vtc4*Δ cells expressing Apl5-GFP and resolved via NuPAGE. Representative of N=4. Relates to Figures 3 and 4.



S3 Figure. PASK sequences within the AP3 complex. (**A**) PASK sequences of Apl5 and Apl6. Numbers indicate amino acid positions. (**B**) PASK sequences of AP3b and AP3d. Numbers indicate amino acid positions. Relates to Figure 4.



S4 Figure. Strategy for TAG checking. (**A**) Diagram of SYH1-GFP tagged locus (top) and WT locus (bottom). Primers used for confirmation are indicated. (**B**) gDNA prepared from the indicated strains was used in PCR reactions with the primers indicated in A. Strains used in the analysis are YMD2258, YMD2259 and YMD963. Relates to *Materials and Methods*.

2.8. Supplemental tables

Note: The tables that are important for the interpretation of the data presented have been included in the thesis. Please see the link provided below for all Supplemental Tables related to this article.

List of tables presented:

S1 Table. PASK containing proteins screened for polyphosphorylation in this study.

S2 Table. Yeast strains used in this study.

Online version of tables (S1 – S3):
feb213588-sup-0002-TableS1-S3.xlsx

S1 Table. PASK containing proteins screened for polyphosphorylation in this study.

S2 Table. Yeast strains used in this study.

S3 Table. Antibodies used in this study.

S1 Table – PASK containing proteins screened for polyphosphorylation in this study.

Systematic names from the *Saccharomyces* Genome Database (SGD)	Hits? (Yes/No)	Systematic names from the *Saccharomyces* Genome Database (SGD)	Hits? (Yes/No)
YFR019W		YDR195W	
YHR023W		YBR138C	
YML059C		YGL056C	
YDR457W		YMR215W	
YLR430W		YMR131C	
YOR341W		YKL081W	
YBL034C		YPR169W	
YER164W		YGR189C	
YDR283C		YDL101C	
YML072C		YJL013C	
YAL024C		YFR039C	
YMR280C		YML043C	
YGL197W		YOR229W	
YPR189W		YOR198C	
YNR031C		YOL041C	
YMR190C		YDL189W	
YNL088W		YDR473C	
YLR278C		YPR152C	
YPL137C		YNL206C	
YOL138C		YBR279W	
YDR293C		YDR055W	
YOR227W		YDL150W	
YDR301W		YPR148C	
YLR084C		YDR528W	
YGR270W		YBL091C	
YJR092W		YNL066W	
YDR097C		YNL175C	
YGL140C		YOR051C	
YKR096W		YGR142W	
YGR233C		YDL105W	
YLR371W		YDR309C	
YDR507C		YGR187C	
YNL250W		YOR057W	
YMR012W		YKL114C	

YGL133W	YES	YBR065C	
YCR033W		YDR171W	
YML049C		YHR052W	
YOR188W		YBL029W	
YJR035W		YKR071C	
YML010W		YDR173C	
YDR325W		YLR287C	
YIL112W		YOR261C	
YBR245C		YGR283C	
YKL033W		YML037C	
YBR059C		YOL007C	
YJL098W		YHR156C	
YFL034W		YPL157W	
YHR082C		YNL322C	
YPR104C		YOR006C	
YCR057C		YJR007W	
YGR140W		YDL173W	
YER075C		YDR054C	
YDR028C		YOR083W	
YOR048C		YGR239C	
YMR124W		YJL115W	
YGL241W		YDL051W	
YIL075C		YKR025W	
YDR356W		YCR016W	
YDR495C		YLR003C	
YGL180W		YOR281C	
YLR451W		YDR087C	
YOR373W		YLR132C	
YBR237W		YGL237C	
YPL105C	YES	YGR280C	
YDR409W		YNL148C	
YER151C		YGR075C	
YDL040C		YOR004W	
YGL141W		YER174C	
YGR071C		YDL139C	
YOR233W		YLR194C	
YMR102C		YDR174W	
YLR095C		YKL096W	
YKR099W		YMR233W	

YDL122W		YMR311C	
YLR397C		YLR221C	
YNL258C		YBL057C	
YPL158C		YER079W	
YPL074W		YOR078W	
YAL043C		YBR122C	
YGR237C	YES	YDR022C	
YKR010C		YFR001W	
YHR149C		YGR251W	
YNL059C		YPR067W	
YHR197W		YGL058W	
YOR206W		YLR421C	
YAR014C		YKL160W	
YDR333C		YNL143C	
YDR458C	YES	YCR043C	
YLR002C		YNL149C	
YLR403W		YMR123W	
YDR452W		YDR382W	
YMR075W		YDL081C	
YNL176C		YDR363W-A	
YNL299W		YGL137W	
YDR398W		YCR017C	
YEL060C	YES	YHR079C	
YNR038W		YBR086C	
YNL020C		YIR006C	
YGL023C		YDR080W	
YDR419W		YPL195W	YES
YPL263C	YES	YGR281W	
YOL117W		YPL270W	
YBR060C		YGR261C	
YOR027W		YBL011W	
YGR013W		YHL019C	
YNL039W		YNL275W	
YNL061W	YES	YMR307W	
YKR078W		YKL008C	
YGR246C		YLL010C	
YER140W		YBR127C	
YGR278W		YKL021C	
YKL088W		YHL003C	

YGL244W		YNR041C	
YHR064C		YHR195W	
YBR030W		YDR033W	
YIL045W		YNL173C	
YPL212C		YLR025W	
		YFR033C	

S2 Table – Yeast strains used in this study.

Strain Number	Strain Background	Full Genotype	Source
YMD2256	S288C BY474	MATa his3d1 leu2d0 met15d0 ura3d0 ITC1-GFP-HIS3MX	GFP collection
YMD2257	S288C BY474	MATa can1::STE2pr-LEU2 lyp1 ura 30 LYS2+ ITC1-GFP-HIS3MX ppn1::NATMX vtc4::KANMX	This study
YMD2258	S288C BY474	MATa his3d1 leu2d0 met15d0 ura3d0 SYH1-GFP-HIS3MX	GFP collection
YMD2259	S288C BY474	MATa can1::STE2pr-LEU2 lyp1 ura 30 LYS2+ SYH1-GFP-HIS3MX ppn1::NATMX vtc4::KANMX	This study
YMD2260	S288C BY474	MATa his3d1 leu2d0 met15d0 ura3d0 YGR237C-GFP-HIS3MX	GFP collection
YMD2261	S288C BY474	MATa can1::STE2pr-LEU2 lyp1 ura 30 LYS2+ YGR237C-GFP-HIS3MX ppn1::NATMX vtc4::KANMX	This study
YMD2262	S288C BY474	MATa his3d1 leu2d0 met15d0 ura3d0 HEH2-GFP-HIS3MX	GFP collection
YMD2263	S288C BY474	MATa can1::STE2pr-LEU2 lyp1 ura 30 LYS2+ HEH-GFP-HIS3MX ppn1::NATMX vtc4::KANMX	This study
YMD2264	S288C BY474	MATa his3d1 leu2d0 met15d0 ura3d0 PRB1-GFP-HIS3MX	GFP collection
YMD2265	S288C BY474	MATa can1::STE2pr-LEU2 lyp1 ura 30 LYS2+ PRB1-GFP-HIS3MX ppn1::NATMX vtc4::KANMX	This study
YMD2266	S288C BY474	MATa his3d1 leu2d0 met15d0 ura3d0 KEL3-GFP-HIS3MX	GFP collection
YMD2267	S288C BY474	MATa can1::STE2pr-LEU2 lyp1 ura 30 LYS2+ KEL3-GFP-HIS3MX ppn1::NATMX vtc4::KANMX	This study
YMD2268	S288C BY474	MATa his3d1 leu2d0 met15d0 ura3d0 NOP2-GFP-HIS3MX	GFP collection
YMD2269	S288C BY474	MATa can1::STE2pr-LEU2 lyp1 ura 30 LYS2+ NOP2-GFP-HIS3MX ppn1::NATMX vtc4::KANMX	This study
YMD2272	S288C BY474	MATa his3d1 leu2d0 met15d0 ura3d0 APL5-GFP-HIS3MX	GFP collection
YMD2273	S288C BY474	MATa can1::STE2pr-LEU2 lyp1 ura 30 LYS2+ APL5-GFP-HIS3MX ppn1::NATMX vtc4::KANMX	This study
YMD2380	S288C BY474	MATa his3d1 leu2d0 met15d0 ura3d0 APL5-GFP-HIS3MX	This study
YMD2381	S288C BY474	MATa his3d1 leu2d0 met15d0 ura3d0 APL6-GFP-HIS3MX	This study
YMD2382	S288C BY474	MATa his3d1 leu2d0 met15d0 ura3d0 APS3-GFP-HIS3MX	This study
YMD2531	S288C BY474	MATa his3d1 leu2d0 met15d0 ura3d0 APL5-GFP-HIS3MX vtc4::NATMX	This study

YMD2537	S288C BY474	MATa his3d1 leu2d0 met15d0 ura3d0 APL6-GFP-HIS3MX vtc4::NATMX	This study
YMD2539	S288C BY474	MATa his3d1 leu2d0 met15d0 ura3d0 APS3-GFP-HIS3MX vtc4::NATMX	This study
YMD2548	S288C BY474	MATa leu2d0 ura3d0 his3-1 met15d0 LYS2+ APM3-GFP-HIS3MX	This study
YMD2551	S288C BY474	MATa leu2d0 ura3d0 his3-1 met15d0 LYS2+ APM3-GFP-HIS3MX vtc4::NATMX	This study
YMD2583	S288C BY474	MATa leu2d0 ura3d0 his3-1 met15d0 LYS2+ APL5PASKΔ896-932-GFP-HIS3MX	This study
YMD2644	S288C BY474	MATa leu2d0 ura3d0 his3-1 met15d0 LYS2+ KANMX-GALpr-PRB1	This study
YMD2647	S288C BY474	MATa leu2d0 ura3d0 his3-1 met15d0 LYS2+ KANMX-GALpr-PRB1 vtc4::NATMX	This study
YMD2663	S288C BY474	MATa leu2d0 ura3d0 his3-1 met15d0 LYS2+ APL5PASKΔ896-932-GFP-HIS3MX vtc4::NATMX	This study
YMD2330	S288C BY474	MATa leu2d0 ura3d0 his3-1 met15d0 LYS2+ ppn1::KANMX ppn2::NATMX	Bentley-DeSousa *et al*., PMID: 29590613
YMD963	S288C BY474	MATa his3d1 leu2d0 met15d0 ura3d	Boone lab via Adam Rudner

CHAPTER 3 – MANUSCRIPT #2

Ddp1 cooperates with Ppx1 to counter a stress response initiated by nonvacuolar polyphosphate

Publication information:
McCarthy, L., Abramchuk, I., Wafy, G., Denoncourt, A., Lavallée-Adam, M., & Downey, M. (2022). Ddp1 cooperates with Ppx1 to counter a stress response initiated by nonvacuolar polyphosphate. *mBio*, 13(4), e0039022. https://doi.org/10.1128/mbio.00390-22

Authors' contributions:
Conceptualization: L.M., M.D. Methodology: L.M., I.A., M.L.A., M.D. Investigation: L.M., I.A., G.W., A.D., Supervision: M.D. Writing – original draft: L.M., M.D. Writing – review and editing: All authors.

Ddp1 cooperates with Ppx1 to counter a stress response initiated by nonvacuolar polyphosphate

Liam McCarthy[1,2], Iryna Abramchuk[2,3], Gamal Wafy[1,2], Alix Denoncourt[1,2], Mathieu Lavallée-Adam[2,3], Michael Downey[1,2]

1. Department of Cellular and Molecular Medicine, University of Ottawa, Ottawa, Ontario, Canada

2. Ottawa Institute of Systems Biology, University of Ottawa, Ottawa, Ontario, Canada

3. Department of Biochemistry, Microbiology and Immunology, University of Ottawa, Ottawa, Ontario, Canada

* Correspondence: mdowne2@uottawa.ca

3.1. Abstract

In diverse cells from bacterial to mammalian species, inorganic phosphate is stored in long chains called polyphosphate (polyP). These nearly universal polymers, ranging from three to thousands of phosphate moieties in length, are associated with molecular functions, including energy homeostasis, protein folding, and cell signaling. In many cell types, polyphosphate is concentrated in subcellular compartments or organelles. In the budding yeast *Saccharomyces cerevisiae*, polyP synthesis by the membrane-bound vacuolar transporter chaperone (VTC) complex is coupled to its translocation into the lumen of the vacuole, a lysosome-like organelle, where it is stored at high concentrations. In contrast, the ectopic expression of the bacterial polyphosphate kinase (PPK) results in the toxic accumulation of polyP outside the vacuole. In this study, we used label-free mass spectrometry to investigate the mechanisms underlying this toxicity. We find that PPK expression results in the activation of a stress response mediated in part by the Hog1 and Yak1 kinases and the Msn2/Msn4 transcription factors as well as by changes in protein kinase A (PKA) activity. This response is countered by the combined action of the Ddp1 and Ppx1 polyphosphatases that function together to counter polyP accumulation and downstream toxicity. In contrast, the ectopic expression of previously proposed mammalian polyphosphatases did not impact PPK-mediated toxicity in this model, suggesting either that these enzymes do not function directly as polyphosphatases *in vivo* or that they require cofactors unique to higher eukaryotes. Our work provides insight into why polyP accumulation outside lysosome-like organelles is toxic. Furthermore, it serves as a resource for exploring how polyP may impact conserved biological processes at a molecular level.

3.2. Importance

Cells from bacteria to humans have a molecule called polyphosphate (polyP) that functions in diverse processes. In many microbes, polyP is sequestered in granules or lysosome-related organelles such as vacuoles. In this study, we use an ectopic expression system to force budding yeast to accumulate polyP outside the vacuole. We use proteomics to demonstrate that this nonvacuolar polyP initiates a stress response mediated by a signaling cascade involving the Yak1 and Hog1 kinases and the Msn2 and Msn4 transcription factors. This response is countered by a pair of polyphosphatases with different enzymatic activities that function in concert to degrade polyP. Our results provide new insights into why polyP is confined to specific cell locations in many microbial cells.

3.3. Introduction

Inorganic phosphates can be joined in linear chains that range from three to thousands of residues in length. These polymers, called polyphosphate, or "polyP," have been implicated in diverse biological processes spanning both prokaryotic and eukaryotic species. In the budding yeast *Saccharomyces cerevisiae*, polyP is synthesized by the vacuolar transporter chaperone (VTC) complex (1). The VTC complex is composed of the catalytic subunit Vtc4 along with Vtc1 and either Vtc2 or Vtc3 (1). Cells mutated for Vtc4, Vtc1, or both Vtc2 and Vtc3 have no detectable polyphosphate (2). An accessory subunit called Vtc5 increases the activity of the complex but is not strictly required for polyP synthesis (3,4). The majority of the VTC complex localizes to the membrane of the yeast vacuole, a lysosome-like organelle (1). The VTC complex spans the vacuolar membrane and synthesizes polyP chains by hydrolyzing the gamma phosphate of cytoplasmic ATP, adding it to growing polyP chains that are simultaneously translocated into the vacuole lumen (5). Vacuolar polyP comprises the majority of total cellular polyP stores, exceeding 10 to 20% of the dry cell weight (2,6). Other areas of the cell beyond the vacuole, including the plasma membrane, cytoplasm, and mitochondria, have lower levels of polyP (2). PolyP is also found in the nucleus, although the reported levels vary drastically (2). These variations are likely due to differences in growth conditions as well as differences in the methods of sample preparation and detection. Whether polyP outside the vacuole is synthesized locally or somehow transported from polyP stores that first accumulate in the vacuole lumen is unknown. Although some VTC proteins localize in part to the plasma membrane and/or the endoplasmic reticulum (1,7), it is unknown if these pools of VTC proteins participate in polyP synthesis.

The subcellular enrichment of polyP is conserved in higher eukaryotes (8). For example, in human myeloma cells (9) and various cancer cell lines treated with cisplatin (10), polyP

accumulates in the nucleolus. In platelets, it is concentrated in lysosome-related organelles called dense granules (11). The localization of polyP to such hot spots likely promotes specific functions. In yeast, vacuolar polyP is important for phosphate homeostasis (12) and vacuole fusion (13). PolyP released from dense granules following injury interacts directly with specific clotting factors to promote blood coagulation (11,14). In contrast, less is known about whether there are physiological reasons why the levels of polyP in some areas of the cell must be kept low.

Unlike the VTC complex, the ectopic expression of the *Escherichia coli* polyphosphate kinase (called PPK) in yeast results in the accumulation of polyP outside the vacuole, and this correlates with slow growth, altered cellular morphology, and dramatic sensitivity to the translation inhibitor cycloheximide and the mTOR inhibitor rapamycin (5,15). The amount of polyP made by PPK is 20% of that produced by VTC (5), and PPK-induced toxicity is observed in both wild-type (WT) and *vtc4*Δ cells (15). Together, these data point to the location of PPK-synthesized polyP, rather than changes in the total amount, as the driving force behind the observed toxicity. Finding the mechanisms underlying this toxicity will provide a foundation for a better understanding of the spatial and temporal regulation of polyP metabolism in eukaryotic cells.

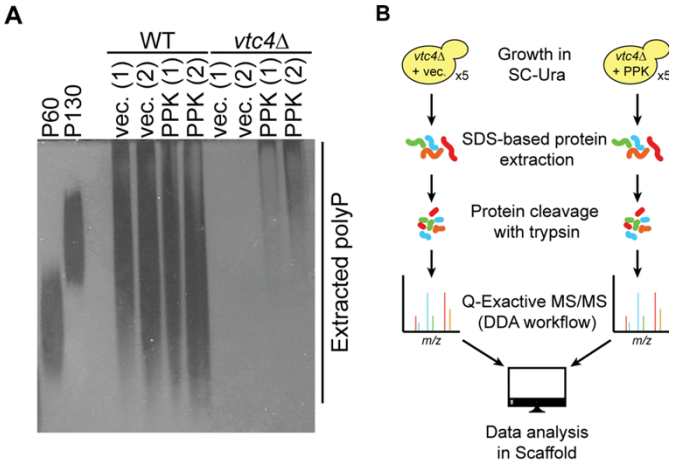
Here, we use label-free mass spectrometry (MS) to determine why PPK expression and the concomitant accumulation of nonvacuolar polyP are toxic in yeast. Our results demonstrate that PPK-expressing cells remodel their proteome with changes to protein networks controlling fundamental aspects of metabolism. In follow-up work, we present evidence that a Yak1/Hog1-Msn2/Msn4 pathway limits the viability of these cells and that protein kinase A (PKA) activity is also altered by PPK expression. Finally, we demonstrate that polyP accumulation outside the vacuole is countered by the combined activities of the endopolyphosphatase Ddp1 (diphosphoinositol polyphosphate phosphohydrolase) and the exopolyphosphatase Ppx1 that work

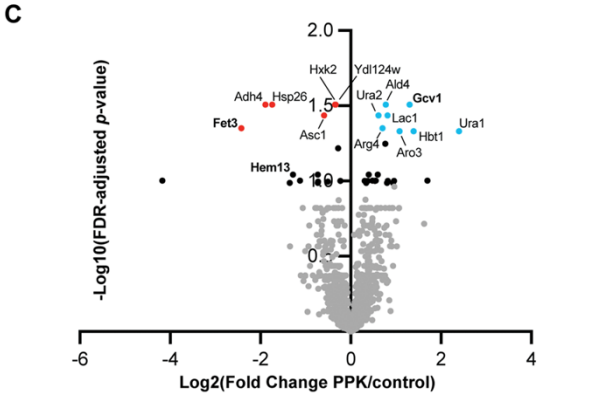
together to degrade long-chain polyP synthesized by PPK. Our results provide an explanation for why polyP is sequestered, elaborate functions of polyphosphatases outside the vacuole, and suggest new avenues for exploring polyP functions at the molecular level.

3.4. Results

3.4.1. Remodeling of the yeast proteome in response to ectopic PPK expression

To determine why PPK expression and the accumulation of nonvacuolar polyP are toxic in yeast, we used label-free mass spectrometry to survey changes to the proteome in strains expressing PPK versus the empty vector control. Our initial experiments were carried out in a *vtc4*Δ background, which enabled us to confirm the production of the polyP in each isolate used for analysis, as judged by the lysine polyphosphorylation of the Fpr3 protein (15) (see **Figure S1A** in the supplemental material). The polyP made by PPK in yeast was of the long-chain type, like that produced by *E. coli* under starvation (**Figure 1A**) (16). Total protein from 5 isolates of the control and 5 isolates of PPK-expressing cells was isolated using an SDS lysis protocol prior to trypsinization and tandem mass spectrometry (MS/MS) analysis using a Thermo Scientific Q Exactive Plus Orbitrap mass spectrometer (**Figure 1B**). As expected, peptides from bacterial PPK were detected only in the PPK-expressing strains (**Supplementary Table 1B**). At the level of a false discovery rate (FDR)-adjusted *P* value of <0.05, 8 proteins were deemed significantly upregulated, while 6 were downregulated (**Figure 1C** and **Figure 1D**). An additional 24 proteins showed up- or downregulation with an associated statistical significance of $0.05 \leq P \leq 0.1$ (**Figure 1C** and **Supplementary Table 1A**). Finally, there were 2 proteins (Snl1 and Rpl22b) that were detected in all five replicates of the empty vector control but not in any replicates of the PPK-expressing strains (**Figure 1D** and **Supplementary Table 1B**).





D

Protein	Function	Log2FC (PPK/cont.)
Fet3	Ferro-O2-oxidoreductase (iron uptake)	-2.42
Adh4	Alcohol dehydrogenase	-1.89
Hsp26	Heat shock protein	-1.74
Asc1	40S ribosome component	-0.59
Hxk2	Hexokinase isozyme (glucose metabolism)	-0.35
Ydl124w	Alpha-keto amide reductase	-0.33
Snl1	Hsp70 co-chaperone	N/A
Rpl22b	Large ribosomal subunit protein	N/A
Arg4	Arginine biosynthesis	+0.62
Aro3	Aromatic amino acid biosynthesis	+0.70
Ald4	Aldehyde dehydrogenase (mitochondrial)	+0.77
Ura2	Pyrimidine biosynthesis	+0.81
Lac1	Ceramide synthesis	+1.08
Gcv1	Glycine decarboxylase complex (mitochondrial)	+1.30
Hbt1	Cell morphogenesis	+1.39
Ura1	Pyrimidine biosynthesis	+2.39
PPK	*E. coli* polyP kinase	N/A

Figure 1. The proteome of PPK-expressing yeast. (**A**) PPK expression in yeast allows the production of polyP outside the vacuole. Polyphosphate was extracted from the strains expressing the indicated constructs and visualized using DAPI staining following separation on a 15.8% acrylamide–TBE–urea gel. Two biological replicates are presented for each condition. (**B**) Workflow for data-dependent acquisition (DDA)-based label-free mass spectrometry analysis. (**C**) Volcano plot with proteins up- or downregulated following PPK expression in a *vtc4*Δ background. Red proteins are downregulated (adjusted *P* value of <0.05), and blue proteins are upregulated (adjusted *P* value of <0.05). Black proteins are those with an adjusted *P* value of ≤0.1. (**D**) Table of the top differentially expressed proteins identified with an adjusted *P* value of <0.05. Images are representative of data from ≥3 experiments. FC, fold change; N/A, not applicable.

3.4.2. Vacuolar polyP does not impact the cellular response to PPK expression

To validate our proteomics data set, we expressed up- or downregulated proteins as C-terminal 3FLAG fusions from their endogenous loci and transformed these strains with control or PPK-expressing vectors. We first carried out this analysis in a *vtc4*Δ background, mirroring the conditions used for our mass spectrometry experiments. For differentially expressed proteins with a *P* value of ≤0.1, we confirmed 6 of 6 upregulations chosen for analysis (e.g., Gcv1) and 3 of 4 downregulations chosen for analysis (e.g., Fet3 and Hem13), for an overall confirmation rate of 90% (**Figure 2A**, **Supplementary Table 2**, **Supplementary Figure 1B** and **Supplementary Figure 1D**). The validation of protein changes in the ranges of both a *P* value of <0.05 and a *P* value of ≤0.1 supports our use of the cutoff of a *P* value of ≤0.1 for downstream bioinformatics analyses (see below). Notably, we also confirmed 5 of 6 differentially expressed proteins beyond the range of a *P* value of 0.1 (**Supplementary Table 2**, **Supplementary Figure 1B** and **Supplementary Figure 1D**), highlighting the overall high quality of our data set and the stringency of our statistical approach.

To test if these changes are influenced by the presence of vacuolar polyP, we repeated our Western blot analyses in a wild-type strain (i.e., *VTC4*$^{+}$), with a confirmation rate of 86% ($P \leq 0.1$) (**Figure 2B**, **Supplementary Table 2** and **Supplementary Figure 1C**). This observation is consistent with our previous work demonstrating that PPK expression sensitizes cells to rapamycin and cycloheximide regardless of *VTC4* status (15). As suggested previously (5), PPK is not simply replacing polyP that is missing in *vtc4*Δ cells. Instead, nonvacuolar polyP appears to have unique consequences for the cell. Finally, to test if the catalytic activity of PPK was required for the observed effects, we generated a mutant version of the enzyme where three histidine residues shown or proposed to be required for catalytic activity (17-19) were mutated to alanine. This

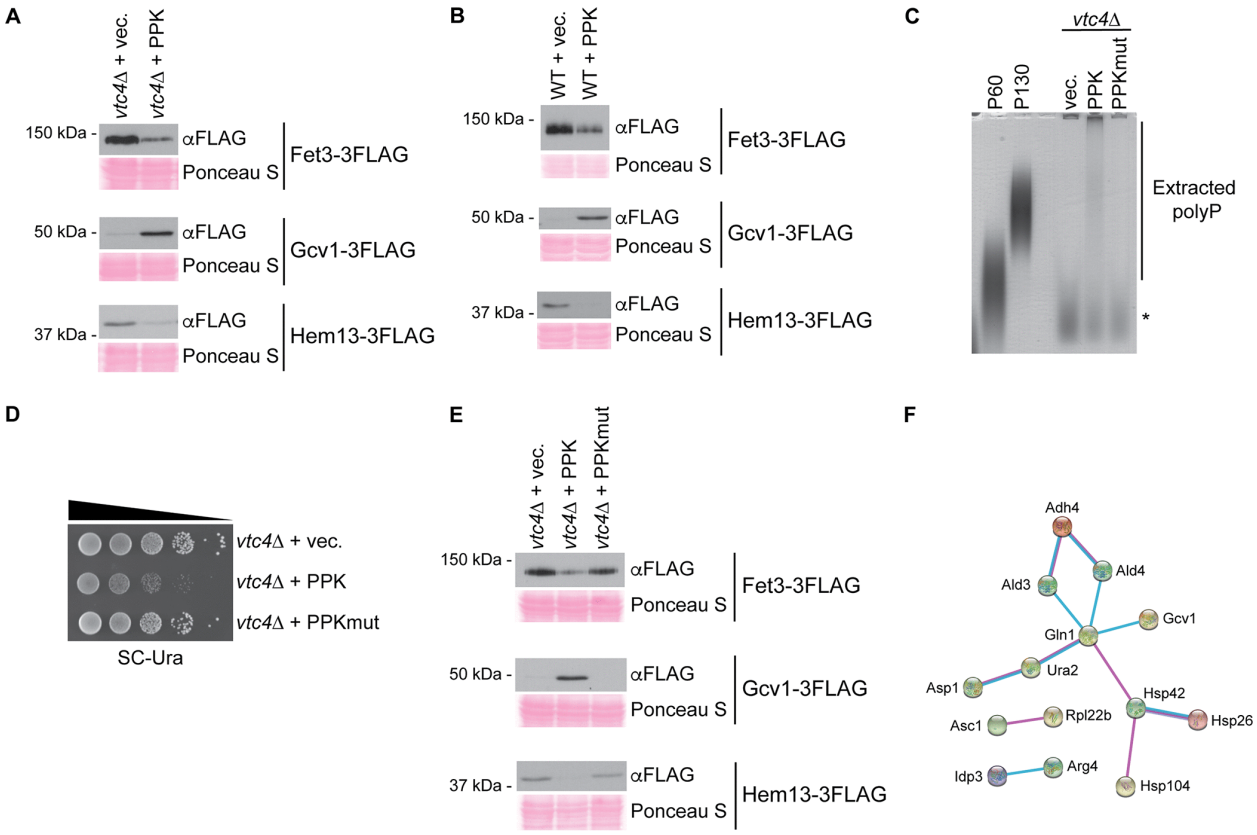


Figure 2. The response to PPK expression is not impacted by the presence of vacuolar polyP. (**A** and **B**) Protein extracts from the indicated strains were prepared using a TCA lysis protocol and separated on SDS-PAGE gels. Separated proteins were transferred to a PVDF membrane prior to probing with anti-FLAG antibody to detect candidate proteins. Ponceau S staining of the PVDF membrane is shown as a loading control. (**C**) Polyphosphate was extracted from the strains expressing the indicated constructs and visualized using toluidine blue staining following separation on a 15.8% acrylamide–TBE–urea gel. The asterisk indicates nonspecific staining of an unknown product that is not polyP, as it is present in *vtc4*Δ cells. (**D**) Tenfold dilutions of the indicated strains were spotted onto SC-Ura medium and incubated for 48 h at 30°C. (**E**) Protein extracts from the indicated strains were analyzed as described above for panel A. (**F**) STRING analysis locates differentially expressed proteins in subnetworks of physically interacting proteins. Magenta, experimental evidence; cyan, database evidence; purple, database evidence (specifically protein homology). Images are representative of results from ≥3 experiments.

mutant enzyme did not produce detectable polyP *in vivo* (**Figure 2C**). Furthermore, it did not result in the same slow-growth defects seen for wild-type PPK expression (**Figure 2D**). For 8 of 8 candidates tested ($P \leq 0.1$), mutant PPK did not impact protein levels (**Figure 2E**, **Supplementary Table 2** and **Supplementary Figure 1D**) despite being expressed at higher levels than wild-type PPK (**Supplementary Figure 1E**). One interesting exception (although beyond the cutoff of a *P* value of ≤0.1) is Ctt1-3FLAG, which was also upregulated in strains expressing the catalytic mutant (**Supplementary Table 2** and **Supplementary Figure 1D**). Still, our data confirm that PPK catalytic activity seems to be required for most changes measured. Finally, we note that proteins encoded by the phosphate (PHO) regulon (e.g., Pho8, Pho86, and Vtc2) (20) did not show significant changes in PPK-expressing cells (**Supplementary Table 1A**). Therefore, the effects of PPK expression are not easily explained by changes in phosphate signaling.

3.4.3. Expression changes for proteins involved in fundamental metabolism in PPK-expressing cells

To identify the molecular functions impacted by PPK expression, we carried out Gene Ontology (GO) (21) enrichment analysis of up- or downregulated proteins ($P \leq 0.1$). We found a statistically significant enrichment (FDR-adjusted *P* value of 0.036) of GO:0006082 (organic acid metabolic process) (**Supplementary Table 1F**). Differentially expressed proteins belonging to this group include those involved in glucose metabolism (Hxk2 and Tdh3), B vitamin synthesis (Snz1 and Fol2), and amino acid biogenesis or turnover (e.g., Aro3, Gcv1, and Gln1) (22). These changes suggest that polyP accumulation outside the vacuole influences important aspects of primary metabolism. Using STRING (Search Tool for the Retrieval of Interacting Genes/Proteins) (23) to model protein interactions, we found that proteins involved in amino acid metabolism had physical interactions with each other and with 3 heat shock proteins (Hsp26, Hsp42, and Hsp104) (22) that

were also significantly up- or downregulated with PPK expression (**Figure 2F**). The identification of heat shock proteins in this network is interesting in light of the proposed role of polyP itself as a molecular chaperone (24). Other heat shock or "quality control" proteins up- or downregulated in our data set include Hsp12, Hsp104, and Snl1, a cochaperone for Hsp70 (22).

PolyP can function as an ion chelator, and recent work from Beaufay et al. suggests that it can act as an inhibitor of the Fenton reaction, in which Fe^{2+} reacts with hydrogen peroxide to form reactive hydroxyl radicals (25). Interestingly, we noted that a number of proteins downregulated with PPK expression either are involved in ion transport (e.g., Fet3, which oxidizes Fe^{2+} to Fe^{3+} (26)) or require divalent ions as cofactors (e.g., Adh4, which requires zinc for its catalytic activity (27)). Genes encoding other differentially expressed proteins confer resistance to metal ions (e.g., *HIS1* (28)) or are induced in response to metal deficiency (e.g., *ADH4*, induced in response to low zinc (29)). While the toxicity associated with PPK expression was not impacted by the addition of various divalent cations (Fe^{2+}, Mg^{2+}, Zn^{2+}, and Ca^{2+}) to growth media (**Supplementary Figure 2**), we cannot yet rule out that disruption of ion homeostasis impacts proteome changes independently of the overt toxicity observed in PPK-expressing cells.

3.4.4. An Msn2/Msn4-dependent signaling pathway limits viability in PPK-expressing cells

We next used the Yeast Search for Transcriptional Regulators and Consensus Tracking (YEASTRACT) (30) tool to identify candidate transcription factors involved in the regulation of genes encoding proteins up- or downregulated in our data set (**Figure 3A**). We were particularly interested in Msn2 (regulating 85% of hits) and its paralog Msn4 (regulating 74% of hits) for two reasons. First, these transcription factors are involved in the response to diverse cellular stresses via the activation of stress response element (STRE) genes (31,32) (**Figure 3B**). Second, the constitutive activation of Msn2 is associated with slow growth (33,34). We reasoned that the mis-

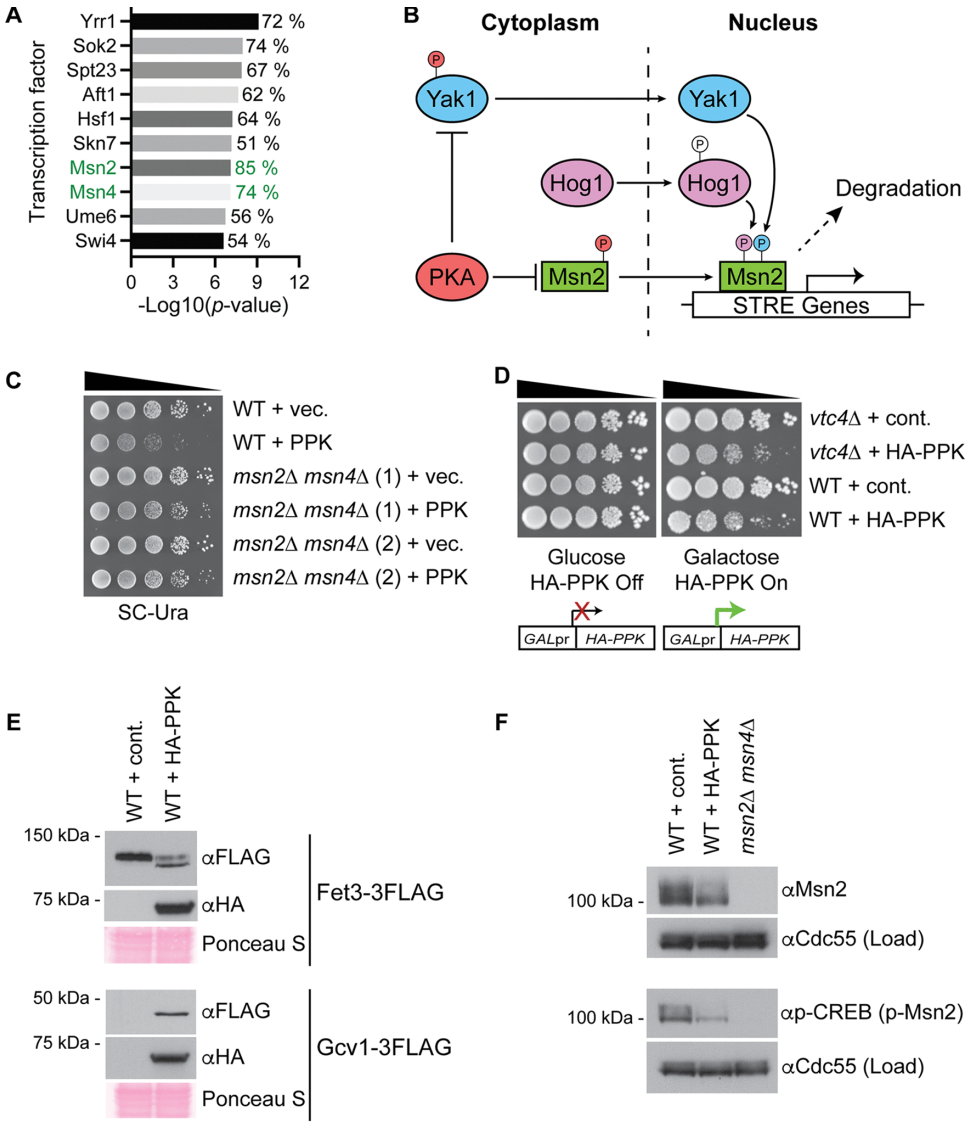


Figure 3. The Msn2 and Msn4 transcription factors limit viability in PPK-expressing cells. (**A**) YEASTRACT analysis was used to identify candidate transcriptional regulators based on proteins up- and downregulated in the mass spectrometry analysis. See Materials and Methods for details. The percentages show the fractions of differentially expressed proteins (adjusted *P* value of ≤0.1) whose encoding genes are regulated by the indicated transcription factors. (**B**) Relationship between PKA/Yak1/Hog1 and Msn2/Msn4 in stress signaling. (**C**) Tenfold serial dilutions of the indicated strains transformed with an empty or PPK-expressing vector were spotted onto the indicated media and incubated for 48 h at 30°C. Two biological replicates for the *msn2*Δ *msn4*Δ mutant are shown for each condition. (**D**) Schematic of an inducible HA-PPK expression system under the control of the GAL promoter. Gal-induced HA-PPK expression results in decreased growth in both the *vtc4*Δ and wild-type backgrounds. Tenfold serial dilutions of the indicated strains were spotted onto the indicated media and incubated for 72 h at 30°C. (**E**) Protein extracts from the indicated strains harboring an empty GAL promoter or the inducible HA-PPK expression system were prepared using a TCA lysis protocol and separated on SDS-PAGE gels. Separated proteins were transferred to a PVDF membrane prior to the detection of proteins

with the indicated antibodies. Ponceau S staining of the PVDF membranes is shown as a loading control. (**F**) Protein extracts from the indicated strains were prepared and analyzed as described above for panel E. A phospho-CREB antibody was used to detect the NLS-specific phosphorylation of Msn2. Cdc55 is used as a loading control. Images are representative of results from ≥3 experiments.

regulation of Msn2 and/or Msn4 impacts cell growth and/or division in PPK-expressing cells. Indeed, the deletion of *MSN2* and *MSN4* in PPK-expressing strains improved growth in serial dilution assays (**Figure 3C**), suggesting that these transcription factors hinder growth in the presence of nonvacuolar polyP. We next examined changes to Msn2 via Western blotting. For these experiments, we developed an integrated galactose (Gal)-inducible version of the PPK expression system (**Figure 3D**). This allowed better control over PPK expression and prevented strains from adapting to the presence of nonvacuolar polyP. The PPK construct contains an N-terminal hemagglutinin (HA) epitope tag, which allowed us to monitor expression in mutant strains. Notably, Gal-induced HA-PPK expression resulted in growth defects in both the *vtc4*Δ and WT strain backgrounds (**Figure 3D**). HA-PPK-synthesized polyP was quantified in *vtc4*Δ cells and amounted to approximately 50% of that produced in wild-type cells grown in galactose (**Supplementary Figure 3A**). We further validated our Gal-inducible system by demonstrating that Gcv1-3FLAG and Hsp42-3FLAG are upregulated and that Fet3-3FLAG and Adh4-3FLAG are downregulated following HA-PPK expression (**Figure 3E** and **Supplementary Figure 1F**), mirroring what was observed for the plasmid-based expression system used in previous experiments. The loss of PKA-dependent Msn2 nuclear localization signal (NLS) phosphorylation is associated with its nuclear localization and transcriptional activation of stress response element genes (35) (**Figure 3B**). HA-PPK-expressing cells had lower levels of this phosphorylated form of Msn2, which can be fortuitously detected using an antibody against human pCREB (35,36)

(**Figure 3F**). Notably, the levels of total Msn2 were also reduced with PPK expression (**Figure 3F**), an observation that may seem at odds with the idea of enhanced Msn2 activity. However, we note that nuclear Msn2 is thought to be destabilized under conditions of chronic stress and low PKA activity as well as heat shock (34,37). Importantly, Msn2/Msn4-induced genes whose encoded proteins were upregulated with PPK expression showed increased mRNA expression, consistent with regulation occurring at the transcriptional level (**Supplementary Figure 3B**).

Hog1 and Yak1 are upstream kinases that act on Msn2 to regulate its nuclear import and at the promoter level to stimulate stress-dependent gene induction (38,39) (**Figure 3B**). Therefore, we next tested if Hog1 and Yak1 might be involved in the response to HA-PPK expression and polyP accumulation outside the vacuole. While we saw no change in the expression of Hog1-green fluorescent protein (GFP) or Yak1-GFP (**Figure 4A** and **Figure 4B**), the electrophoretic mobility of Yak1-GFP was slightly but reproducibly increased with PPK expression (**Figure 4B**). We surmised that this could represent a loss of autophosphorylation or PKA-dependent phosphorylation that accompanies Yak1 activation or translocation to the nucleus, respectively (40). Indeed, some PKA-dependent phosphoproteins show misregulation in PPK-expressing cells (**Figure 4C**). The deletion of *HOG1* or *YAK1* partially rescued the slow growth associated with PPK expression (**Figure 4D**). As a control, these strains had equal levels of HA-PPK expression (**Supplementary Figure 3C**). We also observed a comparable effect on cells deleted for *VTC4*, which were confirmed to accumulate similar levels of PPK-synthesized polyP (**Supplementary Figure 3D** and **Supplementary Figure 3F**). Collectively, our data suggest that Hog1 and Yak1 may signal through Msn2/Msn4 in response to polyP accumulation outside the vacuole and that the activation of this signaling pathway inhibits growth. However, we cannot completely rule out a role for these proteins in the metabolism or distribution of polyP itself.

3.4.5. Ddp1 cooperates with Ppx1 to degrade nonvacuolar polyP

Since aberrant polyP outside the vacuole leads to changes in the expression of the proteome, we expect that mechanisms may exist to counter its accumulation. In yeast, work on polyphosphatase enzymes has focused on four proteins: Ppn1, Ppn2, Ppx1, and Ddp1. Ppn2 and Ddp1 are thought to act as endopolyphosphatases, which cleave polyP chains internally (2). Ppx1 functions as an exopolyphosphatase that cleaves polyP chains starting at the end (2). Ppn1 has been proposed to have both functions (2). Work by Gerasimaitė et al. demonstrated that *GAL*pr-*PPX1* strains show decreased growth when grown in glucose (repressed *PPX1*) versus galactose (*PPX1* overexpression) in the presence of nonvacuolar polyP (5). Whether Ppx1 works alone or in conjunction with additional polyphosphatases is unknown. Therefore, we tested the contribution of each of the four polyphosphatase enzymes in our system. The deletion of the polyphosphatase gene *PPN1* or *PPN2* had no impact on the growth or viability of HA-PPK-expressing cells (**Figure 5A**). This observation is consistent with their roles as vacuolar enzymes and the lack of an impact of vacuolar polyP stores on PPK-induced toxicity (**Figure 3D**). In contrast, and as expected, *PPX1* deletion greatly enhanced the toxicity associated with PPK expression (**Figure 5B**). Interestingly, a similar phenotype was observed in cells disrupted for *DDP1*. In contrast to the slow-growth phenotype conferred by PPK expression alone, the deletion of these genes resulted in a dramatic decrease in viability in addition to slow growth (**Figure 5B**). Interestingly, the simultaneous deletion of *DDP1* and *PPX1* showed an effect that was not more dramatic than that observed for either single mutant (**Figure 5B**). This largely epistatic relationship was recapitulated in the context of a liquid growth assay (**Supplementary Figure 4A**), suggesting that Ddp1 and Ppx1 function in the same pathway to counter the toxicity of polyP outside the vacuole. However, we note that HA-PPK expression levels are lower in the *ppx1*Δ *ddp1*Δ double mutant

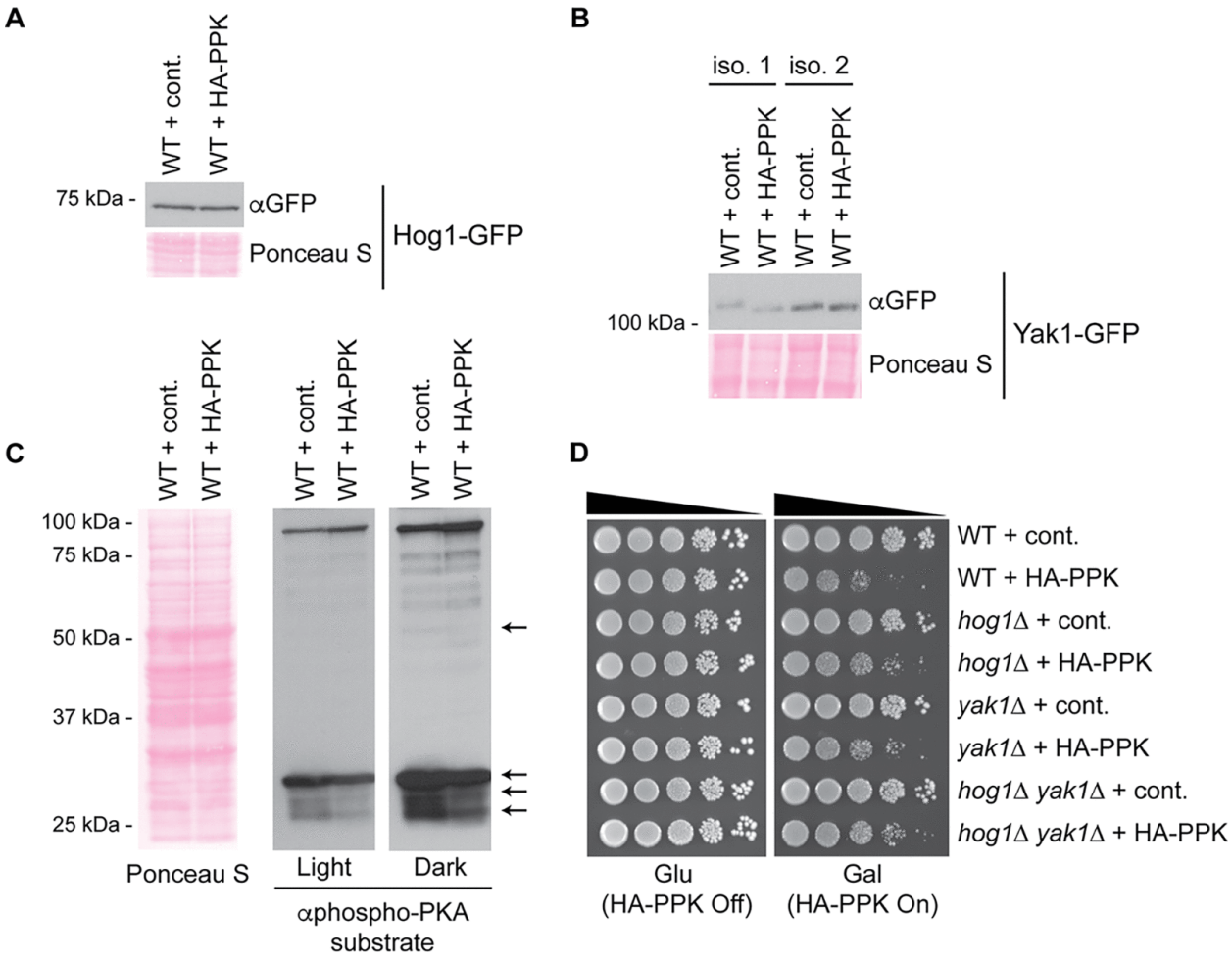


Figure 4. Yak1 and Hog1 kinases modulate the response to PPK expression. (**A**) Hog1-GFP levels are unaffected by PPK expression. Protein extracts from the indicated strains were prepared using a TCA lysis protocol and separated on SDS-PAGE gels. Separated proteins were transferred to a PVDF membrane before probing with the indicated antibodies to detect the proteins of interest. Ponceau S staining of the PVDF membrane is shown as a loading control. (**B**) PPK expression leads to an increase in the electromobility of Yak1. Protein extracts from the indicated strains were prepared and analyzed as described above for panel A, but proteins were run on a 10% SDS-PAGE gel with a 77:1 acrylamide-to-bis ratio. Two biological replicates are shown for each condition. (**C**) Phosphorylated PKA substrates were detected using an antibody that detects phosphorylated serine or threonine residues with arginine at the −3 and −2 positions (RRXS*/T*). Arrows indicate misregulated phosphorylated PKA substrates. Ponceau S staining of the PVDF membrane is shown as a loading control. (**D**) Tenfold serial dilutions of the indicated strains were spotted onto the indicated media and incubated for 72 h at 30°C. Images are representative of results from ≥3 experiments.

than in wild-type cells or either single mutant (**Supplementary Figure 4C** and **Supplementary Figure 4G**), which somewhat complicates this interpretation. To test if Ddp1 and Ppx1 physically interact to degrade polyP in a concerted fashion, we attempted to coimmunoprecipitate 3HA-Ddp1 and Ppx1 but did not detect any interaction between the two proteins (**Supplementary Figure 4B**).

To understand the mechanisms of Ppx1 and Ddp1 action, we analyzed polyP from our panel of polyphosphatase mutants. These experiments were conducted in a *vtc4*Δ background to allow the visualization of HA-PPK-synthesized polyP rather than the VTC-synthesized polyP stored in the vacuole but released during the polyP isolation protocol. As we observed in the plasmid-based system, HA-PPK-synthesized polyP accumulated as predominantly long chains reminiscent of those synthesized by *E. coli* in response to cellular stress (**Figure 5C**). Here again, the amount of polyP is smaller than that in a wild-type yeast cell, consistent with the notion that it is the localization of PPK-synthesized polyP rather than the amount of that polyP that drives changes in cell growth (5). HA-PPK-expressing strains lacking *PPX1* had more polyP, and the chains were of a medium length (**Figure 5C**). Strains lacking *DDP1* also showed increased polyP, but these chains were of the long form (**Figure 5C**). The *ppx1*Δ *ddp1*Δ double mutant accumulated both medium and long polyP chains, with long chains being predominant. The overexpression of either enzyme reduced the level of HA-PPK-synthesized polyP to background levels (**Figure 5C**) and rescued the slow growth associated with PPK expression (**Supplementary Figure 4D**). While these experiments suggest that Ddp1 and Ppx1 act sequentially to degrade long chains of polyP, Ppx1 may also target a distinct population of medium-length chains synthesized by HA-PPK. Interestingly, PKA activity was drastically reduced in *ppx1*Δ cells expressing HA-PPK (**Figure 5D**). This observation reinforces the connection between polyP accumulation outside the vacuole

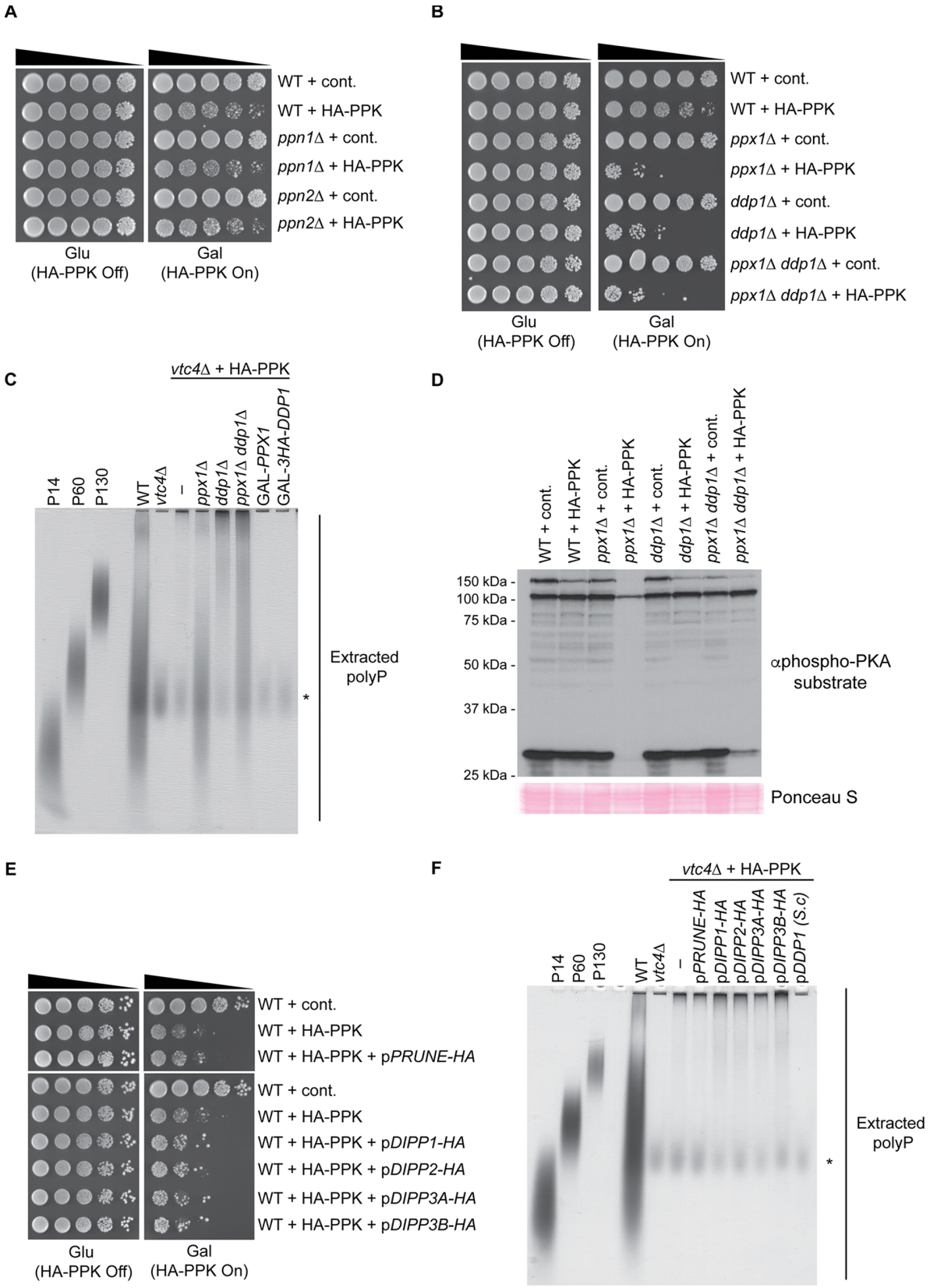


Figure 5 – Figure legend on the next page

Figure 5. PolyP accumulation outside the vacuole is countered by Ppx1 and Ddp1. (**A** and **B**) The indicated strains were spotted in a 5-fold dilution series onto plates containing 2% glucose or 1.8% raffinose with 0.2% galactose and incubated at 30°C for 72 h. (**C**) Polyphosphate was extracted from the indicated strains and visualized using toluidine blue staining following separation on a 15.8% acrylamide–TBE–urea gel. The asterisk indicates nonspecific staining of an unknown product that is not polyP, as it is present in *vtc4*Δ cells. (**D**) PKA activity is drastically reduced in *ppx1*Δ cells expressing PPK. Protein extracts from the indicated strains were prepared using a TCA lysis protocol and separated on SDS-PAGE gels. Separated proteins were transferred to a PVDF membrane before probing with a phospho-PKA substrate antibody. Ponceau S staining of the membrane is used as a loading control. In these experiments, protein levels seem to be lower in PPK-expressing strains, which may be indicative of cell death. (**E**) Strains with the indicated plasmids expressing yeast or candidate human polyphosphatase enzymes were spotted in 10-fold dilution series and incubated at 30°C for 72 h. (**F**) Polyphosphate was extracted from the strains expressing the indicated plasmids and analyzed as described above for panel D. Images are representative of results from ≥3 experiments.

and signaling through this pathway. In contrast, the deletion of *DDP1* had little effect (**Figure 5D**), suggesting that the impact on PKA may be chain length dependent.

To corroborate and extend our findings with yeast Ppx1 and Ddp1, we analyzed lysine polyphosphorylation of previously identified targets (15). Since lysine polyphosphorylation is a nonenzymatic modification, it is thought to be controlled largely by the concentration of polyP itself. We carried out these experiments in a *vtc4*Δ background to prevent the interference of vacuolar polyP, which can polyphosphorylate proteins during cell lysis (41). The deletion of *PPX1* or *DDP1* in HA-PPK-expressing cells resulted in the decreased electrophoretic mobility of the polyphosphorylation targets Rts1 and Fpr3 on NuPAGE gels, indicative of lysine polyphosphorylation (**Supplementary Figure 4E-G**) (15). Therefore, the "extra" polyP in these cells is competent to participate in lysine polyphosphorylation reactions. The decreased electrophoretic mobility observed in *ppx1*Δ and *ddp1*Δ cells could result from the modification of additional lysines at higher concentrations of polyP (42). The greater impact of *ddp1*Δ may reflect the addition of longer chains to individual target lysines in these cells. We propose that the enhanced toxicity of PPK expression observed in *ddp1*Δ and *ppx1*Δ mutants may be due in part to

the aberrant polyphosphorylation of proteins in the cytoplasm, although the identities of these remain unknown.

Yeast Ppx1 and Ddp1 show homology to human Prune and DIPP1-DIPP3, respectively (43,44). Prune and DIPP1-DIPP3 have exo- or endopolyphosphatase activity *in vitro* (43-35). Only DIPP1 (also called NUDT3) has been described to have activity *in vivo* (45). Samper-Martín et al. showed that DIPP1 overexpression confers a zinc-dependent reduction in polyP detected in HEK293T cells via a polyP binding probe (45). Conversely, DIPP1 knockdown caused an increase in polyP in both HEK293T and SH-SY5Y cells using this same method of detection (45). To determine if candidate polyphosphatases could impact PPK-induced toxicity and/or polyP accumulation in yeast, we expressed them in yeast under the control of the strong glyceraldehyde-3-phosphate dehydrogenase (GPD) promoter (**Supplementary Figure 5A**). In contrast to *DDP1* overexpression, the ectopic expression of human Prune or DIPP1-DIPP3 proteins did not improve growth in PPK-expressing cells (**Figure 5E**) and did not decrease polyP accumulation (**Figure 5F**). Since DIPP1 activity is thought to be zinc dependent (45), we added zinc to the growth media used for these experiments. Although the highest concentrations of zinc used caused a slight improvement in the growth of strains expressing HA-PPK alone or in the presence of Prune, the growth of DIPP1-DIPP3-expressing strains was unaffected (**Supplementary Figure 5B**). Similarly, although the addition of zinc resulted in a slight decrease in polyP levels in all strains tested, this was not impacted by the ectopic expression of DIPP1 (**Supplementary Figure 5C**). Either Prune and DIPP1-DIPP3 do not directly impact the accumulation of long-chain polyP *in vivo* or their activities are not faithfully recapitulated in yeast under the conditions tested.

3.5. Discussion

3.5.1. Nonvacuolar polyP reprograms the yeast proteome

There are conflicting data concerning the concentration of polyP that accumulates outside the vacuole in wild-type yeast, although it is generally accepted that the vacuole harbors substantially higher concentrations than other areas of the cell (2). The sequestration of polyphosphate in specific subcompartments is not unique to yeast. Human cells accumulate high concentrations of polyP in the nucleolus or in dense granules of platelets (9.11). Trypanosomes accumulate high levels of polyP in acidocalcisomes (46) as well as in glycosomes and the nucleolus in smaller amounts (47). Even in many bacteria, polyP produced in response to stress is concentrated in granules (2). While the concentration of polyP in these areas is important for specific cellular functions (i.e., blood clotting in the case of dense granules (48)), it is less clear if polyP is actively excluded from (or limited within) some areas of the cell and why this might be important. The expression of bacterial PPK in yeast, coincident with the production of polyP outside the vacuole, was previously demonstrated to reduce growth and sensitize cells to rapamycin and cycloheximide (5,15). Our new study provides a critical advance by (i) identifying molecular pathways that mediate the toxic effects of PPK expression and (ii) providing molecular insight into how exo- and endopolyphosphatases cooperate to counter the accumulation of nonvacuolar polyP in yeast.

We are not able to rule out that other enzymatic activities of the PPK enzyme (e.g., the phosphorylation of nucleotides) contribute to the proteomic changes measured in our mass spectrometry experiments. However, the fact that PPK's impact is greatly exacerbated in strains lacking the Ddp1 and/or Ppx1 polyphosphatase suggests that downstream changes in growth and/or viability are related to changes in polyP metabolism. PolyP could influence the expression or stability of some proteins directly, perhaps by binding to transcription factors or proteins

themselves. We expect that the investigation of such direct modes of action will provide clues to the molecular functions of polyP that are broadly applicable, even under endogenous scenarios. Protein changes following PPK expression could also be indirect, for example, as a downstream result of polyP-mediated ion chelation or the cell's response to more direct activities. Importantly, we consider such indirect effects to be equally interesting as they provide valuable insights into how eukaryotic cells respond to mislocalized polyP and may aid in the identification of scenarios when this occurs in the absence of PPK expression.

3.5.2. Ddp1 and Ppx1 limit the toxic effects of nonvacuolar polyP

In *ppx1*Δ and *ppx1*Δ *ddp1*Δ cells expressing PPK, polyP accumulates as medium-length chains, similar to those made by the VTC complex in wild-type cells. This argues against the idea that PPK expression is toxic only because it makes long chains that are not normally seen in yeast. However, we cannot rule out that different chain lengths have unique impacts on cell signaling and physiology, and this remains an important area for future research. Indeed, there is precedent for chain-length-dependent effects of polyP. For example, polyP chains of different lengths affect different parts of the blood coagulation cascade (49), and long chains preferentially stimulate changes in macrophage signaling important for the immune response (50). Since we have not recovered any evidence of a physical interaction between Ddp1 and Ppx1, we propose that they act sequentially to degrade long polyP chains (**Figure 6**), with Ddp1 first cleaving chains to generate free polyP "ends" on which Ppx1 can then act. Notably, Ppx1 has also been shown to directly remove polyP chains from the nuclear polyphosphorylated target Nsr1 (51) and could act on other proteins in PPK-expressing cells to limit toxicity.

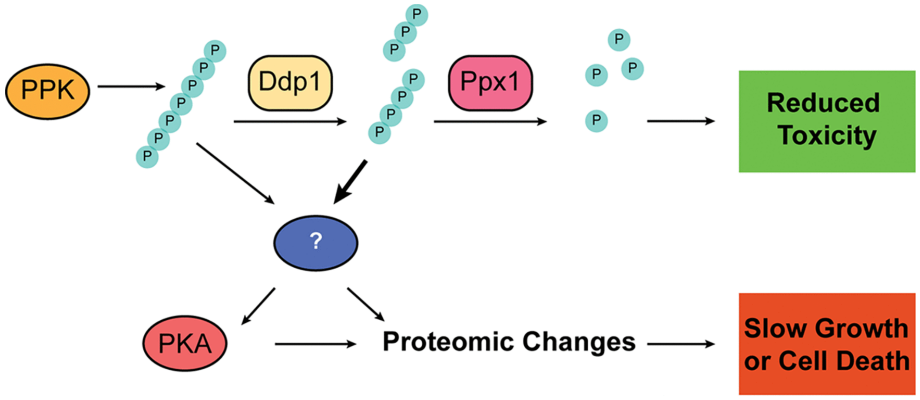


Figure 6. Working model for the cellular response to nonvacuolar polyP in yeast. PPK-produced polyP accumulates in the cytoplasm and slows growth by a variety of pathways, which include the activation of a Yak1/Hog1-Msn2/Msn4 signaling cascade. The accumulation of polyP outside the vacuole is countered by Ppx1 and Ddp1, which work together to degrade polyP. See the text for details.

3.5.3. PolyP as an activator of stress signaling

We propose that polyP escaping degradation by polyphosphatases activates a stress-signaling pathway that limits cell growth or viability (**Figure 6**). It is unclear if polyP is indeed causing some type of intracellular stress (i.e., the accumulation of unfolded proteins) or if it is inappropriately activating stress-signaling pathways in the absence of stress. Regardless, the downstream consequences appear to involve the PKA pathway, which plays a central role in the regulation of cell metabolism, growth, as well as diverse stress responses (52). Our results show that the accumulation of nonvacuolar polyP leads to the broad misregulation of PKA substrates. Some of these substrates may include differentially expressed proteins identified in our mass spectrometry experiments. For example, Ura2, which is downregulated in PPK-expressing cells, is phosphorylated by PKA *in vitro* (53). Moreover, PKA regulates the activity of Msn2/Msn4 and Yak1 through direct phosphorylation (35,40), and recently, it was suggested that PKA might modulate the activation of the Hog1 pathway during impaired sphingolipid biosynthesis (54). Previous work has shown that the deletion of *YAK1* or *MSN2* and *MSN4* under conditions of low PKA activity rescues related slow-growth phenotypes (55,56). We have shown that the deletion of *YAK1* or *MSN2* and *MSN4* also rescues growth in PPK-expressing cells, which is in accordance with scenarios of low PKA activity. Furthermore, low PKA activity imparted by the accumulation of nonvacuolar polyP could explain the sensitivity of PPK-expressing cells to rapamycin (15) since mutants with low PKA activity have increased sensitivity to this drug (57). Our results suggest that nonvacuolar polyP might affect PKA activity directly or indirectly and that these changes may explain the observed toxicity (**Figure 6**).

3.5.4. Endogenous functions of nonvacuolar polyP

The polyphosphate functions outside the vacuole are poorly understood. The Ppx1 and Ppn1

polyphosphatases localize in part to the mitochondria, and here, polyP is suggested to play a role in energy homeostasis and metabolism (58). Within the nucleus, polyphosphorylation may also inhibit the interaction of the Top1 and Nsr1 proteins in addition to modulating their localization to the nucleolus (51). It is also tempting to speculate that the nuclear localization of polyphosphate underlies its poorly understood role in cell cycle regulation (59). How polyP that functions in or transits through the cytoplasm in a wild-type cell avoids degradation by polyphosphatases is an intriguing question. It may be that these polyP molecules are bound by proteins or small molecules that prevent enzyme access to the phosphoanhydride bonds. It is also possible that Ddp1 and Ppx1 become activated to degrade cytoplasmic polyP only when the concentration exceeds a particular threshold. We further speculate that polyP could be released from vacuoles following damage with lysosomotropic agents such as *N*-dodecylimidazole (60) or during sporulation, where the vacuole undergoes programmed lysis (61). Ddp1 and Ppx1 are ideally placed to regulate these responses.

3.5.5. Regulation of polyP in human cells

Our study suggests that the degradation of long-chain polyP in human cells will require the combined action of both endo- and exopolyphosphatases, akin to what we observed for Ddp1 and Ppx1. Mammalian polyphosphatases may also play a role in degrading long-chain polyP made by pathogenic bacteria, which has been suggested to enter cells during infection to reprogram macrophages and thereby subvert host defense mechanisms (50). The identities of intracellular human polyphosphatases had long remained unknown, but Prune and DIPP1-DIPP3 have emerged as candidates based on their *in vitro* activities (43,44,62). Notably, mutations that reduce Prune activity *in vitro* give rise to a rare disease called neurodevelopmental disorder with microcephaly, hypotonia, and variable brain anomalies (NMIHBA) (62). However, expressing either Prune or DIPP1-DIPP3 in yeast resulted in no appreciable change in viability

and no obvious decrease in PPK-synthesized polyP. We note that the *in vitro* exopolyphosphatase activity of Prune is mostly against very short chains (3 to 4 phosphate units in length) (44,62). In our experiments, Prune was also expressed at substantially lower levels than the DIPP1-DIPP3 proteins in yeast despite the fact that both constructs used the GPD promoter. Together, these observations could account for the lack of an effect observed in our system. More surprising is the observation that the expression of DIPP1 had no effect in either the presence or absence of zinc. This finding is seemingly at odds with the exciting work of Samper-Martín et al., who describe a zinc-dependent activity of DIPP1 (also called NUDT3) in HEK293T and SH-SY5Y cells (45). One exciting possibility is that DIPP1 or other mammalian polyphosphatase enzymes require additional cofactors besides zinc that are not normally present in yeast. Such proteins could serve as important regulators of *in vivo* polyphosphatase activity and should be a focus of future work.

3.6. Methods

Yeast strains and handling

Yeast strains were constructed using standard methods as previously described (63-65). The locations of gene deletion and tagging cassettes were confirmed using PCR analyses (65). The full genotypes of all yeast strains used in this work are listed in **Supplementary Table 3** in the supplemental material. Cells were grown in yeast extract-peptone-dextrose (YPD), YEP-raffinose, YEP-galactose, or synthetic complete (SC) medium as described below for individual experiments. In general, SC-Ura and SC-Leu media were used to maintain *URA3*-based and *LEU2*-based selection plasmids, respectively.

Plasmids

All plasmids used for this work are listed in **Supplementary Table 5A**. All plasmids generated for this work are available from Addgene (www.Addgene.org).

Polyphosphate extractions.

(i) Cell growth

Cells expressing the plasmids indicated in **Figure 1A** and **Figure 2C** were diluted to an optical density at 600 nm (OD_{600}) of 0.2 in SC-Ura medium with 2% glucose and grown at 30°C with shaking until the OD_{600} reading reached a final value of 0.8 to 1. Cells in **Figure 5C** and **Supplementary Figure 3F** were diluted to an OD_{600} of 0.2 in YEP medium with 2% raffinose and grown for 3 h before the addition of 2% galactose and growth for another 3 h. Cells expressing the plasmids indicated in **Figure 5F** and **Supplementary Figure 5C** were diluted to an OD_{600} of 0.2 in SC-Ura medium with 2% raffinose and grown for 3 h before the addition of 2% galactose and growth for another 3 h.

(ii) PolyP extraction

The polyP isolation protocol was adapted from a protocol first described by Bru *et al.* (66) and described elsewhere (16). The protocol is repeated here using similar language. Yeast cell pellets of approximately 8 OD_{600} units in size were resuspended in 400 µL of cold LETS buffer (100 mM LiCl, 10 mM EDTA, 10 mM Tris-HCl [pH 7.4], 0.2% SDS), transferred to a screw-cap tube containing 600 µL of phenol (pH 8) and 150 µL of MilliQ water (mqH_2O), and vortexed for 20 s. Samples were then heated for 5 min at 65°C and cooled on ice for 1 min. Once cooled, 600 µL of chloroform was added, and the samples were vortexed for 20 s. Vortexed samples were centrifuged at 13,000 × *g* for 2 min at room temperature, and the top layer was transferred to a new tube containing 600 µL of chloroform. Samples were vortexed for 20 s and centrifuged again at 13,000 × *g* for 2 min, and the top layer was transferred to a clean 1.5-mL tube. To degrade RNA and DNA, 2 µL of 10 mg/mL of RNase A and 2 µL of 10 mg/mL of DNase I were added to samples, and the samples were incubated at 37°C for 1 h. Digested samples were transferred to prechilled 1.5-mL tubes containing 1 mL of 100% ethanol and 40 µL of 3 M sodium acetate (pH 5.3), and polyP was left to precipitate at −20°C for at least 3 h or overnight. PolyP was pelleted by centrifugation at 13,000 × *g* for 20 min at 4°C, and the supernatant was discarded. The pellet was washed with 500 µL of cold 70% ethanol and centrifuged at 13,000 × *g* for an additional 5 min. The supernatant was discarded, and the pellets were air dried before being resuspended in 20 to 30 µL of mqH_2O.

(iii) Gel analysis

Extracted polyP was diluted 1:1 with polyP loading buffer (10 mM Tris-HCl [pH 7], 1 mM EDTA, 30% glycerol, bromophenol blue), and 15 µL was loaded onto a 15.8% Tris-borate-EDTA (TBE)–urea gel (5.25 g urea, 7.9 mL 30% acrylamide, 3 mL 5× TBE, 150 µL 10% ammonium persulfate

[APS], 15 µL *N*,*N*,*N*′,*N*′-tetramethylethylenediamine [TEMED]) and run at 100 V for 1 h 45 min in 1× TBE running buffer. For toluidine blue staining, the gel was incubated in fixative solution with toluidine blue (25% methanol, 5% glycerol, 0.05% toluidine blue) for 20 min and destained with fixative solution without toluidine blue. For 4′,6-diamidino-2-phenylindole (DAPI) staining, the protocol was adapted from the one described previously by Smith and Morrissey (67). The extracted polyP was diluted 1:60 for wild-type or 1:10 for *vtc4*Δ background strains with polyP loading buffer, and 15 µL was loaded. The gel was incubated in fixative solution with DAPI (25% methanol, 5% glycerol, 50 mM Tris base, 2 µg/mL DAPI) for 30 min. The gel was destained with fixative solution without DAPI for 1 h, changing solution once halfway through. The destained gel was exposed to 365 nM UV light on a transilluminator to photobleach the DAPI-polyP until it became dark. Pictures were taken with a Bio-Rad ChemiDoc UV transilluminator.

Polyphosphate quantification

Polyphosphate was quantified using the Phosfinity total polyphosphate quantification kit (Aminoverse) according to the manufacturer's protocol.

Label-free mass spectrometry

The sample preparation and mass spectrometry protocols are based on an experimental setup that we have used previously for work in HEK293T cells (16). Similar language is used in the description here. Cells were diluted to an OD_{600} of 0.2 in SC-Ura medium with 2% glucose and grown at 30°C with shaking until an OD_{600} of 1 was reached. Yeast pellets of approximately 50 OD_{600} units in size were resuspended in 600 µL of lysis buffer (5% SDS and 50 mM triethylammonium bicarbonate [TEAB] supplemented with protease and phosphatase inhibitor tablets [Roche]), and a 2-mL screw-cap tube was filled with acid-washed glass beads. Cells were lysed with 12 1-min pulses on a BioSpec minibeadbeater with incubation on ice in between pulses.

The lysates were clarified by centrifugation at 15,000 × *g* for 10 min at 4°C. The supernatant was collected and centrifuged again at 15,000 × *g* for 10 min at 4°C before being collected again and frozen at −80°C. Frozen protein extracts were shipped overnight on dry ice to the UC Davis Proteomics core. Trypsin digestion was performed using S-Trap Mini spin columns (Protifi) according to the manufacturer's protocol.

Liquid chromatography and mass spectrometry analysis

At UC Davis, digested peptides were first separated using Proxeon Easy-nLC II high-performance liquid chromatography (HPLC) (Thermo Scientific) coupled to a Proxeon nanospray source. The peptides were loaded onto a 100-µm by 25-mm Magic C_{18} 100-Å 5-micron reverse-phase trap and desalted online prior to being separated using a 75-µm by 150-mm Magic C_{18} 200-Å 3-micron reverse-phase column. For all runs, peptides were eluted using a 140-min gradient with a flow rate of 300 nL/min into a Thermo Scientific Q Exactive Plus Orbitrap mass spectrometer. First, an MS survey scan was obtained for the *m/z* range of 350 to 1,600. MS/MS spectra were acquired with the top 15 ions in the MS spectra subjected to higher-energy collisional dissociation, with resolutions at 400 *m/z* of 70,000 and 17,500 at the MS1 and MS2 levels, respectively. For precursor ion selection, an isolation mass window of 1.6 *m/z* was used. A normalized collision energy of 27% was used for fragmentation. Dynamic exclusion was set for 15 s.

Bioinformatics analyses

For mass spectrometry data, the bioinformatics pipeline used for analysis is similar to the one previously described (16). The details are presented here with minimal rewording for clarity.

Protein identification

Tandem mass spectra were extracted using the msConvert program (68). X!Tandem (version X!Tandem ALANINE [2017.2.1.4]; thegmp.org) was used to analyze MS/MS spectra and identify

peptide sequences (69). The X!Tandem program was used to search the Swiss-Prot/UniProt *S. cerevisiae* database (70) (proteome identifier UP000002311; downloaded 21 December 2018), along with 110 common laboratory contaminants (thegpm.org/crap/) and the *E. coli* PPK protein sequence, and all of these sequences were reversed for a decoy database search. A database search was performed on MS/MS spectra from precursor ions with a charge state of 4 at most. Trypsin was set as the digestion enzyme. Using an X!Tandem two-pass search, the initial search was performed with one miscleavage considered, and a refinement search looked for additional unanticipated miscleavages in peptides from proteins identified in the first pass. Fragment ion and parent ion mass tolerances were set to 20 ppm. Single-amino-acid polymorphisms were checked for each peptide residue in the first search, using a default list of polymorphisms from the single nucleotide polymorphism (SNP) annotations in ENSEMBL (71). Carbamidomethylations of cysteine and selenocysteine were specified as fixed modifications. Variable modifications included were glutamic acid→pyroglutamic acid of the N terminus, glutamine→pyroglutamine of the N terminus, ammonia loss of the N terminus, deamidation of asparagine and glutamine, oxidation and dioxidation of both methionine and tryptophan, and N-terminal acetylation. Validation of peptide and protein identifications was done using the Scaffold program (version 4.11.1; Proteome Software, Inc., Portland, OR). The ProteinProphet algorithm was used to assign protein identification probabilities. Peptide identifications associated with an FDR of <1% were deemed of high confidence. Protein identifications with an FDR of <1% and associated with at least 2 high-confidence peptides were then used in all downstream analyses. Proteins were grouped into protein groups if they shared significant peptide evidence. To satisfy the principles of parsimony, proteins sharing the same peptides were grouped if it was not possible to differentiate them based on MS/MS analyses.

Differential protein expression analysis

Protein and protein group spectral counts were retrieved from Scaffold. To account for missing values, spectral counts were imputed for all spectral count values equal to zero by randomly sampling spectral count values from the bottom 20% of nonzero spectral counts. Spectral counts were normalized by the total number of spectral counts in each MS/MS run. Protein differential expression was assessed using two-tailed, two-sample Student's *t* test assuming unequal variance on normalized spectral counts. Differential expression was assessed using a *t* test only for proteins that were reproducibly identified in 3 or more replicates under both experimental conditions. The Benjamini-Hochberg procedure (72) was used to correct for multiple-hypothesis testing. Proteins were deemed differentially expressed when their FDR-adjusted *P* value was ≤0.1. In addition, proteins with extreme expression differences (i.e., detected in all replicates under one condition and in none under the other condition) are also reported and named "all-or-none" proteins.

Gene Ontology enrichment analysis

In order to investigate key functional changes in response to the ectopic expression of PPK, a Gene Ontology (73) enrichment analysis was performed using Ontologizer (74). Differentially expressed proteins (FDR-adjusted *P* value of ≤0.1) and all-or-none proteins were evaluated for enrichment against a background of all identified proteins in all MS/MS runs (FDR of <1%). The OBO ontology file and GAF annotation file used for Gene Ontology enrichment analysis were downloaded from the Gene Ontology database (http://geneontology.org/) on 22 August 2019 and 20 January 2020, respectively. The *P* values were adjusted using the Benjamini-Hochberg procedure to correct for multiple-hypothesis testing.

Protein-protein interaction network

The STRING (23) database was used to construct a protein-protein interaction network between differentially expressed proteins (FDR-adjusted *P* value of ≤0.1) and all-or-none proteins. The network was constructed using the STRING medium-confidence (0.4) threshold for experimental evidence and database evidence of interactions. Proteins without any protein-protein interactions were removed from the network.

YEASTRACT analysis

Genes of differentially expressed proteins (FDR-adjusted *P* value of ≤0.1) and all-or-none proteins were ranked by transcription factor using YEASTRACT (http://www.yeastract.com/formrankbytf.php) (30). Documented regulations were filtered by DNA binding or expression evidence, and transcription factors acting as an activator or inhibitor and all transcription factors were checked.

Immunoprecipitation

Cells were diluted to an OD_{600} of 0.2 in YEP medium with 2% raffinose and grown for 3 h before inducing 3HA-Ddp1 expression with 2% galactose for 2 h. Yeast cell pellets of approximately 50 OD_{600} units were resuspended in 750 µL of lysis buffer (0.1% NP-40, 150 mM NaCl, 50 mM Tris-HCl [pH 8], 10% glycerol); 15 mL of buffer was supplemented with 30 µL of 1 M imidazole, 15 µL of 1 M sodium fluoride, 17.25 µL of 1 M sodium molybdate, 75 µL of 200 mM sodium orthovanadate, 75 µL of 1 M dithiothreitol (DTT), 15 µL of 5 mM cantharidin, 150 µL of 2.5 mM (−)-*p*-bromotetramisole oxalate, 75 µL of 1 M glycerol-2-phosphate, 15 µL of 0.1 M phenylmethylsulfonyl fluoride (PMSF), and a 15-mL Roche cOmplete protease inhibitor tablet with EDTA (15, 51); and 2-mL screw-cap tubes were filled with acid-washed glass beads. Cells were lysed with 8 1.5-min pulses on a BioSpec minibeadbeater with incubation on ice between

pulses. Lysates were clarified by centrifugation at 15,000 × *g* for 10 min at 4°C. The supernatant was collected and centrifuged again at 15,000 × *g* for 10 min at 4°C. Anti-HA antibody was added to each lysate at a dilution of 1/650, and the mixture was rotated end over end for 1 h at 4°C. After incubation, 20 μL of protein A magnetic beads was washed 3 times with 700 μL of lysis buffer and added to each sample, and the samples were rotated end over end for 1 h at 4°C. The samples were centrifuged briefly to pellet the beads, and the lysate was removed. The beads were washed 3 times with 700 μL of lysis buffer and eluted with sample buffer by boiling for 10 min.

Immunoblotting

Proteins were extracted using a method that was described previously (15). That method is described again here for convenience. Cell pellets at an OD_{600} of 3 to 6 (measured using an Eppendorf BioPhotometer) were resuspended in 300 μL of a solution containing 20% trichloroacetic acid (TCA) and 100 μL of acid-washed glass beads. Cells were lysed with 2 3-min pulses on a BioSpec minibeadbeater. The supernatant was removed and kept. Beads were washed with 300 μL 5% TCA, and this supernatant was combined with the first 300 μL. This mixture was clarified via centrifugation at 16,000 × *g* for 4 min at 4°C. The resulting pellet was dissolved in 100 μL of SDS-PAGE loading buffer supplemented with a 1/10 volume of 1.5 M Tris-HCl (pH 8.8) and a 1/10 volume of 1 M DTT and boiled for 8 min. The samples were centrifuged again at 16,000 × *g* for 4 min, and the supernatant was recovered. Approximately 10 to 20 μL was loaded per gel (corresponding to about 75 μg of protein). Unless stated otherwise in the figure legends, protein samples were run on 10% SDS-PAGE gels made from a 30% acrylamide/bis-acrylamide (37.5:1). To resolve polyphosphorylation-induced shifts, protein samples were run on NuPAGE 4 to 12% bis-Tris gels. Buffers used for both gel types were described previously (15). All proteins

were transferred to polyvinylidene difluoride (PVDF) membranes before probing with antibodies. The antibodies used for this work are detailed in **Supplementary Table 4**.

Spot tests

Cells from freshly grown plates were diluted in water, and 5- or 10-fold serial dilutions were spotted onto the indicated media and allowed to dry prior to incubation at 30°C for 2 to 3 days.

Liquid growth curves

Cultures grown overnight in YEP medium with 2% raffinose were diluted to an OD_{600} of 0.2 in YEP medium with 2% raffinose and incubated at 30°C with shaking for 4.5 h (OD_{600} = 0.6 to 0.8). Cultures were subsequently diluted to an OD_{600} of 0.1 (measured using an Eppendorf BioPhotometer) in YEP medium with 2% raffinose or YEP medium with 2% galactose. Two hundred microliters of cells was pipetted into the wells of a 100-well honeycomb plate, and the plate was incubated in a Bioscreen C plate reader (Oy Growth Curves) set at 30°C with continuous shaking. A wavelength of 600 nm was used to measure the optical density every 15 min for 24 h.

RT-qPCR analysis

(i) RNA extraction

Cell pellets of 12 OD_{600} units were resuspended in a solution containing 1 mL of cold TRIzol and 200 µL of acid-washed glass beads. Cells were lysed with 6 30-s pulses on a BioSpec minibeadbeater with 2 min on ice between cycles. Two hundred microliters of chloroform was added, and the samples were vortexed for 20 s and incubated at room temperature for 5 min. The samples were centrifuged at 16,000 × *g* for 15 min at 4°C. The aqueous phase was transferred to a fresh screw-cap tube containing 400 µL of chloroform, and the extraction step was repeated as described above. The aqueous phase was transferred to a fresh 1.5-mL Eppendorf tube, RNA was precipitated by adding 500 µL (1:1 volume) of cold isopropanol and 1 µL of Glycoblue, and the

mixture was incubated for 30 min at −20°C. RNA was pelleted by centrifugation for 20 min at 20,000 × *g* at 4°C, and the supernatant was discarded. The pellet was washed with 1 mL of cold 70% ethanol and centrifuged at 20,000 × *g* for 10 min at 4°C. The ethanol was discarded, and the pellets were allowed to air dry for 10 min in a fume hood. The pellets were dissolved in 30 µL of RNase-free water and heated at 55°C for 5 min to ensure resolubilization of the RNA. The quality of the RNA was analyzed by nanodrop and agarose gel methods. Extracted RNA was DNase treated according to the Invitrogen Ambion DNase I (RNase-free) protocol. DNase was removed by phenol-chloroform extraction; a 1:1 volume of a phenol-chloroform-isoamyl solution (25:24:1) was added, and the samples were vortexed for 2 min. The samples were centrifuged at 20,000 × *g* for 10 min at 4°C. The aqueous phase was transferred to an Eppendorf tube containing 1 mL of cold ethanol and 16 µL of sodium acetate, and RNA was left to precipitate overnight at −20°C. RNA was pelleted by centrifugation for 20 min at 20,000 × *g* at 4°C, and the supernatant was discarded. The pellet was washed with 1 mL of cold 70% ethanol and centrifuged at 20,000 × *g* for 10 min at 4°C. The ethanol was discarded, and the pellets were allowed to air dry for 10 min in a fume hood. The pellets were dissolved in 25 µL of RNase-free water and heated at 55°C for 5 min.

(ii) cDNA synthesis and qPCR

One microgram of RNA was reverse transcribed to cDNA using 5× All-In-One reverse transcription (RT) master mix (Applied Biological Materials). Reaction mixtures were incubated in a thermocycler at 37°C for 15 min, 25°C for 10 min, 60°C for 50 min, and 85°C for 5 min. cDNA was diluted 1:5 with RNase-free water, aliquoted into 20-µL working solutions, and stored at −80°C. Quantitative PCRs (qPCRs) were carried out using iQ SYBR green supermix according to the manufacturer's protocol under the following conditions: 95°C for 3 min and 40 cycles of

95°C for 15 s, 60°C for 30 s, and 72°C for 30 s. Melt curve analysis was performed at the end of each run, and standard curves using genomic DNA were performed to assess the primer efficiency for each primer pair. All qPCRs were completed in 3 technical replicates with 5 biological replicates. Changes in mRNA expression were calculated using the $\Delta\Delta C_T$ method, and statistical analysis was performed using Bio-Rad CFX Maestro 2.3 version 5.3.022.1030 software, which uses unpaired two-tailed Student's *t* test based on the geometric mean. Significance was also determined using standard unpaired two-tailed Student's *t* test performed using GraphPad Prism version 9. The primers used are listed in **Supplementary Table 5B**.

Data availability

The mass spectrometry proteomics data have been deposited to the ProteomeXchange Consortium via the PRIDE (75) partner repository with the data set identifier PXD031326.

3.7. Acknowledgements

We thank T. Shiba (RegeneTiss, Japan) for the gift of polyP standards and Andreas Mayer for the original p416-GPD and p416-GPD-PPK plasmids. We thank the UC Davis Proteomics Core Facility for mass spectrometry analysis and Brett Phinney for help with relevant methods text. We also thank the Rudner lab for the Cdc55 antibody as well as the Baetz lab for the Msn2 and p-PKA substrate antibodies.

Work for this project was funded by Canadian Institutes of Health Research (CIHR) project grants to M.D. (PJT-148722) and M.D. and M.L.-A. (PJT-174987) and a Natural Sciences and Engineering Research Council of Canada (NSERC) discovery grant to M.L.-A. Trainees in the Downey lab are supported in part by an early researcher award from the Ontario Ministry of Research, Innovation, and Science. L.M. was supported by an Ontario graduate scholarship and an NSERC Canada graduate scholarship. I.A. was supported by an Ontario graduate scholarship and an NSERC Canada graduate scholarship.

We declare no conflicts.

3.8. References

1. Hothorn M, Neumann H, Lenherr ED, Wehner M, Rybin V, Hassa PO, Uttenweiler A, Reinhardt M, Schmidt A, Seiler J, Ladurner AG, Herrmann C, Scheffzek K, Mayer A. 2009. Catalytic core of a membrane-associated eukaryotic polyphosphate polymerase. *Science* 324:513–516.
2. Denoncourt A, Downey M. 2021. Model systems for studying polyphosphate biology: a focus on microorganisms. *Curr Genet* 67:331–346.
3. Desfougères Y, Gerasimaitė RU, Jessen HJ, Mayer A. 2016. Vtc5, a novel subunit of the vacuolar transporter chaperone complex, regulates polyphosphate synthesis and phosphate homeostasis in yeast. *J Biol Chem* 291:22262–22275.
4. Bentley-DeSousa A, Downey M. 2021. Vtc5 is localized to the vacuole membrane by the conserved AP-3 complex to regulate polyphosphate synthesis in budding yeast. *mBio* 12:e00994-21.
5. Gerasimaitė R, Sharma S, Desfougères Y, Schmidt A, Mayer A. 2014. Coupled synthesis and translocation restrains polyphosphate to acidocalcisome-like vacuoles and prevents its toxicity. *J Cell Sci* 127(Part 23):5093–5104.
6. Kornberg A, Rao NN, Ault-Riche D. 1999. Inorganic polyphosphate: a molecule of many functions. *Annu Rev Biochem* 68:89–125.
7. Uttenweiler A, Schwarz H, Neumann H, Mayer A. 2007. The vacuolar transporter chaperone (VTC) complex is required for microautophagy. *Mol Biol Cell* 18:166–175.
8. Baijal K, Downey M. 2021. The promises of lysine polyphosphorylation as a regulatory modification in mammals are tempered by conceptual and technical challenges. *Bioessays* 43:e2100058.
9. Jimenez-Nuñez MD, Moreno-Sanchez D, Hernandez-Ruiz L, Benítez-Rondán A, Ramos-Amaya A, Rodríguez-Bayona B, Medina F, Brieva JA, Ruiz FA. 2012. Myeloma cells contain high levels of inorganic polyphosphate which is associated with nucleolar transcription. *Haematologica* 97:1264–1271.
10. Xie L, Rajpurkar A, Quarles E, Taube N, Rai AS, Erba J, Sliwinski B, Markowitz M, Jakob U, Knoefler D. 2019. Accumulation of nucleolar inorganic polyphosphate is a cellular response to cisplatin-induced apoptosis. *Front Oncol* 9:1410.
11. Ruiz FA, Lea CR, Oldfield E, Docampo R. 2004. Human platelet dense granules contain polyphosphate and are similar to acidocalcisomes of bacteria and unicellular eukaryotes. *J Biol Chem* 279:44250–44257.
12. Austin S, Mayer A. 2020. Phosphate homeostasis—a vital metabolic equilibrium maintained through the INPHORS signaling pathway. *Front Microbiol* 11:1367.
13. Desfougeres Y, Neumann H, Mayer A. 2016. Organelle size control—increasing vacuole content activates SNAREs to augment organelle volume through homotypic fusion. *J Cell Sci* 129:2817–2828.
14. Smith SA, Mutch NJ, Baskar D, Rohloff P, Docampo R, Morrissey JH. 2006. Polyphosphate modulates blood coagulation and fibrinolysis. *Proc Natl Acad Sci USA* 103:903–908.
15. Bentley-DeSousa A, Holinier C, Moteshareie H, Tseng Y-C, Kajjo S, Nwosu C, Amodeo GF, Bondy-Chorney E, Sai Y, Rudner A, Golshani A, Davey NE, Downey M. 2018. A screen for candidate targets of lysine polyphosphorylation uncovers a conserved network implicated in ribosome biogenesis. *Cell Rep* 22:3427–3439.

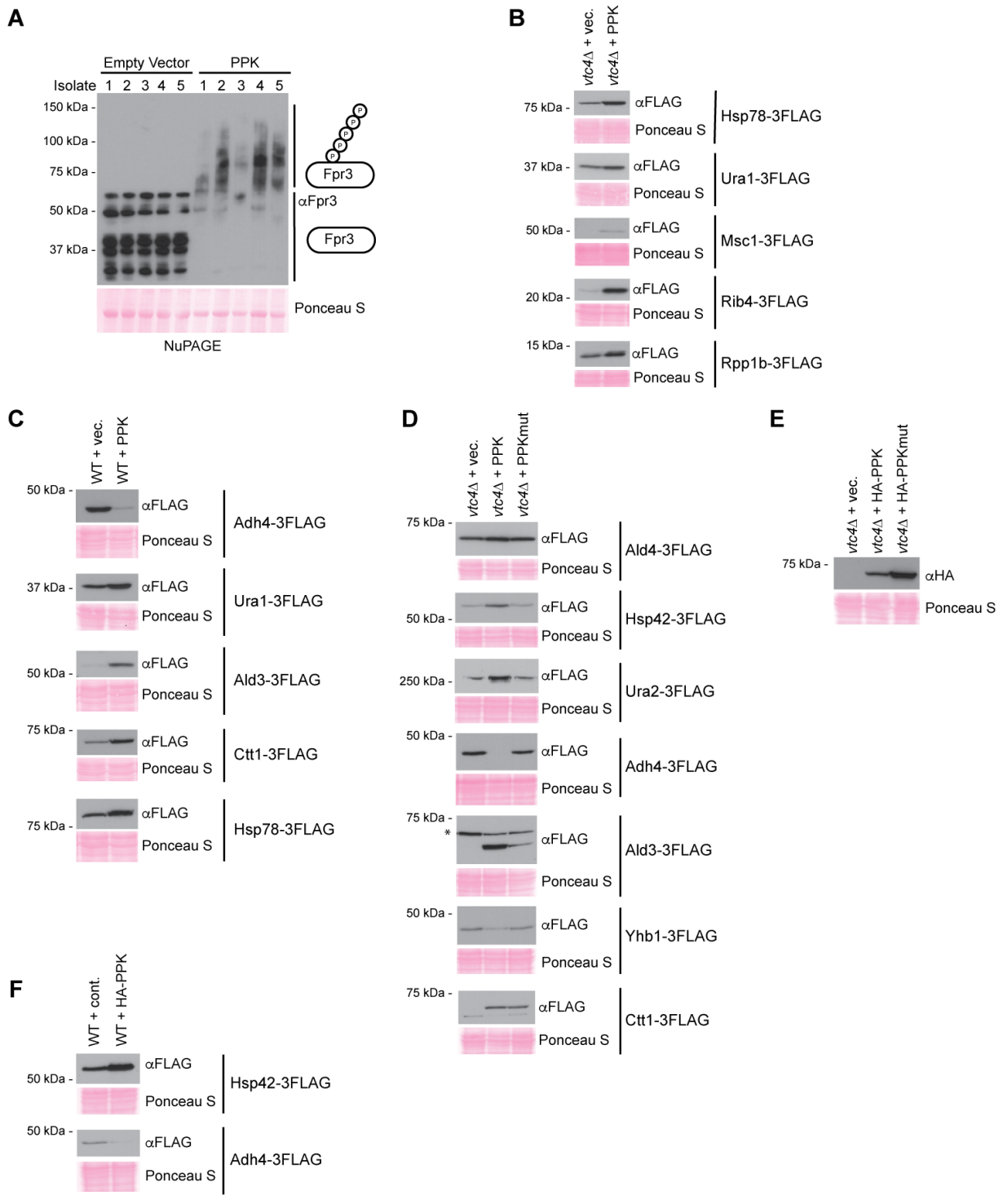
16. Bondy-Chorney E, Abramchuk I, Nasser R, Holinier C, Denoncourt A, Baijal K, McCarthy L, Khacho M, Lavallée-Adam M, Downey M. 2020. A broad response to intracellular long-chain polyphosphate in human cells. *Cell Rep* 33:108318.
17. Kumble KD, Ahn K, Kornberg A. 1996. Phosphohistidyl active sites in polyphosphate kinase of Escherichia coli. *Proc Natl Acad Sci USA* 93:14391–14395.
18. Zhu J, Loubéry S, Broger L, Zhang Y, Lorenzo-Orts L, Utz-Pugin A, Fernie AR, Young-Tae C, Hothorn M. 2020. A genetically validated approach for detecting inorganic polyphosphates in plants. *Plant J* 102:507–516.
19. Zhu Y, Huang W, Lee SS, Xu W. 2005. Crystal structure of a polyphosphate kinase and its implications for polyphosphate synthesis. *EMBO Rep* 6:681–687.
20. Ogawa N, DeRisi J, Brown PO. 2000. New components of a system for phosphate accumulation and polyphosphate metabolism in Saccharomyces cerevisiae revealed by genomic expression analysis. *Mol Biol Cell* 11:4309–4321.
21. Harris MA, Clark J, Ireland A, Lomax J, Ashburner M, Foulger R, Eilbeck K, Lewis S, Marshall B, Mungall C, Richter J, Rubin GM, Blake JA, Bult C, Dolan M, Drabkin H, Eppig JT, Hill DP, Ni L, Ringwald M, Balakrishnan R, Cherry JM, Christie KR, Costanzo MC, Dwight SS, Engel S, Fisk DG, Hirschman JE, Hong EL, Nash RS, Sethuraman A, Theesfeld CL, Botstein D, Dolinski K, Feierbach B, Berardini T, Mundodi S, Rhee SY, Apweiler R, Barrell D, Camon E, Dimmer E, Lee V, Chisholm R, Gaudet P, Kibbe W, Kishore R, Schwarz EM, Sternberg P, Gwinn M, et al. 2004. The Gene Ontology (GO) database and informatics resource. *Nucleic Acids Res* 32:D258–D261.
22. Cherry JM, Hong EL, Amundsen C, Balakrishnan R, Binkley G, Chan ET, Christie KR, Costanzo MC, Dwight SS, Engel SR, Fisk DG, Hirschman JE, Hitz BC, Karra K, Krieger CJ, Miyasato SR, Nash RS, Park J, Skrzypek MS, Simison M, Weng S, Wong ED. 2012. Saccharomyces Genome Database: the genomics resource of budding yeast. *Nucleic Acids Res* 40:D700–D705.
23. Szklarczyk D, Gable AL, Lyon D, Junge A, Wyder S, Huerta-Cepas J, Simonovic M, Doncheva NT, Morris JH, Bork P, Jensen LJ, von Mering C. 2019. STRING v11: protein-protein association networks with increased coverage, supporting functional discovery in genome-wide experimental datasets. *Nucleic Acids Res* 47:D607–D613.
24. Gray MJ, Wholey W-Y, Wagner NO, Cremers CM, Mueller-Schickert A, Hock NT, Krieger AG, Smith EM, Bender RA, Bardwell JCA, Jakob U. 2014. Polyphosphate is a primordial chaperone. *Mol Cell* 53:689–699.
25. Beaufay F, Quarles E, Franz A, Katamanin O, Wholey WY, Jakob U. 2020. Polyphosphate functions in vivo as an iron chelator and Fenton reaction inhibitor. *mBio* 11:e01017-20.
26. Askwith C, Eide D, Van Ho A, Bernard PS, Li L, Davis-Kaplan S, Sipe DM, Kaplan J. 1994. The FET3 gene of S. cerevisiae encodes a multicopper oxidase required for ferrous iron uptake. *Cell* 76:403–410.
27. Drewke C, Ciriacy M. 1988. Overexpression, purification and properties of alcohol dehydrogenase IV from Saccharomyces cerevisiae. *Biochim Biophys Acta* 950:54–60.
28. Pearce DA, Sherman F. 1999. Toxicity of copper, cobalt, and nickel salts is dependent on histidine metabolism in the yeast Saccharomyces cerevisiae. *J Bacteriol* 181:4774–4779.
29. Yuan DS. 2000. Zinc-regulated genes in Saccharomyces cerevisiae revealed by transposon tagging. *Genetics* 156:45–58.
30. Teixeira MC, Monteiro PT, Palma M, Costa C, Godinho CP, Pais P, Cavalheiro M, Antunes M, Lemos A, Pedreira T, Sá-Correia I. 2018. YEASTRACT: an upgraded database for the

analysis of transcription regulatory networks in Saccharomyces cerevisiae. *Nucleic Acids Res* 46:D348–D353.
31. Martinez-Pastor MT, Marchler G, Schuller C, Marchler-Bauer A, Ruis H, Estruch F. 1996. The Saccharomyces cerevisiae zinc finger proteins Msn2p and Msn4p are required for transcriptional induction through the stress response element (STRE). *EMBO J* 15:2227–2235.
32. Schmitt AP, McEntee K. 1996. Msn2p, a zinc finger DNA-binding protein, is the transcriptional activator of the multistress response in Saccharomyces cerevisiae. *Proc Natl Acad Sci USA* 93:5777–5782.
33. Pfanzagl V, Görner W, Radolf M, Parich A, Schuhmacher R, Strauss J, Reiter W, Schüller C. 2018. A constitutive active allele of the transcription factor Msn2 mimicking low PKA activity dictates metabolic remodeling in yeast. *Mol Biol Cell* 29:2848–2862.
34. Durchschlag E, Reiter W, Ammerer G, Schuller C. 2004. Nuclear localization destabilizes the stress-regulated transcription factor Msn2. *J Biol Chem* 279:55425–55432.
35. Gorner W, Durchschlag E, Wolf J, Brown EL, Ammerer G, Ruis H, Schuller C. 2002. Acute glucose starvation activates the nuclear localization signal of a stress-specific yeast transcription factor. *EMBO J* 21:135–144.
36. Ma L, Ho K, Piggott N, Luo Z, Measday V. 2012. Interactions between the kinetochore complex and the protein kinase A pathway in Saccharomyces cerevisiae. *G3 (Bethesda)* 2:831–841.
37. Lallet S, Garreau H, Poisier C, Boy-Marcotte E, Jacquet M. 2004. Heat shock-induced degradation of Msn2p, a Saccharomyces cerevisiae transcription factor, occurs in the nucleus. *Mol Genet Genomics* 272:353–362.
38. Lee P, Cho BR, Joo HS, Hahn JS. 2008. Yeast Yak1 kinase, a bridge between PKA and stress-responsive transcription factors, Hsf1 and Msn2/Msn4. *Mol Microbiol* 70:882–895.
39. Capaldi AP, Kaplan T, Liu Y, Habib N, Regev A, Friedman N, O'Shea EK. 2008. Structure and function of a transcriptional network activated by the MAPK Hog1. *Nat Genet* 40:1300–1306.
40. Lee P, Paik SM, Shin CS, Huh WK, Hahn JS. 2011. Regulation of yeast Yak1 kinase by PKA and autophosphorylation-dependent 14-3-3 binding. *Mol Microbiol* 79:633–646.
41. Azevedo C, Desfougères Y, Jiramongkol Y, Partington H, Trakansuebkul S, Singh J, Steck N, Jessen HJ, Saiardi A. 2020. Development of a yeast model to study the contribution of vacuolar polyphosphate metabolism to lysine polyphosphorylation. *J Biol Chem* 295:1439–1451.
42. Bentley-DeSousa A, Downey M. 2019. From underlying chemistry to therapeutic potential: open questions in the new field of lysine polyphosphorylation. *Curr Genet* 65:57–64.
43. Lonetti A, Szijgyarto Z, Bosch D, Loss O, Azevedo C, Saiardi A. 2011. Identification of an evolutionarily conserved family of inorganic polyphosphate endopolyphosphatases. *J Biol Chem* 286:31966–31974.
44. Tammenkoski M, Koivula K, Cusanelli E, Zollo M, Steegborn C, Baykov AA, Lahti R. 2008. Human metastasis regulator protein H-prune is a short-chain exopolyphosphatase. *Biochemistry* 47:9707–9713.
45. Samper-Martín B, Sarrias A, Lázaro B, Pérez-Montero M, Rodríguez-Rodríguez R, Ribeiro MPC, Bañón A, Wolfgeher D, Jessen HJ, Alsina B, Clotet J, Kron SJ, Saiardi A, Jiménez J, Bru S. 2021. Polyphosphate degradation by Nudt3-Zn(2+) mediates oxidative stress response. *Cell Rep* 37:110004.

46. Moreno B, Urbina JA, Oldfield E, Bailey BN, Rodrigues CO, Docampo R. 2000. 31P NMR spectroscopy of Trypanosoma brucei, Trypanosoma cruzi, and Leishmania major. Evidence for high levels of condensed inorganic phosphates. *J Biol Chem* 275:28356–28362.
47. Negreiros RS, Lander N, Huang G, Cordeiro CD, Smith SA, Morrissey JH, Docampo R. 2018. Inorganic polyphosphate interacts with nucleolar and glycosomal proteins in trypanosomatids. *Mol Microbiol* 110:973–994.
48. Travers RJ, Smith SA, Morrissey JH. 2015. Polyphosphate, platelets, and coagulation. *Int J Lab Hematol* 37(Suppl 1):31–35.
49. Smith SA, Choi SH, Davis-Harrison R, Huyck J, Boettcher J, Rienstra CM, Reinstra CM, Morrissey JH. 2010. Polyphosphate exerts differential effects on blood clotting, depending on polymer size. *Blood* 116:4353–4359.
50. Roewe J, Stavrides G, Strueve M, Sharma A, Marini F, Mann A, Smith SA, Kaya Z, Strobl B, Mueller M, Reinhardt C, Morrissey JH, Bosmann M. 2020. Bacterial polyphosphates interfere with the innate host defense to infection. *Nat Commun* 11:4035.
51. Azevedo C, Livermore T, Saiardi A. 2015. Protein polyphosphorylation of lysine residues by inorganic polyphosphate. *Mol Cell* 58:71–82.
52. Conrad M, Schothorst J, Kankipati HN, Van Zeebroeck G, Rubio-Texeira M, Thevelein JM. 2014. Nutrient sensing and signaling in the yeast Saccharomyces cerevisiae. *FEMS Microbiol Rev* 38:254–299.
53. Denis-Duphil M, Lecaer JP, Hardie DG, Carrey EA. 1990. Yeast carbamoyl-phosphate-synthetase-aspartate-transcarbamylase multidomain protein is phosphorylated in vitro by cAMP-dependent protein kinase. *Eur J Biochem* 193:581–587.
54. Urita A, Ishibashi Y, Kawaguchi R, Yanase Y, Tani M. 2022. Crosstalk between protein kinase A and the HOG pathway under impaired biosynthesis of complex sphingolipids in budding yeast. *FEBS J* 289:766–786.
55. Smith A, Ward MP, Garrett S. 1998. Yeast PKA represses Msn2p/Msn4p-dependent gene expression to regulate growth, stress response and glycogen accumulation. *EMBO J* 17:3556–3564.
56. Garrett S, Broach J. 1989. Loss of Ras activity in Saccharomyces cerevisiae is suppressed by disruptions of a new kinase gene, YAKI, whose product may act downstream of the cAMP-dependent protein kinase. *Genes Dev* 3:1336–1348.
57. Zurita-Martinez SA, Cardenas ME. 2005. Tor and cyclic AMP-protein kinase A: two parallel pathways regulating expression of genes required for cell growth. *Eukaryot Cell* 4:63–71.
58. Kulakovskaya TV, Lichko LP, Vagabov VM, Kulaev IS. 2010. Inorganic polyphosphates in mitochondria. *Biochemistry (Mosc)* 75:825–831.
59. Bru S, Martínez-Laínez JM, Hernández-Ortega S, Quandt E, Torres-Torronteras J, Martí R, Canadell D, Ariño J, Sharma S, Jiménez J, Clotet J. 2016. Polyphosphate is involved in cell cycle progression and genomic stability in Saccharomyces cerevisiae. *Mol Microbiol* 101:367–380.
60. Hussain M, Leibowitz MJ, Lenard J. 1987. Killing of Saccharomyces cerevisiae by the lysosomotropic detergent N-dodecylimidazole. *Antimicrob Agents Chemother* 31:512–517.
61. Eastwood MD, Cheung SW, Meneghini MD. 2013. Programmed nuclear destruction in yeast: self-eating by vacuolar lysis. *Autophagy* 9:263–265.
62. Nistala H, Dronzek J, Gonzaga-Jauregui C, Chim SM, Rajamani S, Nuwayhid S, Delgado D, Burke E, Karaca E, Franklin MC, Sarangapani P, Podgorski M, Tang Y, Dominguez MG, Withers M, Deckelbaum RA, Scheonherr CJ, Gahl WA, Malicdan MC, Zambrowicz B, Gale

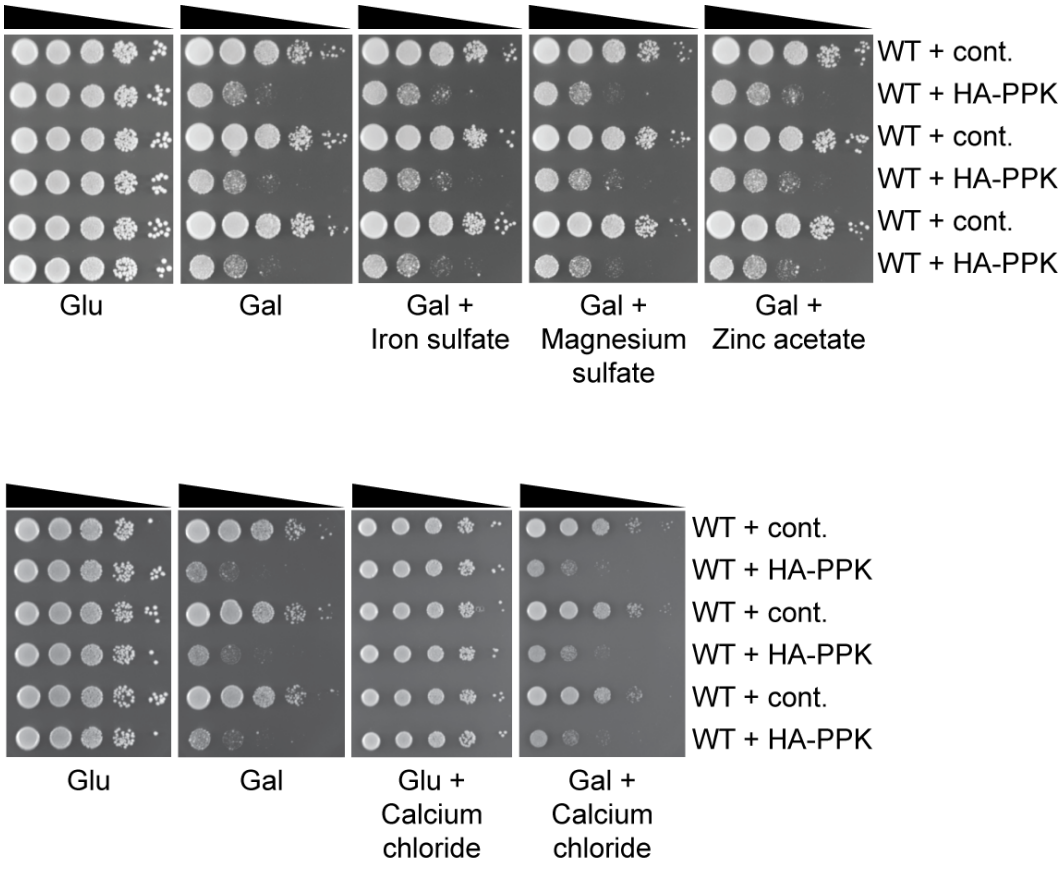
NW, Gibbs RA, Chung WK, Lupski JR, Economides AN. 2021. NMIHBA results from hypomorphic PRUNE1 variants that lack short-chain exopolyphosphatase activity. *Hum Mol Genet* 29:3516–3531.
63. Goldstein AL, McCusker JH. 1999. Three new dominant drug resistance cassettes for gene disruption in Saccharomyces cerevisiae. *Yeast* 15:1541–1553.
64. Longtine MS, Mckenzie A, III, Demarini DJ, Shah NG, Wach A, Brachat A, Philippsen P, Pringle JR. 1998. Additional modules for versatile and economical PCR-based gene deletion and modification in Saccharomyces cerevisiae. *Yeast* 14:953–961.
65. McCarthy L, Bentley-DeSousa A, Denoncourt A, Tseng YC, Gabriel M, Downey M. 2020. Proteins required for vacuolar function are targets of lysine polyphosphorylation in yeast. *FEBS Lett* 594:21–30.
66. Bru S, Samper-Martín B, Quandt E, Hernández-Ortega S, Martínez-Laínez JM, Garí E, Rafel M, Torres-Torronteras J, Martí R, Ribeiro MPC, Jiménez J, Clotet J. 2017. Polyphosphate is a key factor for cell survival after DNA damage in eukaryotic cells. *DNA Repair (Amst)* 57:171–178.
67. Smith SA, Morrissey JH. 2007. Sensitive fluorescence detection of polyphosphate in polyacrylamide gels using 4′,6-diamidino-2-phenylindol. *Electrophoresis* 28:3461–3465.
68. Kessner D, Chambers M, Burke R, Agus D, Mallick P. 2008. ProteoWizard: open source software for rapid proteomics tools development. *Bioinformatics* 24:2534–2536.
69. Craig R, Beavis RC. 2004. TANDEM: matching proteins with tandem mass spectra. *Bioinformatics* 20:1466–1467.
70. Bairoch A, Boeckmann B. 1994. The SWISS-PROT protein sequence data bank: current status. *Nucleic Acids Res* 22:3578–3580.
71. Howe KL, Achuthan P, Allen J, Allen J, Alvarez-Jarreta J, Amode MR, Armean IM, Azov AG, Bennett R, Bhai J, Billis K, Boddu S, Charkhchi M, Cummins C, Da Rin Fioretto L, Davidson C, Dodiya K, El Houdaigui B, Fatima R, Gall A, Garcia Giron C, Grego T, Guijarro-Clarke C, Haggerty L, Hemrom A, Hourlier T, Izuogu OG, Juettemann T, Kaikala V, Kay M, Lavidas I, Le T, Lemos D, Gonzalez Martinez J, Marugán JC, Maurel T, McMahon AC, Mohanan S, Moore B, Muffato M, Oheh DN, Paraschas D, Parker A, Parton A, Prosovetskaia I, Sakthivel MP, Salam AIA, Schmitt BM, Schuilenburg H, Sheppard D, et al. 2021. Ensembl 2021. *Nucleic Acids Res* 49:D884–D891.
72. Benjamini Y, Hochberg Y. 1995. Controlling the false discovery rate: a practical and powerful approach to multiple testing. *J R Stat Soc Series B Stat Methodol* 57:289–300.
73. Ashburner M, Ball CA, Blake JA, Botstein D, Butler H, Cherry JM, Davis AP, Dolinski K, Dwight SS, Eppig JT, Harris MA, Hill DP, Issel-Tarver L, Kasarskis A, Lewis S, Matese JC, Richardson JE, Ringwald M, Rubin GM, Sherlock G. 2000. Gene Ontology: tool for the unification of biology. The Gene Ontology Consortium. *Nat Genet* 25:25–29.
74. Bauer S, Grossmann S, Vingron M, Robinson PN. 2008. Ontologizer 2.0—a multifunctional tool for GO term enrichment analysis and data exploration. *Bioinformatics* 24:1650–1651.
75. Perez-Riverol Y, Bai J, Bandla C, García-Seisdedos D, Hewapathirana S, Kamatchinathan S, Kundu DJ, Prakash A, Frericks-Zipper A, Eisenacher M, Walzer M, Wang S, Brazma A, Vizcaíno JA. 2022. The PRIDE database resources in 2022: a hub for mass spectrometry-based proteomics evidences. *Nucleic Acids Res* 50:D543–D552.

3.9. Supplemental figures

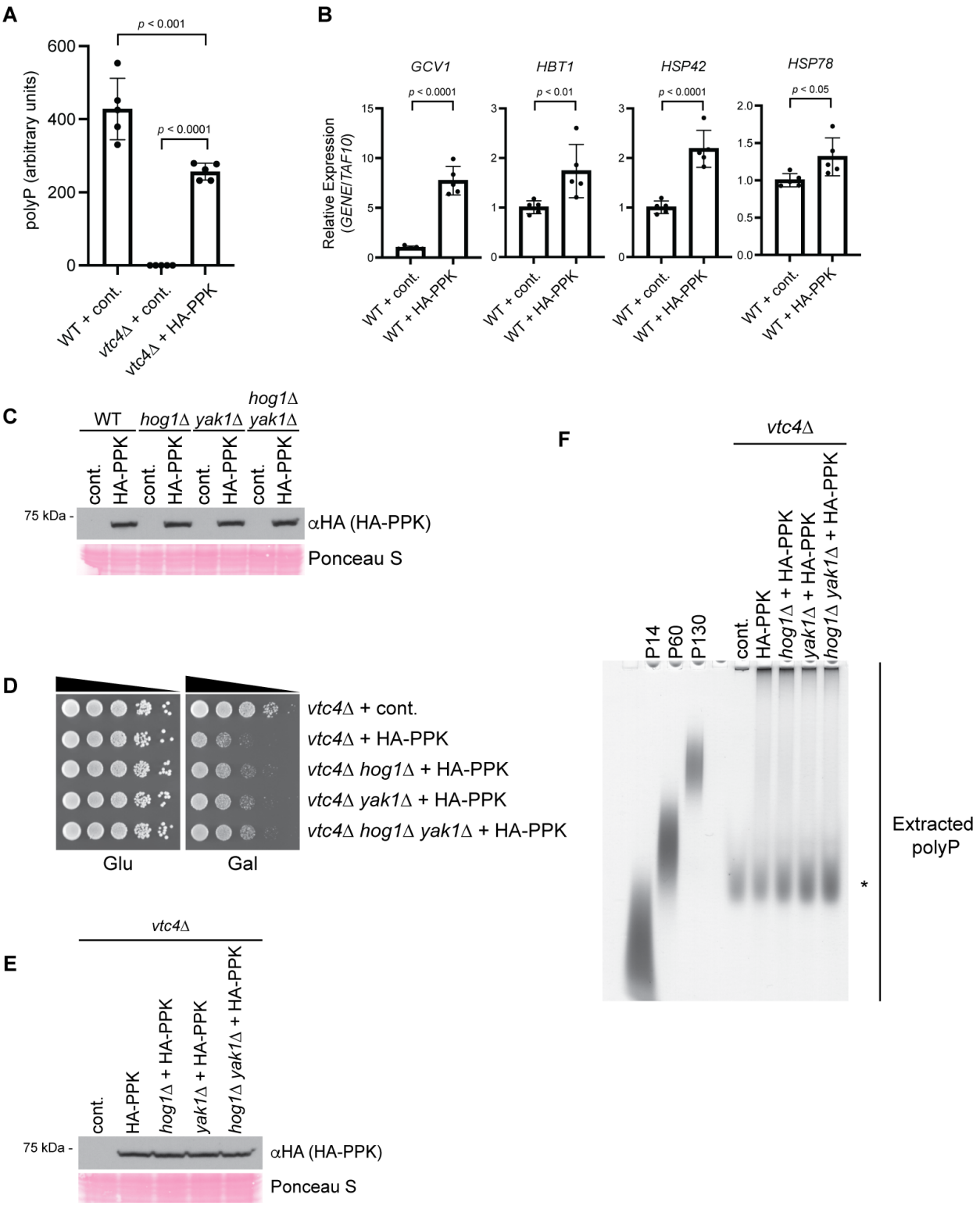


S1 Figure. Changes to the *S. cerevisiae* proteome with ectopic PPK expression. (**A**) PPK expression restores polyphosphate levels in samples used for mass spectrometry. Protein extracts were prepared from the indicated strains carrying either control or PPK-expressing plasmids using an SDS lysis protocol and separated on a NuPAGE gel. Separated proteins were transferred to a

PVDF membrane before probing with an antibody that recognizes yeast Fpr3. Ponceau S staining of the membrane is shown as a loading control. The shift observed in PPK-expressing samples is a sign of lysine polyphosphorylation and polyP production. (**B**) Supplemental protein expression validation of mass spectrometry candidates in a *vtc4*Δ background. (**C**) Supplemental protein expression validation of mass spectrometry candidates in a wild-type background. (**D**) Supplemental protein expression validation of mass spectrometry candidates in a *vtc4*Δ background with mutant PPK included. Asterisks indicate nonspecific bands. (**E**) Expression levels of HA-PPK and mutant HA-PPK expressed from plasmids in a *vtc4*Δ background. These cell extracts were prepared from Fet3-3FLAG-tagged strains. (**F**) Supplemental protein expression validations of mass spectrometry candidates using the Gal-inducible HA-PPK system. All protein extracts from the indicated strains in panels B to F were prepared using a TCA lysis protocol and separated on SDS-PAGE gels. Separated proteins were transferred to a PVDF membrane before probing with an anti-FLAG antibody. Ponceau S staining of the membrane is used as a loading control. Images are representative of results from ≥2 experiments.

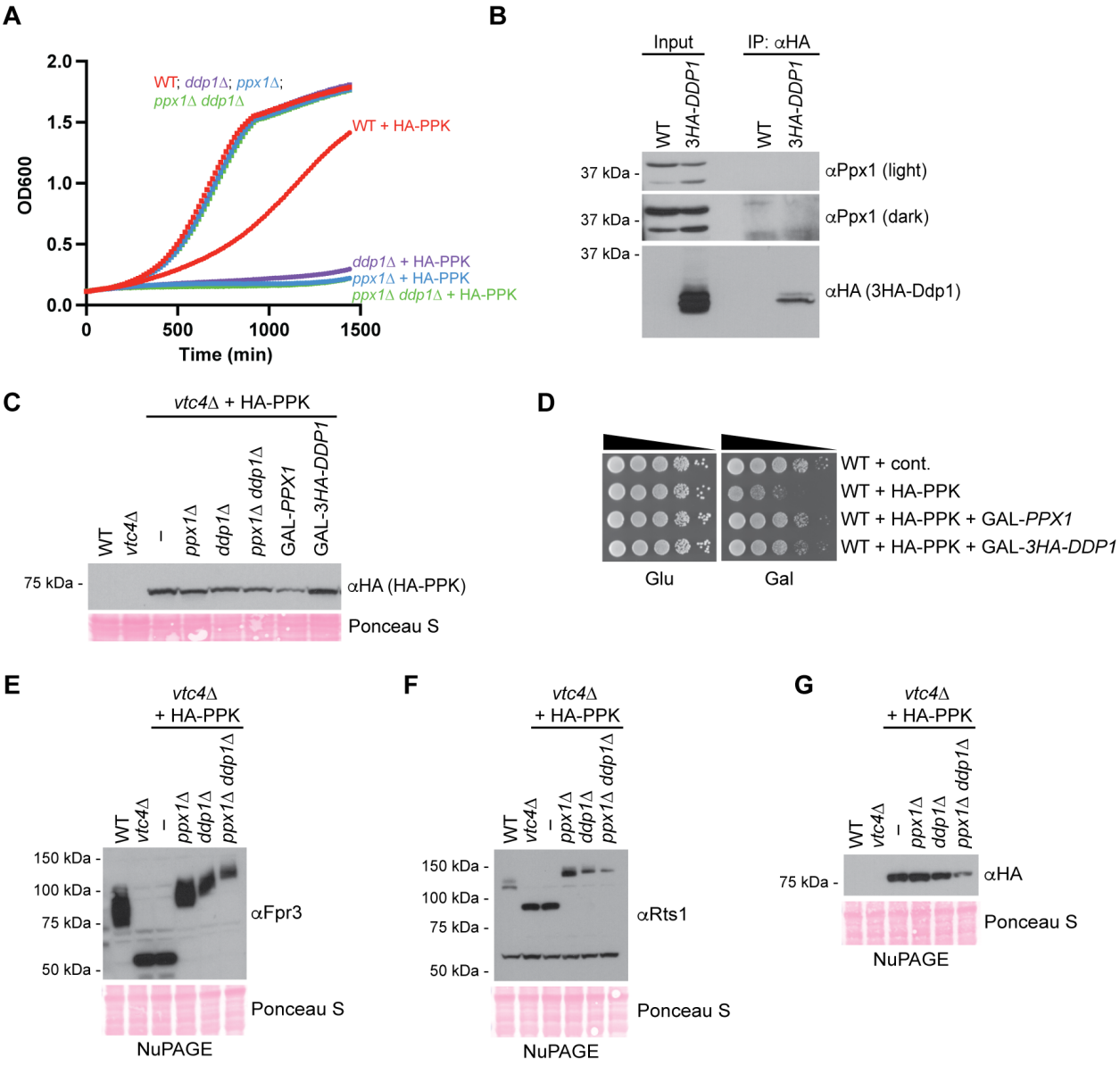


S2 Figure. Supplementing media with excess metals does not rescue PPK-induced growth defects. The indicated strains were spotted in 10-fold dilution series. All metals were used at a concentration of 200 μM with the exception of calcium chloride, which was used at 100 mM. Plates were incubated at 30°C for 48 h. Images are representative of results from 2 experiments, except for calcium chloride, which is representative of results from 3 experiments.



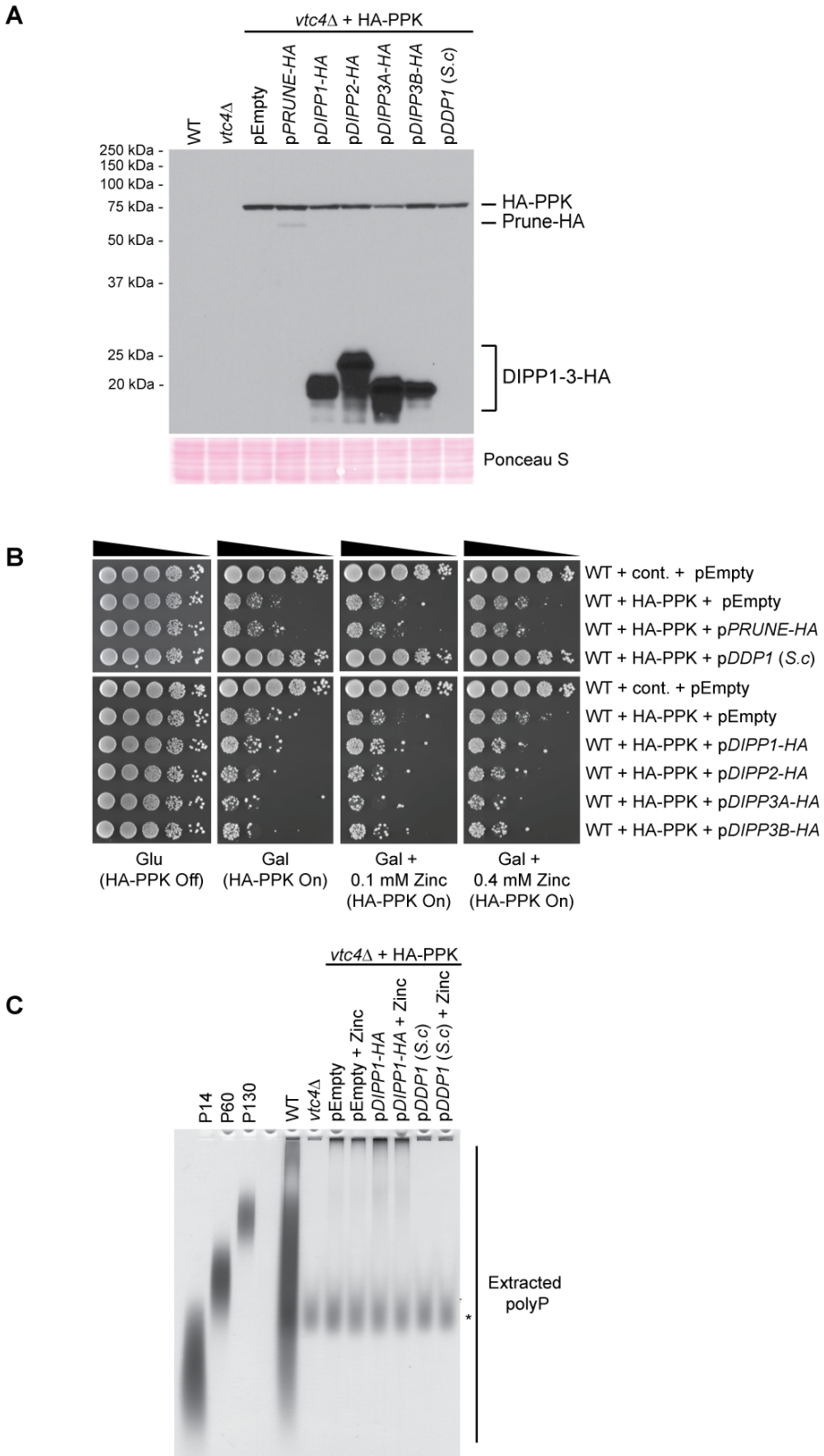
S3 Figure. PolyP quantification, qPCR analysis of Msn2/Msn4 targets, and HA-PPK levels in the *HOG1* and *YAK1* mutants. (**A**) Quantification of polyP produced by the Gal-inducible HA-PPK system. Extracted polyP was quantified from 5 biological replicates using the Phosfinity

kit. Error bars represent standard deviations. Significance was determined by 2-tailed Student's *t* test. (**B**) qPCR analysis of differentially expressed proteins regulated by the Msn2/Msn4 transcription factors. qPCR was performed on 5 biological replicates. Error bars represent standard errors of the means. The indicated *P* values were determined by Bio-Rad CFX Maestro 2.3 version 5.3.022.1030 software, which uses Student's *t* test based on the geometric mean. (**C**) Protein extracts from the indicated strains were prepared using a TCA lysis protocol and separated on SDS-PAGE gels. Separated proteins were transferred to a PVDF membrane and probed with anti-HA to detect HA-PPK. Ponceaus S staining is shown as a loading control. (**D**) The indicated strains were spotted in 10-fold dilution series, and plates were incubated at 30°C for 48 h. (**E**) Protein extracts from the indicated strains were prepared using a TCA lysis protocol and separated on SDS-PAGE gels. Separated proteins were transferred to a PVDF membrane and probed with anti-HA to detect HA-PPK. Ponceaus S staining is shown as a loading control. (**F**) PolyP levels are unaffected in *hog1*Δ and *yak1*Δ mutants. Polyphosphate was extracted from the indicated strains and visualized using toluidine blue staining following separation on a 15.8% acrylamide–TBE–urea gel. The asterisk indicates nonspecific staining of an unknown product that is not polyP, as it is present in *vtc4*Δ cells. Images are representative of results from ≥3 experiments, except for panel E, which is representative of results from 2 experiments.



S4 Figure. HA-PPK regulation in polyphosphatase mutants. (**A**) Growth curves for the indicated strains were generated using the Bioscreen C system described in Materials and Methods. (**B**) Ppx1 does not coimmunoprecipitate with Ddp1. 3HA-Ddp1 was immunoprecipitated using an anti-HA antibody and then recovered using protein A-agarose beads before elution in sample buffer. Eluted proteins from the indicated strains were separated on SDS-PAGE gels and transferred to a PVDF membrane prior to probing with anti-HA to detect 3HA-Ddp1 and anti-Ppx1 to detect Ppx1. (**C**) HA-PPK levels in polyphosphatase mutants. Protein extracts from the indicated strains were prepared using a TCA lysis protocol and separated on SDS-PAGE gels. Separated proteins were transferred to a PVDF membrane and probed with anti-HA to detect HA-PPK. Ponceau S staining is shown as a loading control. (**D**) The indicated strains were spotted in 10-fold dilution series, and plates were incubated at 30°C for 48 h. (**E** to **G**) After a 1-h galactose induction of HA-PPK, lysine polyphosphorylation of Fpr3 and Rts1 was analyzed by NuPAGE,

followed by transfer to a PVDF membrane and the detection of proteins using the indicated antibodies. Ponceau S staining of the membrane is used as a loading control. Images are representative of results from ≥3 experiments for all panels except panel B, which is representative of results from 2 experiments.



S5 Figure. Overexpression of potential mammalian polyphosphatases. (**A**) Protein extracts from the indicated strains were analyzed using a 12% SDS-PAGE gel following TCA-style lysis,

prior to transfer to a PVDF membrane and detection with anti-HA to detect HA-PPK. Strains were transformed with the empty vector or HA-tagged Prune-, HA-tagged DIPP1-, HA-tagged DIPP2-, HA-tagged DIPP3A-, HA-tagged DIPP3B-, or yeast Ddp1-expressing plasmids. Ponceau S staining is shown as a loading control. (**B**) Strains with the indicated plasmids expressing potential mammalian polyphosphatases or yeast Ddp1 were spotted in 10-fold serial dilutions onto the indicated media supplemented with or without zinc sulfate. (**C**) Polyphosphate was extracted from strains expressing the indicated plasmids and visualized using toluidine blue staining following separation on a 15.8% acrylamide–TBE–urea gel. The asterisk indicates nonspecific staining of an unknown product that is not polyP, as it is present in *vtc4*Δ cells. Images are representative of results from 3 experiments.

3.10. Supplemental tables

Note: The tables that are important for the interpretation of the data presented have been included in the thesis. Please see the link provided below for all Supplemental Tables related to this article.

List of tables presented:

S1 Table. Mass spectrometry data.

1. S1-Tab 2: Significantly differentially expressed proteins identified.
2. S1-Tab 3: All-or-none proteins identified.

S2 Table. Summary of MS data set confirmations.

1. S2-Tab 1: MS confirmations using PPK plasmid.
2. S2-Tab 2: MS confirmations using gal-inducible PPK expression system.

S3 Table. Yeast strains used in this work.

S5 Table. Plasmids and qPCR primers used in this work.

1. S5-Tab 1: Plasmids used in this work.

Online version of tables (S1 – S3):

S1 Table. Mass spectrometry data.
See online: Table S1, XLSX file, 2.2 MB.

S2 Table. Summary of MS data set confirmations.
See online: Table S2, XLSX file, 0.01 MB.

S3 Table. Yeast strains used in this work.
See online: Table S3, XLSX file, 0.01 MB.

S4 Table. Antibodies used in this work.
See online: Table S4, XLSX file, 0.01 MB.

S5 Table. Plasmids and qPCR primers used in this work.
See online: Table S5, XLSX file, 0.01 MB.

S1 Table-Tab 2 – Significantly differentially expressed proteins identified.

Significantly differentially expressed proteins	
Protein name	**FDR-adjusted p-value**
HXK2	0.031045414
YDL124W	0.031045414
ALD4	0.031045414
ADH4	0.031045414
HSP26	0.031045414
GCV1	0.031045414
URA2	0.03671704
ASC1	0.03671704
ARG4	0.03671704
ARO3	0.044613425
FET3	0.044613425
URA1	0.046720606
HBT1	0.046720606
LAC1	0.046720606
HSP42	0.056464909
TDH3	0.0605642
TY1B-NL1	0.090697301
SSZ1	0.090697301
HMO1	0.090697301
HEM13	0.090697301
URA3	0.099597571
ZPS1	0.099597571
CCP1	0.099597571
HIS1	0.099597571
SNZ1	0.099597571
DED1	0.099911428
HSP12	0.099911428
GLN1	0.099911428
ALD3	0.099911428
GUT2	0.099911428
IDP3	0.099911428
ASP1	0.100905939
MSC7	0.101021044
HSP104	0.102839886
TUF1	0.102839886
PMT4	0.102839886
FOL2	0.102839886
FIS1	0.102839886

S1 Table-Tab 3 – All-or-none proteins identified.

All-or-none proteins										
Protein Name	**PPK_1**	**PPK_2**	**PPK_3**	**PPK_4**	**PPK_5**	**Ctrl_1**	**Ctrl_2**	**Ctrl_3**	**Ctrl_4**	**Ctrl_5**
RPL22B	0	0	0	0	0	4	2	2	4	3
SNL1	0	0	0	0	0	4	4	2	2	4
PPK1	35	33	34	28	28	0	0	0	0	0

S2 Table-Tab 1 – MS confirmations using PPK plasmid.

Proteins	Regulation PPK vs. Control	Confirmations	
		*vtc4*Δ (n)#	wild-type (n)#
Ald4	Up	Yes (4)	Not tested
Adh4	Down	Yes (6)	Yes (2)
Hsp26	Down	Inconsistent (3)	Inconsistent (2)
Gcv1	Up	Yes (6)	Yes (4)
Ura2	Up	Yes (4)	Not tested
Fet3	Down	Yes (8)	Yes (5)
Ura1	Up	Yes (3)	Yes (3)
Hsp42	Up	Yes (5)	Not tested
Hem13	Down	Yes (6)	Yes (3)
Ald3	Up	Yes (5)	Yes (4)
Msc1	Up	Yes (2)	Not tested
Rib4	Up	Yes (2)	Not tested
Ctt1	Up	Yes (5)	Yes (2)
Hsp78	Up	Yes (2)	Yes (2)
Yhb1	Down	Yes (4)	Not tested
Rpp1b	Down	Opposite (2)	Not tested

Legend:
$p<0.05$
$0.05<p\leq0.1$
$p>0.1$

S2 Table-Tab 2 – MS confirmations using gal-inducible PPK expression system.

Proteins	Regulation PPK vs. Control	Confirmations	
		*vtc4*Δ (n)	wild-type (n)
Ald4	Up	Not tested	Not tested
Adh4	Down	Not tested	Yes (2)
Hsp26	Down	Not tested	Opposite (3)
Gcv1	Up	Not tested	Yes (3)
Ura2	Up	Not tested	Not tested
Fet3	Down	Not tested	Yes (3)
Ura1	Up	Not tested	Not tested
Hsp42	Up	Not tested	Yes (3)
Hem13	Down	Not tested	Not tested
Ald3	Up	Not tested	Not tested
Msc1	Up	Not tested	Not tested
Rib4	Up	Not tested	Not tested
Ctt1	Up	Not tested	Not tested
Hsp78	Up	Not tested	Not tested
Yhb1	Down	Not tested	Inconsistent (3)
Rpp1b	Down	Not tested	Not tested

Legend:
$p<0.05$
$0.05<p\leq0.1$
$p>0.1$

S3 Table – Yeast strains used in this work.

Reference number	Strain background	Genotype	Source
963	S288C BY474	MATa leu2d0 ura3d0 his3-1 met15d0 LYS2+	Rudner Lab via Boone Lab
1574	S288C BY474	MATa leu2d0 ura3d0 his3-1 met15d0 LYS2+ vtc4::NATMX	Bentley-DeSousa et al., PMID: 29590613
2723A	S288C BY474	MATa leu2d0 ura3d0 his3-1 met15d0 LYS2+ vtc4::NATMX FET3-3FLAG-HYGMX	This study
2727A	S288C BY474	MATa leu2d0 ura3d0 his3-1 met15d0 LYS2+ vtc4::NATMX HEM13-3FLAG-HYGMX	This study
2823	S288C BY474	MATa leu2d0 ura3d0 his3-1 met15d0 LYS2+ vtc4::NATMX GCV1-3FLAG-HYGMX	This study
2919	S288C BY474	MATa leu2d0 ura3d0 his3-1 met15d0 LYS2+ FET3-3FLAG-HYGMX	This study
2914	S288C BY474	MATa leu2d0 ura3d0 his3-1 met15d0 LYS2+ GCV1-3FLAG-HYGMX	This study
2925	S288C BY474	MATa leu2d0 ura3d0 his3-1 met15d0 LYS2+ HEM13-3FLAG-HYGMX	This study
1106	S288C BY474	MATa leu2d0 ura3d0 his3-1 met15d0 LYS2+ msn4::KANMX msn2::HIS3MX	Rössl et al., PMID: 27527516
3219	S288C BY474	MATα leu2d0 ura3d0 his3::GAL-HIS3 MET15+ LYS2+	This study
3222	S288C BY474	MATα leu2d0 ura3d0 his3::GAL-HA-PPK-HIS3 MET15+ LYS2+	This study
3333	S288C BY474	MATa leu2d0 ura3d0 his3::GAL-HIS3 met15d0 LYS2+	This study
3336	S288C BY474	MATa leu2d0 ura3d0 his3::GAL-HA-PPK-HIS3 met15d0 LYS2+	This study
3305	S288C BY474	MATa leu2d0 ura3d0 his3::GAL-HIS3 met15d0 lys2d0 FET3-3FLAG-HYGMX	This study
3307	S288C BY474	MATa leu2d0 ura3d0 his3::GAL-HA-PPK-HIS3 met15d0 lys2d0 FET3-3FLAG-HYGMX	This study
3751	S288C BY474	MATα leu2d0 ura3d0 his3::GAL-HIS3 MET15+ LYS2+ GCV1-3FLAG-HYGMX	This study
3754	S288C BY474	MATα leu2d0 ura3d0 his3::GAL-HA-PPK-HIS3 MET15+ LYS2+ GCV1-3FLAG-HYGMX	This study
3788	S288C BY474	MATα leu2d0 ura3d0 his3::GAL-HIS3 MET15+ LYS2+ msn4::KANMX msn2::NATMX	This study
3236	S288C BY474	MATα leu2d0 ura3d0 his3::GAL-HIS3 met15d0 LYS2+ ppn1::KANMX	This study

3240	S288C BY474	MATα leu2d0 ura3d0 his3::GAL-HA-PPK-HIS3 met15d0 LYS2+ ppn1::KANMX	This study
3243	S288C BY474	MATa leu2d0 ura3d0 his3::GAL-HIS3 MET15+ LYS2+ ppn2::KANMX	This study
3246	S288C BY474	MATa leu2d0 ura3d0 his3::GAL-HA-PPK-HIS3 MET15+ LYS2+ ppn2::KANMX	This study
3226	S288C BY474	MATα leu2d0 ura3d0 his3::GAL-HIS3 MET15+ LYS2+ ppx1::KANMX	This study
3229	S288C BY474	MATa leu2d0 ura3d0 his3::GAL-HA-PPK-HIS3 MET15+ LYS2+ ppx1::KANMX	This study
3232	S288C BY474	MATa leu2d0 ura3d0 his3::GAL-HIS3 MET15+ LYS2+ ddp1::KANMX	This study
3233	S288C BY474	MATα leu2d0 ura3d0 his3::GAL-HA-PPK-HIS3 MET15+ LYS2+ ddp1::KANMX	This study
3301	S288C BY474	MATα leu2d0 ura3d0 his3::GAL-HIS3 MET15+ LYS2+ ppx1::KANMX ddp1::NATMX	This study
3303	S288C BY474	MATa leu2d0 ura3d0 his3::GAL-HA-PPK-HIS3 MET15+ LYS2+ ppx1::KANMX ddp1::NATMX	This study
3340	S288C BY474	MATa leu2d0 ura3d0 his3::GAL-HIS3 met15d0 LYS2+ vtc4::NATMX ppx1::KANMX	This study
3341	S288C BY474	MATa leu2d0 ura3d0 his3::GAL-HA-PPK-HIS3 MET15+ LYS2+ vtc4::NATMX ppx1::KANMX	This study
3343	S288C BY474	MATα leu2d0 ura3d0 his3::GAL-HIS3 MET15+ LYS2+ vtc4::NATMX ddp1::KANMX	This study
3346	S288C BY474	MATa leu2d0 ura3d0 his3::GAL-HA-PPK-HIS3 MET15+ lys2d0 vtc4::NATMX ddp1::KANMX	This study
3387	S288C BY474	MATα leu2d0 ura3d0 his3::GAL-HIS3 MET15+ LYS2+ vtc4::HYGMX ppx1::KANMX ddp1::NATMX	This study
3391	S288C BY474	MATα leu2d0 ura3d0 his3::GAL-HA-PPK-HIS3 MET15+ LYS2+ vtc4::HYGMX ppx1::KANMX ddp1::NATMX	This study
3546	S288C BY474	MATa leu2d0 ura3d0 his3::GAL-HA-PPK-HIS3 met15d0 LYS2+ vtc4::HYGMX KANMX-GAL-PPX1	This study
3550	S288C BY474	MATa leu2d0 ura3d0 his3::GAL-HA-PPK-HIS3 MET15+ lys2d0 vtc4::HYGMX KANMX-GAL-3HA-DDP1	This study
3955	S288C BY474	MATα leu2d0 ura3d0 his3::GAL-HIS3 MET15+ LYS2+ HOG1-GFP-HIS3MX	This study
3958	S288C BY474	MATα leu2d0 ura3d0 his3::GAL-HA-PPK-HIS3 MET15+ LYS2+ HOG1-GFP-HIS3MX	This study
3949	S288C BY474	MATα leu2d0 ura3d0 his3::GAL-HIS3 MET15+ LYS2+ YAK1-GFP-HIS3MX	This study
3952	S288C BY474	MATα leu2d0 ura3d0 his3::GAL-HA-PPK-HIS3 MET15+ LYS2+ YAK1-GFP-HIS3MX	This study
3727	S288C BY474	MATα leu2d0 ura3d0 his3::GAL-HIS3 MET15+ LYS2+ hog1::NATMX	This study

3731	S288C BY474	MATα leu2d0 ura3d0 his3::GAL-HA-PPK-HIS3 MET15+ LYS2+ hog1::NATMX	This study
3721	S288C BY474	MATα leu2d0 ura3d0 his3::GAL-HIS3 MET15+ LYS2+ yak1::NATMX	This study
3724	S288C BY474	MATα leu2d0 ura3d0 his3::GAL-HA-PPK-HIS3 MET15+ LYS2+ yak1::NATMX	This study
3782	S288C BY474	MATα leu2d0 ura3d0 his3::GAL-HIS3 MET15+ LYS2+ yak1::NATMX hog1::HYGMX	This study
3785	S288C BY474	MATα leu2d0 ura3d0 his3::GAL-HA-PPK-HIS3 MET15+ LYS2+ yak1::NATMX hog1::HYGMX	This study
3452	S288C BY474	MATa leu2d0 ura3d0 his3-1 met15d0 LYS2+ KANMX-GAL-3HA-DDP1	This study
2725A	S288C BY474	MATa leu2d0 ura3d0 his3-1 met15d0 LYS2+ vtc4::NATMX HSP26-3FLAG-HYGMX	This study
2729A	S288C BY474	MATa leu2d0 ura3d0 his3-1 met15d0 LYS2+ vtc4::NATMX YHB1-3FLAG-HYGMX	This study
2814	S288C BY474	MATa leu2d0 ura3d0 his3-1 met15d0 LYS2+ vtc4::NATMX ADH4-3FLAG-HYGMX	This study
2818	S288C BY474	MATa leu2d0 ura3d0 his3-1 met15d0 LYS2+ vtc4::NATMX RPP1B-3FLAG-HYGMX	This study
2820	S288C BY474	MATa leu2d0 ura3d0 his3-1 met15d0 LYS2+ vtc4::NATMX URA1-3FLAG-HYGMX	This study
2821	S288C BY474	MATa leu2d0 ura3d0 his3-1 met15d0 LYS2+ vtc4::NATMX CTT1-3FLAG-HYGMX	This study
2825	S288C BY474	MATa leu2d0 ura3d0 his3-1 met15d0 LYS2+ vtc4::NATMX ALD3-3FLAG-HYGMX	This study
2826	S288C BY474	MATa leu2d0 ura3d0 his3-1 met15d0 LYS2+ vtc4::NATMX RIB4-3FLAG-HYGMX	This study
2828	S288C BY474	MATa leu2d0 ura3d0 his3-1 met15d0 LYS2+ vtc4::NATMX MSC1-3FLAG-HYGMX	This study
2830	S288C BY474	MATa leu2d0 ura3d0 his3-1 met15d0 LYS2+ vtc4::NATMX HSP78-3FLAG-HYGMX	This study
2836	S288C BY474	MATa leu2d0 ura3d0 his3-1 met15d0 LYS2+ vtc4::NATMX URA2-3FLAG-HYGMX	This study
2838	S288C BY474	MATa leu2d0 ura3d0 his3-1 met15d0 LYS2+ vtc4::NATMX ALD4-3FLAG-HYGMX	This study
2840	S288C BY474	MATa leu2d0 ura3d0 his3-1 met15d0 LYS2+ vtc4::NATMX HSP42-3FLAG-HYGMX	This study
2910	S288C BY474	MATa leu2d0 ura3d0 his3-1 met15d0 LYS2+ URA1-3FLAG-HYGMX	This study
2912	S288C BY474	MATa leu2d0 ura3d0 his3-1 met15d0 LYS2+ CTT1-3FLAG-HYGMX	This study
2916	S288C BY474	MATa leu2d0 ura3d0 his3-1 met15d0 LYS2+ ALD3-3FLAG-HYGMX	This study

2917	S288C BY474	MATa leu2d0 ura3d0 his3-1 met15d0 LYS2+ HSP78-3FLAG-HYGMX	This study
2921	S288C BY474	MATa leu2d0 ura3d0 his3-1 met15d0 LYS2+ ADH4-3FLAG-HYGMX	This study
2923	S288C BY474	MATa leu2d0 ura3d0 his3-1 met15d0 LYS2+ HSP26-3FLAG-HYGMX	This study
3751	S288C BY474	MATα leu2d0 ura3d0 his3::GAL-HIS3 MET15+ LYS2+ GCV1-3FLAG-HYGMX	This study
3754	S288C BY474	MATα leu2d0 ura3d0 his3::GAL-HA-PPK-HIS3 MET15+ LYS2+ GCV1-3FLAG-HYGMX	This study
3757	S288C BY474	MATα leu2d0 ura3d0 his3::GAL-HIS3 MET15+ LYS2+ YHB1-3FLAG-HYGMX	This study
3760	S288C BY474	MATα leu2d0 ura3d0 his3::GAL-HA-PPK-HIS3 MET15+ LYS2+ YHB1-3FLAG-HYGMX	This study
3763	S288C BY474	MATα leu2d0 ura3d0 his3::GAL-HIS3 MET15+ LYS2+ ADH4-3FLAG-HYGMX	This study
3766	S288C BY474	MATα leu2d0 ura3d0 his3::GAL-HA-PPK-HIS3 MET15+ LYS2+ ADH4-3FLAG-HYGMX	This study
3769	S288C BY474	MATα leu2d0 ura3d0 his3::GAL-HIS3 MET15+ LYS2+ HSP26-3FLAG-HYGMX	This study
3772	S288C BY474	MATα leu2d0 ura3d0 his3::GAL-HA-PPK-HIS3 MET15+ LYS2+ HSP26-3FLAG-HYGMX	This study
3775	S288C BY474	MATα leu2d0 ura3d0 his3::GAL-HIS3 MET15+ LYS2+ HSP42-3FLAG-HYGMX	This study
3776	S288C BY474	MATα leu2d0 ura3d0 his3::GAL-HA-PPK-HIS3 MET15+ LYS2+ HSP42-3FLAG-HYGMX	This study
4135	S288C BY474	MATα leu2d0 ura3d0 his3::HIS3-GAL-HA-PPK MET15+ LYS2+ yak1::NATMX vtc4::KANMX	This study
4138	S288C BY474	MATα leu2d0 ura3d0 his3::HIS3-GAL-HA-PPK MET15+ LYS2+ hog1::NATMX vtc4::KANMX	This study
4141	S288C BY474	MATα leu2d0 ura3d0 his3::HIS3-GAL-HA-PPK MET15+ LYS2+ yak1::NATMX hog1::HYGMX vtc4::KANMX	This study

S5 Table-Tab 1 – Plasmids used in this work.

Plasmid	Details	Reference
pRS415-GPD	Empty vector control with GPD promoter expressing nothing (Leu2 selection)	This study
pRS415-GPD-PPK	Expresses E. coli PPK from yeast GPD promoter (Leu2 selection)	This study
p416-GPD	Empty vector control with GPD promoter expressing nothing (Ura3 selection)	Gerasimaitė et al., PMID: 25315834
p416-GPD-PPK	Expresses E. coli PPK from yeast GPD promoter (Ura3 selection)	Gerasimaitė et al., PMID: 25315834
p416-GPD-HA-PPK	Expresses HA-tagged E. coli PPK from yeast GPD promoter (Ura3 selection)	This study
p416-GPD-PPK(mutant)	Expresses catalytic mutant of E. coli PPK from yeast GPD promoter (Ura3 selection)	This study
p416-GPD-HA-PPK(mutant)	Expresses catalytic mutant of HA-tagged E. coli PPK from yeast GPD promoter (Ura3 selection)	This study
p416-GPD-PRUNE-HA	Expresses human HA-tagged PRUNE from yeast GPD promoter (Ura3 selection)	This study
p416-GPD-DIPP1-HA	Expresses human HA-tagged DIPP1 from yeast GPD promoter (Ura3 selection)	This study
p416-GPD-DIPP2-HA	Expresses human HA-tagged DIPP2 from yeast GPD promoter (Ura3 selection)	This study
p416-GPD-DIPP3A-HA	Expresses human HA-tagged DIPP3A from yeast GPD promoter (Ura3 selection)	This study
p416-GPD-DIPP3B-HA	Expresses human HA-tagged DIPP3B from yeast GPD promoter (Ura3 selection)	This study
p416-GPD-DDP1	Expresses yeast *DDP1* from yeast GPD promoter (Ura3 selection)	This study

CHAPTER 4 – MANUSCRIPT #3

Exploring the structure and function of the Ddp1 polyphosphate phosphohydrolase in yeast.

Publication information:
This work is in preparation for submission.
Liam McCarthy[1,2], Onyekachi Ononye[1,2] & Michael Downey[1,2].

Authors' contributions:
Conceptualization: L.M., O.O., M.D. Methodology: L.M., M.D. Investigation: L.M. Supervision: M.D. Writing – original draft: L.M., M.D.

Exploring the structure and function of the Ddp1 polyphosphate phosphohydrolase in yeast.

Liam McCarthy[1,2], Onyekachi Ononye[1,2] & Michael Downey[1,2]

1. Department of Cellular and Molecular Medicine, University of Ottawa, Ottawa, Ontario, Canada

2. Ottawa Institute of Systems Biology, University of Ottawa, Ottawa, Ontario, Canada

* Correspondence: mdowne2@uottawa.ca

4.1. Abstract

Inositol pyrophosphate and polyphosphate are two critical phosphate molecules important for maintaining phosphate homeostasis in yeast. The Ddp1 protein is a Nudix protein that can degrade both of these phosphate substrates, but how these activities are regulated *in vivo* is still unclear. In this study we set out to explore the regulation of the Ddp1 protein as a polyphosphatase and a pyrophosphatase. We first performed a protein mutagenesis screen to explore the structure and function of the Ddp1 endopolyphosphatase. We used our previously described ectopic PPK expression system to compare the ability of Ddp1 mutants and wild-type Ddp1 to rescue the PPK-induced toxicity. Our screen confirms many phosphate recognition residues important for Ddp1's polyphosphatase activity *in vivo*. We also developed a plasmid shuffle system in a pyrophosphatase mutant strain that presumably accumulates toxic levels of 1,5-bisdiphosphoinositol tetrakisphosphate (1,5-IP8) to expand our Ddp1 mutagenesis screen and study the regulation of its pyrophosphatase activity *in vivo*. We identify the intrinsically disordered N-terminal region, as well as a potential phosphorylation site that follows the IDR, as potential regulators of pyrophosphatase activity. Moreover, DIPP1, the mammalian homologue of Ddp1, can complement the loss of the yeast protein in the plasmid shuffle system, highlighting that this system could be used to perform mutagenesis screens on other pyrophosphatases in the future.

4.2. Introduction

High energy phosphate molecules such as polyphosphate and inositol pyrophosphate are important for regulating phosphate homeostasis in yeast (1–3). The timely synthesis and degradation of these phosphate molecules is critical for phosphate signaling. The yeast diadenosine and diphosphoinositol polyphosphate phosphohydrolase (Ddp1) was first described as a diadenosine phosphohydrolase (4). Since then, Ddp1's cleavable substrates have expanded to include inositol pyrophosphates (5–7), polyphosphate (6), and the 5'-7-methylguanosine cap of RNA (8). Its broad specificity for a variety of substrates is unsurprising considering it is a member of the Nudix (nucleoside diphosphate linked to any moiety) hydrolase family (9). Nudix proteins are conserved from prokaryotes to eukaryotes and have been shown to hydrolyze nucleoside polyphosphates, dinucleoside polyphosphates, inositol pyrophosphates, polyphosphate, nucleotide sugars, and a variety of RNA cap structures (9). Nudix proteins all share a Nudix motif $GX_5EX_7REUXEEXGU$, in which X is any amino acid and U is isoleucine, leucine or valine (I/L/V), that forms a loop-helix-loop structure with multiple metal binding sites (10,11). It is still unclear how these broad specificity proteins might be regulated *in vivo* to selectively target certain substrates over others.

The relevance of Ddp1's diadenosine polyphosphate hydrolase activity has remained unclear. *In vitro*, Ddp1 can cleave nucleoside polyphosphates such as Ap6A, Ap5A, Ap5, and Ap4, but not Ap4A or Ap3A (4). However, the existence of Ap6A and Ap5A in yeast has yet to be demonstrated. Moreover, yeast cells do not produce Ap5 or Ap4 during normal vegetative growth, but both have been detected during later stages of sporulation (12). It was initially proposed that Ddp1 might be responsible for degrading these potentially toxic dinucleoside polyphosphates during sporulation (4). It is still unclear if this nucleoside polyphosphatase activity is relevant *in vivo* or if it is simply an evolutionary artifact of Nudix proteins (9,11). Since first being

characterized as a diadenosine polyphosphate hydrolase, Ddp1 has been shown to catalyze a multitude of other substrates.

The strongest *in vivo* data for Ddp1 activity can be attributed to its inositol pyrophosphatase activity (13–15). Inositol pyrophosphates consist of phosphorylated, 6 carbon, inositol rings that can carry one or two diphosphate moieties (16). These molecules act as important signalling molecules by binding to SPX (Syg1/Pho81/Xpr1) domains of proteins (17). In yeast, 1,5-IP8, denoting diphosphates at carbon ring positions 1 (C1) and 5 (C5), can bind and inactivate the cyclin-dependent kinase inhibitor Pho81 (15). When cells are starved for phosphate, inositol pyrophosphates are rapidly degraded leading to Pho85-Pho80 inactivation and a phosphate starvation transcriptional response (15). Moreover, inositol pyrophosphates have been shown to positively modulate the activity of the VTC complex (18). Recent work demonstrated that 1,5-IP8, and to a lesser degree 5-IP7 and IP6, increase VTC activity by binding to the SPX domains of Vtc2 and Vtc3, and preventing SPX-SPX interactions between these subunits and Vtc4 (19). As a result, the inositol pyrophosphate and polyphosphate pathways appear to be intertwined (3,6). Inositol pyrophosphates are degraded by a variety of pyrophosphatases including Ddp1, Siw14, and Vip1 which is a dual pyrophosphate kinase and phosphatase (**Figure 3A**). Ddp1 preferentially removes the β-phosphate from C1 and can convert 1,5-IP8 into 5-IP7 or 1-IP7 into IP6 (5–7). On the other hand, Siw14 preferentially removes the β-phosphate from C5 and can convert 1,5-IP8 into 1-IP7 or 5-IP7 into IP6 (20). As expected, *ddp1*Δ mutants accumulate significantly more 1-IP7 whereas *siw14*Δ mutants accumulate more 5-IP7, and both show increased levels of 1,5-IP8 (13,15,20). Vip1 is a unique dual inositol pyrophosphate kinase and phosphatase which can phosphorylate the C1 position of IP6 to generate 1-IP7 or remove the β-phosphate from C1 to convert 1,5-IP8 into 5-IP7 (21). Together these enzymes control the turnover of inositol pyrophosphates in yeast.

Ddp1 also has endopolyphosphatase activity and can cleave polyphosphate chains internally to generate two shorter chains (6). Interestingly, Ddp1 shows preference for polyP degradation over pyrophosphate *in vitro* when both substrates are present (6). This may be because more phosphate recognition residues interact with polyP than with inositol pyrophosphate (22). Recently, we demonstrated that Ddp1 can degrade polyphosphate *in vivo* using an ectopic *E. coli* PPK expression system (23). Expression of the *E. coli* PPK synthetase in yeast leads to nonvacuolar polyP accumulation which is toxic to the cell (23,24). Deletion of the nonvacuolar polyphosphatases Ppx1 or Ddp1 sensitizes yeast cells to the cytotoxic effects of PPK expression, whereas their overexpression can degrade PPK-synthesized polyP and rescue the toxicity (23).

Recent crystallography work solved Ddp1's structure bound by dinucleoside polyphosphate, pyrophosphates, and polyphosphate (15 residues in length), and identified important phosphate recognition residues that drive substrate binding and catalysis. However, how these various activities might be regulated *in vivo* is still unclear. Here, we set out to explore how Ddp1 activity is regulated *in vivo* by performing a large-scale mutagenesis screen. Using our *E. coli* PPK expression system, we were able to investigate residues that contribute to Ddp1's activity as an endopolyphosphatase. Moreover, we developed a plasmid shuffle system to begin to study the regulation of its inositol pyrophosphatase function *in vivo*.

We confirm essential phosphate binding sites that are important for Ddp1's polyphosphatase activity *in vivo*. We show that the intrinsically disordered N-terminus is dispensable for polyphosphatase activity but potentially critical for pyrophosphatase activity. We identify the serine 26, which is a potential phosphorylation site, as a possible regulator of

pyrophosphatase activity. Finally, we show that the N-terminus is not involved in RNA binding, but that the nose might be.

4.3. Results

4.3.1. Confirming Ddp1 polyphosphate recognition sites *in vivo*

To identify potential regulatory regions of Ddp1, we performed a structural mutagenesis screen by mutating amino acids of interest to alanine and generated N- and C-terminal truncations. A plasmid expressing *DDP1-HA* from its native promoter and terminator was used for site directed mutagenesis. We previously demonstrated that cells lacking *DDP1* are sensitive to PPK expression, because of nonvacuolar polyP accumulation, and show a drastic reduction in growth compared to wild-type cells expressing PPK (23). Complementation of Ddp1 from a plasmid can rescue this growth phenotype **(Figure 1A)**. The mutagenized plasmids were transformed into *ddp1*Δ cells expressing PPK, and spot tests were used to determine whether the mutations impair or ameliorate the expected rescue (**Figure 1B**). Out of the 112 mutants screened, almost 50% influenced the level of rescue as assessed by spot test (**Table S1**). However, some of these mutations negatively affected protein levels making it difficult to discern a functional role. This may be because mutation of residues that contribute to Ddp1's tertiary structure can easily disrupt its folding and stability. Thus, mutations that negatively impact protein levels might represent amino acids that are important for protein folding and stability rather than regulatory sites.

Nonetheless, using our PPK expression system we were able to confirm a multitude of phosphate recognition residues that were previously uncovered using crystallography (22). These include R32, H55, K56, K57, R58, K63, R102, R171, which when mutated impacted the ability of Ddp1 to rescue growth to varying degrees (**Figure 1B**). We first explored the role of the 54-

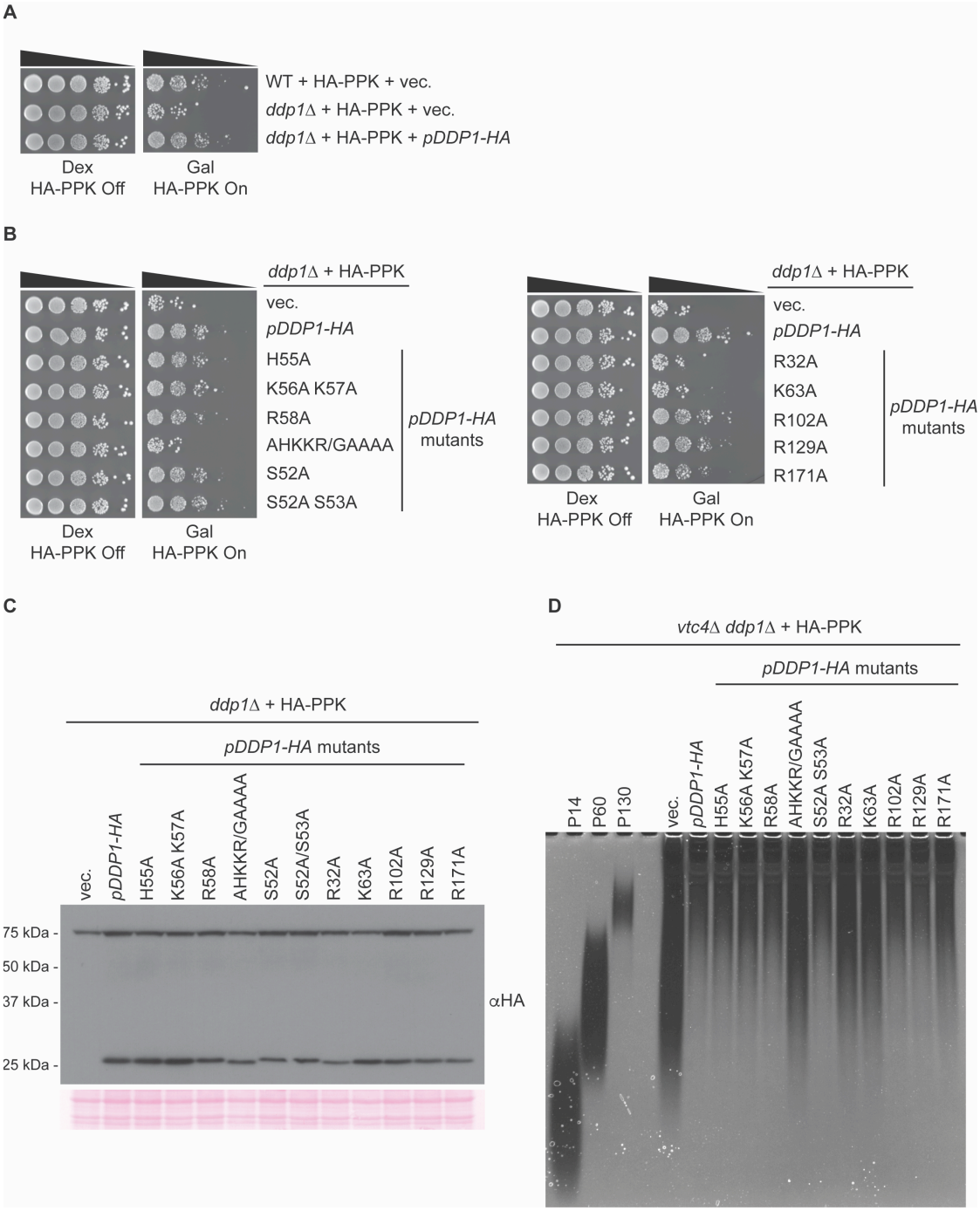


Figure 1. Using the PPK system to identify critical Ddp1 polyphosphate binding sites *in vivo*. (**A**) Complementation of *DDP1-HA* from a plasmid can rescue *ddp1*Δ cells expressing PPK. Tenfold dilutions of the indicated galactose inducible HA-PPK strains transformed with an empty vector plasmid or a plasmid expressing *DDP1-HA* were spotted onto SC-Ura plates containing 2% dextrose or galactose and grown for 3 days. (**B**) Mutation of some Ddp1 phosphate binding sites affect the *DDP1*-dependent rescue. Tenfold dilutions of the *ddp1*Δ GAL-HA-PPK strains transformed with an empty vector or a plasmid expressing *DDP1-HA* or the indicated *DDP1-HA* mutant were spotted onto SC-Ura plates containing 2% dextrose or galactose and grown for 3 days.

(**C**) Effect of phosphate binding site mutations on Ddp1-HA expression. Protein extracts from the indicated strains were prepared using a TCA lysis protocol and separated on a 12% SDS-PAGE gel. Separated proteins were transferred to a PVDF membrane and HA-PPK (~75 kDa) and Ddp1-HA (~25 kDa) were detected using an HA antibody. Ponceau S staining of the PVDF membrane is shown as a loading control. (**D**) PPK-synthesized polyP levels in cells expressing Ddp1-HA phosphate binding site mutants. Polyphosphate was extracted from the indicated strains and visualized using DAPI staining following separation on a 20% acrylamide/bis-acrylamide(19:1)–TBE gel. Images are representative of ≥3 experiments.

AHKKR motif for Ddp1's polyphosphatase activity. This motif was proposed to be involved in polyphosphate binding and is not fully conserved in the DIPP1 mammalian homologue (22). Mutation of individual residues within the motif (e.g. H55A, K56A K57A, R58A) did not impact the Ddp1-dependent rescue (**Figure 1B**). However, when we mutated the entire AHKKR motif to GAAAA no rescue was observed suggesting that this stretch of residues is important for polyphosphatase activity (**Figure 1B**). Importantly, this mutant was expressed at similar levels to that of the wild-type protein highlighting that the effect is not due to protein stability (**Figure 1C**). In fact, mutation of most phosphate binding sites did not impact Ddp1 levels dramatically (**Figure 1C**). We surmise that their side chains are used to interact with substrates rather than forming intramolecular interactions important for protein structure. Because this motif is not fully conserved in the human homologue DIPP1 we wondered if these differences could account for the inability of DIPP1 expression to rescue PPK-induced toxicity in yeast (23). Mutation of DIPP1's semi-conserved RHPDR sequence to AHHKR did not significantly improve its ability to rescue PPK-induced toxicity (**Supplemental Figure 1**). Thus, differences in the AHKKR motif cannot account for the differences in activity between Ddp1 and DIPP1 in yeast expressing PPK.

Interestingly, S52 and S53, which were proposed to form a short loop within Ddp1's catalytic site essential for phosphate binding (22), were dispensable for polyphosphatase activity (**Figure 1B and 1D**). Moreover, we did not see the same level of instability when the S52A S53A

mutant was expressed in yeast (**Figure 1C**), which was unstable and insoluble when expressed in *E. coli* (22). Interestingly, despite the slight reduction in protein levels the S52A S53A mutant had little impact on polyphosphatase activity in yeast expressing PPK (**Figure 1D**). Although these serine residues do not appear to be essential for polyphosphatase activity, as previously thought, they may be essential for inositol pyrophosphate and dinucleoside polyphosphate recognition.

To assess how mutation of the previously identified phosphate binding sites H55, K56 K57, R58, 54-AHHKR, S52 S53, R32, K63, R102, R129, and R171 might affect polyphosphatase activity we extracted the polyP from *vtc4*Δ yeast expressing PPK and the Ddp1 mutants of interest. By deleting *VTC4*, we were able to ablate vacuolar polyP and specifically extract PPK-synthesized polyP for analysis. Lack of Ddp1 led to a dramatic increase in PPK-synthesized polyP accumulation which was reduced by the expression of Ddp1-HA (**Figure 1D**). Ddp1 mutants that showed the worst rescue via spot tests, such as AHHKR/GAAAA, R32A, K63A, and R171A, had polyP profiles that looked most like the *ddp1*Δ mutant expressing PPK (**Figure 1D**). Other mutations which were not as detrimental to the Ddp1-dependent rescue, such as S52A S53A, R102A, and R129A, did not show as dramatic increases in PPK-synthesized polyP (**Figure 1D**). Altogether, we were able confirm essential phosphate binding sites of Ddp1 including R32, 54-AHHKR, K63, and R171. Moreover, we show that S52 and S53 are not essential for polyphosphate binding as previously thought. These results highlight that our PPK expression system can be used to study the structure and function of polyphosphatase enzymes targeted outside the vacuole.

4.3.2. The nose and the intrinsically disordered N-terminus are dispensable for polyphosphatase activity

The crystal structure of Ddp1 revealed an interesting 26 amino acid insertion that projects out of the Nudix fold which the authors termed the “nose” (22). The nose is a partly disordered region

that is conserved in the *Saccharomyces pombe* homolog Aps1, but not in the mammalian homologue DIPP1 (22). The authors showed that the nose is not required for Ddp1's pyrophosphatase activity *in vitro*. To test whether this structure was involved in Ddp1's polyphosphatase activity, we assessed its ability to rescue the PPK-induced toxicity in yeast. Cells expressing wild-type Ddp1 or the noseΔ mutant had comparable growth phenotypes (**Figure 2A**), suggesting that the nose is not involved in degrading polyP, at least in the context of our PPK expression system. Moreover, the noseΔ did not show appreciable differences in protein levels or PPK-synthesized polyP levels compared to wild-type Ddp1 (**Figure 2B and 2C**).

Additionally, Márquez-Moñino *et al.* had proposed that the nose could be important for Ddp1 dimerization and oligomerization (22). However, in co-immunoprecipitation assays using strains expressing Ddp1-3FLAG transformed with a plasmid expressing *DDP1-HA* or *DDP1(noseΔ)-HA* we were not able to detect an interaction between Ddp1-3FLAG and Ddp1-HA (**Supplemental Figure 2**). Certainly, it is possible that the FLAG and HA epitope tags, and the conditions under which the co-immunoprecipitation was performed could impact the potential interaction.

We were also interested in Ddp1's N-terminus as a potential regulatory region since the first 23 amino acids are predicted to be intrinsically disordered (25) and no structure for the first 20 amino acids was recovered during crystallization (22). Moreover, like the nose, it is not conserved in the mammalian homolog DIPP1 (22). Truncation of the first 20 N-terminal amino acids (N20Δ) did not significantly affect the ability of this mutant to deal with PPK-induced toxicity (**Figure 2A**). However, truncation of the first 25 N-terminal amino acids N25Δ had a slightly more dramatic effect on the ability of Ddp1 to rescue growth (**Figure 2A**). Strikingly, the N25Δ mutant had much lower protein levels compared to wildtype (**Figure 2B**). When we

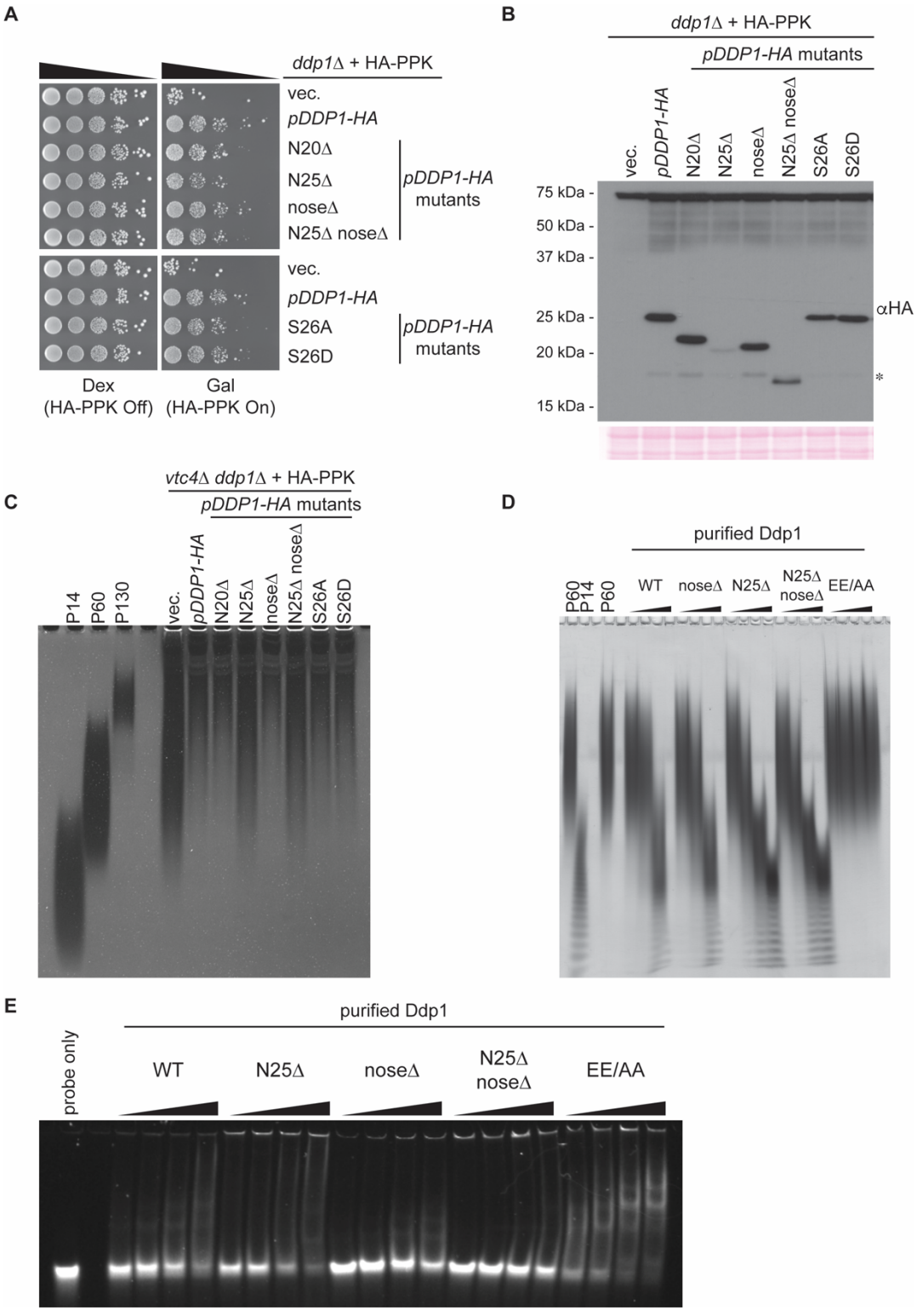


Figure 2. The disordered N-terminus and nose of Ddp1 are not required for polyphosphatase activity, but the nose might be involved in RNA binding. (**A**) N-terminal truncations and phosphorylation site mutations do not significantly affect Ddp1-dependent rescue of PPK-expressing cells. Tenfold dilutions of the indicated galactose inducible HA-PPK strains

transformed with an empty vector or a plasmid expressing *DDP1-HA* or the indicated *DDP1-HA* mutant were spotted on SC-Ura plates containing 2% dextrose or galactose and grown for 3 days. (**B**) Effect of N-terminal truncations and phosphorylation site mutations on Ddp1-HA expression. Protein extracts from the indicated strains were prepared using a TCA lysis protocol and separated on a 12% SDS-PAGE gel. Separated proteins were transferred to a PVDF membrane and HA-PPK (~75 kDa) and Ddp1-HA (~25 kDa) were detected using an HA antibody. Ponceau S staining of the PVDF membrane is shown as a loading control. The * indicates a non-specific band of unknown origin. (**C**) N25Δ mutants show slightly higher polyP accumulation in PPK-expressing cells. Polyphosphate was extracted from the indicated strains and visualized using DAPI staining following separation on a 20% acrylamide/bis-acrylamide (19:1)–TBE gel. (**D**) In vitro polyphosphatase assays of various Ddp1 truncation mutants. Polyphosphatase assays were conducted with 5 mM polyP with an average chain length of 60 residues (P60) and increasing equimolar amounts of the indicated purified Ddp1 proteins. Concentrations of proteins used were 200, 400, 800, and 1600 nM. Reactions were incubated for 1 h at 37°C before being stopped with EDTA. Samples were run on a 20% acrylamide/bis-acrylamide(19:1)–TBE gel and stained with toluidine blue to visualize polyP. (**E**) The nose is important for RNA binding. Electromobility shift assays were conducted with increasing equimolar amounts of purified proteins and 1 nM of an IR800 Dye-labelled RNA probe. Concentrations of proteins used were 625, 1250, 2500, 5000 nM. Reactions were incubated at 4°C for 1 h before being run on a 6% non-denaturing 0.5X Tris-Glycine acrylamide/bis-acrylamide (37.5:1) gel. Images are representative of ≥3 experiments.

extracted polyP from the N25Δ mutant we saw increased polyP levels as compared to Ddp1-HA (**Figure 2C**). Similarly, *in vitro* assays with the purified N25Δ Ddp1 mutant revealed slightly worse polyphosphatase activity compared to wild-type Ddp1 (**Figure 2D**). Combining the N25Δ and noseΔ truncations improved the rescue slightly compared to N25Δ truncation alone (**Figure 2A**), but the double truncation showed similar polyphosphatase activity to the N25Δ mutant (**Figure 2C and D**). The slight growth improvement is likely because truncation of the nose stabilized the protein levels, as seen by western blot (**Figure 2B**). This stabilization effect is in line with previous work which demonstrated that truncation of the nose increases the thermal stability of Ddp1 *in vitro* (22). However, it's unclear why this stabilization effect is seen when the N25Δ truncation is combined with the nose, but not with the noseΔ alone *in vivo* (**Figure 2B**).

Next, we investigated the regulatory function of a putative phosphorylation site on serine 26 (S26) that has been detected by many mass spectrometry experiments (26–29). This serine is

followed by a proline and bears a similarity to the consensus sequence recognized by cyclin-dependent kinases like Pho85, involved in phosphate metabolism and cell cycle regulation (30), and Cdc28 involved in cell cycle regulation (31). Intrinsically disordered regions (IDR) are hot spots for phosphorylation and can promote the folding or unfolding of disordered regions, as well as promote the binding or dissociation of protein interactors (32). Mutation of S26 to alanine (S26A), to prevent phosphorylation, or to aspartic acid (S26D), to mimic phosphorylation, had no impact on the ability of Ddp1 to rescue PPK-induced toxicity (**Figure 2A**). However, compared to wild-type and S26D Ddp1, whose expression were comparable, the S26A mutant was expressed at slightly lower levels (**Figure 2B**). Together, we conclude that the disordered N-terminus and the phosphorylation site that follows are dispensable for polyphosphatase activity.

4.3.3. The nose is involved in nucleic acid binding

Many Nudix hydrolases have been shown to have 5'-7-methylguanosine RNA decapping activity *in vitro*, including Ddp1 (8). Unsurprisingly, many of these hydrolases can bind to nucleic acids (33). Since IDRs are often associated with nucleic acid binding (34), we next tested the role of the N-terminus and the nose in binding RNA using electromobility shift assays (EMSA). Our EMSAs suggest that the nose might be involved in nucleic acid binding, but the N-terminus is not (**Figure 2E**). The N25Δ mutant displayed similar binding to the RNA probe compared to wild-type Ddp1, whereas the noseΔ mutant showed less binding to the RNA probe (**Figure 2E**). When both mutations were combined the ability of Ddp1 to bind nucleic acids was like that of the *nose*Δ mutant (**Figure 2E**). Interestingly, the catalytically dead E83A E84A Ddp1 protein had a higher affinity for RNA (**Figure 2E**). Moreover, more distinct banding patterns could be seen with the catalytically dead mutant (**Figure 2E**). Nudix proteins have previously been reported to form smears as seen in our EMSA and it has been suggested that this could be due to the ability of these

proteins to form dimers or oligomers on nucleic acids (33). Therefore, Ddp1 might oligomerize in the presence of RNA and these oligomers might be stabilized in the catalytic mutant allowing them to better survive the electrophoresis conditions. Moreover, previous modelling of Ddp1 crystals suggested that the nose might make intermolecular interactions to form apparent Ddp1 oligomers, but whether these are physiologically relevant is unclear (22). The reduction in RNA binding in the noseΔ mutant may result from reduced oligomerization on the RNA substrate. Considering this possibility, it would be interesting to repeat the co-immunoprecipitations in the presence of RNAse inhibitors to see if an RNA-dependent Ddp1-Ddp1 interaction can be demonstrated. Moreover, oligomerization on RNA could act as a means of enzymatic regulation. Repeating in vitro polyphosphatase assays in the presence and absence of RNA could begin to test this possibility.

This data suggests that the nose of Ddp1 is important for nucleic acid binding. Whether this structure is also important for Ddp1's ability to decap RNA remains to be tested. Interestingly, it could also represent a novel regulatory mechanism within the context of the cell which should be explored further.

4.3.4. A plasmid shuffle system for studying the structure and function of pyrophosphatases *in vivo*

In addition to studying the structure and function of Ddp1 as a polyphosphatase, we also wanted to develop a system to study the regulation of its pyrophosphatase activity *in vivo*. In *S. pombe*, overaccumulation of 1,5-IP8 is toxic to cells. In fact, deletion of *aps1* (homologue of *DDP1*) in a mutant expressing the inactive pyrophosphatase *asp1-D333A* (homologue of *VIP1*) is synthetically lethal (35). Furthermore, deletion of *aps1* in combination with *siw14* is also synthetically lethal (36). In both cases, the observed lethality is thought to result from 1,5-IP8 overaccumulation. In *S. cerevisiae*, homologous mutations that increase 1,5-IP8 accumulation such

as *ddp1*Δ *siw14*Δ and *ddp1*Δ *vip1*Δ *VIP1(H548A)* (equivalent to the Asp1 phosphatase mutant) are not synthetically lethal (**Supplemental Figure 3**). It is unclear if *S. pombe* might be more sensitive to 1,5-IP8 levels compared to *S. cerevisiae*. Therefore, in an effort to drive 1,5-IP8 accumulation higher we generated a *ddp1*Δ *siw14*Δ *vip1*Δ mutant and transformed it with a plasmid expressing *VIP1-H548A* from its native promoter and terminator. Mutation of H548A prevents Vip1 from dephosphorylating 1,5-IP8, but its kinase domain can still phosphorylate 5-IP7 into 1,5-IP8 or IP6 into 1-IP7 (21) (**Figure 3A**). Expression of the Vip1 pyrophosphatase mutant in this triple mutant was inviable suggesting that 1,5-IP8 is also toxic in *S. cerevisiae*.

Next, we generated a *URA3*-marked plasmid expressing wild-type *VIP1* and a *LEU2*-marked plasmid expressing *VIP1-H548A* from their native promoters and terminators. To demonstrate that the expression of *VIP1-H548A* is synthetically lethal in the *ddp1*Δ *siw14*Δ *vip1*Δ mutant we co-transformed both aforementioned plasmids and performed a 5-FOA plasmid shuffle to select against the *URA3* plasmid. Loss of the wild-type copy of *VIP1* was lethal (**Figure 3B**), suggesting that 1,5-IP8 accumulation driven by the loss of Ddp1 and Siw14, and the mutation of the pyrophosphatase domain of Vip1 is lethal.

We then exploited this plasmid shuffle system to study the regulation of Ddp1's pyrophosphatase activity *in vivo*. To accomplish this, we took our *LEU2* plasmid expressing *VIP1-H548A* and subcloned wild-type *DDP1* or mutants thereof. This way we could co-express the Vip1 pyrophosphatase mutant and Ddp1 mutants of interest from the *LEU2* plasmid and select for *VIP1* loss using 5-FOA. As expected, expression of wild-type Ddp1 was able to rescue cells that lost the *VIP1* plasmid (**Figure 3C**). On the other hand, expression of the catalytically dead mutant *DDP1(EE/AA)* was unable to rescue cells from the presumed 1,5-IP8 toxicity (**Figure 3C**). In line

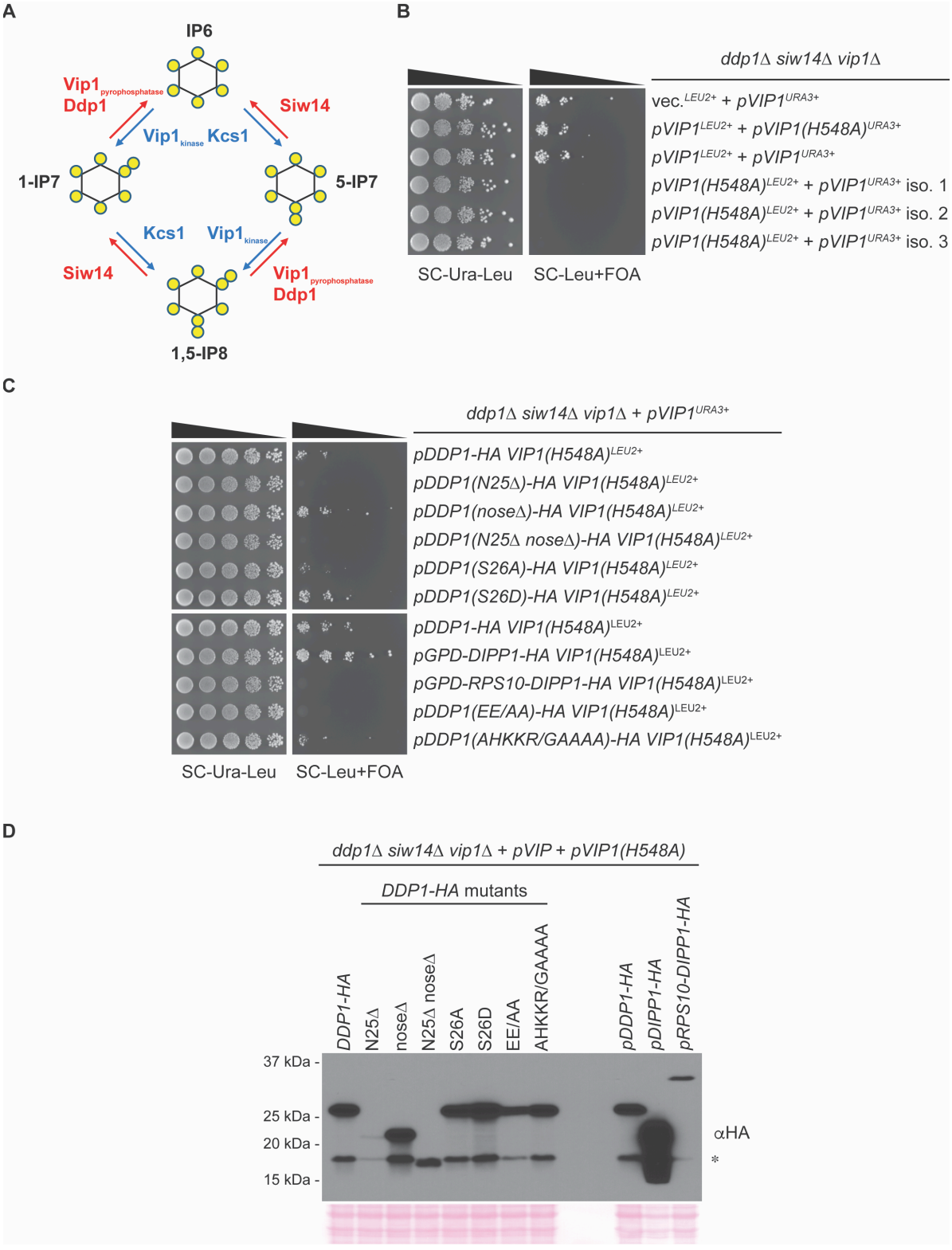


Figure 3. Ddp1's N-terminus is required for pyrophosphatase activity. (**A**) Schematic of inositol pyrophosphate synthesis and degradation. Enzymes in blue represent kinases that

phosphorylate inositol and enzymes in red represent pyrophosphatases that dephosphorylate inositol pyrophosphates. (**B**) Loss of *VIP1* is lethal in *ddp1*Δ *siw14*Δ *vip1*Δ cells expressing the *VIP1(H548A)* pyrophosphatase domain mutant. Tenfold dilutions of the *ddp1*Δ *siw14*Δ *vip1*Δ mutants co-transformed with the indicated plasmids were spotted onto SC-Ura-Leu plates or SC-Leu + FOA plates and grown for 3 days at 30°C. (**C**) Plasmid shuffle assay used to assess the ability of Ddp1 mutants to rescue inositol pyrophosphate toxicity. Fivefold dilutions of the *ddp1*Δ *siw14*Δ *vip1*Δ cells co-transformed with a *URA3*-marked plasmid expressing *VIP1* and a *LEU2*-marked plasmid co-expressing *VIP1(H548A)* and *DDP1-HA* or the indicated *DDP1-HA* mutants. (**D**) Protein expression levels of various Ddp1 mutants and the DIPP1 protein in the pyrophosphatase mutant strain. Protein extracts from *ddp1*Δ *siw14*Δ *vip1*Δ mutants co-transformed with a *LEU2*-marked plasmid expressing *VIP1* and a *URA3*-marked plasmid co-expressing *VIP1(H548A)* and *DDP1-HA* or the indicated *DDP1-HA* mutants were prepared using a TCA lysis protocol and separated on a 13% SDS-PAGE gel. Half the amount of protein was loaded for GPD-DIPP1-HA. The * indicates a non-specific band of unknown origin. Images are representative of ≥3 experiments.

with previous *in vitro* pyrophosphatase assays (22), truncation of the nose had no significant impact on Ddp1's ability to deal with inositol pyrophosphate (**Figure 3C**). Mutation of the 54-AHKKR motif, which was essential for polyphosphatase activity (**Figure 2B and 2D**), showed a reduction in rescue rather than complete death (**Figure 3C**). Moreover, it was expressed to a similar degree as the wild-type protein (**Figure 3D**). This suggests that the AHKKR motif is also important for pyrophosphate substrate binding, but not necessarily essential. Next, it will be interesting to test whether the S52 S53 serine loop is important for pyrophosphatase activity. By comparing which phosphate binding sites are important for pyrophosphatase activity we will be able to determine whether they overlap with sites essential for polyP binding. This could provide insight into substrate selection *in vivo*.

Interestingly, truncation of the N-terminus (N20Δ and N25Δ) resulted in no growth on 5-FOA (**Figure 3C and Supplemental Figure 4A**), suggesting that the N-terminus of Ddp1 might be important for inositol pyrophosphatase activity. Moreover, combining the N25Δ truncation with the noseΔ truncation was insufficient to rescue growth (**Figure 3C**). However, these results were somewhat difficult to interpret because all three of these mutants, which were unable to rescue

growth, had lower expression levels than wild-type Ddp1-HA to varying degrees (**Figure 3D and Supplemental Figure 4B**). We were also interested in the potential regulatory role of S26 phosphorylation. Despite seeing no effect with the PPK expression system (**Figure 2A**), we wondered if it might regulate its pyrophosphatase activity. Expression of the S26A mutant showed worse viability on 5-FOA plates and the colonies that did appear were small and slow growing compared to cells expressing wild-type Ddp1-HA (**Figure 3C**). Conversely the phosphomimetic mutant S26D showed a similar rescue in viability comparable to wild-type Ddp1 (**Figure 3C**). Protein levels of the S26A Ddp1 mutant were slightly lower than that of wildtype or the S26D mutant (**Figure 3D**), but it is unclear if this can account for the effects seen. Nonetheless, these data suggest that the phosphorylation of S26 could be important for regulating the pyrophosphatase activity of Ddp1. This phosphorylation site could potentially serve to regulate the structure of the disordered N-terminus.

Finally, we also tested the ability of DIPP1 (the human homologue of Ddp1) to rescue the 1,5-IP8 mediated toxicity. DIPP1 expression was able to rescue viability similarly to Ddp1 (**Figure 3B**), demonstrating that its mammalian homologue can complement the yeast pyrophosphatase. Importantly, this also confirmed, for the first time, that DIPP1 is functional when expressed in yeast. An important fact considering that we previously had shown that it was unable to degrade PPK-synthesized polyP in yeast, unlike Ddp1 (23). Finally, we were interested in testing potential mutant isoforms of DIPP1 and their impact on its function. As a first test, we cloned a readthrough transcript isoform of DIPP1 where RPS10 is fused to DIPP1 (37). The RPS10-DIPP1-HA fusion protein was unable to rescue the pyrophosphate mediated toxicity (**Figure 3C**). However, the fusion protein was also expressed at a much lower level compared to wild-type DIPP1-HA even though both were expressed from the same constitutive GPD promoter (**Figure 3C**). Nonetheless,

these results highlight that our plasmid shuffle system could be a useful tool for performing structure function analysis screens of DIPP1 as well as other mammalian pyrophosphatases.

4.4. Discussion

In this work, we used our previously described PPK expression system to perform a structure and function analysis of Ddp1's polyphosphatase activity *in vivo*. Consistent with the published crystal structure of Ddp1 bound by various substrates, mutation of residues involved in phosphate binding disrupted the polyphosphatase activity of Ddp1. Moreover, we showed that the intrinsically disordered N-terminus is dispensable for polyphosphatase activity and RNA binding. Using purified proteins, we showed that Ddp1's nose structure is involved in binding RNA which may have implications for its decapping activity. Finally, we developed a novel plasmid shuffle system to investigate the pyrophosphatase activity of Ddp1 *in vivo*. This system allowed us to identify the N-terminus as a potentially critical region for Ddp1's pyrophosphatase activity. Additionally, a phosphorylation site on S26, which follows the IDR, might also be important for regulating this activity. These results raise the interesting possibility that the phosphorylation site at S26 might regulate the structure of the disordered N-terminus and promote pyrophosphatase activity. More work is needed to validate these potential modes of Ddp1 regulation.

Our work demonstrates that the PPK expression system is a valuable tool for performing structure function analyses of cytoplasmic polyphosphatases in yeast. Using this system, we were able to build upon crystal structure work to confirm the importance of most phosphate recognition residues important for Ddp1's polyphosphatase activity *in vivo*. We identified the phosphate binding residues R32, 54-AHHKR, K63, and R171 as critical residues for Ddp1's ability to degrade PPK-synthesized polyP *in vivo*. Based on these results, this system could be expanded to

study the structure and function of other polyphosphatases, such as the Ppx1 exopolyphosphatase in yeast. Similarly to Ddp1 there is a lack of data regarding its regulation as well as its function *in vivo*.

Although the intrinsically disordered N-terminus does not appear to be important for polyphosphatase activity, it appears to be important for its pyrophosphatase activity. More work will need to be done to establish if the N-terminus is directly involved in pyrophosphatase activity or if the lack of rescue in our plasmid shuffle is simply due to lowered protein levels. *In vitro* assays using synthesized inositol pyrophosphates and purified Ddp1 proteins could begin to answer these questions. We propose that the N-terminus might be important for acting as a capture site for inositol pyrophosphate substrates. Inositol pyrophosphate is a bulky substrate that needs to be orientated properly into Ddp1's catalytic site for productive binding and catalysis (22). Similar pyrophosphate capture sites have been demonstrated for Vip1's pyrophosphatase domain (21) and the mammalian PPIP5K (Vip1 homologue) kinase domain (38). In both cases, the capture site is thought to be important for ensuring the proper rotation of the pyrophosphate molecule into the active site (21,38). It is possible that inositol pyrophosphates are first bound to the N-terminal IDR before being shuttled and properly rotated into to the catalytic site to promote catalysis. The IDR contains many arginine residues that could be important for binding inositol pyrophosphate. Moreover, phosphorylation of S26 might induce structural changes in the IDR that promote inositol pyrophosphate binding or shuttling. Protein phosphorylation has previously been shown to affect the structure of IDRs in a variety of ways (32). One interesting possibility is that the phosphorylation might affect the cis-trans conformation of its neighbouring proline, which could impact the orientation and structure of the N-terminus (32).

A second possibility is that the N-terminus is important for Hsc82 (Hsp90) client recognition and subsequent folding and activation. Hsc82 was previously found to target IDRs of client proteins and Ddp1 was identified as a potential interactor of Hsc82 via mass spectrometry after crosslinking (39). Notably, Ddp1 interacted with all three domains of Hsc82 and one of these crosslinked interacting peptides was mapped between residues 33 and 44 of Ddp1 (39), just downstream of the IDR. It is possible that Hsc82 binds Ddp1 to promote the proper folding and activation of Ddp1. This could potentially explain why N25Δ mutants show decreased levels of Ddp1 protein. Moreover, several mutations of charged amino acids within or near the Hsc82-recognized peptide (residues 33-44) of Ddp1 had similar detrimental effects on Ddp1 levels (**Table S1**).

In mammals it has been proposed that Hsp90 binds to IPPK6B, the homologue of Kcs1, to inhibit its ability to phosphorylate IP6 to IP7 (40). An increase in IP7 was seen in *hsc82*Δ yeast mutants which the authors assigned to an increase in Kcs1 activity (40). However, it is also possible that deletion of *HSC82* might negatively impact Ddp1 folding and activity which could account for this 2-fold increase in IP7. Deletion mutants of *DDP1* have previously been shown to have 10-fold higher levels of 1-IP7 (15). Interestingly, many PHO regulated genes were recently identified as differentially expressed proteins in *hsc82-W296A* mutant yeast using proteomics (41). Most Vtc proteins as well as many PHO regulated proteins such as Pho5 and Pho84 were found to be downregulated (41). These results suggest the Hsc82 might play an important role in the phosphate response and the potential interplay between Hsc82 and inositol pyrophosphate metabolism should be investigated further.

Whether Pho85 or Cdc28 can directly phosphorylate Ddp1 on S26 to regulate its function is still unclear. Recent work demonstrated that 1,5-IP8 is likely the master regulator of the

phosphate response following phosphate depletion (15). When cells are exposed to phosphate limitation, 1,5-IP8 and all other inositol pyrophosphates are rapidly depleted (15). The loss of 1,5-IP8 binding to Pho81's SPX domain causes a conformational change that results in Pho85 inhibition (15). This inhibition allows Pho4 to localize to the nucleus and activate the transcription of PHO regulon genes (15). Ddp1 can degrade 1,5-IP8, as well as 1-IP7, and may be important for rapidly depleting inositol pyrophosphate and maintaining their levels until phosphate becomes available again. Based on our results, the phosphorylation of S26 could be important for promoting the inositol pyrophosphatase activity of Ddp1. Identifying physiological conditions under which phosphorylation at this site increases or decreases could provide more insight into its potential regulatory function.

Like *S. pombe*, too much 1,5-IP8 accumulation appears to be lethal in *S. cerevisiae*. We have shown that *ddp1*Δ *siw14*Δ *vip1*Δ mutants expressing *VIP1-H548A* are inviable. In *S. pombe* genetic experiments suggest that 1,5-IP8 toxicity is driven by early 3'-processing/transcription termination (36). Interestingly, this 1,5-IP8 toxicity can be abrogated by the deletion of SPX domain proteins Gde1, Spx1, Vtc2, and Vtc4 (42). Mutation of the SPX domain of Gde1 and Spx1 is sufficient to supress toxicity whereas mutation of Vtc4's SPX domain is not (42). It will be important to determine whether 1,5-IP8 toxicity is driven by similar mechanisms in budding yeast. Notably, *S. pombe* appears to be more sensitive to 1,5-IP8 levels since *ddp1*Δ *siw14*Δ and *ddp1*Δ *vip1*Δ *VIP1(H548A) S. cerevisiae* mutants are viable. Moreover, Spx1 which was identified as a transducer of 1,5-IP8 toxicity in *S. pombe* is not conserved in *S. cerevisiae* (42). Additionally, Pho81 and Pho85 are not conserved in *S. pombe* (15). These differences in conservation suggest that 1,5-IP8 toxicity could be driven by different molecular mechanisms. One interesting possibility raised by Schwer et al. is that overaccumulation of 1,5-IP8 drives nonvacuolar polyP

synthesis (42). Under phosphate replete conditions, GFP subunits localize around the nucleus (believed to be the ER) and the plasma membrane suggesting that VTC pools might produce polyP beyond the vacuole (43,44). Recent work has shown that 1,5-IP8 can bind to the SPX domains of Vtc2 and Vtc3 to promote the catalytic activity of the VTC complex (19). Thus increased 1,5-IP8 levels could promote the accumulation of nonvacuolar polyP which is toxic to cells. Ddp1 would be well positioned to deal with inositol pyrophosphate as well as nonvacuolar polyP in this scenario. Future work will explore the genetic and molecular mechanisms that drive 1,5-IP8 toxicity in *S. cerevisiae*.

Finally, we have demonstrated that our plasmid shuffle system using the *ddp1*Δ *siw14*Δ *vip1*Δ pyrophosphatase mutant strain expressing *VIP1-H548A* can be used to study the regulation of the Ddp1 pyrophosphatase and its mammalian homologue DIPP1. By modifying plasmids used for the plasmid shuffle, this system could easily be expanded to study the structure and function of Siw14 or Vip1 *in vivo*. Moreover, our system could be leveraged to explore cancer related mutations of DIPP1. This would allow us to determine whether these mutations correspond to loss of function mutations. Eventually this information could be used to determine whether certain DIPP1 mutations might drive negative outcomes in specific cancer types.

4.5. Methods

Yeast growth and maintenance

Yeast strains were constructed using standard methods as previously described (45–47). The locations of gene deletion and tagging cassettes were confirmed using PCR analyses (47). The full genotypes of all yeast strains used in this work are listed in **Table S2**. Cells were grown in yeast extract-peptone-dextrose (YPD) or synthetic complete (SC) medium as described for individual experiments. In general, SC-Ura and Sc-Leu media were used to maintain *URA3*-based and *LEU2*-based selection plasmids, respectively. Double dropout media (SC-Ura-Leu) was used to maintain both plasmids simultaneously when needed. For experiments where gal-HA-PPK was induced (Fig. 1D and 1E, and Fig. 2B and 2C) cells were grown in SC-Ura with 2% raffinose overnight. The next morning, cultures were diluted to OD_{600} = 0.25 in SC-Ura with 2% raffinose and grown for 3 hours. Cultures were then supplemented with 2% galactose for 3 hours to induce HA-PPK expression. For other experiments (Fig. 3C, and Sup. Fig. 4B), cells were grown in SC-Ura-Leu with 2% dextrose overnight, diluted to OD_{600} = 0.2 the next morning and grown until cells had doubled twice to OD_{600} = ~0.8-1. All strains were grown at 30°C.

Plasmids

All plasmids used for this work are listed in **Table S2**. Some plasmids generated for this work will be made available from Addgene (www.Addgene.org).

Mutagenesis of the first 101 plasmids was performed by GenScript. For the other plasmids, site directed mutagenesis was performed using a protocol adapted from Edelheit et al. (48). Primers for site directed mutagenesis were designed using Agilent's QuikChange Primer Design Program. Two individual 50 µL PCR reactions for each forward and reverse primer were prepared using 32.5 µL H2O, 10 µL 5X HF buffer, 2.5 µL DMSO, 1 µL 10 mM dNTPs, 2.5 µL 10 µM primer, 1 µL 50

ng/μL plasmid, and 0.5 μL Phusion enzyme. PCR was carried out using the following settings: 98°C for 2 min, followed by 25 cycles of 98°C for 15 sec, 55°C for 30 sec, 72°C for 30 sec/kb of plasmid, and a final extension at 72°C for 5 min. The reactions were cooled and 10 μL from each PCR reaction were combined. The combined reactions were denatured at 95°C for 5 minutes and then gradually cooled to 37°C to allow random annealing of the PCR products. After cooling, 2 μL of 10X CutSmart buffer and 1 μL of Dpn1 enzyme were added to the reaction and incubated for at least 1 hour at 37°C to degrade any non-mutated methylated parental plasmid. Finally, 5 μL of the Dpn1 treated reaction mixture was transformed into XL10-gold ultracompetent cells following Agilent's transformation protocol. All plasmids were sequenced to confirm the presence of the desired mutations.

Spot tests

Cells from freshly grown plates were diluted in water, and 5- or 10-fold serial dilutions were spotted onto the indicated media and allowed to dry before incubation at 30°C for 3 days. For 5-FOA selection assays, SC-Leu plates contained 50 mg/L uracil and 1 g/L of 5-FOA (49). FOA is used to select against cells expressing *URA3* (49).

Immunoblotting

Cell pellets equivalent to an OD_{600} of 5 (measured using an Eppendorf BioPhotometer) were resuspended in 300 μL of 20% trichloroacetic acid (TCA) and 100 μL of acid-washed glass beads. Cells were lysed with 2 x 1.5 min pulses on a BioSpec mini-beadbeater. The supernatant was transferred to a new tube. Beads were washed with 300 μL 5% TCA by vortexing for 10 sec, and this supernatant was combined with the first 300 μL. This mixture was clarified via centrifugation at 16,000 × g for 4 min at 4°C. The resulting pellet was resuspended in 100 μL of SDS-PAGE loading buffer supplemented with a 1/10 volume of 1.5 M Tris-HCl (pH 8.8) and a 1/10 volume

of 1 M DTT and boiled for 5 min. The samples were centrifuged again at 16,000 × g for 4 min at room temperature, and the supernatant was recovered. Approximately 10 to 20 µL was loaded per gel (corresponding to about 75 µg of protein). Unless stated otherwise in the figure legends, protein samples were run on 12% SDS-PAGE gels made from a 30% acrylamide/bis-acrylamide (37.5:1) solution. Buffers used were described previously (15). All proteins were transferred to polyvinylidene difluoride (PVDF) membranes and blocked with 5% milk in TBST before probing with antibodies.

Immunoprecipitation

Cell pellet equivalent to an OD600 of 40 (measured using an Eppendorf BioPhotometer) were resuspended in 600 µL of lysis buffer (20 mM Tris-HCl pH 7.4, 137 mM NaCl, 1 mM EDTA, 0.1 % NP-40, 1 mM PMSF, Roche c0mplete protease inhibitor tablet) in 2 mL screw cap tubes. Tubes were filled with acid-washed glass beads, leaving about 100 µL of empty space at the top. Cells were lysed by bead beating 5 x 1 min on a BioSpec mini-beadbeater, with 2 min on ice water in between cycles. After lysis, cell debris were removed by centrifuging lysates at 16,000 x g for 10 minutes at 4°C. Anti-FLAG M2 magnetic beads equilibrated in lysis buffer were added to the clarified lysate and rotated end over end for 1 hour at 4°C. Beads were subsequently washed 3 times with 750 µL lysis buffer. Proteins were eluted by incubating beads in sample buffer without DTT and heating at 65°C for 10 min. The eluate was collected and DTT was added to 100 mM before heating again for 5 min.

Polyphosphate extraction and gel electrophoresis

The polyP extraction protocol was adapted from a protocol first described by Bru et al. (50). Yeast pellets of 8 OD_{600} units in size were resuspended in 400 µL of cold LETS buffer (10 mM Tris-HCl pH 7.4, 100 mM LiCl, 10 mM EDTA, 0.2% SDS). Resuspended cells were transferred to a 2 mL

screw cap tube containing 600 µL of phenol (pH 8) and 150 µL of MilliQ water (mqH2O), and vortexed for 20 sec. Samples were heated for 10 min at 65°C and cooled on ice for 2 min. Once cooled, 600 µL of chloroform was added, and the samples were vortexed for 20 sec. Samples were centrifuged at 16,000 x g for 2 min at room temperature, and the top aqueous phase (600 µL) was transferred to a new 2 mL screw cap tube containing 600 µL of chloroform. Samples were vortexed for 20 sec and centrifuged again at 16,000 x g for 2 min. The top aqueous phase (400 µL) was transferred to a prechilled 1.5 mL tube containing 1 mL of ethanol and 40 µL (1/10 volume) of 3 M sodium acetate (pH 5.3). The polyP was left to precipitate overnight and then pelleted by centrifugation at 16,000 x g for 20 min at 4°C. The supernatant was discarded, and the pellet was washed with 500 µL of cold 70% ethanol and centrifuged at 16,000 x g for an additional 5 min. The supernatant was discarded, and the pellets were air dried before being resuspended in 30 µL of mqH_2O.

Extracted polyP was diluted 1:20 with water and polyP loading buffer (10 mM Tris-HCl [pH 7], 1 mM EDTA, 30% glycerol, bromophenol blue) and 10 uL was loaded onto a 20% Tris-borate-EDTA (TBE) gel (19:1) and run at 100 V for 2 h 30 min in 1X TBE running buffer. For 4′,6-diamidino-2-phenylindole (DAPI) staining, the protocol was adapted from the one described previously by Smith and Morrissey (51). The gel was incubated in fixative solution with DAPI (25% methanol, 5% glycerol, 50 mM Tris base, 2 µg/mL DAPI) for 30 min with rocking. The gel was destained with fixative solution without DAPI for 1 h with rocking, changing the solution once halfway through. The destained gel was exposed to 365 nm UV light on a transilluminator to photobleach the DAPI-polyP until it became dark. Pictures were taken with a Bio-Rad ChemiDoc UV transilluminator.

Protein purification

N-terminally 6HIS-TEV-tagged Ddp1 constructs were expressed in BL21 (DE3) pLysS Escherichia coli cells. Bacteria were grown in LB media supplemented with 100 µg/mL ampicillin, 34 µg/mL chloramphenicol, and 0.5% dextrose overnight at 37 °C. The next morning cells were diluted to an OD_{600} of 0.1 in 1 L of fresh LB media supplemented with 100 µg/mL ampicillin, 34 µg/mL chloramphenicol, 0.5% dextrose, and 1 mM $MgCl_2$, and grown at 37°C to an OD_{600} of 0.5-0.6. Cells were shifted to 30°C and expression was induced with 0.2 mM isopropyl-β-d-thiogalactopyranoside (IPTG) for 4 hours at 30°C. Cells were harvested by centrifugation and pellets were washed once with mqH_2O before freezing in liquid nitrogen and storing them at -80 °C. Cells were resuspended in 30 mL of lysis buffer (50 mM HEPES-KOH pH 7.4, 500 mM NaCl, 10% glycerol, 10 mM imidazole pH 7.4, 0.5% triton X-100, 10 mM BME, 1 mM $MgCl_2$, 1 mM PMSF, EDTA-free c0mplete protease inhibitor tablet). Cells were lysed by addition of 0.4 mg/mL lysozyme and incubated on ice for 30 minutes before sonicating 4 x 20 sec on a Misonix sonicator 3000 on power level 5. Cell debris were removed from the lysate by spinning at 16,000 rpm for 30 min at 4°C and filtering through a 0.45 µM filter. TALON resin (1.5 mL slurry) washed and equilibrated in 50 mM HEPES-KOH pH 7.4, 500 mM NaCl, 10% glycerol, 10 mM imidazole pH 7.4, 0.5% triton X-100, and 1 mM $MgCl_2$ was added to the clarified lysate and rotated for 30 min at 4°C. The beads were pelleted by centrifuging at 500 x g for 5 min at 4°C and batch washed with 20 mL of wash buffer (50 mM HEPES-KOH pH 7.4, 500 mM NaCl, 10% glycerol, 10 mM imidazole pH 7.4, 0.1% triton X-100, 10 mM BME, 1 mM MgCl2, 0.1 mM PMSF) by rotation for 5 mins at 4°C. The beads were spun again at 500 x g for 2 mins at 4°C and transferred to a chromatography column in a cold room. The column with beads was washed with 10 mL of wash buffer followed by 10 mL of high salt wash buffer containing 1 M NaCl. Finally, the protein was

eluted with 5 mL elution buffer (50 mM HEPES-KOH pH 7.4, 300 mM NaCl, 150 mM imidazole pH 7.4, 10% glycerol, 1 mM $MgCl_2$, 10 mM BME). Fractions were collected and analyzed by SDS-PAGE. Fractions containing the protein were pooled, and excess 6HIS-TEV protease was added before dialyzing overnight in dialysis buffer (25 mM HEPES-KOH pH 7.4, 200 mM NaCl, 10% glycerol, 10 mM imidazole pH 7.4, 1 mM $MgCl_2$, 10 mM BME). The protein + TEV mixture was dialyzed two more times for at least 3 hours in fresh dialysis buffer. The tag-free Ddp1 protein was separated from the fusion tag and the 6His-TEV protease using a second TALON bead affinity chromatography step. The eluate was collected and dialyzed against storage buffer (20 mM HEPES-KOH pH 7.4, 100 mM NaCl, 10% glycerol, 1 mM $MgCl_2$, 1 mM DTT). Proteins were concentrated to at least 1 mg/mL using Amicon Ultra-15 Centrifugal Filters with a 10 kDa MWCO, aliquoted into PCR tubes in single use aliquots, and flash frozen in liquid nitrogen. Proteins were stored at -80°C until needed. Final protein concentrations were determined by running the purified proteins on an SDS-PAGE gel with known concentrations of a BSA standard and quantified after Coomassie staining using the standard curve.

Polyphosphatase activity assays

Proteins were flash thawed and diluted to appropriate concentrations in storage buffer (20 mM HEPES-KOH pH 7.4, 100 mM NaCl, 10% glycerol, 1 mM $MgCl_2$, 1 mM DTT). Two-fold serial dilutions of the proteins were prepared to the desired concentrations. Polyphosphatase reactions were prepared in 10 µL volumes containing 10 mM HEPES-KOH pH 7.4, 50 mM NaCl, 2 mM MgCl2, 5 mM P60 and equimolar concentrations of protein as indicated in the figure legend. Reactions were incubated at 37°C for 1 h in a thermocycler. After 1 h, 2 µL of a 100 mM EDTA solution was added to each tube to stop the reaction. Samples were either stored at -80°C or immediately run on a 20% acrylamide/bis-acrylamide (19:1)-TBE gel (12.5 mL 40%

acrylamide/bis-acrylamide (19:1), 2.5 mL 10X TBE, 9.8 mL H_2O, 125 µL 10% APS, and 20 µL TEMED). Samples were run on large 18 cm x 18 cm gels using a 19:1 acrylamide/bis-acrylamide solution to resolve short chain polyP products. Gels were run at 360 V for 3 h in a cold room before staining in fixative solution with toluidine blue (25% methanol, 5% glycerol, 0.05% toluidine blue) for 30 min. Gels were subsequently destained with the same solution without toluidine blue and scanned.

Electromobility shift assays

Proteins were flash thawed and diluted in storage buffer (20 mM HEPES-KOH pH 7.4, 100 mM NaCl, 10% glycerol, 1 mM $MgCl_2$, 1 mM DTT). EMSA reactions were prepared in 10 µL reactions containing 10 mM HEPES-KOH pH 7.4, 50 mM KCl, 5% glycerol, 5 mM $MgCl_2$, 0.05% NP-40, 50 ug/mL BSA, 1 nM IR800-labelled RNA probe, and the molar concentrations of protein as indicated in the figure legend. In probe only reactions, the volume of protein (2 µL) was replaced with storage buffer. Reactions were incubated in a thermocycler at 4°C for 1 h and run on a 6% non-denaturing Tris-Glycine polyacrylamide/bis-acrylamide gel (37.5:1) with 2.5% glycerol that had been pre-run at 80 V for 30 min in a cold room. Gels were run for 160 V for 5 min before reducing the voltage to 80 V for 1 h. Gels were imaged with a BioRad Chemidoc MP using the IR800 dye filter setting. The RNA probe sequence is: 5'-UAGUACCGCCACCCUCAGAACCUUUUUUUUUUUUU-3' and is the same sequence as the RNA36 probe from Ray and Frick (33).

4.6. Acknowledgements

We thank T. Shiba (RegeneTiss, Japan) for the gift of polyP standards. Polyphosphate research in the Downey lab is funded by Canadian Institutes of Health Research Project Grants (PJT-198016 and PJT-174987) to M.D. L.M. was supported by an NSERC Canada graduate scholarship and an Ontario Graduate Scholarship.

We declare no conflicts.

4.7. References

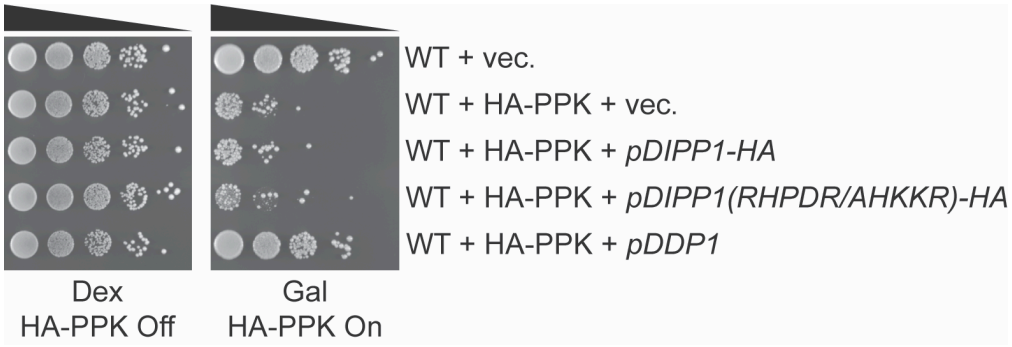
1. Austin S, Mayer A. Phosphate Homeostasis − A Vital Metabolic Equilibrium Maintained Through the INPHORS Signaling Pathway. Front Microbiol [Internet]. 2020;Volume 11. Available from: https://www.frontiersin.org/journals/microbiology/articles/10.3389/fmicb.2020.01367
2. Azevedo C, Saiardi A. Eukaryotic phosphate homeostasis: the inositol pyrophosphate perspective. Trends Biochem Sci. 2017;42(3):219–31.
3. Kim G-D, Qiu D, Jessen HJ, Mayer A. Metabolic consequences of polyphosphate synthesis and imminent phosphate limitation. MBio. 2023;14(3):e00102-23.
4. Cartwright JL, McLennan AG. The Saccharomyces cerevisiae YOR163w gene encodes a diadenosine 5',5'''- P1,P6-hexaphosphate (Ap6A) hydrolase member of the MutT motif (Nudix hydrolase) family. J Biol Chem [Internet]. 1999;274(13):8604–10. Available from: http://dx.doi.org/10.1074/jbc.274.13.8604
5. Safrany ST, Ingram SW, Cartwright JL, Falck JR, McLennan AG, Barnes LD, et al. The diadenosine hexaphosphate hydrolases from Schizosaccharomyces pombe and Saccharomyces cerevisiae are homologues of the human diphosphoinositol polyphosphate. Overlapping substrate specificities in a Mutt-type protein phosphohydrolase. J Biol Chem [Internet]. 1999;274(31):21735–40. Available from: http://dx.doi.org/10.1074/jbc.274.31.21735
6. Lonetti A, Szijgyarto Z, Bosch D, Loss O, Azevedo C, Saiardi A. Identification of an evolutionarily conserved family of inorganic polyphosphate endopolyphosphatases. J Biol Chem. 2011;286(37):31966–74.
7. Kilari RS, Weaver JD, Shears SB, Safrany ST. Understanding inositol pyrophosphate metabolism and function: Kinetic characterization of the DIPPs. FEBS Lett. 2013;587(21):3464–70.
8. Song MG, Bail S, Kiledjian M. Multiple Nudix family proteins possess mRNA decapping activity. Rna. 2013;19(3):390–9.
9. McLennan AG. Substrate ambiguity among the nudix hydrolases: biologically significant, evolutionary remnant, or both? Cell Mol life Sci. 2013;70:373–85.
10. Koonin E V. A highly conserved sequence motif defining the family of MutT-related proteins from eubacteria, eukaryotes and viruses. Nucleic Acids Res. 1993;21(20):4847.
11. Srouji JR, Xu A, Park A, Kirsch JF, Brenner SE. The evolution of function within the Nudix homology clan. Proteins Struct Funct Bioinforma. 2017;85(5):775–811.
12. Jakubowski H. Sporulation of the yeast Saccharomyces cerevisiae is accompanied by synthesis of adenosine 5'-tetraphosphate and adenosine 5'-pentaphosphate. Proc Natl Acad Sci. 1986;83(8):2378–82.
13. Padmanabhan U, Dollins DE, Fridy PC, York JD, Downes CP. Characterization of a selective inhibitor of inositol hexakisphosphate kinases. Use in defining biological roles and metabolic relationships of inositol pyrophosphates. J Biol Chem. 2009;284(16):10571–82.
14. York SJ, Armbruster BN, Greenwell P, Petes TD, York JD. Inositol diphosphate signaling regulates telomere length. J Biol Chem [Internet]. 2005;280(6):4264–9. Available from: http://dx.doi.org/10.1074/jbc.M412070200
15. Chabert V, Kim G-D, Qiu D, Liu G, Michaillat Mayer L, Jamsheer K M, et al. Inositol pyrophosphate dynamics reveals control of the yeast phosphate starvation program

through 1,5-IP8 and the SPX domain of Pho81. Gutjahr C, Ron D, editors. Elife [Internet]. 2023;12:RP87956. Available from: https://doi.org/10.7554/eLife.87956
16. Shears SB. Inositol pyrophosphates: Why so many phosphates? Adv Biol Regul. 2015;57:203–16.
17. Secco D, Wang C, Shou H, Whelan J. Phosphate homeostasis in the yeast Saccharomyces cerevisiae, the key role of the SPX domain-containing proteins. FEBS Lett [Internet]. 2012 Feb 17;586(4):289–95. Available from: https://doi.org/10.1016/j.febslet.2012.01.036
18. Gerasimaite R, Pavlovic I, Capolicchio S, Hofer A, Schmidt A, Jessen HJ, et al. Inositol Pyrophosphate Specificity of the SPX-Dependent Polyphosphate Polymerase VTC. ACS Chem Biol. 2017;12(3):648–53.
19. Pipercevic J, Kohl B, Gerasimaite R, Comte-Miserez V, Hostachy S, Müntener T, et al. Inositol pyrophosphates activate the vacuolar transport chaperone complex in yeast by disrupting a homotypic SPX domain interaction. Nat Commun [Internet]. 2023;14(1):2645. Available from: https://doi.org/10.1038/s41467-023-38315-w
20. Steidle EA, Chong LS, Wu M, Crooke E, Fiedler D, Resnick AC, et al. A novel inositol pyrophosphate phosphatase in Saccharomyces cerevisiae: Siw14 protein selectively cleaves the β-phosphate from 5-diphosphoinositol pentakisphosphate (5PP-IP5). J Biol Chem. 2016;291(13):6772–83.
21. Raia P, Lee K, Bartsch SM, Rico-Resendiz F, Portugal-Calisto D, Vadas O, et al. A small signaling domain controls PPIP5K phosphatase activity in phosphate homeostasis. Nat Commun [Internet]. 2025;16(1):1753. Available from: https://doi.org/10.1038/s41467-025-56937-0
22. Márquez-Moñino MÁ, Ortega-García R, Shipton ML, Franco-Echevarría E, Riley AM, Sanz-Aparicio J, et al. Multiple substrate recognition by yeast diadenosine and diphosphoinositol polyphosphate phosphohydrolase through phosphate clamping. Sci Adv. 2021;7(17):1–16.
23. McCarthy L, Abramchuk I, Wafy G, Denoncourt A, Lavallée-Adam M, Downey M. Ddp1 Cooperates with Ppx1 to Counter a Stress Response Initiated by Nonvacuolar Polyphosphate. MBio. 2022;13(4).
24. Gerasimaitė R, Sharma S, Desfougères Y, Schmidt A, Mayer A. Coupled synthesis and translocation restrains polyphosphate to acidocalcisome-like vacuoles and prevents its toxicity. J Cell Sci. 2014;127(23):5093–104.
25. Piovesan D, Del Conte A, Mehdiabadi M, Aspromonte MC, Blum M, Tesei G, et al. MOBIDB in 2025: integrating ensemble properties and function annotations for intrinsically disordered proteins. Nucleic Acids Res. 2025;53(D1):D495–503.
26. Lanz MC, Yugandhar K, Gupta S, Sanford EJ, Faça VM, Vega S, et al. In-depth and 3-dimensional exploration of the budding yeast phosphoproteome. EMBO Rep. 2021;22(2):e51121.
27. Hu Z, Raucci S, Jaquenoud M, Hatakeyama R, Stumpe M, Rohr R, et al. Multilayered control of protein turnover by TORC1 and Atg1. Cell Rep. 2019;28(13):3486–96.
28. Dokladal L, Stumpe M, Hu Z, Jaquenoud M, Dengjel J, De Virgilio C. Phosphoproteomic responses of TORC1 target kinases reveal discrete and convergent mechanisms that orchestrate the quiescence program in yeast. Cell Rep. 2021;37(13).
29. Caligaris M, Nicastro R, Hu Z, Tripodi F, Hummel JE, Pillet B, et al. Snf1/AMPK fine-tunes TORC1 signaling in response to glucose starvation. Elife. 2023;12:e84319.
30. Moffat J, Huang D, Andrews B. Functions of Pho85 cyclin-dependent kinases in budding

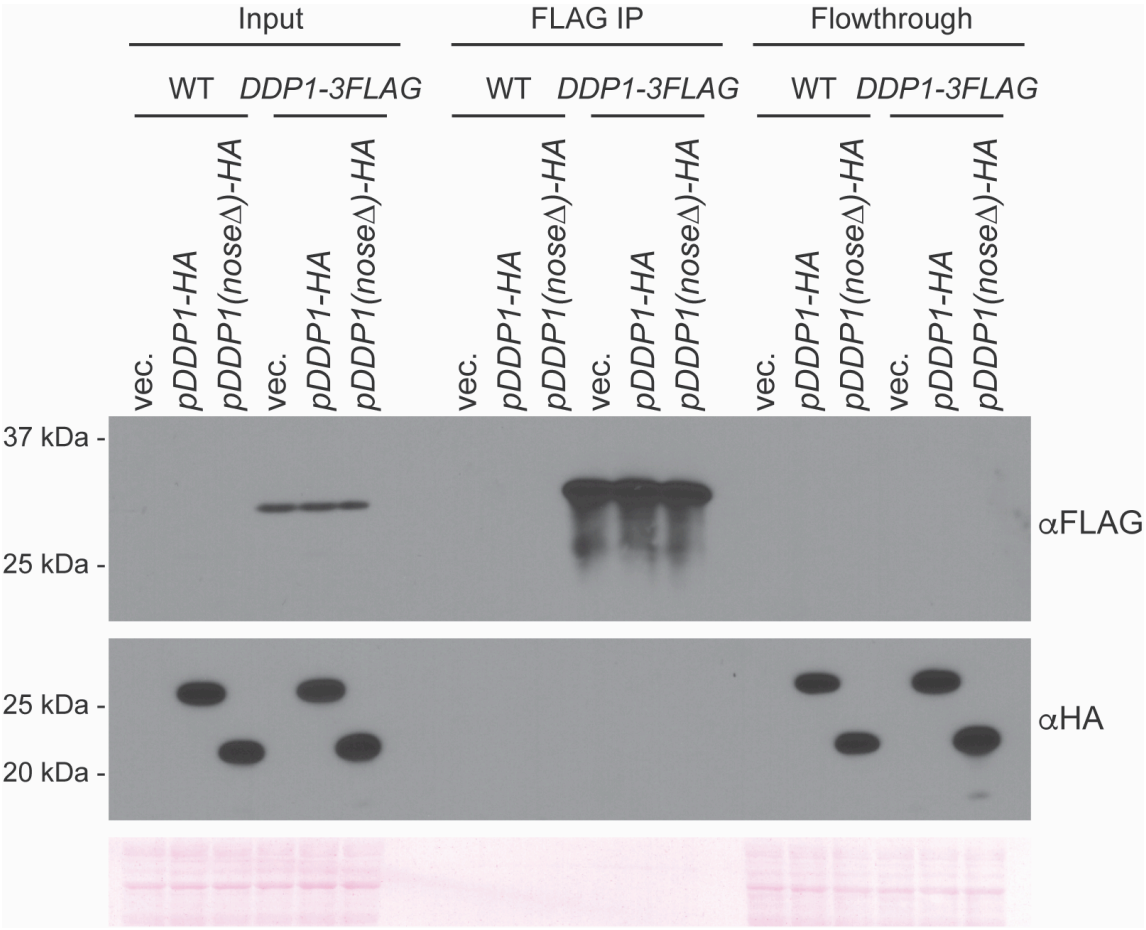
yeast. Prog Cell Cycle Res. 1998;97–106.
31. Enserink JM, Kolodner RD. An overview of Cdk1-controlled targets and processes. Cell Div. 2010;5:1–41.
32. Newcombe EA, Delaforge E, Hartmann-Petersen R, Skriver K, Kragelund BB. How phosphorylation impacts intrinsically disordered proteins and their function. Essays Biochem. 2022;66(7):901–13.
33. Ray A, Frick DN. Fluorescent probe displacement assays reveal unique nucleic acid binding properties of human nudix enzymes. Anal Biochem. 2020;595:113622.
34. Dyson HJ. Roles of intrinsic disorder in protein–nucleic acid interactions. Mol Biosyst. 2012;8(1):97–104.
35. Sanchez AM, Garg A, Shuman S, Schwer B. Inositol pyrophosphates impact phosphate homeostasis via modulation of RNA 3′ processing and transcription termination. Nucleic Acids Res. 2019;47(16):8452–69.
36. M. SA, Beate S, Nikolaus J, J. JH, Stewart S. Activities, substrate specificity, and genetic interactions of fission yeast Siw14, a cysteinyl-phosphatase-type inositol pyrophosphatase. MBio [Internet]. 2023 Sep 29;14(5):e02056-23. Available from: https://doi.org/10.1128/mbio.02056-23
37. Mungall AJ, Palmer SA, Sims SK, Edwards CA, Ashurst JL, Wilming L, et al. The DNA sequence and analysis of human chromosome 6. Nature. 2003;425(6960):805–11.
38. Wang H, Godage HY, Riley AM, Weaver JD, Shears SB, Potter BVL. Synthetic inositol phosphate analogs reveal that PPIP5K2 has a surface-mounted substrate capture site that is a target for drug discovery. Chem Biol. 2014;21(5):689–99.
39. Kolhe JA, Babu NL, Freeman BC. The Hsp90 molecular chaperone governs client proteins by targeting intrinsically disordered regions. Mol Cell. 2023;83(12):2035–44.
40. Chakraborty A, Koldobskiy MA, Sixt KM, Juluri KR, Mustafa AK, Snowman AM, et al. HSP90 regulates cell survival via inositol hexakisphosphate kinase-2. Proc Natl Acad Sci. 2008;105(4):1134–9.
41. Rios EI, Gonçalves D, Morano KA, Johnson JL. Quantitative proteomic analysis reveals unique Hsp90 cycle-dependent client interactions. Genetics. 2024;227(2):iyae057.
42. Schwer B, Garg A, Sanchez AM, Bernstein MA, Benjamin B, Shuman S. Cleavage-polyadenylation factor Cft1 and SPX domain proteins are agents of inositol pyrophosphate toxicosis in fission yeast. MBio. 2022;13(1):e03476-21.
43. Hothorn M, Neumann H, Lenherr ED, Wehner M, Rybin V, Hassa PO, et al. Catalytic core of a membrane-associated eukaryotic polyphosphate polymerase. Science (80-). 2009;324(5926):513–6.
44. Uttenweiler A, Schwarz H, Neumann H, Mayer A. The vacuolar transporter chaperone (VTC) complex is required for microautophagy. Mol Biol Cell. 2007;18(1):166–75.
45. Goldstein AL, McCusker JH. Three new dominant drug resistance cassettes for gene disruption in Saccharomyces cerevisiae. Yeast. 1999;15(14):1541–53.
46. Longtine MS, Mckenzie III A, Demarini DJ, Shah NG, Wach A, Brachat A, et al. Additional modules for versatile and economical PCR-based gene deletion and modification in Saccharomyces cerevisiae. Yeast. 1998;14(10):953–61.
47. McCarthy L, Bentley-DeSousa A, Denoncourt A, Tseng YC, Gabriel M, Downey M. Proteins required for vacuolar function are targets of lysine polyphosphorylation in yeast. FEBS Lett. 2019;1–10.
48. Edelheit O, Hanukoglu A, Hanukoglu I. Simple and efficient site-directed mutagenesis

using two single-primer reactions in parallel to generate mutants for protein structure-function studies. BMC Biotechnol. 2009;9:1–8.
49. Boeke JD, La Croute F, Fink GR. A positive selection for mutants lacking orotidine-5′-phosphate decarboxylase activity in yeast: 5-fluoro-orotic acid resistance. Mol Gen Genet MGG. 1984;197(2):345–6.
50. Bru S, Jiménez J, Canadell D, Ariño J, Clotet J. Improvement of biochemical methods of polyP quantification. Microb Cell. 2016;4(1):6.
51. Smith SA, Morrissey JH. Sensitive fluorescence detection of polyphosphate in polyacrylamide gels using 4′, 6-diamidino-2-phenylindol. Electrophoresis. 2007;28(19):3461–5.

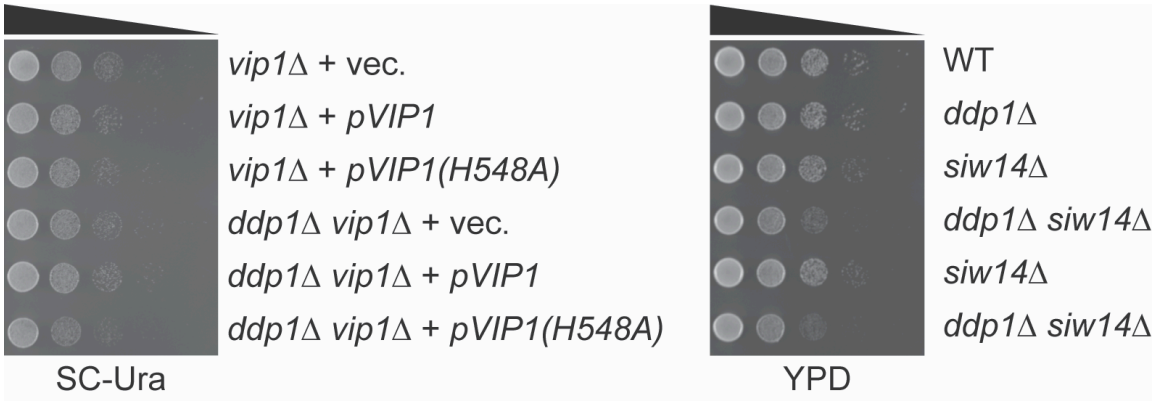
4.8. Supplemental figures



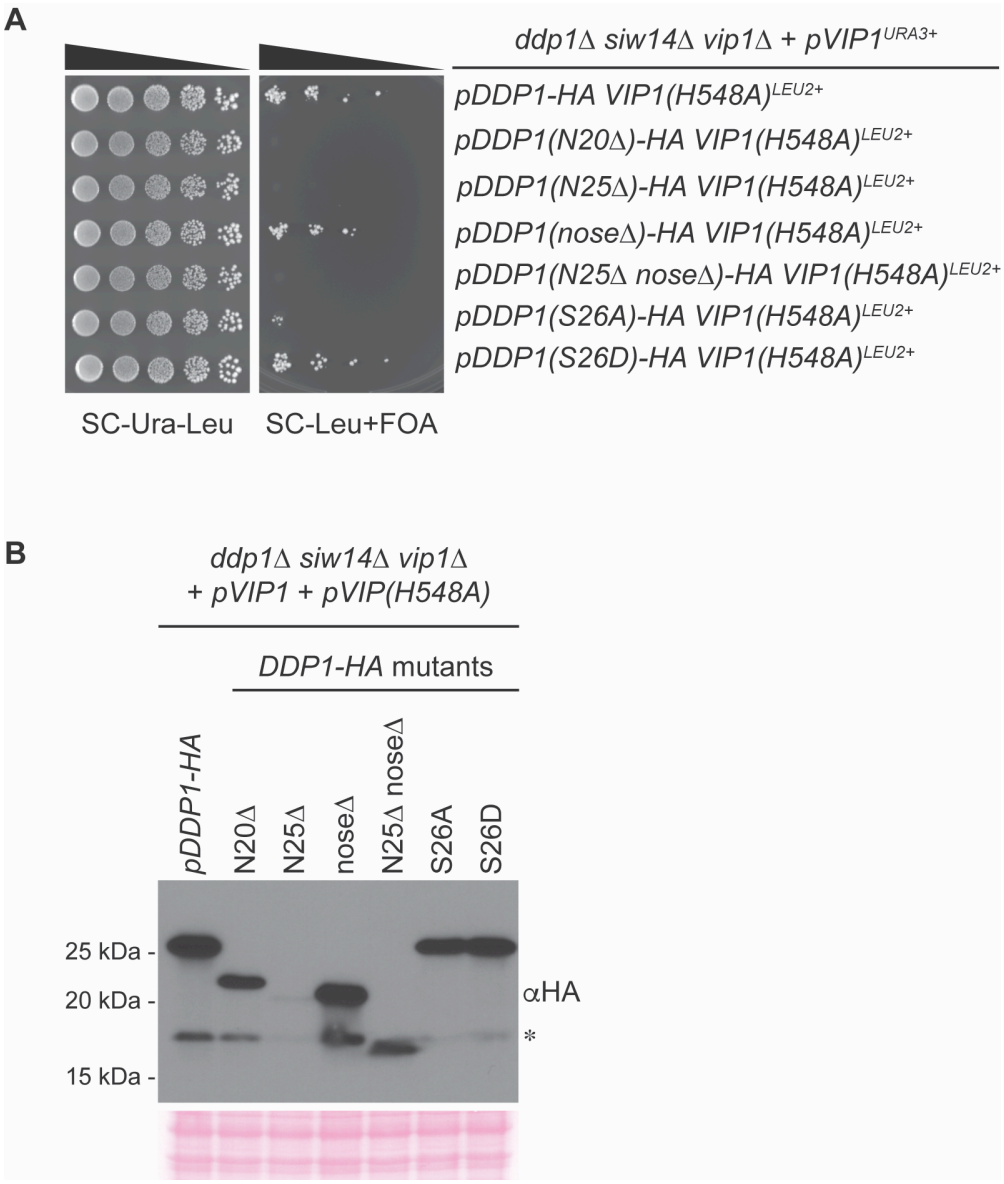
S1 Figure. Mutation of DIPP1's RHPDR sequence to AHKKR does not significantly improve rescue. Ten-fold dilutions of wild-type galactose inducible HA-PPK yeast strains transformed with the indicated GPD overexpression plasmids were spotted onto SC-Ura plates with 2% dextrose or galactose and grown for 3 days. Images are representative of ≥3 experiments.



S2 Figure. Ddp1 does not interact with itself. Ddp1-3FLAG was immunoprecipitated from yeast cells co-expressing Ddp1-HA or Ddp1(noseΔ)-HA. Protein samples were separated on a 12% SDS-PAGE gel. Separated proteins were transferred to a PVDF membrane and Ddp1-HA was detected using an HA antibody and Ddp1-3FLAG was detected using a FLAG-HRP antibody. Image is representative of 1 experiment.



S3 Figure. The *ddp1*Δ *siw14*Δ and *siw14*Δ *vip1*Δ *VIP1(H548A)* mutant strains are viable *in S. cerevisiae.* Ten-fold dilutions of the indicated strains were spotted onto SC-Ura or YPD plates as indicated and grown for 1 day. The slight toxicity observed in both strains was only visible during the first 24 h of growth. Images are representative of ≥3 experiments.



S4 Figure. The first 20 amino acids of Ddp1 are important for its pyrophosphatase activity. (**A**) Plasmid shuffle assay used to assess the ability of Ddp1 mutants to rescue inositol pyrophosphate toxicity. Fivefold dilutions of the *ddp1*Δ *siw14*Δ *vip1*Δ cells co-transformed with a *URA3*-marked plasmid expressing *VIP1* and a *LEU2*-marked plasmid co-expressing *VIP1(H548A)* and *DDP1-HA* or the indicated *DDP1-HA* mutants. (**B**) Protein expression levels of various Ddp1-HA mutants. Protein extracts from *ddp1*Δ *siw14*Δ *vip1*Δ mutants co-transformed with a *LEU2*-marked plasmid expressing *VIP1* and a *URA3*-marked plasmid co-expressing *VIP1(H548A)* and *DDP1-HA* or the indicated mutant were prepared using a TCA lysis protocol and separated on a 13% SDS-PAGE gel. The * indicates a non-specific band of unknown origin. Images are representative of ≥3 experiments.

4.9. Supplemental tables

List of tables presented:

S1 Table. Summary of the Ddp1 mutant screen.

1. S1-Tab 1: List of mutants screened, their phenotypes and expression levels.

S2 Table. Strains and plasmids used in this work.

1. S2-Tab 1: Strains used in this work.
2. S2-Tab 2: Plasmids used in this work.

S1 Table-Tab 1 – List of mutants screened, their phenotypes and expression levels.

Description	Name	Mutation site	Phenotype	Expression
Repeated amino acids	Mut1	K44A K45A	dead	lower
	Mut2	K56A K57A	slightly worse	same
	Mut3	S52A S53A	same	slightly lower
	Mut4	G64A G65A	dead	lower
	Mut5	T75A T76A	same	lower
	Mut6	E83A E84A	dead	lower
	Mut7	P103A P104A	same	lower
	Mut8	P127A P128A	same	lower
	Mut9	L142A L143A	worse	lower
	Mut10	L174A L175A	dead	lower
	Mut11	I183A I184A	dead	lower
	Mut12	D186A D187A	same	slightly higher
Possible phosphorylation sites	Mut13	S13A	same	same
	Mut14	S26A	same	slightly lower
	Mut15	S52A	same	same
	Mut16	S117A S121A	same	same
	Mut17	S158A	same	same
	Mut18	S181A	worse	lower
	Mut19	T4A	same	same
	Mut20	T15A	slightly worse	same
	Mut21	T29A	same	same
	Mut22	T41A T51A	dead	lower
	Mut23	T75A	same	same
	Mut24	T76A	same	same
	Mut25	T81A	dead	same
	Mut26	T97A	same	same
	Mut27	T130A	slightly worse	same
	Mut28	T160A	same	slighly lower
	Mut29	Y25A	same	slighly lower
	Mut30	Y73A	same	same
	Mut31	Y135A	dead	lower
	Mut32	Y157A	same or slightly worse	slightly lower
Possible acetylation/ubiquitination sites	Mut33	K3	same or slightly worse	slightly lower
	Mut34	K44A	slightly worse	lower
	Mut35	K45A	slightly worse	lower

	Mut36	K56A	slightly worse	same
	Mut37	K57A	worse	same
	Mut38	K63A	dead	same
	Mut39	K68A	same	same
	Mut40	K90A	same	untested
	Mut41	K105A K109A	slightly worse	same
	Mut42	K112A	potentially better	higher
	Mut43	K119A	same	higher
	Mut44	K125A	same	same
	Mut45	K145A	same	same
	Mut46	K151A	slightly worse	slightly lower
	Mut47	K155A	worse	lower
	Mut48	K163A	same	same
	Mut49	K170A	same	same
	Mut50	K185A	slightly worse	lower
	Mut51	K188A	slightly worse	lower
Aligned to DIPP1 (N-term) difference	Mut52	G2M	same	same
	Mut53	E18K G19S R20N	slightly worse	more
	Mut54	E21Q N22T Q23R	same	lower
	Mut55	V24G S26Y P27D	worse	lower
	Mut56	V28G T29D A31Y	worse	lower
	Mut57	R32K L33K V34R	dead	lower
Aligned to DIPP1 (Nudix box) difference	Mut58	K63G V66M K68P	dead	lower
	Mut59	D69E P71E N72P	worse	lower
	Mut60	Y73S E74A T75V	slightly worse	lower
	Mut61	T76A Q78V T81V	same	more
	Mut62	W82C C87V I88K	dead	lower
Aligned to DIPP1 (C-term) difference	Mut63	R154V K155V L156A	dead	hardly detectable
	Mut64	Y157T S158T T160S	same	same
	Mut65	E161V A162S K163A	dead	hardly detectable
	Mut66	N165S L166S I167M	dead	hardly detectable
	Mut67	D168S A169G K170I	dead	lower
Aligned to DIPP1 (N-term) similar	Mut68	G30A	same	same
	Mut69	A35G	same	same
	Mut70	C37A C39A	same	same
	Mut71	V47A L48A	dead	hardly detectable
	Mut72	H55A	slightly worse	same

Aligned to DIPP1 (C-term) Similar	Mut73	L142A	even worse	lower
	Mut74	Y159A	dead	hardly detectable
	Mut75	Q164A	worse	lower
	Mut76	R171A	worse	same
Aligned to DIPP1 (Nudix Box) Similar	Mut77	R58A W59A I60A V61A P62A	dead	hardly detectable
Motifs	Mut78	E83A E84A A85G G86A	dead	hardly detectable
	Mut79	I60A V61A P62A K63A G64A G65A	dead	hardly detectable
	Mut80	E136A L137A E138A I139A E140A	dead	hardly detectable
	Mut81	K185A D186A D187A K188A	dead	lower
PolyP binding	Mut82	A54G H55A K56A K57A R58A	dead	same
	Mut83	R58A	slightly worse	slightly lower
	Mut84	R102A	slightly worse	slightly lower
	Mut85	R129A	slightly worse	same
	Mut86	R171A	worse	same
Key interaction sites	Mut87	R32A	dead	lower
	Mut88	E80A	dead	lower
	Mut89	E84A	dead	lower
N-term modifications	Mut90	N term -5	same	same
	Mut91	N term -10	slightly better	slightly higher
	Mut92	N term -15	same	slightly higher
	Mut93	N term -20	slightly worse	slightly lower
	Mut94	N term -25	slightly worse	lower
C-term modifications	Mut95	C term -28	dead	?
	Mut96	C term -23	dead	?
	Mut97	C term -18	dead	?
	Mut98	C term -13	dead	?
	Mut99	C term -8	dead	?
	Mut100	C term -3	dead	?
	Mut101	noseΔ	same	same
	Mut102	N term - 25 and noseΔ	slightly worse	lower
Phosphomimetic	Mut103	S26D	same	same
Potential phospho site	Mut104	T41A	same	lower
Phosphomimetic	Mut105	T41D	worse	lower
Potential phospho site	Mut106	S26A T41A	dead	lower

Phosphomimetic	Mut107	S26D T41D	dead	lower
Potential W-Y dyad	Mut108	W59A	dead	lower
Y157 interacts with W59	Mut109	Y157A Y159A	dead	lower
KEN box-like motif	Mut110	G19A E21A N22A	worse	lower
D-box motif	Mut111	R171A L174A	dead	same
Predicted bipartite NLS	Mut112	148-174Δ	dead	undetectable

S2 Table-Tab 1 – Strains used in this work.

Reference number	Strain background	Genotype	Source
963	S288C BY474	MATa leu2d0 ura3d0 his3-1 met15d0 LYS2+	Adam Rudner's Lab via Boone Lab
3222	S288C BY474	MATα leu2d0 ura3d0 his3::GAL-HA-PPK-HIS3 MET15+ LYS2+	McCarthy et al. 2023 (PMID: 35862758)
3234	S288C BY474	MATα leu2d0 ura3d0 his3::GAL-HA-PPK-HIS3 met15d0 LYS2+ ddp1::KANMX	McCarthy et al. 2023 (PMID: 35862758)
3347	S288C BY474	MATa leu2d0 ura3d0 his3::GAL-HA-PPK-HIS3 MET15+ LYS2+ vtc4::NATMX ddp1::KANMX	McCarthy et al. 2023 (PMID: 35862758)
3512	S288C BY474	MATa leu2d0 ura3d0 his3-1 met15d0 LYS2+ DDP1-3FLAG-HYGMX	This study
4340	S288C BY474	MATa leu2d0 ura3d0 his3-1 met15d0 LYS2+ ddp1::NATMX	This study
4944	S288C BY474	MATa leu2d0 ura3d0 his3-1 met15d0 siw14::URA3	This study
4946	S288C BY474	MATa leu2d0 ura3d0 his3-1 met15d0 LYS2+ siw14::URA3 ddp1::NATMX	This study
4968	S288C BY474	MATa leu2d0 ura3d0 his3-1 met15d0 lys2d0 vip1::HYGMX	This study
5032	S288C BY474	MATa leu2d0 ura3d0 his3-1 met15d0 LYS2+ ddp1::NATMX vip1::HYGMX	This study
5321	S288C BY474	MATa leu2d0 ura3d0 his3-1 met15d0 LYS2+ ddp1::NATMX vip1::HYGMX siw14::KANMX	This study

S2 Table-Tab 2 – Plasmids used in this work.

Plasmid	Details	Source
pRS316	Empty vector control (*URA3* selection)	Sikorski and Hieter 1989 (PMID: 2659436)
pRS316-DDP1-HA	Expresses *DDP1-HA* from its endogenous promoter and terminator (*URA3* selection)	This study
pRS316-DDP1(H55A)-HA	Expresses *DDP1(H55A)-HA* from its endogenous promoter and terminator (*URA3* selection)	This study
pRS316-DDP1(K56A K57A)-HA	Expresses *DDP1(K56A K57A)-HA* from its endogenous promoter and terminator (*URA3* selection)	This study
pRS316-DDP1(R58A)-HA	Expresses *DDP1(R58A)-HA* from its endogenous promoter and terminator (*URA3* selection)	This study
pRS316-DDP1(54-AHHKR/GAAAA)-HA	Expresses *DDP1(54-AHHKR/GAAAA)-HA* from it endogenous promoter and terminator (*URA3* selection)	This study
pRS316-DDP1(S52A)-HA	Expresses *DDP1(S52A)-HA* from its endogenous promoter and terminator (*URA3* selection)	This study
pRS316-DDP1(S52A S53A)-HA	Expresses *DDP1(S52A S53A)-HA* from its endogenous promoter and terminator (*URA3* selection)	This study
pRS316-DDP1(R32A)-HA	Expresses *DDP1(R32A)-HA* from its endogenous promoter and terminator (*URA3* selection)	This study
pRS316-DDP1(K63A)-HA	Expresses *DDP1(K63A)-HA* from its endogenous promoter and terminator (*URA3* selection)	This study
pRS316-DDP1(R102A)-HA	Expresses *DDP1(R102A)-HA* from its endogenous promoter and terminator (*URA3* selection)	This study
pRS316-DDP1(R129A)-HA	Expresses *DDP1(R129A)-HA* from its endogenous promoter and terminator (*URA3* selection)	This study
pRS316-DDP1(R171A)-HA	Expresses *DDP1(R171A)-HA* from its endogenous promoter and terminator (*URA3* selection)	This study
pRS316-DDP1(N20Δ)-HA	Expresses *DDP1(N20Δ)-HA* from its endogenous promoter and terminator (*URA3* selection)	This study
pRS316-DDP1(N25Δ)-HA	Expresses *DDP1(N25Δ)-HA* from its endogenous promoter and terminator (*URA3* selection)	This study
pRS316-DDP1(noseΔ)-HA	Expresses *DDP1(noseΔ)-HA* from its endogenous promoter and terminator (*URA3* selection)	This study
pRS316-DDP1(N25Δ noseΔ)-HA	Expresses *DDP1(N25Δ noseΔ)-HA* from its endogenous promoter and terminator (*URA3* selection)	This study
pRS316-DDP1(S26A)-HA	Expresses *DDP1(S26A)-HA* from its endogenous promoter and terminator (*URA3* selection)	This study
pRS316-DDP1(S26D)-HA	Expresses *DDP1(S26D)-HA* from its endogenous promoter and terminator (*URA3* selection)	This study
pRS316-VIP1	Expresses *VIP1* from its endogenous promoter and terminator (*URA3* selection)	This study

pRS316-VIP1(H548A)	Expresses *VIP1(H548A)* from its endogenous promoter and terminator (*URA3* selection)	This study
pRS415	Empty vector control (*LEU2* selection)	Kristin Baetz Lab
pRS415-VIP1	Expresses *VIP1* from its endogenous promoter and terminator (*LEU2* selection)	This study
pRS415-VIP1(H548A)	Expresses *VIP1(H548A)* from its endogenous promoter and terminator (*LEU2* selection)	This study
pRS415-VIP1(H548A)-DDP1-HA	Co-expresses *VIP(H548A)* pyrophosphatase mutant and *DDP1-HA* from their endogenous promoters and terminators (*LEU2*)	This study
pRS415-VIP1(H548A)-DDP1(N20Δ)-HA	Co-expresses *VIP(H548A)* pyrophosphatase mutant and *DDP1(N20Δ)-HA* from their endogenous promoters and terminators (*LEU2*)	This study
pRS415-VIP1(H548A)-DDP1(N25Δ)-HA	Co-expresses *VIP(H548A)* pyrophosphatase mutant and *DDP1(N25Δ)-HA* from their endogenous promoters and terminators (*LEU2*)	This study
pRS415-VIP1(H548A)-DDP1(N25Δ noseΔ)-HA	Co-expresses *VIP(H548A)* pyrophosphatase mutant and *DDP1(N25Δ noseΔ)-HA* from their endogenous promoters and terminators (*LEU2*)	This study
pRS415-VIP1(H548A)-DDP1(S26A)-HA	Co-expresses *VIP(H548A)* pyrophosphatase mutant and *DDP1(S26A)-HA* from their endogenous promoters and terminators (*LEU2*)	This study
pRS415-VIP1(H548A)-DDP1(S26D)-HA	Co-expresses *VIP(H548A)* pyrophosphatase mutant and *DDP1(S26D)-HA* from their endogenous promoters and terminators (*LEU2*)	This study
pRS415-VIP1(H548A)-DDP1(E83A E84A)-HA	Co-expresses *VIP(H548A)* pyrophosphatase mutant and *DDP1(E83A E84A)-HA* from their endogenous promoters and terminators (*LEU2*)	This study
pRS415-VIP1(H548A)-DDP1(54-AHKKR/GAAAA)-HA	Co-expresses *VIP(H548A)* pyrophosphatase mutant and *DDP1(54-AHKKR/GAAAA)-HA* from their endogenous promoters and terminators (*LEU2*)	This study
pRS415-VIP1(H548A)-GPD-DIPP1-HA	Co-expresses *VIP(H548A)* pyrophosphatase mutant and human *DIPP1-HA* from yeast GPD promoter (*LEU2*)	This study
pRS415-VIP1(H548A)-GPD-RPS10-DIPP1-HA	Co-expresses *VIP(H548A)* pyrophosphatase mutant and human RPS10-*DIPP1-HA* from the constitutive GPD promoter (*LEU2*)	This study
p416	Empty vector control (*URA3* selection)	Gerasimaitė et al., PMID: 25315834
p416-DIPP1-HA	Expresses human *DIPP1-HA* from GPD promoter (*URA3* selection)	McCarthy et al. 2023 (PMID: 35862758)
p416-DIPP1(RHPDR/AHKKR)-HA	Expresses human *DIPP1(RHPDR/AHKKR)-HA* from yeast GPD promoter (*URA3* selection)	This study
p416-DDP1	Expresses yeast *DDP1* from yeast GPD promoter (*URA3* selection)	McCarthy et al. 2023 (PMID: 35862758)
p6HIS-TEV-Ddp1	Expresses 6HIS TEV-cleavable Ddp1 from IPTG inducible promoter	This study

p6HIS-TEV-Ddp1(N25Δ)	Expresses 6HIS TEV-cleavable Ddp1(N25Δ) from IPTG inducible promoter	This study
p6HIS-TEV-Ddp1(noseΔ)	Expresses 6HIS TEV-cleavable Ddp1(noseΔ) from IPTG inducible promoter	This study
p6HIS-TEV-Ddp1(N25Δ noseΔ)	Expresses 6HIS TEV-cleavable Ddp1(N25Δ noseΔ) from IPTG inducible promoter	This study
p6HIS-TEV-Ddp1(E83A E84A)	Expresses 6HIS TEV-cleavable Ddp1(E83 E84) from IPTG inducible promoter	This study

CHAPTER 5 – GENERAL DISCUSSION

Statement of rights and permissions
The articles listed below were used under the following licences:

(1) **McCarthy, L.***, Baijal, K.*, Downey, M. (2025) A framework for understanding and investigating polyphosphate-protein interactions. *Biochem Soc Trans*, 21:BST20240678. https://doi.org/10.1042/BST20240678

*Co-first authors

© 2025 McCarthy et al. This is an open access article published by Portland Press Limited on behalf of the Biochemical Society and distributed under the Creative Commons Attribution 4.0 International (CC BY) license.

Note: Sections 5.2, 5.3, 5.4, and 5.5 were taken directly from this review article with no modifications made.

(2) **McCarthy, L.**, Abramchuk, I., Wafy, G., Denoncourt, A., Lavallée-Adam, M., & Downey, M. (2022). Ddp1 cooperates with Ppx1 to counter a stress response initiated by nonvacuolar polyphosphate. *mBio*, 13(4), e0039022. https://doi.org/10.1128/mbio.00390-22

© 2022 McCarthy et al. This is an open-access article distributed under the terms of the Creative Commons Attribution 4.0 International (CC BY) license.

Note: Some of the ideas discussed in Section 5.6 and 5.7 are taken from this research article and were modified to fit the flow of the discussion.

5.1. Role of polyP-protein interactions and vacuolar function

At the time of my first publication (1) (Chapter 2) polyphosphorylation was believed to be covalent based on its ability to survive denaturing conditions (2). New evidence (discussed in Chapter 1 – Introduction) suggests that polyphosphorylation is non-covalent (3) and our lab now refers to target proteins as polyP-binding proteins rather than polyphosphorylated proteins. Whether the interaction is covalent or non-covalent does not necessarily matter, although different binding modes could potentially lead to different outcomes in the cell. To date, most polyP-binding proteins uncovered in yeast are nucleolar proteins involved in ribosome biogenesis (2,4). This is seemingly at odds with the fact that the majority of polyP in yeast is stored in the vacuole (5,6). By performing an expanded screen for polyP-binding proteins using the NuPAGE analysis we were able to uncover 8 additional targets in yeast. Notably, these targets included two vacuolar proteins, Prb1 and Apl5. We focused on these vacuolar proteins since we believed that they were more likely to be effectors of polyP-mediated signaling based on polyP levels in the vacuole. We showed that polyP binds to the precursor peptide of Prb1 which is removed by a self-catalyzed cleavage event in the endoplasmic reticulum (ER) (7). Moreover, Prb1 processing was slightly slower in *vtc4*Δ cells, which lack polyP, suggesting that polyP binding could be important for Prb1 processing. Notably, the Ppn1 endopolyphosphatase also binds polyP when analyzed via NuPAGE, whereas Ppn2 does not (data not shown). Similarly to Prb1, polyP binds Ppn1 within its precursor peptide which is eventually cleaved by vacuolar proteases, including Prb1 (8). How polyphosphatases in the vacuole are regulated is still unclear, but their activity must be regulated in some manner to avoid the degradation of polyP as it is synthesized in the vacuole. Otherwise, the synthesis and storage of polyP in the vacuole would be a futile task (9). The fact that polyP binds the propeptide of Prb1 suggests a potentially interesting cross-regulatory mechanism between polyP, vacuolar

proteases, and the subsequent processing of polyphosphatases in the vacuole. It is possible that small pools of polyP in the ER could be important for regulating protease and polyphosphatase processing and activation in the vacuole. This idea is particularly interesting since some Vtc proteins localize around the nucleus (thought to be the ER) and the cell periphery in phosphate replete conditions (10,11). Future studies should aim to investigate the regulatory role of polyP in the processing and activation of vacuolar proteases and polyphosphatases.

5.2. Characteristics of polyP-binding elements

PolyP-binding sequence elements are positively charged in nature, suggesting that polyP interaction might simply be determined by the charged state of proteins and the corresponding anionic nature of the polymer. However, it is unlikely that charge is the only consideration. Interestingly, mutation of lysine and histidine residues in PASK and polyHis motifs to arginine prevents polyP interaction (2,4,12,13). Why does positively charged arginine not support binding in these contexts? Neville et al. (14) have previously discussed the idea that the guanidinium group in the arginine side chain results in a delocalized charge that prevents polyP binding. However, we also note that loss of polyP binding for arginine mutations has only been demonstrated using NuPAGE analysis (2,4,12,13). It is possible that polyP still binds to arginine-rich sequences, but with a lower affinity that does not permit detection on NuPAGE gels. As such, we encourage the use of alternative techniques, described below, to investigate the binding properties of arginine-rich sequences. This same logic extends to investigating the contribution of neighboring amino acids such as acidic and serine residues found in the PASK motif (2,15). Finally, it is curious that in contrast with PASK and polyHis motifs, arginines have been implicated in polyP binding for the endopolyphosphatase Ddp1 (16), the polyP kinase PPK2 (17), and the polyP-binding CHAD

domain (18). Therefore, it could also be true that context is important — PASK and polyHis sequences are shorter motifs often located in regions of little structure, whereas Ddp1, PPK2, and CHAD domains bind to polyP across folded protein surfaces. Finally, we do not discount the possibility that polyP binding to protein targets could be impacted by direct or indirect interactions with peptide backbones.

5.3. Methodological considerations for studying polyP-binding proteins

While NuPAGE analysis may be useful for identification of the strongest polyP binders, the fact that these gels are (largely) denaturing, presents a challenge for understanding how proteins might interact with polyP *in vivo*. Under denaturing conditions, polyP binding could be mediated by amino acids that are not normally exposed in natively folded proteins. Immobilization of natively folded proteins on beads, followed by washing prior to NuPAGE would help to address these concerns (12). Still, other more precise methods than gel electrophoresis are needed to identify and study the kinetics of polyP-binding proteins under native conditions. For example, plate-based enzyme-linked immunosorbent assays have recently been used to measure the affinity of polyP for three different plasma proteins (19), as well as the SARS-CoV-2 ACE2 receptor (20). Even more sophisticated tools such as surface plasmon resonance analysis (21–23) and grating-coupled interferometry (18) have also been used to accurately measure dissociation constants for polyP-protein interactions. Since polyP concentrations vary across different cell types and even within regions of a single cell, accurate measurements of polyP binding parameters are critical to establish whether an interaction is likely to occur *in vivo*.

5.4. Regulation of polyP binding by post-translation modifications (PTMs)

A consideration that has not been explored in detail is the potential interplay between PTMs and polyP binding. Direct modification of lysine residues, by acetylation or methylation for example (24,25), could prevent polyP from interacting with these residues. Azevedo et al. (2) also previously suggested the possibility of interplay between polyP binding and covalent pyrophosphorylation of eukaryotic PASK containing proteins. Pyrophosphorylation involves the magnesium dependent non-enzymatic transfer of the β-phosphoryl group from inositol pyrophosphate to a pre-phosphorylated residue (26). This modification occurs primarily on serine residues within intrinsically disordered regions (27). Indeed, recent work suggests that pyrophosphorylation occurs on a global scale and many of the proteins modified are localized to the nucleolus (27), as is the case with polyP-binding proteins (2,4). It is important to note that polyP binding is not strictly dependent on pyrophosphorylation since Nsr1 extracted from yeast cells with no diphosphoinositol pentakisphosphate, the phosphate donor for pyrophosphorylation, can bind polyP (2), and proteins purified from *E. coli* can also bind polyP *in vitro* (3). Nonetheless, we postulate that pyrophosphorylation might regulate polyP binding *in vivo* under specific conditions. As a first step, proteins known to bind polyP that are also pyrophosphorylated, such as Nsr1 (2,26) or DEK (4,27), could be used to test whether this modification can alter the extent of polyP binding *in vitro*. Alternatively, polyP binding could precede pyrophosphorylation, either by promoting the recruitment of kinases responsible for priming phosphorylations, or the subsequent reaction with inositol pyrophosphates (26).

5.5. Regulation of polyP binding by polyphosphatases

Polyphosphatases are ubiquitous enzymes, from prokaryotes to eukaryotes (28). The ability of

these enzymes to degrade polyP chains makes them candidate regulators that could turn off or dampen signaling cascades initiated by polyP-protein interactions. *In vitro* work has shown that recombinant yeast Ppx1 can cleave protein-bound polyP (2), and many studies have used exogenous Ppx1 expression to study the effects of polyP in mammalian cells (29,30). Polyphosphatases were initially proposed to remove the covalent interacting polyP chains from proteins (2,31,32), although there is no reason to assume that the mode of interaction would have any bearing on the ability of these enzymes to act on polyP bound to protein targets. Understanding how these polyphosphatases are regulated could shed light on pathways mediated by polyP-protein interactions. Since most polyphosphatase enzymes are dependent on cations for their function (28), we speculate that local concentrations of these cofactors are important determinants for the reversal of polyP-protein interactions *in vivo*.

5.6. Importance of polyP compartmentalization

Compartmentalization of polyP into acidocalcisome-like organelles is conserved across most eukaryotic organisms that produce polyP (33,34). Acidocalcisomes are acidic membrane-bound organelles where phosphorous is stored as pyrophosphate and polyP often complexed to calcium or other ions (35). Although bacteria don't have membrane-bound organelles, polyP is often "compartmentalized" into fluid-like granules that may arise from phase separation (36,37). The sequestration of polyP into granules and vacuole-like organelles suggests a tight control of polyP localization to prevent nonspecific interactions with effector proteins or cations (38). Indeed, accumulation of nonvacuolar polyP in yeast is toxic and we have shown that this mislocalization activates a constitutive Msn2/Msn4-driven stress response likely driven by low PKA activity (Chapter 3) (39). It is unclear if nonvacuolar polyP is causing some type of intracellular stress (i.e. the accumulation of unfolded proteins) or if it is inappropriately activating these stress-signaling

pathways in the absence of stress. Importantly, this toxicity is dampened by the cytoplasmic polyphosphatases Ddp1 and Ppx1, which combine their endo- and exopolyphosphatase activities to regulate nonvacuolar polyP accumulation. Thus, these two enzymes likely ensure that nonvacuolar polyP levels are kept at bay under normal physiological conditions.

In yeast, the most obvious reason for polyP synthesis and storage within the vacuole is to serve as a phosphate store to deal with fluctuations in the environment, such as phosphate availability (9,38). To this end, it is thought that when phosphate is plentiful it is imported into the cell and subsequently converted into polyP and stored in the vacuole (9,38). When phosphate becomes limiting, polyP stores are mobilized by the Ppn1 and Ppn2 polyphosphatases and exported into the cytoplasm as inorganic phosphate by the Pho91 phosphate transporter (9,40–42). How the synthesis and degradation of polyP is regulated to prevent degradation of polyP stores is still unclear (9). Potential interplay between polyP, vacuolar proteases, and the subsequent processing of polyphosphatases was discussed above. Another possibility is that polyphosphatases are inhibited by inorganic phosphate levels in the vacuole. There is some *in vitro* evidence that Ppn1 is inhibited by phosphate and pyrophosphate (43), thus Ppn1 might be regulated by enzyme product inhibition. Similar inhibition is seen for the pyrophosphatase activity of *S. pombe* Siw14 (44) and *S. cerevisiae* Vip1 (45) where inorganic phosphate is inhibitory *in vitro*. New work from Bru et al. suggests that polyphosphatase activity in the vacuole is inhibited by inorganic phosphate (46). When phosphate levels are abundant, the VTC complex converts ATP in the cytoplasm into polyP for storage. As polyP is synthesized a portion is converted into inorganic phosphate by Ppn1 and Ppn2 until it reaches an inhibitory threshold that inactivates the polyphosphatases and allows for polyP accumulation (46). When phosphate becomes limiting, Pho91 exports phosphate from

the vacuole allowing for polyP chains to be degraded and further exported as inorganic phosphate (46). Thus, the compartmentalization of polyP allows for a dynamic phosphate buffering system.

5.7. Physiological scenarios of nonvacuolar polyP accumulation

Herein we used the *E. coli* PPK expression system to investigate the consequences of nonvacuolar polyP accumulation in yeast. This artificial system allowed us to explore the importance of polyP compartmentalization in eukaryotes and the molecular mechanisms that lead to the toxic effects of mislocalized polyP accumulation (33,39). One important question that still needs to be addressed is if, when, and how polyP might make its way outside the vacuole? There are a few potential scenarios of interest wherein polyP might be released from the vacuole via vacuolar lysis or permeabilization. First, polyP might be released from the vacuole during sporulation when cells undergo meiosis (47,48). During this process the vacuole is lysed, and its contents are released into the cytosol to promote bulk degradation of the nuclear content that is not protected by a spore wall (47,48). Second, hydrogen peroxide stress (49) and heat stress (50) have both been shown to lead to vacuole membrane permeabilization and eventual cell death. These could be potential scenarios when polyP might be released from the confines of the vacuole and may interact with proteins outside the vacuole. It would be interesting to test whether proteins that we identified as being differentially regulated by PPK expression are also differentially regulated during these physiological scenarios. Moreover, if polyP is released into the cytoplasm during these events, it would be interesting to investigate the impact of deleting the cytoplasmic polyphosphatases Ddp1 and Ppx1 to see whether phenotypes, such as cell death, are exaggerated.

5.8. Protein kinase A (PKA) regulation by polyP

Our findings in Chapter 3, suggest that nonvacuolar polyP accumulation leads to lowered PKA activity in yeast cells expressing PPK and that this effect is amplified in polyphosphatase mutants (39). However, it is still unclear if this regulation is direct or indirect. A first step in determining a direct effect of polyP on PKA activity would be to perform *in vitro* phosphorylation assays. PKA is composed of 3 catalytic subunits: Tpk1, Tpk2, and Tpk3, and a regulatory subunit Bcy1 (51). *In vitro* a single catalytic subunit, like Tpk1, can be used to perform in vitro phosphorylation of known PKA targets, such as Yak1 (52). Comparing the ability of Tpk1 to phosphorylate Yak1 in the presence or absence of polyP in vitro would begin to delineate the direct versus indirect effects of polyP on PKA. Moreover, the effects on PKA substrate phosphorylation are greater in *ppx1*Δ cells than the effects seen in *ddp1*Δ mutants. These results suggest there might be a chain length-dependent effect on PKA activity since *ppx1*Δ mutants accumulate more medium and short chain polyP than *ddp1*Δ mutants, which accumulate a greater amount of long chain polyP. This potential chain length-dependent effect could be tested by using commercially available synthetic polyP chains of varying lengths in the *in vitro* assays described above. Chain-length dependent effects have previously been described, for example short chain and long chain polyP activate different parts of the blood coagulation cascade (53), and long chain polyP is better for interfering with macrophage signaling (54). Thus, chain length-dependent effects could represent an important mechanism of polyP signaling.

The effects of polyP on PKA activity could also be indirect via an upstream target in the cAMP-PKA pathway. An obvious target would be the Ras GTPase pathway, which when active (GTP-bound), interacts with the adenylate cyclase Cyr1 to produce cAMP (51,55,56). This cAMP can then bind to the regulatory subunit Bcy1 allowing the catalytic subunits to phosphorylate their

targets (51,56). Interestingly, K-Ras, the human homologue of yeast Ras1 and Ras2 has been shown to bind polyP and the addition of exogenous polyP to media or ectopic expression of PPK reduces the amount of GTP-bound K-Ras in HELA cells (57). A similar Ras2-GTP pulldown assay could be used to investigate if PPK expression reduces the amount of GTP-bound Ras2 in yeast (58,59). Moreover, if nonvacuolar polyP affects Ras2 activation and subsequently PKA activity, deletion of the Ddp1 and Ppx1 polyphosphatases would be expected to reduce Ras2-GTP to a greater degree based on the reduced PKA substrate phosphorylation we see in these mutants. These experiments would begin to answer whether nonvacuolar polyP affects PKA activity directly or indirectly.

5.9. Regulation of Ddp1 activity

Our work in Chapter 4 has confirmed critical residues for Ddp1 polyphosphate binding and catalysis *in vivo* using our PPK expression system. We have shown that the intrinsically disordered N-terminus might also be important for its pyrophosphatase activity. Moreover, our data suggest that the phosphorylation of serine 26 is potentially important for regulating this pyrophosphatase activity. However, there are still many questions regarding Ddp1's regulation to be answered (some of these are discussed in Chapter 4).

First, although Ddp1 is primarily localized in the cytoplasm it is still unclear how a small portion of Ddp1 is localized to the nucleus. Using the cNLS mapper tool (60), we identified a potential bipartite nuclear localization signal between amino acids 148-172. Unfortunately, when we generated a deletion mutant of this region the protein was not expressed to a detectable level (data not shown). In the future, a more targeted mutational analysis of key basic residues might allow us to determine whether this region is in fact a nuclear localization signal (61).

Previous works have shown that protein chaperones can facilitate the nuclear import of client proteins, which might target misfolded cytoplasmic proteins for degradation in the nucleus (62,63). Another interesting possibility is that chaperone interactions with Hsc82 (64) and Ssa1 (65) may allow for the nuclear import of Ddp1. Analyzing the localization of Ddp1 in chaperone deletion mutants could begin to test this possibility. Moreover, Hsc82 was previously shown to target IDRs of client proteins and prevent them from being recruited into RNA-containing stress granules and processing bodies (P-bodies) (64). We have shown that Ddp1 can bind to RNA which may promote oligomerization via the nose. The RNA-dependent oligomerization of Ddp1 could serve to regulate the enzymatic activity of Ddp1 in the cell. Co-localization experiments could be performed to determine whether Ddp1 can localize to stress granules or P-bodies under specific conditions and whether Hsc82 might regulate its inclusion into these RNA-containing cytoplasmic bodies.

The possibility that Ddp1 activity might be regulated by phosphate levels in the cell should also be investigated. Performing *in vitro* polyphosphatase or pyrophosphatase assays in the presence of increasing orthophosphate concentrations could begin to determine whether Ddp1 activity is directly regulated by phosphate. Similar phosphate-dependent inhibition has been demonstrated for the mammalian PPIP5K pyrophosphatase domain (66), Vip1's pyrophosphatase domain (45), and *S. pombe* Siw14 (44). However, it is still unclear how phosphate acts on these proteins to inhibit their activity. In the case of Vip1, it has been proposed that orthophosphate might bind to the highly basic "capture site" to prevent 1,5-IP8 from binding (45). If the N-terminus of Ddp1, which also contains many basic amino acids, does is in fact act as a capture site, a similar phosphate dependent-inhibition could be true. Moreover, the phosphorylation of Ddp1 S26 could potentially serve to prevent this phosphate-dependent inhibition by preventing phosphate from

binding the basic residues in the N-terminus or the nearby R32 residue which is critical for polyP binding and may be critical for inositol binding as well.

5.10. Could Ddp1 dephosphorylate pyrophosphorylated proteins?

Since the coordinated addition and removal of phosphorylation is important for regulating protein function and cell signaling (67) it is safe to assume that timely removal of pyrophosphorylation is likely also important. Ddp1 can accommodate various substrates into its active site for catalysis raising the possibility that it could also dephosphorylate pyrophosphorylated proteins. Interestingly, pyrophosphorylation removal was shown to be resistant to various phosphatases including lambda phosphatase (26). Further work using pyrophosphorylated peptides demonstrated that protein phosphatases like PP1, PP2C were ineffective in removing pyrophosphate, but that the alkaline phosphatases CIP, rSAP, and phoA were effective (68). By incubating pyrophosphorylated peptides with lysates prepared from wild-type yeast cells and *pho8*Δ mutants, the authors were able to show that the alkaline phosphatase Pho8 can hydrolyze pyrophosphate from proteins (68). Interestingly, there was still some hydrolysis activity in *pho8*Δ lysates suggesting that there are other yeast proteins that can hydrolyze protein pyrophosphate (68). This residual activity was lost in the presence of EDTA, suggesting that the protein is metal dependent (68). Ddp1 is a metal-dependent pyrophosphatase which could be responsible for this residual activity and its ability to remove pyrophosphate from proteins should be tested.

Notably, DIPP1, the mammalian homologue of Ddp1, was unable to remove pyrophosphate from any of the peptides tested (68). Although the mammalian homologue cannot remove the pyrophosphate moiety from peptides there are several differences in the Ddp1 structure that could promote protein binding and its ability to remove the pyrophosphate moiety. For

example, intrinsically disordered regions are known to be important for protein-protein interactions (69). The intrinsically disordered N-terminus and the nose could serve as regions important for promoting protein-protein interactions with pyrophosphorylated proteins. Future work should determine whether Ddp1 can remove pyrophosphate moieties from proteins.

5.11. 1,5-IP8 toxicity in yeast

Our work has shown that the *ddp1*Δ *siw14*Δ *vip1*Δ pyrophosphatase mutant expressing *VIP1(H548A)* is inviable and that this toxicity is presumably driven by excess 1,5-IP8 accumulation. It will be important to confirm whether this lethality is in fact driven by 1,5-IP8 by measuring inositol pyrophosphate levels using a conditional mutant (e.g. galactose-inducible *VIP1(H548A)* in *ddp1*Δ *siw14*Δ *vip1*Δ background). Recent advances in the extraction and mass spectrometry analysis of pyrophosphate extracted from yeast has enabled more precise measurements of pyrophosphate extracted from yeast (70–72). Nonetheless, genetic studies in *S. pombe* suggest that 1,5-IP8 overaccumulation is also toxic (44). Here, the toxicity seems to be driven in part by early 3'-processing/transcription termination (73). Notably, deletion of various SPX binding domain proteins can rescue this toxicity (73). As a first step, SPX domain containing proteins in *S. cerevisiae* should be deleted to see if a similar phenomenon is true. These include Vtc2, Vtc3, Vtc4, Vtc5, Pho81, Pho87, Pho90, Pho91, Gde1, and Syg1 (74). These proteins could be screened using our plasmid shuffle system to see if their deletion can rescue growth in the *ddp1*Δ *siw14*Δ *vip1*Δ *VIP1(H548A)* mutant. We note that the transducers of 1,5-IP8 toxicity may differ between *S. pombe* and *S. cerevisiae*. In S. pombe, Spx1 was identified has a transducer of 1,5-IP8 toxicity but is not conserved in *S. cerevisiae* (73). Moreover, the SPX domain protein Pho81 and the Pho85 cyclin-dependent kinase are not conserved in *S. pombe* (72). Our results also

suggest that *S. pombe* may be more sensitive to 1,5-IP8 accumulation compared to *S. cerevisiae* where pyrophosphatase double mutants are viable. Differences in SPX binding domain protein conservation and inositol pyrophosphate signaling could account for these differences.

One interesting possibility raised by Schwer et al. is that excess 1,5-IP8 drives nonvacuolar polyP accumulation in the nucleus (73) (See discussion Chapter 4). A small portion of the VTC complex may reside around the nuclear membrane under phosphate replete conditions to produce a small pool of nuclear polyP (10). Although it was initially thought that 5-IP7 could activate the VTC complex *in vivo* (75), more recent work showed that 1,5-IP8 is likely the regulatory pyrophosphate that can activate the VTC complex to promote polyP synthesis (76). Thus increased 1,5-IP8 levels could promote the accumulation of nonvacuolar polyP which is toxic. To test this possibility, the Ppx1 exopolyphosphatase could be targeted to the nucleus using a nuclear localization signal. If nuclear polyP accumulation is driving 1,5-IP8 toxicity we would expect Ppx1 expression in the nucleus to rescue growth.

5.12 Concluding remarks

Overall, the work presented in this thesis has expanded our understanding of the role of polyP and its regulation in the budding yeast *S. cerevisiae*. We have shown that polyP can bind to the propeptide of the vacuolar protease Prb1 and may be important for its processing. Prb1 itself is directly involved in the processing and activation of the Ppn1 endopolyphosphatase suggesting a potential cross-regulatory mechanism between polyP, vacuolar proteases, and the subsequent processing of polyphosphatases in the vacuole that should be explored further.

Additionally, our work has uncovered potential pathways that drive the toxicity of nonvacuolar polyP accumulation. We find that nonvacuolar polyP accumulation in yeast activates

an Msn2/Msn4-dependent stress response that appears to be driven by a reduction in PKA activity. Nonvacuolar polyP accumulation and toxicity is mitigated by the cytoplasmic Ddp1 and Ppx1 polyphosphatases. These results highlight the importance of polyP compartmentalization in eukaryotes and suggest that polyphosphatases likely play important roles in mitigating the negative impacts of mislocalized polyP in other eukaryotes. Moreover, we identify a potential link between the conserved PKA pathway and polyP signaling.

Finally, we have used our PPK expression system to better characterize critical polyphosphate binding residues of the Ddp1 endopolyphosphatase *in vivo*. Additionally, we have developed a plasmid shuffle system to study its pyrophosphatase activity *in vivo* and have identified potentially important regulatory regions, including its intrinsically disordered N-terminus. These tools have allowed us to explore how this multifunctional enzyme might be regulated *in vivo*. Understanding how these enzymes are regulated will be critical for the development of potential therapeutic interventions for polyP-driven disorders.

Importantly, this work has highlighted two tools that can potentially be used to further characterize these important enzymes. The PPK expression system can be used to explore the regulation and function of other cytoplasmic polyphosphatases, such as Ppx1 in yeast, as well as potential mammalian candidate enzymes. In addition, our pyrophosphatase plasmid shuffle system could be expanded to explore the function of other key yeast pyrophosphatases including Siw14 and Vip1. Similarly, it could be used to characterize mammalian pyrophosphatases such as the DIPP1 homologue. If the inositol pyrophosphate and polyphosphate pathways in higher eukaryotes are interconnected, as they are in yeast, both classes of enzymes may be important drivers of polyP dysregulation in human cells. Eventually, these enzymes may provide therapeutic targets in disorders driven by the overaccumulation or mislocalization of polyP. Additionally, understanding

how these enzymes function will be critical in efforts to deliver polyP in therapeutic contexts. Thus, it will be critical to understand how these enzymes are regulated in the context of the cell.

5.13. References

1. McCarthy L, Bentley-DeSousa A, Denoncourt A, Tseng YC, Gabriel M, Downey M. Proteins required for vacuolar function are targets of lysine polyphosphorylation in yeast. FEBS Lett. 2019;1–10.
2. Azevedo C, Livermore T, Saiardi A. Protein polyphosphorylation of lysine residues by inorganic polyphosphate. Mol Cell [Internet]. 2015;58(1):71–82. Available from: http://dx.doi.org/10.1016/j.molcel.2015.02.010
3. Neville N, Lehotsky K, Klupt KA, Downey M, Jia Z. Polyphosphate attachment to lysine repeats is a non-covalent protein modification. Mol Cell [Internet]. 2024 May 2;84(9):1802-1810.e4. Available from: https://doi.org/10.1016/j.molcel.2024.03.028
4. Bentley-DeSousa A, Holinier C, Moteshareie H, Tseng YC, Kajjo S, Nwosu C, et al. A Screen for Candidate Targets of Lysine Polyphosphorylation Uncovers a Conserved Network Implicated in Ribosome Biogenesis. Cell Rep [Internet]. 2018;22(13):3427–39. Available from: https://doi.org/10.1016/j.celrep.2018.02.104
5. Urech K, Dürr M, Boller T, Wiemken A, Schwencke J. Localization of polyphosphate in vacuoles of Saccharomyces cerevisiae. Arch Microbiol. 1978;116(3):275–8.
6. Saito K, Ohtomo R, Kuga-Uetake Y, Aono T, Saito M. Direct labeling of polyphosphate at the ultrastructural level in Saccharomyces cerevisiae by using the affinity of the polyphosphate binding domain of Escherichia coli exopolyphosphatase. Appl Environ Microbiol. 2005;71(10):5692–701.
7. Naik RR, Nebes V, Jones EW. Regulation of the proteinase B structural gene PRB1 in Saccharomyces cerevisiae. J Bacteriol. 1997;179(5):1469–74.
8. Shi X, Kornberg A. Endopolyphosphatase in Saccharomyces cerevisiae undergoes post-translational activations to produce short-chain polyphosphates. FEBS Lett. 2005;579(9):2014–8.
9. Austin S, Mayer A. Phosphate Homeostasis − A Vital Metabolic Equilibrium Maintained Through the INPHORS Signaling Pathway. Front Microbiol [Internet]. 2020;Volume 11. Available from: https://www.frontiersin.org/journals/microbiology/articles/10.3389/fmicb.2020.01367
10. Hothorn M, Neumann H, Lenherr ED, Wehner M, Rybin V, Hassa PO, et al. Catalytic core of a membrane-associated eukaryotic polyphosphate polymerase. Science (80-). 2009;324(5926):513–6.
11. Uttenweiler A, Schwarz H, Neumann H, Mayer A. The vacuolar transporter chaperone (VTC) complex is required for microautophagy. Mol Biol Cell. 2007;18(1):166–75.
12. Neville N, Lehotsky K, Yang Z, Klupt KA, Denoncourt A, Downey M, et al. Modification of histidine repeat proteins by inorganic polyphosphate. Cell Rep [Internet]. 2023 Sep 26;42(9). Available from: https://doi.org/10.1016/j.celrep.2023.113082
13. Gauthier CM, LeGallais J, Savic N, Moradi-Fard S, Grew A, Loe M, et al. Intrinsic disorder of a nucleoplasmin-like histone chaperone specifies its discrete nuclear and nucleolar functions. FEBS Lett. 2024;598(2):187–98.
14. Neville N, Lehotsky K, Jia Z. Back on the chain gang: polyphosphate modification of proteins. Trends Biochem Sci [Internet]. 2024 Sep 1;49(9):757–60. Available from: https://doi.org/10.1016/j.tibs.2024.06.010
15. Azevedo C, Desfougères Y, Jiramongkol Y, Partington H, Trakansuebkul S, Singh J, et al. Development of a yeast model to study the contribution of vacuolar polyphosphate

metabolism to lysine polyphosphorylation. J Biol Chem. 2020;295(6):1439–51.
16. Márquez-Moñino MÁ, Ortega-García R, Shipton ML, Franco-Echevarría E, Riley AM, Sanz-Aparicio J, et al. Multiple substrate recognition by yeast diadenosine and diphosphoinositol polyphosphate phosphohydrolase through phosphate clamping. Sci Adv. 2021;7(17):1–16.
17. Parnell AE, Mordhorst S, Kemper F, Giurrandino M, Prince JP, Schwarzer NJ, et al. Substrate recognition and mechanism revealed by ligand-bound polyphosphate kinase 2 structures. Proc Natl Acad Sci. 2018;115(13):3350–5.
18. Lorenzo-Orts L, Hohmann U, Zhu J, Hothorn M. Molecular characterization of CHAD domains as inorganic polyphosphate-binding modules. Life Sci Alliance [Internet]. 2019 Jun 1;2(3):e201900385. Available from: http://www.life-science-alliance.org/content/2/3/e201900385.abstract
19. Malik RA, Zhou J, Fredenburgh JC, Truong TK, Crosby JR, Revenko AS, et al. Polyphosphate-induced thrombosis in mice is factor XII dependent and is attenuated by histidine-rich glycoprotein. Blood Adv. 2021;5(18):3540–51.
20. Ferrucci V, Kong D-Y, Asadzadeh F, Marrone L, Boccia A, Siciliano R, et al. Long-chain polyphosphates impair SARS-CoV-2 infection and replication. Sci Signal. 2021;14(690):eabe5040.
21. Choi SH, Smith SA, Morrissey JH. Polyphosphate is a cofactor for the activation of factor XI by thrombin. Blood, J Am Soc Hematol. 2011;118(26):6963–70.
22. Montilla M, Hernandez-Ruiz L, Garcia-Cozar FJ, Alvarez-Laderas I, Rodriguez-Martorell J, Ruiz FA. Polyphosphate binds to human von Willebrand factor in vivo and modulates its interaction with glycoprotein Ib. J Thromb Haemost. 2012;10(11):2315–23.
23. Wijeyewickrema LC, Lameignere E, Hor L, Duncan RC, Shiba T, Travers RJ, et al. Polyphosphate is a novel cofactor for regulation of complement by a serpin, C1 inhibitor. Blood, J Am Soc Hematol. 2016;128(13):1766–76.
24. Azevedo C, Saiardi A. Why always lysine? The ongoing tale of one of the most modified amino acids. Adv Biol Regul [Internet]. 2016;60:144–50. Available from: https://www.sciencedirect.com/science/article/pii/S2212492615300142
25. Wang ZA, Cole PA. The chemical biology of reversible lysine post-translational modifications. Cell Chem Biol. 2020;27(8):953–69.
26. Bhandari R, Saiardi A, Ahmadibeni Y, Snowman AM, Resnick AC, Kristiansen TZ, et al. Protein pyrophosphorylation by inositol pyrophosphates is a posttranslational event. Proc Natl Acad Sci. 2007;104(39):15305–10.
27. Morgan JAM, Singh A, Kurz L, Nadler-Holly M, Ruwolt M, Ganguli S, et al. Extensive protein pyrophosphorylation revealed in human cell lines. Nat Chem Biol. 2024;20(10):1305–16.
28. McCarthy L, Downey M. The emerging landscape of eukaryotic polyphosphatases. FEBS Lett. 2023;597(11):1447–61.
29. Wang L, Fraley CD, Faridi J, Kornberg A, Roth RA. Inorganic polyphosphate stimulates mammalian TOR, a kinase involved in the proliferation of mammary cancer cells. Proc Natl Acad Sci U S A. 2003;100(20):11249–54.
30. Abramov AY, Fraley C, Diao CT, Winkfein R, Colicos MA, Duchen MR, et al. Targeted polyphosphatase expression alters mitochondrial metabolism and inhibits calcium-dependent cell death. Proc Natl Acad Sci. 2007;104(46):18091–6.
31. Bentley-DeSousa A, Downey M. From underlying chemistry to therapeutic potential:

open questions in the new field of lysine polyphosphorylation. Curr Genet [Internet]. 2018;0(0):1–8. Available from: http://dx.doi.org/10.1007/s00294-018-0854-4
32. Azevedo C, Saiardi A. The new world of inorganic polyphosphates. Biochem Soc Trans. 2016;44(1):13–7.
33. Gerasimaitė R, Sharma S, Desfougères Y, Schmidt A, Mayer A. Coupled synthesis and translocation restrains polyphosphate to acidocalcisome-like vacuoles and prevents its toxicity. J Cell Sci. 2014;127(23):5093–104.
34. Lander N, Cordeiro C, Huang G, Docampo R. Polyphosphate and acidocalcisomes. Biochem Soc Trans [Internet]. 2016 Feb 9;44(1):1–6. Available from: https://doi.org/10.1042/BST20150193
35. Docampo R, Moreno SNJ. Acidocalcisomes. Cell Calcium [Internet]. 2011;50(2):113–9. Available from: https://www.sciencedirect.com/science/article/pii/S0143416011001011
36. Racki LR, Tocheva EI, Dieterle MG, Sullivan MC, Jensen GJ, Newman DK. Polyphosphate granule biogenesis is temporally and functionally tied to cell cycle exit during starvation in Pseudomonas aeruginosa. Proc Natl Acad Sci U S A. 2017;114(12):E2440–9.
37. Guan J, Hurto RL, Rai A, Azaldegui CA, Ortiz-Rodríguez LA, Biteen JS, et al. HP-Bodies – Ancestral Condensates that Regulate RNA Turnover and Protein Translation in Bacteria. bioRxiv [Internet]. 2025 Jan 1;2025.02.06.636932. Available from: http://biorxiv.org/content/early/2025/02/06/2025.02.06.636932.abstract
38. Borghi F, Saiardi A. Evolutionary perspective on mammalian inorganic polyphosphate (polyP) biology. Biochem Soc Trans. 2023;0:1947–56.
39. McCarthy L, Abramchuk I, Wafy G, Denoncourt A, Lavallée-Adam M, Downey M. Ddp1 Cooperates with Ppx1 to Counter a Stress Response Initiated by Nonvacuolar Polyphosphate. MBio. 2022;13(4).
40. Hürlimann HC, Stadler-Waibel M, Werner TP, Freimoser FM. Pho91 is a vacuolar phosphate transporter that regulates phosphate and polyphosphate metabolism in Saccharomyces cerevisiae. Mol Biol Cell. 2007;18(11):4438–45.
41. Sethuraman A, Rao NN, Kornberg A. The endopolyphosphatase gene: Essential in Saccharomyces cerevisiae. Proc Natl Acad Sci U S A [Internet]. 2001;98(15):8542–7. Available from: http://www.pnas.org/content/98/15/8542.abstract
42. Gerasimaitė R, Mayer A. Ppn2, a novel Zn^{2+} -dependent polyphosphatase in the acidocalcisome-like yeast vacuole. J Cell Sci [Internet]. 2017;130(9):1625–36. Available from: http://jcs.biologists.org/lookup/doi/10.1242/jcs.201061
43. Kumble KD, Kornberg A. Endopolyphosphatases for long chain inorganic polyphosphate in yeast and mammals. J Biol Chem. 1996;271(43):27146–51.
44. M. SA, Beate S, Nikolaus J, J. JH, Stewart S. Activities, substrate specificity, and genetic interactions of fission yeast Siw14, a cysteinyl-phosphatase-type inositol pyrophosphatase. MBio [Internet]. 2023 Sep 29;14(5):e02056-23. Available from: https://doi.org/10.1128/mbio.02056-23
45. Raia P, Lee K, Bartsch SM, Rico-Resendiz F, Portugal-Calisto D, Vadas O, et al. A small signaling domain controls PPIP5K phosphatase activity in phosphate homeostasis. Nat Commun [Internet]. 2025;16(1):1753. Available from: https://doi.org/10.1038/s41467-025-56937-0
46. Bru S, Michaillat Mayer L, Kim G-D, Qiu D, Jessen HJ, Mayer A. Acidocalcisome-like vacuoles constitute a feedback-controlled phosphate buffering system for the cytosol.

bioRxiv [Internet]. 2025 Jan 1;2025.05.30.656997. Available from: http://biorxiv.org/content/early/2025/05/30/2025.05.30.656997.abstract
47. Eastwood MD, Cheung SWT, Lee KY, Moffat J, Meneghini MD. Developmentally programmed nuclear destruction during yeast gametogenesis. Dev Cell. 2012;23(1):35–44.
48. Eastwood MD, Meneghini MD. Developmental coordination of gamete differentiation with programmed cell death in sporulating yeast. Eukaryot Cell. 2015;14(9):858–67.
49. Mason DA, Shulga N, Undavai S, Ferrando-May E, Rexach MF, Goldfarb DS. Increased nuclear envelope permeability and Pep4p-dependent degradation of nucleoporins during hydrogen peroxide-induced cell death. FEMS Yeast Res [Internet]. 2005 Dec 1;5(12):1237–51. Available from: https://doi.org/10.1016/j.femsyr.2005.07.008
50. Stolp ZD, Kulkarni M, Liu Y, Zhu C, Jalisi A, Lin S, et al. Yeast cell death pathway requiring AP-3 vesicle trafficking leads to vacuole/lysosome membrane permeabilization. Cell Rep [Internet]. 2022 Apr 12;39(2). Available from: https://doi.org/10.1016/j.celrep.2022.110647
51. Conrad M, Schothorst J, Kankipati HN, Van Zeebroeck G, Rubio-Texeira M, Thevelein JM. Nutrient sensing and signaling in the yeast Saccharomyces cerevisiae. FEMS Microbiol Rev. 2014;38(2):254–99.
52. Lee P, Paik SM, Shin CS, Huh WK, Hahn JS. Regulation of yeast Yak1 kinase by PKA and autophosphorylation-dependent 14-3-3 binding. Mol Microbiol. 2011;79(3):633–46.
53. Smith SA, Choi SH, Davis-Harrison R, Huyck J, Boettcher J, Rienstra CM, et al. Polyphosphate exerts differential effects on blood clotting, depending on polymer size. Blood, J Am Soc Hematol. 2010;116(20):4353–9.
54. Roewe J, Stavrides G, Strueve M, Sharma A, Marini F, Mann A, et al. Bacterial polyphosphates interfere with the innate host defense to infection. Nat Commun [Internet]. 2020;11(1):1–12. Available from: http://dx.doi.org/10.1038/s41467-020-17639-x
55. Broach JR. Ras-regulated signaling processes in Saccharomyces cerevisiae. Curr Opin Genet Dev. 1991;1(3):370–7.
56. Rolland F, Winderickx J, Thevelein JM. Glucose-sensing and -signalling mechanisms in yeast. FEMS Yeast Res [Internet]. 2002 May 1;2(2):183–201. Available from: https://doi.org/10.1111/j.1567-1364.2002.tb00084.x
57. Lehotsky KE. Investigating the polyphosphate interactome with lysine- and histidine-rich proteins [Internet]. Queen's University; 2024. Available from: https://qspace.library.queensu.ca/server/api/core/bitstreams/a27e9bd8-d2c4-42ec-ac00-b5d497a806dc/content
58. Rudoni S, Colombo S, Coccetti P, Martegani E. Role of guanine nucleotides in the regulation of the Ras/cAMP pathway in Saccharomyces cerevisiae. Biochim Biophys Acta - Mol Cell Res [Internet]. 2001;1538(2):181–9. Available from: https://www.sciencedirect.com/science/article/pii/S0167488901000672
59. Colombo S, Ronchetti D, Thevelein JM, Winderickx J, Martegani E. Activation State of the Ras2 Protein and Glucose-induced Signaling in Saccharomyces cerevisiae. J Biol Chem [Internet]. 2004 Nov 5;279(45):46715–22. Available from: https://doi.org/10.1074/jbc.M405136200
60. Kosugi S, Hasebe M, Tomita M, Yanagawa H. Systematic identification of cell cycle-dependent yeast nucleocytoplasmic shuttling proteins by prediction of composite motifs. Proc Natl Acad Sci. 2009;106(25):10171–6.

61. Lu J, Wu T, Zhang B, Liu S, Song W, Qiao J, et al. Types of nuclear localization signals and mechanisms of protein import into the nucleus. Cell Commun Signal. 2021;19(1):60.
62. Shulga N, James P, Craig EA, Goldfarb DS. A nuclear export signal prevents Saccharomyces cerevisiae Hsp70 Ssb1p from stimulating nuclear localization signal-directed nuclear transport. J Biol Chem. 1999;274(23):16501–7.
63. Prasad R, Xu C, Ng DTW. Hsp40/70/110 chaperones adapt nuclear protein quality control to serve cytosolic clients. J Cell Biol. 2018;217(6):2019–32.
64. Kolhe JA, Babu NL, Freeman BC. The Hsp90 molecular chaperone governs client proteins by targeting intrinsically disordered regions. Mol Cell. 2023;83(12):2035–44.
65. Kao C-H, Ryu SW, Kim MJ, Wen X, Wimalarathne O, Paull TT. Growth-regulated Hsp70 phosphorylation regulates stress responses and prion maintenance. Mol Cell Biol. 2020;40(12):e00628-19.
66. Gu C, Nguyen H-N, Hofer A, Jessen HJ, Dai X, Wang H, et al. The significance of the bifunctional kinase/phosphatase activities of diphosphoinositol pentakisphosphate kinases (PPIP5Ks) for coupling inositol pyrophosphate cell signaling to cellular phosphate homeostasis. J Biol Chem. 2017;292(11):4544–55.
67. Ardito F, Giuliani M, Perrone D, Troiano G, Lo Muzio L. The crucial role of protein phosphorylation in cell signaling and its use as targeted therapy. Int J Mol Med. 2017;40(2):271–80.
68. Yates LM, Fiedler D. Establishing the stability and reversibility of protein pyrophosphorylation with synthetic peptides. ChemBioChem. 2015;16(3):415–23.
69. Bondos SE, Dunker AK, Uversky VN. Intrinsically disordered proteins play diverse roles in cell signaling. Cell Commun Signal. 2022;20(1):20.
70. Qiu D, Wilson MS, Eisenbeis VB, Harmel RK, Riemer E, Haas TM, et al. Analysis of inositol phosphate metabolism by capillary electrophoresis electrospray ionization mass spectrometry. Nat Commun. 2020;11(1):6035.
71. Qiu D, Gu C, Liu G, Ritter K, Eisenbeis VB, Bittner T, et al. Capillary electrophoresis mass spectrometry identifies new isomers of inositol pyrophosphates in mammalian tissues. Chem Sci 14: 658–667. 2023.
72. Chabert V, Kim G-D, Qiu D, Liu G, Michaillat Mayer L, Jamsheer K M, et al. Inositol pyrophosphate dynamics reveals control of the yeast phosphate starvation program through 1,5-IP8 and the SPX domain of Pho81. Gutjahr C, Ron D, editors. Elife [Internet]. 2023;12:RP87956. Available from: https://doi.org/10.7554/eLife.87956
73. Schwer B, Garg A, Sanchez AM, Bernstein MA, Benjamin B, Shuman S. Cleavage-polyadenylation factor Cft1 and SPX domain proteins are agents of inositol pyrophosphate toxicosis in fission yeast. MBio. 2022;13(1):e03476-21.
74. Secco D, Wang C, Shou H, Whelan J. Phosphate homeostasis in the yeast Saccharomyces cerevisiae, the key role of the SPX domain-containing proteins. FEBS Lett [Internet]. 2012 Feb 17;586(4):289–95. Available from: https://doi.org/10.1016/j.febslet.2012.01.036
75. Gerasimaite R, Pavlovic I, Capolicchio S, Hofer A, Schmidt A, Jessen HJ, et al. Inositol Pyrophosphate Specificity of the SPX-Dependent Polyphosphate Polymerase VTC. ACS Chem Biol. 2017;12(3):648–53.
76. Pipercevic J, Kohl B, Gerasimaite R, Comte-Miserez V, Hostachy S, Müntener T, et al. Inositol pyrophosphates activate the vacuolar transport chaperone complex in yeast by disrupting a homotypic SPX domain interaction. Nat Commun [Internet]. 2023;14(1):2645. Available from: https://doi.org/10.1038/s41467-023-38315-w.